

University of Warwick institutional repository: <http://go.warwick.ac.uk/wrap>

A Thesis Submitted for the Degree of PhD at the University of Warwick

<http://go.warwick.ac.uk/wrap/59513>

This thesis is made available online and is protected by original copyright.

Please scroll down to view the document itself.

Please refer to the repository record for this item for information to help you to cite it. Our policy information is available from the repository home page.

A STUDY OF THE ORGANOMETALLIC CHEMISTRY OF ALUMINIUM, GALLIUM AND INDIUM.

CHAPTER 1 Introduction

A The Elements of Aluminium, Gallium and Indium

B Oxidation States of Organometallic Compounds of Group 13

B1 Self-Association of MOC Units

B2 Ligand Effects

B3 Neutral Adducts

B4 Alkyl Elimination Reactions

C Organometallic Compounds of Aluminium, Gallium and Indium

C1 Preparation of Simple Triorganometallic Compounds

C2 Neutral Adducts

C3 Reactions of N_2 , M with N_2 and M with N_2

(i) Metal-Nitrogen Multiple Bonds

(ii) Metal-Oxygen Multiple Bonds

(iii) Metal-Carbon Multiple Bonds

(iv) Metal-Hydrogen Multiple Bonds

(v) Metal-Halogen Multiple Bonds

(vi) Metal-Sulfur Multiple Bonds

(vii) Metal-Nitrogen Multiple Bonds

(viii) Metal-Oxygen Multiple Bonds

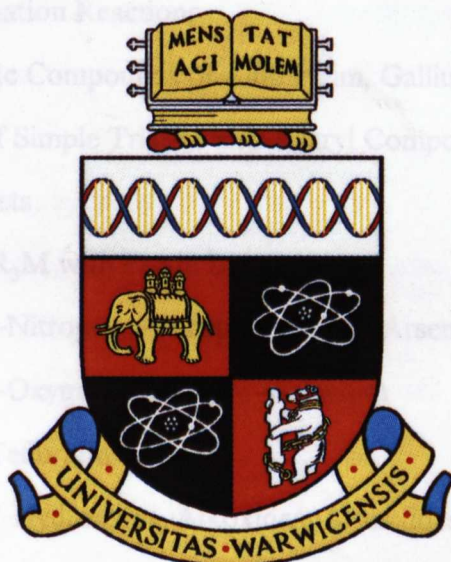
(ix) Metal-Carbon Multiple Bonds

(x) Metal-Hydrogen Multiple Bonds

(xi) Metal-Halogen Multiple Bonds

(xii) Metal-Sulfur Multiple Bonds

Paul Richard Phillips



University of Warwick

Department of Chemistry

**A Thesis submitted as part requirement for the
Degree of Doctor of Philosophy**

January, 1996

CONTENTS

	Page
CHAPTER 1 Introduction	1
A. The Elements of Aluminium, Gallium and Indium	2
B. Oxidation States of Organometallic Compounds of Group 13	4
B1. Self-Association of MX_3 Units	4
B2. Ligand Exchange	6
B3. Neutral Adducts	7
B4. Alkane Elimination Reactions	10
C. Organometallic Compounds of Aluminium, Gallium and Indium	12
C1. Preparation of Simple Trialkyl and Triaryl Compounds	12
C2. Neutral Adducts	15
C3. Reactions of R_3M with Protic Donors	20
(i) Metal-Nitrogen, -Phosphorus and -Arsenic Bonds	20
(ii) Metal-Oxygen, -Sulphur, -Selenium and -Tellurium Bonds	27
(a) Hydroxides, Alkoxides, Aryloxides and Related Complexes	27
(b) Carboxylates and Thiocarboxylates	31
(c) Other Compounds Containing Metal-Oxygen Bonds	33
(iii) Compounds Containing Metal-Nitrogen and -Oxygen Bonds	33

	Page
CHAPTER 2	
A Study of Some Organometallic N,N'-Diarylamidinato Derivatives of Aluminium, Gallium and Indium	36
Introduction	37
Preparation of the Dialkylmetal–Amidinato Complexes of Aluminium, Gallium, and Indium	39
Spectroscopic Characterisation of the Dialkylmetal–Amidinato Complexes	43
X–ray Crystallographic Studies	59
Reactions of the Dialkylmetal-N,N'-diphenylbenzamidinato Complexes of Aluminium, Gallium and Indium with Lewis Bases	69
Spectroscopic Properties of the Adducts	70
X–ray Crystallographic Studies	73
Preparation of the Monoalkylmetal-bis(amidinato) Complexes of Aluminium, Gallium and Indium	80
Spectroscopic Properties of the Monoalkylmetal-bis(amidinato) Complexes	81
X–ray Crystallographic Studies	88
Preparation of the Tris(Amidinato) Complexes of Aluminium, Gallium and Indium	103
Spectroscopic Properties of the Metal–tris(amidinato) Complexes	104
X–ray Crystallographic Studies	110
Discussion	114
CHAPTER 3	
Reactions of Trimethylgallium with Two N,N'-Unsubstituted Amidine Ligands	116
Introduction	117
(1) Reaction of trimethylgallium with <i>tert</i> -butyramidine, [H ₂ NCBu ^t NH]	118

	Page
Discussion	122
(2) Reaction of trimethylgallium with trifluoroacetamide, [H ₂ NCCF ₃ NH]	122
Spectroscopic Properties of [Me ₂ Ga{HNC(CF ₃)NC(CF ₃)NH}]	130
CHAPTER 4 Tetraazamacrocyclic Complexes of Indium(III)	136
Introduction	137
(1) Preparation of the Complexes	141
Spectroscopic Properties	145
X-ray Crystallographic Studies	152
(2) The Synthesis of Further Indium Functionalities	162
CHAPTER 5 Preliminary Investigation of the Photoreactivity of Some Group 13 Metal-Alkyl Bonds	179
Introduction	180
E.S.R Experiments	181
CHAPTER 6 Experimental	189
General Experimental	190
Chapter 2	192
Chapter 3	211
Chapter 4	213
APPENDIX 1 Thermal Decomposition of Some Group 13 Metal Amidinato Compounds	219
Introduction	220
Thermal Decomposition Reactions	221

	Page
APPENDIX 2	
X-ray Crystallographic Studies	229
APPENDIX 3	
Mass Spectra	272
REFERENCES	282

FIGURES AND TABLES

CHAPTER 1

Table 1.1	Some atomic properties of aluminium, gallium and indium	2
------------------	---	---

CHAPTER 2

Table 2.1	Compounds of the type $[R_2M(R'NCR''NR''')]]$ prepared in this study	40
Table 2.2	Summary of Proton decoupled ^{13}C N.M.R. data for dimethylaluminium-amidinato complexes	47
Table 2.3	Summary of Proton decoupled ^{13}C N.M.R. data of dialkylgallium-amidinato complexes	48
Table 2.4	Summary of Proton decoupled ^{13}C N.M.R. data of dialkylindium-amidinato complexes	49
Table 2.5	The major differences between the I.R. spectra of N,N' -diphenylbenzamidine and the dimethylmetal complexes	53
Table 2.6	Principal bond lengths and angles for $[Me_2In(PhNCPPhNPh)]$	63
Table 2.7	Relevant bond angles for dimethylgallium- N,N' -dimethylacetamidinato	65
Table 2.8	Relevant bond lengths and angles for bis(dimethylindium)- N,N',N'',N''' -tetramethyloxamidinato	66
Table 2.9	Structural parameters in bidentate chelate N,N' -diphenylbenzamidinato groups	68
Table 2.10	1H N.M.R. data for the dimethylmetal- N,N' -diphenylbenzamidinato adducts and parent Lewis base	70
Table 2.11	^{13}C N.M.R. data for the dimethylmetal- N,N' -diphenylbenzamidinato adducts and parent Lewis base	71
Table 2.12	Principal bond angles and angles for $[Me_2Ga(PhNCPPhNPh).(4-Bu^t-pyridine)]$	75

	Page
Table 2.13 Summary of Proton decoupled ^{13}C N.M.R. data of alkylmetal-bis(amidinato) complexes	83
Table 2.14 Major aluminium-containing fragments from $[\text{MeAl}(\text{PhNCPhNPh})_2]$	85
Table 2.15 Major aluminium-containing fragments from $[\text{MeAl}(\text{PhNCMeNPh})_2]$	86
Table 2.16 Major gallium-containing fragments from $[\text{MeGa}(\text{PhNCPhNPh})_2]$	86
Table 2.17 Major gallium-containing fragments from $[\text{EtGa}(\text{PhNCMeNPh})_2]$	86
Table 2.18 Major indium-containing fragments from $[\text{EtIn}(\text{PhNCPhNPh})_2]$	87
Table 2.19 Major indium-containing fragments from $[\text{EtIn}(\text{PhNCMeNPh})_2]$	87
Table 2.20 Metal-Ligand Bond Lengths for the Complexes $[\text{RM}(\text{PhNCR}^{\prime}\text{NPh})_2]$	100
Table 2.21 Metal-Ligand Bond Angles for the Complexes $[\text{RM}(\text{PhNCR}^{\prime}\text{NPh})_2]$	101
Table 2.22 Important Ligand Bond Lengths and Angles for the Complexes $[\text{RM}(\text{PhNCR}^{\prime}\text{NPh})_2]$	102
Table 2.23 Dihedral angles between the planes defined in Figure 2.21	95
Table 2.24 Relevant bond lengths and angles for $[\text{MeIn}\{\text{MeNC}(\text{CH})_4\text{N}\}_2]$	97
Table 2.25 Summary of Proton decoupled ^{13}C N.M.R. data of metal-tris(amidinato) complexes	106
Table 2.26 Major aluminium-containing fragments from $[\text{Al}(\text{PhNCPhNPh})_3]$	108
Table 2.27 Major aluminium-containing fragments from $[\text{Al}(\text{PhNCMeNPh})_3]$	108

	Page
Table 2.28	Major gallium-containing fragments from $[\text{Ga}(\text{PhNCPPhNPh})_3]$ 109
Table 2.30	Major indium-containing fragments from $[\text{In}(\text{PhNCPPhNPh})_3]$ 109
Table 2.31	Major indium-containing fragments from $\{\text{In}(\text{PhNCMeNPh})_3\}$ 110
Table 2.32	Principal bond lengths and angles in $[\text{In}(\text{PhNCPPhNPh})_3]$ and $[\text{In}(\text{PhNNNPh})_3]$ 112
Figure 2.1	The amidine group and common amidinato co-ordination modes 37
Figure 2.2	^1H N.M.R. spectra of dimethylaluminium-N,N'-diphenylacetamidinato, dimethylaluminium-N,N'-diphenylbenzamidinato 45
Figure 2.3	^1H N.M.R. spectra of diethylgallium-N,N'-diphenylbenzamidinato, diethylindium-N,N'-diphenylbenzamidinato 46
Figure 2.4	Dimethylindium-N,N'-diphenylbenzamidinato fragmentation pattern 55
Figure 2.5	Diethylindium-N,N'-diphenylacetamidinato fragmentation pattern 56
Figure 2.6	Diethylindium-N,N'-diphenylformamidinato fragmentation pattern 57
Figure 2.7	Proposed co-ordinated amidinato ligand fragmentation scheme 58
Figure 2.8	The molecular structure of dimethylindium-N,N'-diphenylbenzamidinato 62
Figure 2.9	Another view of the molecular structure of dimethylindium-N,N'-diphenylbenzamidinato 64
Figure 2.10	Molecular structure of dimethylgallium-N,N'-dimethylacetamidinato 65
Figure 2.11	Molecular structure of bis(dimethylindium)-N,N',N'',N'''-tetramethyloxamidinato 66

	Page
Figure 2.12 Molecular structure of dimethylgallium-N,N'-diphenylbenzamidinato.4-Bu ^t -pyridine	74
Figure 2.13 Molecular structure of [Me ₂ Ga(PhNCPhNPh). (4-Bu ^t -pyridine)]	75
Figure 2.14 Proposed ligand exchange mechanism scheme for [Me ₂ In(PhNCPhNPh)]	78
Figure 2.15 The molecular structure of methylaluminium-N,N'-diphenylbenzamidinato	89
Figure 2.16 The molecular structure of methylgallium-N,N'-diphenylbenzamidinato	90
Figure 2.17 The molecular structure of ethylgallium-N,N'-diphenylacetamidinato	91
Figure 2.18 The molecular structure of ethylindium-N,N'-diphenylbenzamidinato	92
Figure 2.19 Molecular structures of [MeAl(PhNCPhNPh) ₂], and [EtGa(PhNCMeNPh) ₂]	93
Figure 2.20 Molecular structures of [MeGa(PhNCPhNPh) ₂], and [EtIn(PhNCPhNPh) ₂]	94
Figure 2.21 Schematic view of the co-ordination polyhedron around the metal in [RM(PhNCR"NPh) ₂]	95
Figure 2.22 The molecular structure of [MeIn{MeNC(CH) ₄ N} ₂]	97
Figure 2.23 The molecular structure of indium-tris(N,N'-diphenylbenzamidinato)	111
Figure 2.24 The molecular structures of [In(PhNCPhNPh) ₃] and [In(PhNNNPh) ₃]	112

CHAPTER 3

Table 3.1	Significant gallium-containing ions in the E.I. mass spectrum of $[\text{Me}_2\text{Ga}(\text{HNCBu}^t\text{NH})]$	120
Table 3.2	Bond angles in $[\text{Me}_2\text{Ga}\{\text{HNC}(\text{CF}_3)\text{NC}(\text{CF}_3)\text{NH}\}]$	125
Figure 3.1	Possible amidinato co-ordination modes in $[\{\text{Me}_2\text{Ga}(\text{HNCBu}^t\text{NH})\}_2]$	121
Figure 3.2	The molecular structure of $[\text{Me}_2\text{Ga}\{\text{HNC}(\text{CF}_3)\text{NC}(\text{CF}_3)\text{NH}\}]$	124
Figure 3.3	Another view of the molecular structure of $[\text{Me}_2\text{Ga}\{\text{HNC}(\text{CF}_3)\text{NC}(\text{CF}_3)\text{NH}\}]$	125
Figure 3.4	A further view of the molecular structure of $[\text{Me}_2\text{Ga}\{\text{HNC}(\text{CF}_3)\text{NC}(\text{CF}_3)\text{NH}\}]$	127
Figure 3.5	Infra-red spectrum of $[\text{Me}_2\text{Ga}\{\text{HNC}(\text{CF}_3)\text{NC}(\text{CF}_3)\text{NH}\}]$	131
Figure 3.6	Fragmentation Scheme for the E.I. Mass Spectrum of $[\text{Me}_2\text{Ga}\{\text{HNC}(\text{CF}_3)\text{NC}(\text{CF}_3)\text{NH}\}]$	133
Figure 3.7	Proposed mechanism of formation of $[\text{Me}_2\text{Ga}\{\text{HNC}(\text{CF}_3)\text{NC}(\text{CF}_3)\text{NH}\}]$	135

CHAPTER 4

Table 4.1	Summary of the ^1H N.M.R. data for H_2tmtaa , $[\text{Et}_2\text{In}(\text{Htmtaa})]$ and $[\text{EtIn}(\text{tmtaa})]$	145
Table 4.2	Summary of the ^{13}C N.M.R. data for H_2tmtaa , $[\text{Et}_2\text{In}(\text{Htmtaa})]$ and $[\text{EtIn}(\text{tmtaa})]$	149
Table 4.3	Summary of the E.I. Mass Spectra of H_2tmtaa , $[\text{Et}_2\text{In}(\text{Htmtaa})]$ and $[\text{EtIn}(\text{tmtaa})]$	151
Table 4.4	Summary of important structural parameters for the three $[\text{RM}(\text{tmtaa})]$ structures	158
Table 4.5	Comparison of the indium co-ordination environments in $[\text{EtIn}(\text{tmtaa})]$ and $[\text{MeIn}(\text{TPP})]$	161

	Page
Table 4.6	Bond angles around the indium atom in [ClIn(tmtaa)] 166
Table 4.7	Bond angles around the indium atom in [CpIn(tmtaa)] 171
Table 4.8	Comparison of the important M–N distances in [XM(tmtaa)] 172
Table 4.9	Summary of the E.I. Mass Spectra of Complexes of the type [XIn(tmtaa)] 176
Table 4.10	Summary of proton decoupled ¹³ C N.M.R. data of indium(III)-tmtaa compounds 178
Figure 4.1	Reported organoaluminium–macrocyclic complexes 138
Figure 4.2	Reported organogallium–macrocyclic complexes 139
Figure 4.3	Combined T.G.A. and D.T.A. plot obtained for [Et ₂ In(Htmtaa)] 142
Figure 4.4	Two–step insertion reactions of Et ₃ In with H ₂ tmtaa 143
Figure 4.5	¹ H N.M.R. spectra of H ₂ tmtaa, [Et ₂ In(Htmtaa)] and [EtIn(tmtaa)] 147
Figure 4.6	¹³ C N.M.R. spectra of H ₂ tmtaa, [Et ₂ In(Htmtaa)] and [EtIn(tmtaa)] 148
Figure 4.7	The molecular structure of [Me ₂ Ga(Htmtaa)] 146
Figure 4.8	The molecular structures, showing bond lengths of H ₂ tmtaa and [EtIn(tmtaa)] 153
Figure 4.9	The molecular structure of [EtIn(tmtaa)] 154
Figure 4.10	Side–view of the molecular structure of [EtIn(tmtaa)] 155
Figure 4.11	Side view of the free ligand 156
Figure 4.12	Diagrammatic key of the structural parameters introduced in Table 4.4 159
Figure 4.13	The co–ordination geometry of indium in [MeIn(TPP)] 160
Figure 4.14	The molecular structure of [ClIn(tmtaa)] 164
Figure 4.15	Side–view of the molecular structure of [ClIn(tmtaa)] 165
Figure 4.16	The molecular structure of [ClIn(tmtaa)] 166
Figure 4.17	Reactions of [ClIn(tmtaa)] 167
Figure 4.18	The molecular structure of [CpIn(tmtaa)] 169

	Page
Figure 4.19 Side-view of the molecular structure of [CpIn(tmtaa)]	170
Figure 4.20 The molecular structure of [CpIn(tmtaa)]	171
Figure 4.21 Important Bond Lengths and Angles in the Cyclopentadienyl Ring in [CpIn(tmtaa)]	174
 CHAPTER 5	
Figure 5.1 E.S.R. spectrum of a benzene solution of [MeAl(PhNCPhNPh)] with added TBN upon irradiation. E.S.R. simulation spectrum of TBN-CH ₃	181
Figure 5.2 Spin trap adducts of TBN from irradiation of [MeAl(PhNCPhNPh) ₂]	182
Figure 5.3 E.S.R. spectrum of a benzene solution of [EtGa(PhNCPhNPh) ₂] with added TBN upon irradiation. E.S.R. simulation spectrum of TBN-C ₂ H ₅	184
Figure 5.4 E.S.R. spectrum of a benzene solution of [MeIn(PhNCPhNPh) ₂] with added TBN. E.S.R. spectrum obtained after standing at room temperature overnight	186
 CHAPTER 6	
Table 6.1 Summary of infra-red band frequencies of some dialkyl-metal-amidinato complexes	206
Table 6.2 Summary of infra-red band frequencies of the dialkyl-metal-(N,N'-diphenylbenzamidinato).(4-Bu ^t -pyridine) complexes	208
Table 6.3 Summary of infra-red band frequencies of some monoalkyl-metal-bis(amidinato) complexes	209
Table 6.4 Summary of infra-red band frequencies of some metal-tris(amidinato) complexes	210

	Page	
Table 6.5	Summary of infra-red band frequencies of H_2tmtaa and the indium(III) $tmtaa$ complexes	218
 APPENDIX 1		
Table 1	Summary of T.G.A. Results for the Aluminium, Gallium and Indium Amidinato Derivatives	222
Figure 1	TEM image taken from the thermal decomposition residue of $[MeGa(PhNCPhNPh)_2]$	225
Figure 2	EDX measurements	226
Figure 3	Combined T.G.A. and D.T.A. plot of $[Me_2Ga\{HNC(CF_3)NC(CF_3)NH\}]$	228
 APPENDIX 2		
Table 2	Bond lengths for $[Me_2In(PhNCPhNPh)]$	239
Table 3	Bond angles for $[Me_2In(PhNCPhNPh)]$	240
Table 4	Bond lengths for $[Me_2Ga(PhNCPhNPh).(4-Bu^t\text{-pyridine})]$	242
Table 5	Bond angles for $[Me_2Ga(PhNCPhNPh).(4-Bu^t\text{-pyridine})]$	243
Table 6	Bond lengths and angles for $[MeAl(PhNCPhNPh)_2]$	245
Table 7	Bond lengths for $[MeGa(PhNCPhNPh)_2]$	247
Table 8	Bond angles for $[MeGa(PhNCPhNPh)_2]$	248
Table 9	Bond lengths for $[EtGa(PhNCMeNPh)_2]$	250
Table 10	Bond angles for $[EtGa(PhNCMeNPh)_2]$	251
Table 11	Bond lengths for $[EtIn(PhNCPhNPh)_2]$	253
Table 12	Bond angles for $[EtIn(PhNCPhNPh)_2]$	254
Table 13	Bond lengths for $[In(PhNCPhNPh)_3]$	256
Table 14	Bond angles for $[In(PhNCPhNPh)_3]$	257

	Page	
Table 15	Bond lengths and angles for [Me ₂ Ga{HNC(CF ₃)NC(CF ₃)NH}]	260
Table 16	Bond lengths and angles for [EtIn(tmtaa)]	262
Table 17	Bond lengths and angles for [ClIn(tmtaa)]	265
Table 18	Bond lengths for [CpIn(tmtaa)]	267
Table 19	Bond angles for [CpIn(tmtaa)]	268
Table 20	Bond lengths and angles for [PhN(H)CMeNPh]	270
Figure 4	Space filling representation of [EtIn(tmtaa)]	263
Figure 5	The molecular structure of N,N'-diphenylacetamide	271

APPENDIX 3

Table 21	Summary of E.I. mass spectroscopic data of dimethylaluminium-amidinato complexes	274
Table 22	Summary of E.I. (and C.I. where specified) mass spectroscopic data of dialkylgallium-amidinato complexes	275
Table 23	Summary of E.I. (and C.I. where specified) mass spectroscopic data of dialkylindium-amidinato complexes	276
Table 24	Summary of E.I. mass spectroscopic data of monoalkyl- metal-bis(amidinato) complexes	277
Table 25	Summary of E.I. mass spectroscopic data of metal-tris(amidinato) complexes	279
Table 26	E.I. (and C.I. where specified) mass spectroscopic data of H ₂ tmtaa and indium(III) tmtaa complexes	280

ACKNOWLEDGEMENTS

The author would like to thank the following people for their help during the course of this work:

Professor M G H Wallbridge, for his invaluable advice, guidance and support throughout the past three years.

Dr J Barker, of the Associated Octel Company, for his generous assistance, enthusiasm, and for providing drinks and lunches.

Dr N W Alcock and **Dr W Errington**, for their help and tuition in the art of X-ray crystallography.

Dr J Hastings, for his assistance in obtaining some of the N.M.R. spectra reported in this work.

Mr I K Katyal, for his help by running most of the mass spectra presented in this thesis.

All of the technicians in the Chemistry Department at the University of Warwick and the Analytical Department at Octel for their assistance.

My friends and colleagues at Warwick University, especially Zac, AJ, Andy, Chris, Martin, Jon, Jase, Dave B, H, and the F.O. Cantona Football Team.

A special thank you to you, Helen, for your kindness, and Mum and Dad for your continuous help and support.

Finally the Associated Octel Company and the EPSRC for providing the funding for this work.

DECLARATION

All of the work described in this thesis is original and was, unless otherwise stated, carried out by the author.

Paul R. Phillips

January, 1996

Some of the work presented in Chapters 2, 3 and 4 of this thesis has been published in the following references:

P.R. Phillips, A. McCamley, N.W. Alcock and M.G.H Wallbridge, *Acta Crystallogr, Sect. C.*, 1994, **50**, 1072.

N.W. Alcock, J. Barker, N.C. Blacker, W. Errington, P.R. Phillips and M.G.H. Wallbridge, *J. Chem. Soc., Dalton Trans.*, 1996, 431.

The work presented in Chapters 2 and 3 has been patented under the following application number: PCT/GB94/01696. Title: Organometallic Complexes of Aluminium, Gallium and Indium.

SUMMARY

This thesis describes a study of several aspects of the organometallic chemistry of aluminium, gallium and indium.

A study has been carried out on the products obtained from the reactions of trimethyl- and triethyl-metal derivatives of aluminium, gallium and indium with amidines. The compounds $[R_2M(L)]$ [$L = \text{amidinato } (R'NCR''NR')$; $R' = \text{aryl}$; $R'' = \text{H, Me, Ph}$], $[RM(\text{PhNCR}''\text{NPh})_2]$, and $[M(\text{PhNCR}''\text{NPh})_3]$ ($M = \text{Al, Ga, In}$; $R = \text{Me, Et}$; $R'' = \text{Me, Ph}$) have been isolated from the reactions of the appropriate trialkyl-metal derivative with 1, 2 and 3 moles of amidine $[R'N(H)CR''NR']$ respectively. The compounds have been fully characterised, and mass spectroscopic data indicate that the compounds exist as monomers in the gas phase. An X-ray crystallographic study was carried out on $[\text{Me}_2\text{In}(\text{PhNCPhNPh})]$. It was found to be monomeric and the ligand is attached in a bidentate chelating manner. X-ray crystallographic studies on $[\text{RM}(\text{PhNCPhNPh})_2]$ ($M = \text{Al, Ga, R = Me; M = In, R = Et}$) and $[\text{EtGa}(\text{PhNCMeNPh})_2]$ reveal monomeric structures and the presence of chelating amidinato ligands with highly distorted trigonal bipyramidal co-ordination at the metal centre. Cleavage of the metal-alkyl bond in some of these dialkyl- and monoalkyl-metal derivatives on photolysis in the presence of a spin trapping agent was demonstrated using E.S.R. spectroscopy. An X-ray crystallographic study on $[\text{In}(\text{PhNCPhNPh})_3]$ shows a monomeric structure in which the metal centre is six co-ordinate and the amidinato ligands are bound in a bidentate chelating manner. Some data have been obtained on the thermal decomposition products of the metal-amidinato complexes in view of their potential use as "III-V" semiconductor precursors.

The reactions of the simple N,N' -unsubstituted amidine ligands, butyramidine and trifluoroacetamidine with Me_3Ga have been investigated. The former amidine, $[\text{NH}_2\text{CBu}^i\text{NH}]$, gave the dimethylgallium-butuyramidinato compound and mass spectroscopic data indicate that this compound is oligomeric and exists as both a dimer and monomer in the gas phase. The latter amidine, $[\text{NH}_2\text{CCF}_3\text{NH}]$, underwent a condensation reaction in the presence of Me_3Ga to form the complex $[\text{Me}_2\text{Ga}\{\text{HNC}(\text{CF}_3)\text{NC}(\text{CF}_3)\text{NH}\}]$. The molecular structure of this complex was determined by X-ray crystallography. It was found to consist of a planar six-membered metalocycle containing the N,N' -chelating trifluoroimidoyltrifluoroacetamidinato ligand and a distorted tetrahedral co-ordination environment around the metal.

Several new indium(III) tetraaza-macrocyclic complexes have been prepared using the unsaturated ligand 5,7,12,14-tetramethyldibenzo[b,i][1,4,8,11]tetraazacyclotetradecine $[\text{H}_2\text{tmtaa}]$. The molecule structures of the compounds $[\text{XIn}(\text{tmtaa})]$ ($\text{X} = \text{Et, Cp, Cl}$) have been determined by X-ray crystallography. In each case, the structure consists of an InX fragment bonded to the four nitrogen atoms of the macrocyclic ligand. These structures provide unusual examples of indium in a five co-ordinate square based pyramidal co-ordination geometry in which the indium is centrally bound above the N_4 plane of the macrocycle. The effects of change of both metal size and axial ligand on the molecular geometry of these types of complex have been discussed in detail.

ABBREVIATIONS

R, R' etc.	alkyl group
Me	methyl
Et	ethyl
Pr ⁿ	<i>n</i> -propyl
Pr ⁱ	<i>iso</i> -propyl
Bu ⁿ	<i>n</i> -butyl
Bu ⁱ	<i>iso</i> -butyl
Bu ^t	<i>tert</i> -butyl
Ar	aryl
Ph	phenyl
Cp	cyclopentadienyl
Cp*	pentamethylcyclopentadienyl
M, M'	metal
L, L'	ligand
X	halide
py	pyridine
TMEDA	N,N,N',N'-tetramethylethylenediamine
H ₂ tmtaa	5,7,12,14-tetramethyldibenzo[b,i] [1,4,8,11]-tetraazacyclotetradecine
acac	acetylacetonone
hfac	hexafluoroacetylacetonone
cyclam or [14]aneN ₄	1,5,8,12-tetraazacyclotetradecane
Me ₄ [14]aneN ₄	1,5,8,12-N-tetramethylcyclam
diphos	bis-1,2-diphenylphosphinoethane
triphos	bis(2-diphenylphosphinoethyl)phenylphosphine
tetraphos	bis-1,2-[(2-diphenylphosphinoethyl)phenylphosphino]ethane
TMS	Me ₃ Si
mesityl	2,4,6-CH ₃ -C ₆ H ₂

DMSO	dimethylsulphoxide
I.R.	Infra-Red
vs	very strong
s	strong
m	medium
w	weak
vw	very weak
br	broad
sh	shoulder
F.T.	Fourier Transform
N.M.R.	Nuclear Magnetic Resonance
MHz	megahertz
δ	chemical shift
p.p.m.	parts per million
rel. intens.	relative intensity
s	singlet
d	doublet
t	triplet
q	quartet
m	multiplet
br	broad
E.S.R.	Electron Spin Resonance
E.I.	Electron Impact
C.I.	Chemical Ionisation
F.A.B.	Fast Atom Bombardment
M.W.	Molecular Weight
T.G.A.	Thermogravimetric Analysis
D.T.A.	Differential Thermal Analysis
\AA	Angstrom ($1\text{\AA} = 1 \times 10^{-10}\text{m}$)
λ	wavelength in nm
nm	nanometres ($1\text{nm} = 1 \times 10^{-9}\text{m}$)

CHAPTER 1

Introduction

CHAPTER 1

Introduction

A. The Elements Aluminium, Gallium and Indium

Aluminium, gallium and indium belong to group 13 of the Periodic Table, situated between boron and thallium. Some of the atomic properties of the elements are presented below.¹

Table 1.1 Some atomic properties of aluminium, gallium and indium.

Property	Aluminium	Gallium	Indium
Atomic number	13	31	49
Atomic weight	26.98	69.72	114.82
Natural isotopes (% abundance)	²⁷ Al (100%)	⁶⁹ Ga (60.5%) ⁷¹ Ga (39.5%)	¹¹³ In (4.3%) ¹¹⁵ In (95.7%)
Electronic configuration	[Ne]3s ² 3p ¹	[Ar]3d ¹⁰ 4s ² 4p ¹	[Kr]4d ¹⁰ 5s ² 5p ¹

Much of the research into the chemistry of aluminium has been driven by the numerous industrial applications of its compounds, and since this thesis is concerned primarily with organometallic derivatives of these group 13 elements, it is relevant to note the extensive use of organoaluminium derivatives in Ziegler–Natta polymerisation.² Another area of research has used aluminium alkyls of the type R_nAlE_{3-n} in organic synthesis for the selective formation of C–E bonds (E = C, H, N, O, X).³ These developments have ensured a high level of research activity into organoaluminium compounds. In contrast, the elements of gallium and indium had until recent years received less attention. The previously high costs to obtain these two heavier elements and the lack of extensive industrial applications of their compounds detracted from interest in their chemistry. More recently however, the study of compounds of all these

elements, particularly of gallium and indium, has grown substantially. This greater research activity, most evident since the early 1980s, can be mainly ascribed to the increased application of these metals in the electronics industry. For example, this activity concerns the preparation of semi-conductor materials and a significant amount of the research into the organometallic chemistry of these elements involves the search for new volatile precursor materials for the epitaxial growth of thin films of the "III-V" semi-conductor materials, such as aluminium nitride, gallium arsenide and indium phosphide by, for example, metal organic chemical vapour deposition (MOCVD).^{4,5} A second area of interest is the research into the aqueous solution chemistry of Ga(III) and In(III) ions, which is largely concerned with applications in medical imaging techniques.

These developments have also led to improvements in methods for obtaining and refining these elements and increased production levels and consequently a general expansion of interest in their properties themselves.

However, despite these recent advances, many areas of the chemistry of these elements remain unexplored. This thesis describes some aspects of the co-ordination chemistry of aluminium, gallium and indium, and deals especially with two classes of nitrogen-based ligands and thus can be divided into two sections. Firstly, Chapters 2 and 3 describe the reactions of trialkyl-metal derivatives of aluminium, gallium and indium with amidine ligands and a study of the co-ordination compounds formed following the elimination of alkane. Chapter 5 describes some initial studies on the photochemical behaviour of some of the compounds formed. Preliminary thermal decomposition experiments on these compounds have also been carried out to investigate their potential as precursors to metal nitride materials and these results are presented in Appendix 1. Secondly, the work described in Chapter 4 concerns the preparation and structural characterisation of some tetraazamacrocyclic complexes containing indium(III) moieties.

The following introduction provides a selective review of the organometallic chemistry of the group 13 elements, with emphasis on the metallic elements and the topics relevant to the work presented in the remainder of this thesis. It starts with a concise guide to the general reaction types and trends within the group, followed by a

more in depth review of the organometallic chemistry of aluminium, gallium and indium, concentrating on compounds with ligands containing elements of groups 15 and 16. Comprehensive reviews by Eisch^{6b} and Tuck^{6c} detail these areas of work to 1982 and an extension to these texts has recently appeared covering the intervening years to 1994.⁷

B. Oxidation States of Organometallic Compounds of Group 13

The ground state valence shell electron configuration of the group 13 elements is $ns^2 np^1$ ($n = 2 - 6$ for boron – thallium) and therefore the chemistry of these elements is dominated by the (III) oxidation state, although the (I) oxidation state becomes increasingly stable on descending the group, particularly for thallium. Low valent organometallic compounds of aluminium, gallium and indium are known, such as MCp^* ($M = Al,^8 Ga^9, In^{10}$) [(I) oxidation state] and a growing number of interesting low valent π -bonded arene complexes of gallium, indium and thallium (e.g. $[\{(\eta^6-C_6H_6)_2Ga\}^+(GaCl_4)^-]_2 \cdot 3C_6H_6$ ¹¹). The reader is referred to a review by Schmidbaur for further information on this latter class of compounds.¹²

The metal centre in compounds of the general formula MX_3 has only six electrons associated with it, leaving it two short of the more stable eight electron configuration and thus is conveniently considered to be "electron deficient"; in other words this describes the tendency of these compounds to accept electrons to build up an "octet" configuration around the metal. The Lewis acid properties of group 13 trialkyls and organometallic halides are the driving force behind many of the features of the chemistry of these compounds and the ways by which these attempt to increase the number of electrons associated with the central atom are discussed below.

1. Self-Association of MX_3 Units

A common method by which "electron deficient" metal centres build-up further electron density is by oligomerisation by the formation of bridging donor groups. Aluminium trialkyls, especially the lower alkyls where no steric effects are apparent, have a pronounced tendency for the formation of dimeric units, their structures containing

bridging alkyl groups. The description of the bonding in these compounds involves the concept of three-centre, two-electron bonds. This ability of association is dependent on the ability of the alkyl group to participate in bridge bonding and their steric size. Trimethylaluminium is strongly associated as a dimer, even in the vapour phase. Higher straight chain aluminium trialkyls, up to $(\text{Bu}^n)_3\text{Al}$, are predominately dimeric in benzene solution, but branch-chain trialkyls, such as $(\text{Bu}^i)_3\text{Al}$, are monomeric.^{13,14,15,16} In the case of aryl-, acetylenyl- and vinyl-aluminium compounds, the π -electrons of these bridging groups may also be considered to be involved in the bridge bonding scheme and therefore contribute further electron density to the metal centre. The vinyl groups in the dimeric solid state structure of *trans*-3,3-dimethylbut-1-enyl(di-*iso*-butyl)aluminium bridge the two aluminium centres.¹⁷ In a similar fashion, the dimeric solid state structure of diphenyl(phenylethynyl)aluminium consists of bridging phenylethynyl groups.¹⁸

In contrast, no such association exists in solution at room temperature and in both the liquid and vapour states for even the trimethyl metal derivatives of boron,^{6b} gallium,^{6c,15,19} and thallium,^{6d} which are monomeric. This may be seen as a combination of steric and electronic effects associated with the formation of the four centre $(\text{MC})_2$ bridge system.

The overall structural unit in the crystal structure of trimethylindium is based on a tetramer and consists of trigonal planar Me_3In units in which each indium centre has weak interactions with two adjacent carbon atoms, and the metal has an effective co-ordination number of five.²⁰

Organometallic halides are associated, mostly to dimer, with bridging halogen atoms, such as in $[\{\text{MeAlCl}_2\}_2]$,²¹ although alternative arrangements are known. For example, dimethylindium chloride consists of planar $[\text{Me}_2\text{InCl}]$ molecules, which are stacked in such a way that two chlorine atoms from neighbouring molecules give an apparent metal co-ordination number of five.²² Ionic structures are common for the heavier metal compounds, such as that for MeInI_2 , which has the solid state structure $[\text{Me}_2\text{In}]^+[\text{InI}_4]^-$.^{23,24} The structures of dialkylmetal fluorides often differ from those of

other halides, displaying higher oligomeric structures. For example, Et_2AlF is tetrameric in benzene solution²⁵ and R_2GaF ($\text{R} = \text{Me}, \text{Et}$) are trimeric.²⁶

2. Ligand Exchange

Ligand exchange reactions are frequently encountered for these compounds, because of the availability of the empty p orbital on the central atom of a monomeric MX_3 unit. This orbital provides a route for the formation of bridged intermediates leading to alkyl exchange reactions. Such interactions can occur between a triorgano and another trivalent species, such as the trihalides (Equation 1), or between two triorgano species (Equation 2).



For example, the methyl groups in Me_3Tl , which was noted above to be monomeric in benzene solution, undergo rapid intermolecular exchange, as shown by N.M.R. studies, and a dimeric transition state similar to the structure of $[(\text{Me}_3\text{Al})_2]$ has been assumed.²⁷ Further evidence to support this type of intermediate species with boron trialkyls can be inferred from the following experimental observations. Pure boron trialkyls undergo slow group exchange. However, small quantities of boron hydrides catalyse these reactions, since the sterically undemanding B-H group can easily participate in bridge formation.^{28,29,30} Conversely, exchange reactions are impeded by bulky ligands for example by *tert*-butyl groups in Bu^t_3B .³¹

Alkyl- and aryl-aluminium halides are obtained from mixing R_3Al and AlX_3 , and it has been proposed by Eisch^{6b} that the thermodynamic driving force for this type of redistribution is the formation of the unsymmetrical products which maximise the number of strong bridging units. For the successful preparation of $\text{R}_n\text{AlX}_{3-n}$ ($n = 1, 2$) compounds, the stoichiometry and purity of the reagents must be carefully controlled.



By a series of N.M.R. experiments, Mole demonstrated that for species of the type Me_2AlE the bridge formed by group 15, 16, or 17 donor atoms is always preferred to the possible formation of the methyl bridge.^{32,33}

Ligand exchange can be used to prepare new unsymmetrical triorgano compounds, although the isolation of pure products usually necessitates the bridging priority effect to operate. Mixing Me_3Al and Ph_3Al in a 2:1 ratio allows isolation of pure dimethyl(phenyl)aluminium,^{32,34,35} which possesses phenyl bridges, despite the larger steric size of these groups, and mixing Ph_3Al and AlH_3 in a 2:1 ratio forms diphenylaluminium hydride, which possesses hydride bridges.³⁶ Alternatively, the desired reaction can be driven to completion if one product can be removed. For example, trimethylaluminium can be obtained by distillation from the thermal disproportionation of methylaluminium sesquiodide.³⁷

Ligand redistribution reactions occur between two derivatives containing different metals and this type of reaction is a useful route to the preparation of organometallic derivatives particularly of gallium and indium, as discussed later.

3. Neutral Adducts

There is a strong tendency for Lewis bases to form adducts with these compounds and a large number of adducts have been prepared for all members of group 13, particularly with neutral donors from groups 15 and 16. Reference 6 contains comprehensive lists of this type of complex. The stoichiometry of the adduct is usually 1:1 based on a tetrahedral metal centre, but for the larger elements, particularly indium and thallium, 2:1 and 3:1 adducts become more common, especially when the acceptor strength of the molecule is enhanced, such as for the organometallic halides. These five and six co-ordinate complexes generally show trigonal bipyramidal and octahedral geometries respectively.

The stability of these complexes with respect to dissociation, as shown below, can vary considerably and depends not only on the acceptor and donor strengths of the

Lewis acid and base respectively, but also on factors such as temperature, pressure and stoichiometry of reactants.



The relative acceptor strengths of the trimethyl-group 13 derivatives with the elements of group 15 (N, P) were studied by Coates and Whitcombe, mainly using gas phase heats of dissociation, and this work suggests the series in order of Lewis acidity: $\text{Me}_3\text{B} < \text{Me}_3\text{Al} > \text{Me}_3\text{Ga} > \text{Me}_3\text{In} > \text{Me}_3\text{Tl}$ (with $\text{Me}_3\text{Ga} > \text{Me}_3\text{B}$).³⁸ Similarly, the Lewis acidity of the triphenylmetal derivatives with pyridine is given by the series: $\text{Al} > \text{Ga} > \text{B} > \text{In}$.³⁹ A number of other investigations have been carried out so as to establish orders of both the Lewis acidity of R_3M and basicity of donor species from groups 15 and 16, using a number of different methods, which will be outlined below. These results generally confirm these sequences, in which the position of R_3B is noted to vary. Because of the smaller size of boron, the formation of adducts with this element is more sensitive to steric effects of both the ligands in R_3B and the incoming Lewis base, thus explaining the variable position of its relative Lewis acid strength. Formation of adduct complexes with dimeric organoaluminium complexes, such as trimethylaluminium, will firstly require the breaking of these structures, which is not required to occur for the remaining trimethyl-group 13 derivatives. Despite this, trimethylaluminium is usually the strongest Lewis acid in this series, except with weak Lewis bases, where the sequence can vary, with the monomeric trimethylgallium being a stronger acceptor.⁴⁰

Measurement of Pt-H N.M.R. coupling constants of Lewis acid-base adducts with cyano(hydrido)bis(triethylphosphine)platinum, $[\text{H}(\text{Et}_3\text{P})_2\text{PtCN.L}]$ ($\text{L} = \text{Lewis acid}$), gave a ranking order of $\text{Ar}_3\text{B} > \text{R}_3\text{B} > \text{Ar}_3\text{Al} > \text{R}_3\text{Al}$, illustrating how variation of the nature of the R groups influences the Lewis acidity. The greater acceptor strength of the triaryl over the trialkyl derivatives may be explained by the electron attracting properties of the aryl groups, thus stabilising the adduct.⁴¹

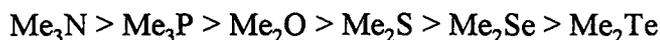
As a general statement, the Lewis acidity of BY_3 molecules increases in the order alkyl < aryl < F < H < Cl < Br < I.⁴² The change in acceptor strength of the trihalides, which is opposite to that which would be expected from consideration of the electronegativities of the halides, is believed to reflect, at least in part, the increasing π -bonding that is known to occur between the boron atom and the halides in the order $BI_3 < BBr_3 < BCl_3 < BF_3$. This increased energetic stability of the trigonal planar structure must be disrupted in order to form an adduct, such as a 1:1 tetrahedral complex, and hence the stronger this π -bonding, the formation of a complex is less favourable.

Successive substitution of the organo groups by halides would reasonably be predicted to lead to increased Lewis acidity. A study of the complexation of $[Et_{3-n}AlCl_n]$ ($n = 0, 1, 2$) with alkali metal chlorides gave the expected acceptor strength sequence, $Et_3Al < Et_2AlCl < EtAlCl_2$.⁴³ It has been proposed for the diethylaluminium halides that Lewis acidity increases in the order $F < Cl < Br < I$,⁴⁴ which is the same as the order of acceptor strength of the aluminium trihalides of $Cl < Br < I$ (AlF_3 is largely ionic) and is consistent with the decreasing strength of the bridging groups in the aluminium trihalides of $Al_2I_6 < Al_2Br_6 < Al_2Cl_6$.⁴⁵

For the gallium trihalides, thermochemical studies of the complexes $GaX_3 \cdot OEt_2$, $GaX_3 \cdot SET_2$ and $GaX_3 \cdot SMe_2$ ($X = Cl, Br, I$) showed that the relative Lewis acidity increased in the series $GaI_3 < GaBr_3 < GaCl_3$.⁴⁶ A similar ranking order was found for the complexes formed between the gallium trihalides and the Lewis bases, triethylamine and pyridine.⁴⁷ For the indium trihalides, similar studies on the complexes formed with ethylacetate showed that $InCl_3$ was a stronger Lewis acid than $InBr_3$.⁴⁸ It would be useful to establish corresponding series for the organometallic halides of gallium and indium.

The stability of the adducts will obviously vary according to the donor strength of the Lewis base. Extensive studies have been performed with trimethylaluminium and a range of Lewis bases. Determinations of the enthalpy of dissociation of $[Me_3Al.L]$ adducts in the vapour phase (thereby preventing the need for corrections of enthalpy of

dimerisation), showed that the relative donor strengths of the Lewis bases decreased in the order shown below:^{49,50}



The relative stabilities of adducts have been studied by allowing two bases to compete for trimethylaluminium. For example, mixing trimethylaluminium etherate with trimethylphosphine oxide yielded the phosphine oxide adduct.⁵¹ Similarly, trimethylamine displaced trimethylphosphine from $\text{Me}_3\text{Al.PMe}_3$.⁴⁹

N.M.R. studies of adducts of trimethylgallium carried out by Coates^{52,53} suggested the sequence (a) shown below. The order of the dimethyl chalcogenides, Me_2Se , Me_2S and Me_2Te appears to be unexpected. Other later studies indicated that the order is as shown in scheme (b).⁵⁴ Similar work on adducts of triethylgallium ranked the relative base strengths of the ligands as shown in scheme (c).⁵⁵

- (a) $\text{Me}_3\text{N} > \text{Me}_3\text{P} > \text{Me}_3\text{As} > \text{Me}_2\text{O} > \text{Me}_2\text{Se} > \text{Me}_2\text{S} \approx \text{Me}_2\text{Te}$
- (b) $\text{Me}_2\text{S} \geq \text{Me}_2\text{Te} > \text{Me}_2\text{Se}$
- (c) $\text{MeNH}_2 > \text{NH}_3 > \text{NHMe}_2 > \text{NMe}_3 > \text{PMe}_3 > \text{OMe}_2 > \text{SMe}_2$

Data on the corresponding indium derivatives are sparse.³⁸ Furthermore, little work has been performed using other alkyl or aryl or halide groups for compounds of gallium and indium.

4. Alkane Elimination Reactions

An important aspect of the chemistry of organometallic derivatives, including those from group 13, is their reaction with compounds containing protic hydrogen atoms to eliminate hydrocarbon. This type of reaction is usually clean and essentially quantitative and therefore is a convenient route to further organometallic derivatives. It

is generally thought that these reactions proceed with the initial formation of an unstable adduct which then undergoes the elimination reaction.

The series of reactions between the trimethyl-group 13 compounds of aluminium, gallium and indium and Ph_2EH ($\text{E} = \text{N}, \text{P}, \text{As}$) have been studied, and dimeric products of the formula, $[(\text{Me}_2\text{MEPh}_2)_2]$ ($\text{M} = \text{Al}, \text{Ga}, \text{In}$) were obtained from the initial adduct between temperatures of $0 - 170^\circ\text{C}$.⁵⁶ For example, the 1:1 reaction of trimethylaluminium and diphenylamine at room temperature leads to the adduct $[\text{Me}_3\text{Al.NHPh}_2]$ which on further heating to around 80°C eliminates methane to form the dimer $[(\text{Me}_2\text{AlNPh}_2)_2]$. The higher temperatures required to eliminate alkane from the corresponding phosphine and arsine adducts of trimethylaluminium indicate the order of reactivity toward alkane elimination, $\text{Ph}_2\text{NH} > \text{Ph}_2\text{PH} > \text{Ph}_2\text{AsH}$, while the reverse behaviour is indicated for trimethylgallium and trimethylindium.

The reaction of R_3M with water has been relatively well studied for all the group 13 derivatives and these reactions illustrate a number of important points. Trimethylborane shows no reaction with water at room temperature, but is slowly hydrolysed at 180°C with the loss of one methyl group over 7 hours to give dimethylborinic acid, $[\text{Me}_2\text{BOH}]$.⁵⁷ Of further note is the resistance of trialkylboranes (and triarylboranes) to reaction with inorganic acids. For example, the reaction of $(\text{Bu}^n)_3\text{B}$ with HCl at 110°C liberates only one mole of alkane to form $(\text{Bu}^n)_2\text{BCl}$.⁵⁸ They are much more reactive towards carboxylic acids and, depending on the conditions, sequential cleavage of one, two and three B-R groups can be achieved.^{59,60,61}

Organoaluminium compounds are highly reactive towards protic reagents and all three Al-R bonds are readily cleaved. Organogallium and organoindium compounds are slightly less reactive, although both can still react violently with water. The controlled hydrolysis of a diethyl ether solution of trimethylgallium with a slight excess of water produces dimethylgallium hydroxide,⁶² which in the solid state exists as a tetramer, based on a puckered $(\text{GaO})_4$ ring.⁶³ Hydrolysis of triethylgallium similarly yields $[\text{Et}_2\text{GaOH}]_n$.⁶⁴ Triethylindium evolves one mole of ethane in cold water, but on heating to 90°C , three

moles of ethane are evolved. Heating at 70°C in ethanol results in the loss of one mole only of ethane.⁶⁵

Hydrolysis of trimethyl- and triethyl-thallium with water also results in the elimination of only one alkyl group.^{66,67} The majority of dialkylthallium compounds are inert to hydrolysis and are usually salts containing the R_2Tl^+ cation, with exceptions such as the molecular $R_2Tl(OR')$ dimers.⁴⁰ $CH_3CO_2TlEt_2$ and $CH_3CO_2TlPh_2$ are known to be stable to excess acetic acid.⁶⁸

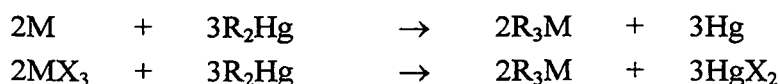
C. Organometallic Compounds of Aluminium, Gallium and Indium.

The discussion of the organometallic chemistry of the group 13 elements above set out the general reactions of these compounds. The following section will describe in more detail areas of the organometallic chemistry of aluminium, gallium and indium which are more relevant to the studies presented in the remainder of this thesis. In particular it will mainly describe reactions of the trialkyl derivatives of these metals with ligands containing acidic hydrogen. Obviously, this discussion can only highlight certain aspects of this chemistry, in view of the extensive chemistry reported, and therefore references 6 and 7 are cited for more comprehensive reviews.

1. Preparation of Simple Trialkyl and Triaryl Compounds.

This section is intended to give a few examples of the more convenient and commonly used procedures for the preparation of trialkyl- and triaryl-metal compounds in the laboratory.

(a) Metal Exchange with Organomercury Compounds.



This route is convenient for the preparation of small quantities of R_3M compounds, especially for $R = \text{alkyl}$, and the preparation can be carried out in the absence of solvent thus making for ease of separation of the product. Examples include the synthesis of Me_3Al , Ph_3Al ,⁶⁹ Me_3Ga ,⁷⁰ $(\text{vinyl})_3Ga$,⁷¹ Ph_3Ga ,⁷² Me_3In ,⁷³ and Ph_3In .⁷⁴ The

main disadvantages involved are (1) the need to prepare and handle highly toxic organomercury reagents and (2) the relatively high temperatures and slow reaction times required to complete the reaction, (e.g. for Me_3Al , 80–100°C, several hours ; for Me_3In , 150°C, several days). Therefore a serious limitation of this route is that it is useful only for the preparation of thermally stable derivatives. The use of an activated form of the group 13 metal is desirable. For example, for the preparation of Me_3In , highly activated indium metal, which can be prepared by the treatment of InCl_3 with potassium, reacts completely with Me_2Hg at 100°C over 3 hours.⁷⁵ Trimesitylaluminium has been prepared by the reaction of aluminium (activated by stirring with HgCl_2) and dimesitylmercury in xylene (yield 61%).⁷⁶

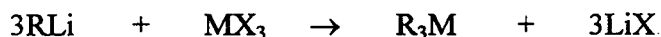
(b) Reaction of Grignard Reagents



The reaction of ethereal Grignard reagents with the trihalides of Al, Ga and In can be used for the preparation of a wide range of alkyl and aryl compounds. It serves as a simple preparation of triphenylaluminium etherate in yields of greater than 50%.⁷⁷ However, as a general procedure for the preparation of pure triorganometal derivatives, it suffers from the disadvantageous presence of co-ordinated solvent. In some cases, (e.g. Ph_3Al , Pr^n_3Ga ^{78,79}) removal of solvent can be achieved by distillation under vacuum at low enough temperatures to prevent thermal decomposition. Pure trimesitylgallium and trimesitylindium have been obtained from the reaction of the mesityl Grignard reagent, MesMgBr , and MCl_3 in Et_2O ($\text{M} = \text{Ga}, \text{In}$), reported in yields of greater than 70%.^{80,81}

An interesting variant of this type of reaction involves the use of In/Mg alloys or mixtures, with RBr in Et_2O ($\text{R} = \text{Me}, \text{Et}, \text{Pr}^n, \text{Pr}^i, \text{Bu}^n, \text{Bu}^i, \text{Bu}^s$),⁸² producing high yields of R_3M . Similarly, Me_3Ga has been prepared from a Ga/Mg alloy and MeI in high yield.⁸³ The reactions of primary alkyl halides with magnesium in hydrocarbon solvents or in the absence of solvent have been reported to alkylate AlCl_3 to produce high yields of a range of trialkylaluminium derivatives (alkyl = C_2H_5 up to C_9H_{19}).⁸⁴

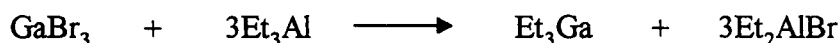
(c) Reaction of Lithium Alkyl Reagents.



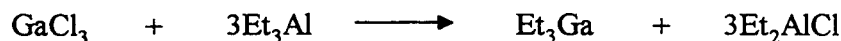
Reaction of the trihalides with organolithium reagents provides a simple and convenient route to trialkyl compounds. If the lithium reagent is to be used as an ethereal solution (e.g. LiMe) then this method also suffers from the presence of co-ordinated solvent, which may be difficult to remove. However, if, as is often the case, the compound is to be reacted with a further Lewis base, the ether is usually displaced easily and hence does not present a problem. Trimethylindium is commonly prepared by this route.⁸⁵ Reaction between AlCl₃ and ethyl-, *n*-butyl-,⁸⁶ or *tert*-butyl-lithium⁸⁷ in heptane, produces the corresponding trialkylaluminium.

(d) Ligand Redistribution Reactions

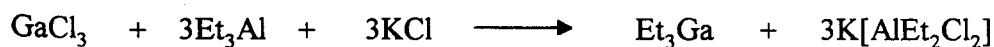
This class of reaction has already been dealt with above in relation to R₂Hg. A further important use of this type of preparation is the reaction between the trihalides of gallium and indium with trialkylaluminium. Triethylgallium can be conveniently prepared in high yield (reportedly over 80%) using triethylaluminium according to the equation below.⁸⁸



The analogous reaction between GaCl₃ and Et₃Al was claimed to give a lower yield, because of the formation of the complex [Ga(Cl₂AlEt₂)₃].



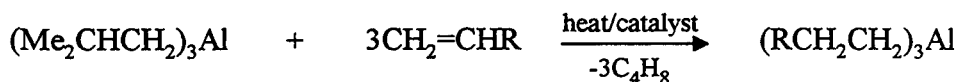
Three equivalents of KCl were added after the initial reaction to complex the aluminium as K[AlEt₂Cl₂], giving Et₃Ga in yields of 80–90%.



Traces of Et_3Al in the product may be removed by distillation over NaF , which complexes with Et_3Al , but not with Et_3Ga . Bu^i_3Ga and Me_3In can be similarly prepared, but Bu^i_3In requires the addition of KF . Dialkyls of zinc have been used in a similar manner. Thus Et_2Zn , prepared from Et_3Al and ZnCl_2 , and GaBr_3 in pentane gave Et_3Ga in 66% yield. Like preparation (a) above, these reactions have the advantage of not requiring Et_2O or other oxygenated solvents.

(e) Displacement reactions of trialkylaluminium.

The so-called displacement reaction has most applications in the preparation of a wide variety of trialkylaluminium derivatives, both in the laboratory and in larger scale production. A useful starting reagent is tri-*iso*-butylaluminium which can react with a less volatile alkene either thermally ($>100^\circ\text{C}$) or with the use of a nickel catalyst.^{89,90}



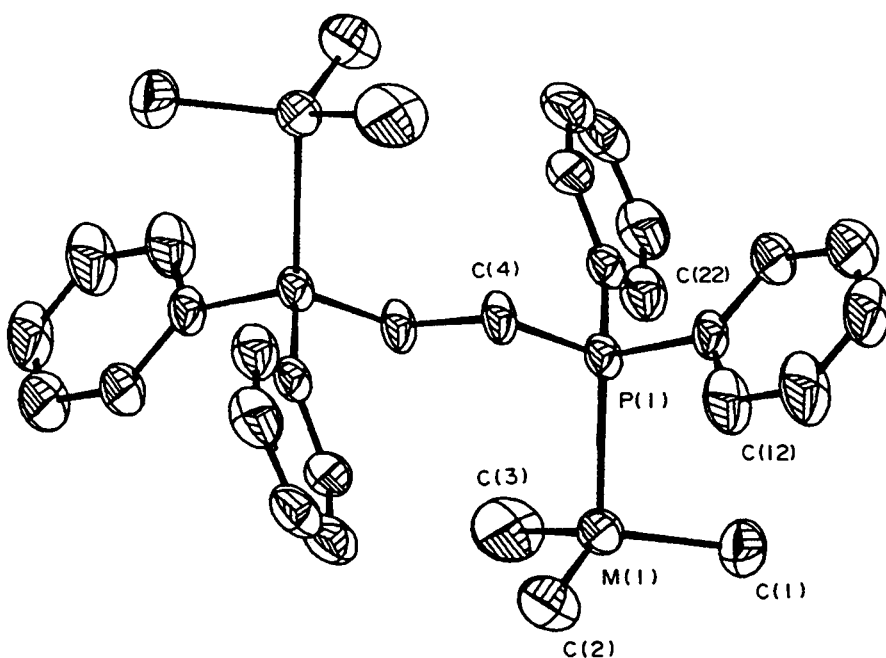
Likewise, the reaction of Bu^i_3Ga with 1-decene yields $\text{Ga}(\text{C}_{10}\text{H}_{21})_3$.^{88,90}

2. Neutral Adducts

As discussed earlier, a large number of neutral adducts of the trialkyls of Al, Ga and In are known with donation via N, P, As, Sb, O, S, Se and Te. Comprehensive lists of reported adducts of R_3M are included in the reviews by Eisch and Tuck.⁶ It is notable that most of this previous work concerns the use of monodentate ligands with the trimethylmetal derivatives. Furthermore, X-ray diffraction work on these adducts is limited compared to the amount available on derivatives obtained from alkane elimination reactions.

More recently, the study of adducts of group 13 organometallic compounds, particularly those of gallium and indium, have become the focus of considerable interest owing to their potential use as precursors for the MOCVD of 13–15 semi-conductors. A number of complexes between R_3M and aryl phosphines have been prepared,^{91,92}

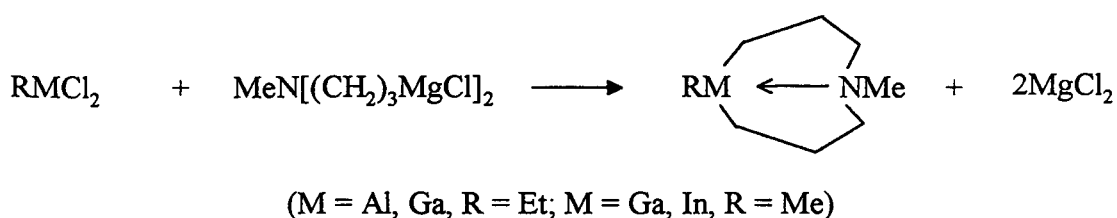
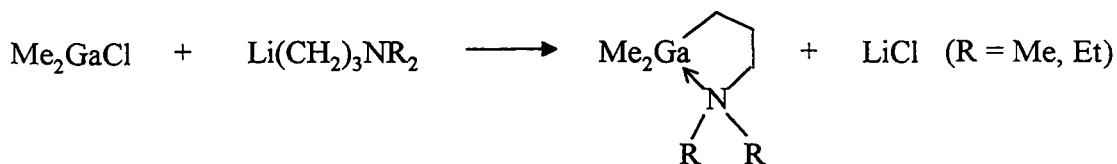
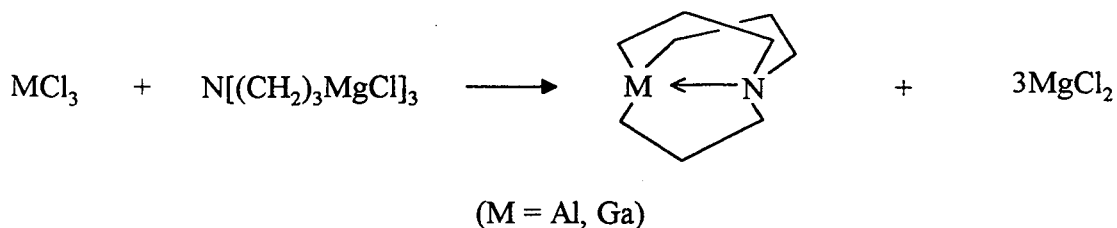
including adducts formed using the multidentate phosphines "diphos", "triphos", and "tetraphos". However, in all cases the metal centre is co-ordinated to one phosphorus donor atom. The molecular structure of $[(\text{Me}_3\text{In})_2(\text{diphos})]$ is shown below.⁹²



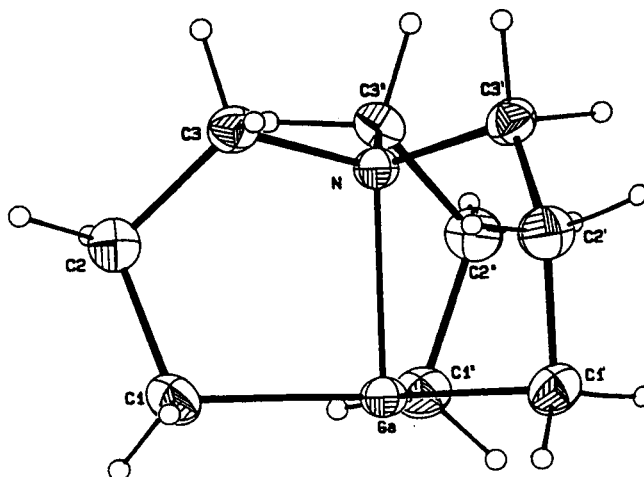
Complexes with tetramethyldiphosphine have also been prepared.⁹³

Other adducts of R_3M with ligands that contain two or more donor atoms that have had their solid state structure definitively characterised include $[\{(\text{TMS}-\text{CH}_2)_3\text{Ga}\}_2(\text{Me}_2\text{NCH}_2\text{CH}_2\text{NMe}_2)]$,⁹⁴ $[(\text{Me}_3\text{M})_2(\text{cyclam})]$ ($\text{M} = \text{Al}, \text{Ga}$),⁹⁵ $[(\text{Me}_3\text{Ga})_2(\text{dibenzo-18-crown-6})]$,⁹⁶ $[(\text{Me}_3\text{Al})_2(\text{Me}_2\text{NCH}_2\text{CH}_2\text{NMe}_2)]$ ⁹⁷ and $[(\text{Me}_3\text{Al})_2(\text{Ph}_2\text{PCH}_2\text{PPh}_2)]$.⁹⁸ In each case, the donation of only one electron pair from the ligand to each metal centre is encountered in the solid state.

An interesting development in this area is the synthesis of a number of intramolecularly base-stabilised complexes, such as those prepared by Schumann *et al*^{99,100} shown overleaf, which are monomeric and appreciably volatile.

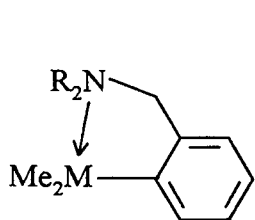


The X-ray crystallographic study performed on $[\text{Ga}\{(\text{CH}_2)_3\text{N}\}]$ revealed a trigonal monopyramidal co-ordination geometry around the metal, with a trigonal planar GaC_3 unit. The molecular structure is shown below: ⁹⁹



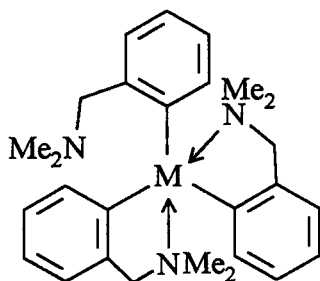
Other examples of this type of complex are shown overleaf. Compounds (1) and (2) are examples of intramolecularly stabilised aromatic derivatives.^{101,102,103} All the complexes discussed previously have one characteristic in common, namely that they possess only one donor atom per metal centre, which is typical for Lewis base adducts of

R_3M . The molecular structures of the gallium and indium complexes of (2)^{102,104}, as determined by X-ray crystallography, differ in this respect in having donation of two lone pairs to the metal.



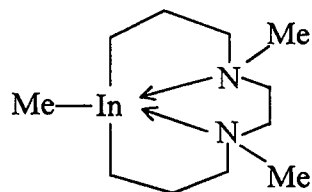
M=Ga, R=Me; M=In, R=Et

(1)



M=Ga, In

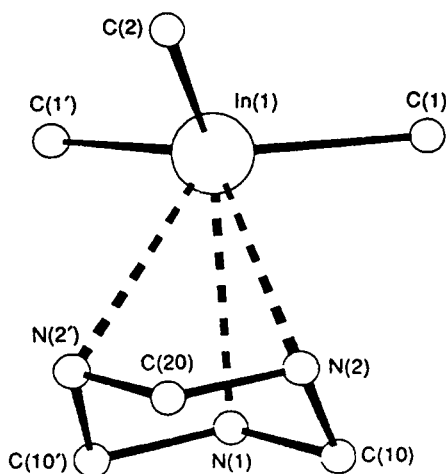
(2)



(3)

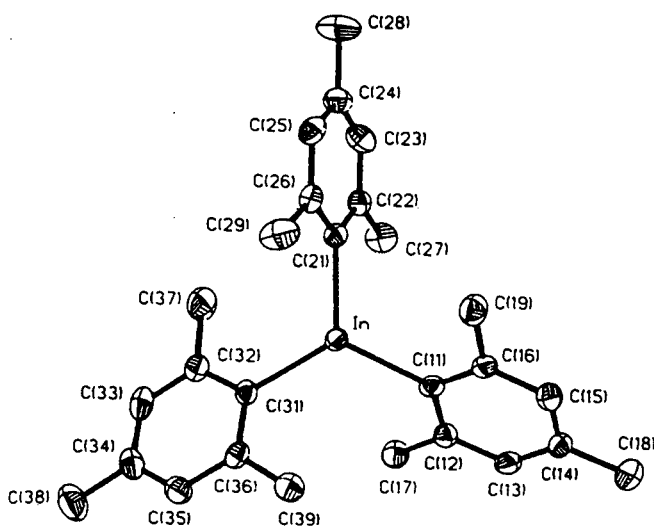
Both complexes show a five co-ordinate trigonal bipyramidal geometry around the metal, with two NMe_2 groups at the axial sites, and the remaining unattached NMe_2 group. Compound (3) has the potential of possessing donation of both N lone pairs to the metal, but has not been definitively structurally characterised.¹⁰¹

The recent X-ray structural characterisation of the trimethylindium adduct of N,N',N'' -tri-*iso*-propyl-1,3,5-triazacyclohexane, $[Me_3In(Pr^iNCH_2)_3]$, reveals an unusual donation of three lone pairs to the metal centre, and the metal sits above the macrocycle ring.¹⁰⁵



The synthesis of $(\text{Mes})_3\text{Al}$ by metal exchange between dimesitylmercury and aluminium was noted earlier.⁷⁶ The molecular structure of this compound, described in the same paper, shows that the effect of the bulky ligands is to give a monomeric, planar molecule. This form contrasts with the known dimeric solid state structure of triphenylaluminium, which contains strong bridge bonds.^{106,107}

The preparation of the analogous gallium and indium compounds via the corresponding mesityl Grignard reagent was also discussed earlier.^{80,81} Mes_3Ga shows little tendency to form adducts with either THF or Et_2O , both being unstable to dissociation at room temperature. This observation indicates that it is a weak Lewis acid presumably because of the large steric size of the mesityl ligands. The indium complex behaves similarly towards Et_2O . The crystal structures of these derivatives have been reported. Both are also monomeric. The solid state structure of the indium complex differs slightly from those of the aluminium and gallium derivatives in the way the aryl rings are arranged around the metal. In the structure of the former complex, each ring is crystallographically inequivalent, whereas in the structures of both the latter two complexes, they are arranged in a propeller-like fashion, with each ring related by a crystallographic C_3 axis. The significance of the different structure of the indium complex is that there may be agostic C–H interactions of the methyl groups. The molecular structure is given below:



Bradley *et al*¹⁰⁸ have reported a number of adducts of trimethylindium of the type $\text{Me}_3\text{In}\cdot\text{L}$ involving protic donors from group 15, where metallation of the donor species has not occurred. The ligands used include dicyclohexylamine, 2,6-dimethylpiperidine, 2,2,6,6-tetramethylpiperidine and $\text{N,N}'$ -dimethylethylenediamine. All these complexes can be sublimed under vacuum repeatedly without decomposition. For example, sublimation of the solid which is obtained from the 1/1 treatment of Me_3In with $\text{N,N}'$ -dimethylethylenediamine at $90^\circ\text{C} / 10^{-1}\text{mm Hg}$, yields a product which has been characterised by X-ray crystallography. The crystal structure shows that one Me_3In moiety is attached to each nitrogen atom, with the N-H group intact and the metal exhibiting near ideal tetrahedral co-ordination geometry.

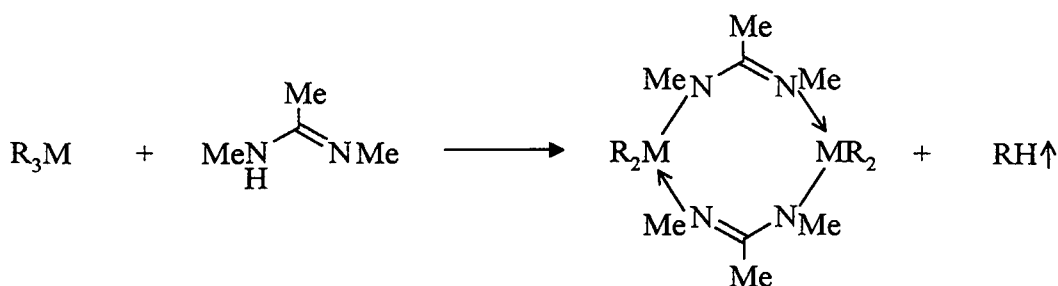
3. Reactions of R_3M with Protic Donors.

This section deals with the important class of reactions of organometallic derivatives with donor species containing protic groups, where metallation of the donor has occurred, as already briefly covered. Most of the derivatives that are to be described are derived from the trialkylmetal derivatives, particularly the trimethyl and triethyl compounds, since these are most relevant to the work presented in this thesis. The discourse is divided into sections according to ligand type, and emphasis will be placed on ligands which are related to those discussed in later chapters, such as the triazenido and carboxylate ligands, which are isoelectronic with the amidinato ligand discussed in the preceding two chapters, and macrocyclic complexes which are discussed in Chapter 4.

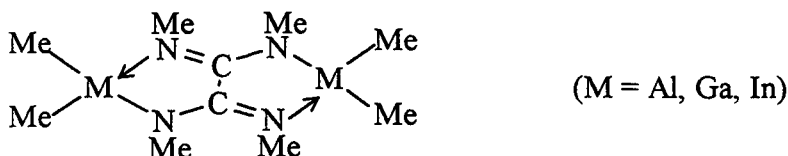
(i) Metal-Nitrogen, -Phosphorus and -Arsenic Bonds

Condensation of R_3M with the amidine ligand, $[\text{MeN(H)CMeNMe}]$ at -196°C , followed by warming to room temperature gives the complexes, $\{[\text{R}_2\text{M}(\text{MeNCMeNMe})]_2\}$ ($\text{M} = \text{Al}, \text{Ga}, \text{R} = \text{Me}, \text{Et}; \text{M} = \text{In}, \text{R} = \text{Me}$).¹⁰⁹ The X-ray structural characterisation of the dimethyl-aluminium and -gallium derivatives reveals a

dimeric structure which has a puckered eight-membered ring. The indium derivative is assigned to be isostructural on the basis of detailed infra-red and Raman studies.



The bi-functional amidine ligand, N,N',N'',N'''-tetramethyloxamidino reacts with two equivalents of Me₃M (M = Al, Ga, In) to generate the corresponding bis(dialkylmetal)-amidinato complex. The X-ray structure determinations reported for the three complexes all show an essentially planar bicyclic structure, which consist of two fused five-membered rings.¹¹⁰



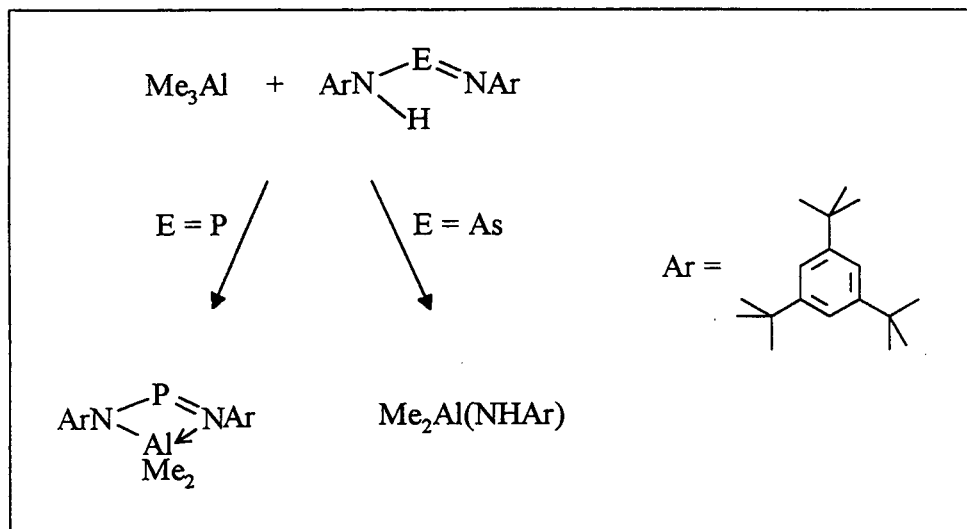
The reaction of Me₃Ga or Me₃In with the N,N'-dialkylcarbodiimide [Me₃SiN=C=NSiMe₃] produces 1:1 adducts, whereas Me₃Al forms the insertion compound [Me₂Al(Me₃SiNCMeNSiMe₃)] producing the amidinato ligand which has been shown by X-ray crystallography to co-ordinate to the aluminium centre in a symmetrical bidentate chelating manner.¹¹¹

Organoaluminium compounds are well-known to undergo insertion reactions with nitriles.^{112,113,114} For example, Me₃Al reacts with PhCN to form the adduct [Me₃Al.NCPh], which rearranges between 160–170°C to give the dimeric product [(Me₂AlNCMePh)₂].¹¹² A related reaction that occurs between diethylaluminium dimethylamide and a range of nitriles has been used to prepare some organoaluminium-

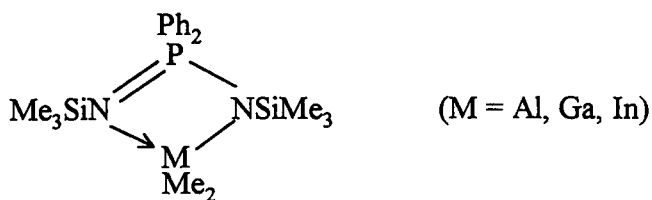
amidine complexes.¹¹⁵ For example, the reactions of this amide with acetonitrile or benzonitrile produce the compounds that are formulated as the diethylaluminium–amidine derivatives, $[\text{Et}_2\text{Al}(\text{N}=\text{CR}-\text{NMe}_2)]$ ($\text{R} = \text{Ph}, \text{Me}$). These compounds are formed by nucleophilic migration of the NMe_2 group to the nitrile. The corresponding gallium and indium reactions have not been reported.

Barron and co-workers^{116,117,118} have prepared a number organoaluminium and organoindium complexes from the reactions of trialkylmetal and the triazene ligands, 1,3-diphenyltriazene, $[\text{PhN}(\text{H})\text{NNPh}]$. This research has shown that the reaction of trimethylaluminium with the triazene results in the condensation of all three methyl groups at room temperature to yield the tris-triazenido complex $[\text{Al}(\text{PhNNNPh})_3]$ even in the presence of excess Me_3Al . The use of the more bulky *iso*-butyl group in $(\text{Bu}^i)_2\text{AlH}$ allows the isolation of the intermediate triazenido products $[\text{Bu}^i_{3-n}\text{Al}(\text{PhNNNPh})_n]$ ($n = 1, 2$), although it is noted in the same paper that the bis-triazenido complex is thermally unstable, even at room temperature, to disproportionation to yield the mono- and tris-triazenido products. In all the complexes prepared and structurally characterised using X-ray crystallography by this group, the triazenido ligand $[\text{ArNNNAr}]^-$ ($\text{Ar} = \text{aryl}$) acts as a bidentate chelate ligand. Coates¹¹⁹ has cursorily reported that dimethylgallium–1,3-diphenyltriazenido is isolated from a 1:1 reaction of Me_3Ga with the triazene at -196°C , followed by warming to room temperature and is believed to be monomeric. The amidine ligand may be expected to undergo similar reactions with these metal derivatives.

Lappert *et al*¹²⁰ have reacted the related arylimides of phosphorus(III) and arsenic(III), $[\text{ArN}(\text{H})\text{ENAr}]$ ($\text{E} = \text{P}, \text{As}$), with trimethylaluminium as shown below. In the case of the phosphorus(III)-containing ligand, the acidic N–H hydrogen is cleaved with the formation of the two co-ordinate phosphorus(III) metallocycle, $[\text{Me}_2\text{Al}(\text{ArNPNAr})]$. The solid state structure of this complex has been determined by X-ray crystallography, and shows it to be monomeric with a symmetrical bidentate chelate NPN unit. The equivalent reaction with the arsenic(III)-containing ligand proceeds with As–N rather than N–H cleavage, to yield $[\text{Me}_2\text{Al}\{\text{N}(\text{H})\text{Ar}\}]$.



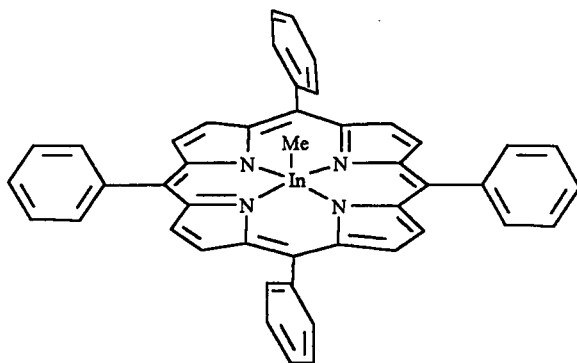
The phosphorus(V)-containing ligand $[\text{Me}_3\text{SiN}=\text{P}(\text{Ph}_2)\text{NHSiMe}_3]$ undergoes a condensation reaction with Me_3M ($\text{M} = \text{Al}, \text{Ga}, \text{In}$), eliminating methane and yielding a monomeric product.¹²¹



A growing area of interest concerns the investigation of the interaction of group 13 organometallic derivatives with macrocyclic amines, mixed nitrogen–oxygen macrocyclic donors, crown ethers and thiacycrown ethers. Much of this work has centred on organoaluminium and organogallium species, particularly with tetradentate amines, the majority of which have been reported by Robinson and co-workers. The corresponding indium complexes have not yet been reported. This work will be discussed in Chapter 4, along with some new indium complexes prepared in this study.

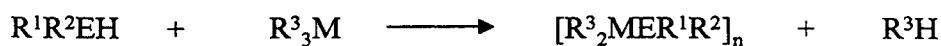
Porphyrins are examples of another important class of cyclic nitrogen-containing ligands. The rigidity of the macrocycle ring framework in these ligand systems predetermines the metal co-ordination stereochemistry, favouring a five co-ordinate square-based pyramidal metal environment. Guilard has prepared a number of

alkylmetal–porphyrin complexes by the reaction of Grignard or organolithium reagents with the corresponding chlorometal–porphyrin derivative.^{122,123,124} The crystal structure of methylindium–tetraphenylporphinato has been determined as shown schematically below and will be discussed in detail in Chapter 4.¹²⁵



A substantial amount of work has centred on the preparation of metal–nitride, –phosphide and –arsenide complexes with interest aimed at the potential application of such compounds for the preparation of semi–conductor materials. In view of the extensive investigation of this class of compounds, it is necessary to limit this discussion to some important and recent derivatives.

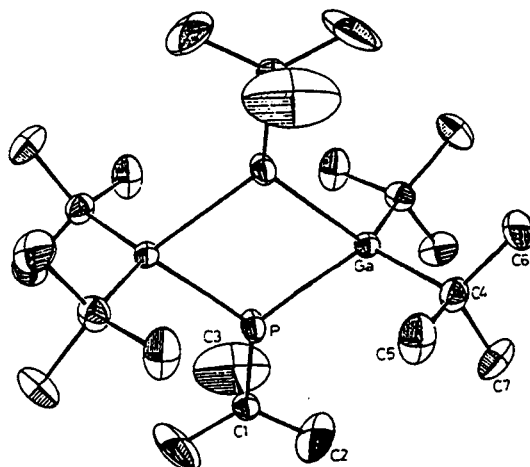
One preparative route to these compounds is the metallation of E–H bonds (E = N, P, As) in ligands generalised as R¹R²EH (R¹, R² = alkyl, aryl or H), with the R³₃M derivatives of aluminium, gallium and indium (R³ = alkyl, aryl). Another common synthetic route involves the displacement of halide from organometallic halides.



Coates and co–workers showed as early as 1963, that the reaction of Me₃M (M = Al, Ga, In) and secondary amines, phosphines, and arsines, R₂EH (R = alkyl or aryl, E = N, P, As) produces complexes formulated as [(Me₂MER₂)₂].^{56,126} Dimeric complexes are known for the dimethylmetal dimethylamide derivatives of Al, Ga and

In.^{53,127,128,129} More recent work has focused on the use of bulky metal and heteroatom groups in an attempt to influence the solid state structures of these derivatives, in particular the extent of oligomerisation. Most of the complexes that have been characterised by X-ray crystallography show dimeric structures, generally with planar four-membered $(ME)_2$ rings.

Examples of this type of structure are *trans*- $[\{Bu^t_2Ga(\mu-E(H)Bu^t)\}_2]$ ($E = P, As$),¹³⁰ in which the $(GaE)_2$ core is isostructural with that in the dimeric amide complex, $[(Me_2InNMe_2)_2]$. The molecular structure of the phosphide is shown below, and illustrates the stereochemistry of the auxiliary groups attached to the ring.

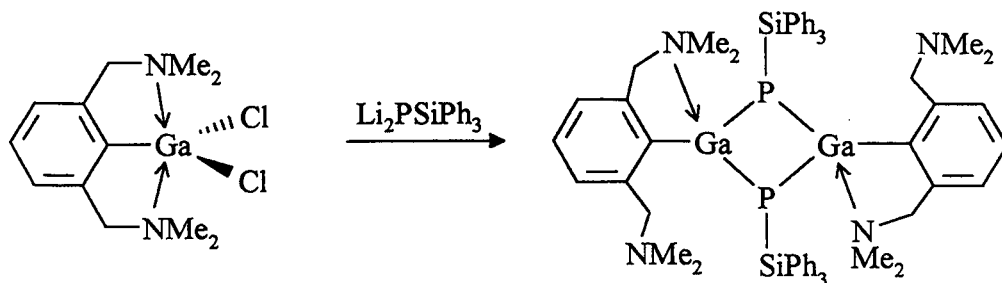


Trimeric structures are relatively rare compared to the number of dimeric examples. Trimeric structures are known for the products $[\{R_2Ga(\mu-EH_2)\}_3]$ obtained from the reactions of EH_3 with R_3Ga ($E = N, R = Me$;¹³¹ $E = N, P, As, R = Bu^t$ ¹³³), and similarly for $[\{Me_2Al(\mu-NH_2)\}_3]$ ¹³⁴. The importance of the characterisation of these compounds can be appreciated by noting that they may be expected to be intermediates in the preparation of ME materials from these precursors.

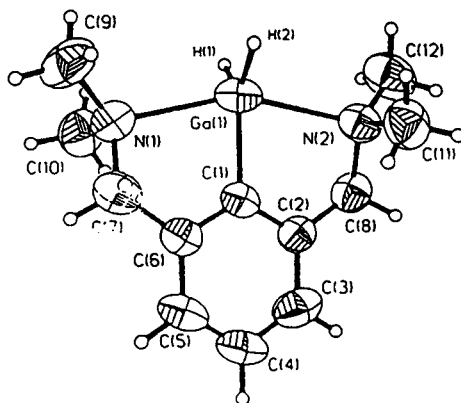
Monomeric amides, phosphides or arsenides of these metals are quite rare in comparison to the more common tendency of such complexes to oligomerise through the formation of M-E bridges. Examples of monomeric complexes are of interest because of the co-ordinative unsaturation of the metal centre, and therefore the possibility of the

formation of M–E π -bonds becomes important. The monomeric amides, $[\text{Bu}'_2\text{GaN}(\text{R})\text{SiPh}_3]$ ($\text{R} = \text{Bu}'$, 1-adamantyl), $[(2,4,6\text{-Pr}^i_3\text{C}_6\text{H}_2)_2\text{GaNH}(2,6\text{-Pr}^i_2\text{C}_6\text{H}_3)]$ and $[(2,4,6\text{-Pr}^i_3\text{C}_6\text{H}_2)_2\text{GaNPh}_2]$ have been synthesised using the bulky substituents on the nitrogen atom, although no clear evidence of Ga–N π -bonding is observed.¹³⁵ X-ray crystallographic characterisation of the monomeric phosphinogallane, $[\text{Bu}'_2\text{GaP}(\text{R})\text{SiPh}_3]$ ($\text{R} = \text{C}_6\text{H}_2\text{Bu}'_3$) has provided evidence to support the existence of weak π interactions.¹³⁶ Other monomeric species include $[\text{M}\{\text{N}(\text{TMS})_2\}_3]$ ($\text{M} = \text{Al}, \text{Ga}$),^{137,138} and $[\text{In}(\text{PBU}'_2)_3]$.¹³⁹ Any potential $p\pi$ – $p\pi$ interactions in these complexes will be extended over all three M–E bonds and therefore are less easily assessed.

Finally, an unusual method of metal stabilisation is seen in $[\{2,6\text{-}(\text{Me}_2\text{NCH}_2)_2\text{C}_6\text{H}_3\}\text{GaCl}_2]$, where the gallium centre is five co-ordinate, and is intramolecularly co-ordinated to both N atoms of the aryl side chains. A metathetical reaction of this compound with $\text{Li}_2\text{PSiPh}_3$ yields the dimeric four co-ordinate gallium complex shown below, which possesses the familiar $(\text{GaP})_2$ ring.¹⁴⁰



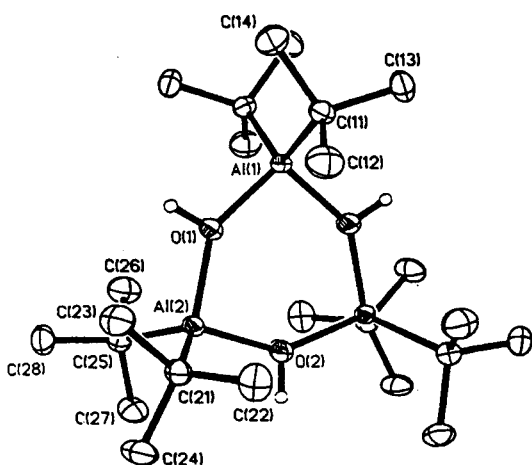
A subsequent paper describes the reaction of the dichloride with LiGaH_4 leading to the dihydride and the molecular structure is shown below.¹⁴¹ Reaction of this product with diethylzinc gave the diethylgallium analogue, which is presumably formed by alkyl/hydride exchange.



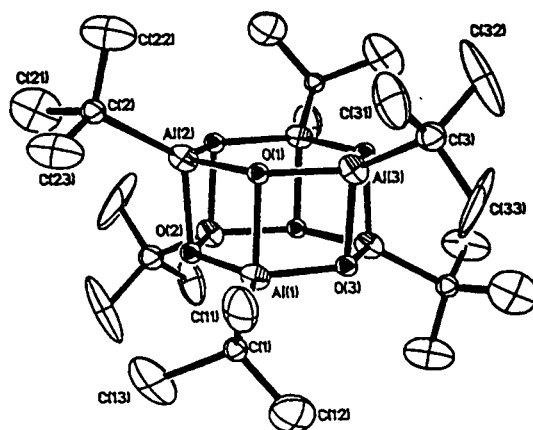
(ii) **Metal–Oxygen, –Sulphur, –Selenium and –Tellurium Bonds**

(a) **Hydroxides, Alkoxides, Aryloxides and Related Complexes**

The hydrolysis of R_3M with water has been briefly discussed (section B4). The partial hydrolysis of aluminium alkyls generates a wide variety of new organoaluminium compounds containing Al–O–Al linkages known as aluminoxanes. Definitive structural characterisation of these compounds is limited, although spectroscopic and theoretical results have been used to propose a vast range of structural possibilities.⁷ Barron and co-workers¹⁴² have recently studied the controlled hydrolysis of Bu^t_3Al and reported the first X-ray structural characterisation of alkylaluminoxanes $[(R_2Al)_2O]_n$ and $(RAlO)_n$. A number of bonding arrangements of Bu^t_2AlO and Bu^tAlO moieties have been shown in the resulting oligomer structures. For example, low-temperature ($-78^\circ C$) hydrolysis of Bu^t_3Al forms the trimeric hydroxide $[\{(Bu^t)_2Al(\mu-OH)\}_3]$ (4) shown below. Thermolysis of this product in refluxing hexane produces the hexameric and nonameric derivatives $[\{(Bu^t)Al(\mu_3-O)\}_6]$ (5) and $[\{(Bu^t)Al(\mu_3-O)\}_9]$.

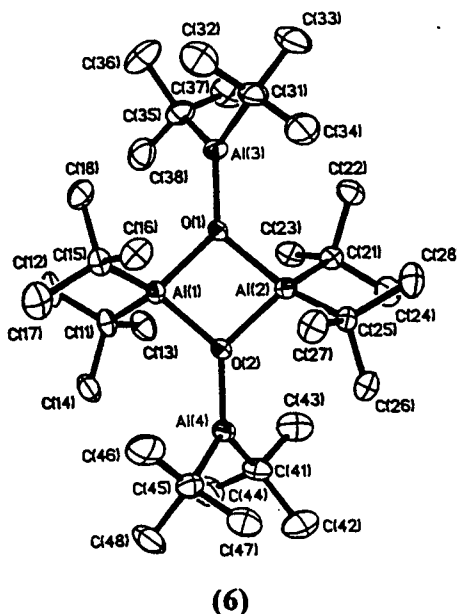


(4)



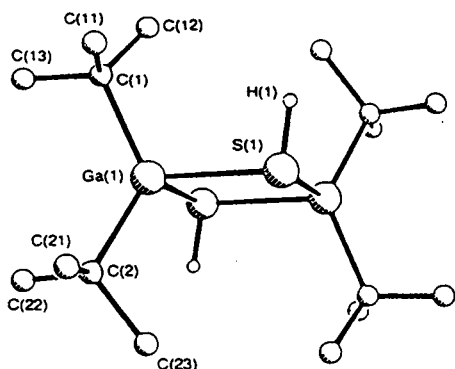
(5)

Hydrolysis of Bu^t_3Al with the hydrated salt, $\text{Al}_2(\text{SO}_4)_3 \cdot 18\text{H}_2\text{O}$ at -78°C followed by thermolysis in refluxing toluene, gives the tetrameric aluminoxane $[(\text{Bu}^t)_2\text{Al}\{\mu\text{-OAl}(\text{Bu}^t)_2\}]_2$ (6) and the octameric aluminoxane $[\{(\text{Bu}^t)\text{Al}(\mu_3\text{-O})\}]_8$.

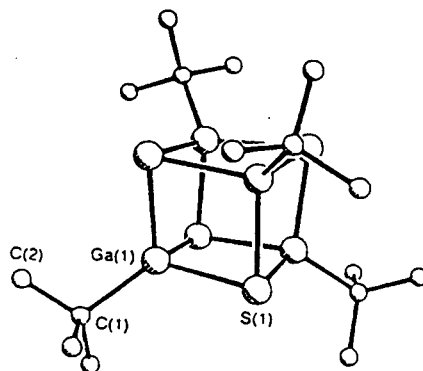


Partial hydrolysis of Me_3Ga gives Me_2GaOH , which is polymeric in benzene solution and its solid state structure is of a tetramer, consisting of a puckered $(\text{GaO})_4$ ring. This colourless, crystalline, sublimable solid dissolves in aqueous perchloric or nitric acids with no decomposition.¹⁴³ On heating the solid to 150°C it loses methane to yield $[(\text{Me}_2\text{GaO})_n]$. It may be noted that $[(\text{Me}_2\text{Ga})_2\text{O}]_n$ has also been proposed to be the hydrolysis product of Me_3Ga .¹⁴⁴ It is likely that the hydrolysis product obtained varies with experimental conditions employed. Bu^t_2GaOH , prepared by the addition of a slight excess of water to Bu^t_3Ga , has a planar $(\text{GaO})_3$ ring structure.¹³² Me_2InOH has not been reported, although $[(\text{Me}_2\text{In})_2\text{O}]$ has apparently been identified as one product of the hydrolysis of Me_3In .¹⁴⁵

The dimeric structure of *trans*- $[\{\text{Bu}^t_2\text{Ga}(\mu\text{-SH})\}]_2$ (7), prepared by the reaction of H_2S with Bu^t_3Ga ,¹⁴⁶ may be compared to the trimeric structures known for the N, P, As and O analogues. Thermolysis of *trans*- $[\{\text{Bu}^t_2\text{Ga}(\mu\text{-SH})\}]_2$ produces the cubane $[\{\text{Bu}^t\text{Ga}(\mu\text{-S})\}]_4$ (8).^{146,147,148}



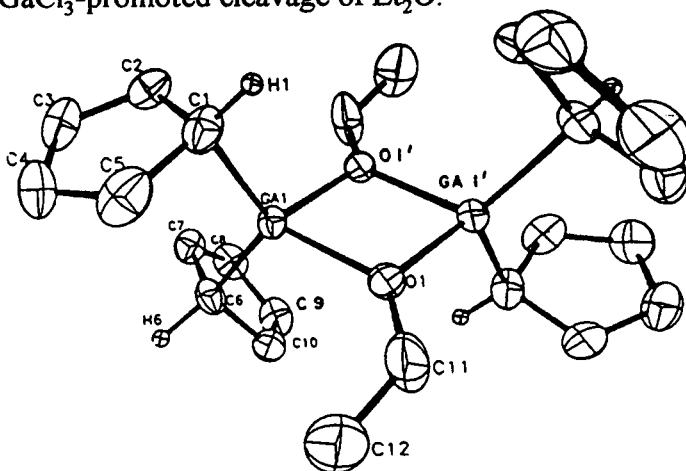
(7)



(8)

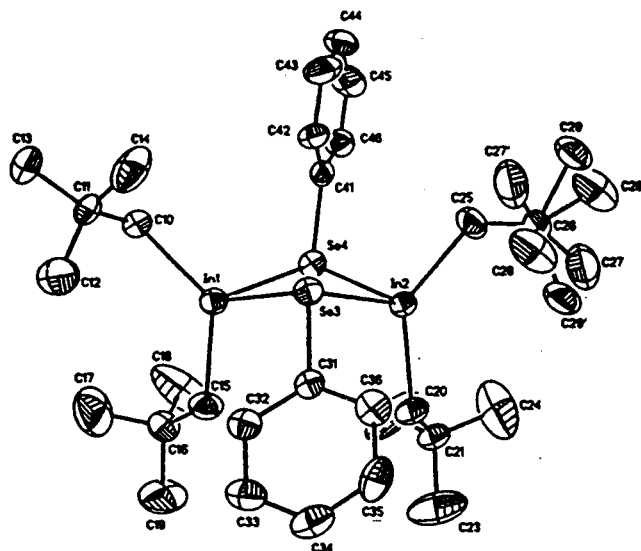
The reactions between alcohols and phenols with group 13 alkyls have been widely studied, with particular interest in determining the physical properties and aggregate size of the products obtained. The reaction of Me_3Al and methanol yields Me_2AlOMe , which is trimeric in benzene.¹⁴⁹ The determination of the solid state structure by X-ray crystallography confirms this degree of association.¹⁵⁰ Me_2AlSMe is dimeric in the vapour phase,⁴⁹ but polymeric in the solid state.¹⁵¹ The gallium compound, Me_2GaOMe , along with the equivalent sulphur and selenium derivatives, are formulated as dimers with bridging group 16 atoms.¹⁵² The dimeric structure of the sulphur and selenium derivatives is disrupted by the addition of trimethylamine to form 1:1 adducts, whereas the structure of the alkoxide derivative remains intact. Me_2InOMe is prepared in a similar manner, and is a glassy colourless material which cannot be crystallised, suggesting extensive polymerisation in the solid state.³⁸ The reaction of R_3M and Bu^tOH ($\text{M} = \text{Al}$, $\text{R} = \text{Et}$,¹⁵³ $\text{M} = \text{Ga}$, In , $\text{R} = \text{Me}$ ³⁸) yields the dimeric structures $[\{\text{R}_2\text{MOBu}^t\}_2]$. Similarly, treatment of Me_3M with Me_3SiOH generates the dimers $[\{\text{Me}_2\text{MSiR}_3\}_2]$ ($\text{M} = \text{Al}$, $\text{R} = \text{Me}$,¹⁵⁴ $\text{M} = \text{Ga}$, In , $\text{R} = \text{Me}$, Ph ¹⁵⁵). The germanium complexes ($\text{M} = \text{Ga}$, In) are prepared in a similar manner.¹⁵⁶ The interaction of Me_3Al with the

common stopcock grease poly(dimethyl)siloxane also yields $[\{\text{Me}_2\text{AlOSiMe}_3\}_2]$.¹⁵⁷ The preparation of $[\{\text{Cp}_2\text{Ga}(\mu\text{-OEt})\}_2]$ is worthy of brief note. Beachley *et al*¹⁵⁸ reported the preparation of $\text{Ga}(\text{Cp})_3$ from LiCp and GaCl_3 carried out using Et_2O as solvent at 0°C . This reaction has also been reported by Cowley *et al*,¹⁵⁹ but carried out at room temperature. The resulting product has been confirmed by X-ray crystallography to be the ethoxy-bridged dimer shown below. The bridging ethoxy groups were presumed to be formed via GaCl_3 -promoted cleavage of Et_2O .



Simple phenols generally give compounds that are dimeric in nature, such as $[\{\text{Me}_2\text{MOPh}\}_2]$ ($\text{M} = \text{Al}$,^{160,161} Ga ¹⁵²). The reaction of the sterically hindered phenol 2,6-di-*tert*-butyl-4-methyl-phenol (HO-BHT) with trimethylaluminium prevents bridge formation and gives the monomeric species, $[\text{Me}_2\text{Al}(\text{OBHT})]$ and $[\text{MeAl}(\text{OBHT})_2]$.^{162,163}

The selenide and telluride complexes, $[\{\text{Me}_3\text{CCH}_2\}_2\text{MEPh}\}_2]$ ($\text{M} = \text{Ga}$, $\text{E} = \text{Te}$;¹⁶⁴ $\text{M} = \text{In}$, $\text{E} = \text{Se}$ ¹⁶⁵), which have been prepared by a chloride elimination reaction with LiEPh , are dimeric with $(\text{ME})_2$ rings. These structures are similar to those seen for the dimeric metal-nitride, -phosphide and -arsenide complexes discussed earlier, but the conformation of the rings differ significantly. Whereas the latter structures generally consist of planar rings, the former complexes have butterfly-shaped $(\text{ME})_2$ rings. The fold angle about $\text{Ga}\cdots\text{Ga}$ in the selenide complex is ca. 150.2° , and in the telluride complex (the molecular structure of which is shown overleaf) the angle about $\text{In}\cdots\text{In}$ is ca. 149.4° .

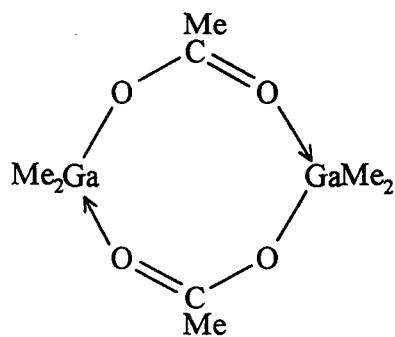


(b) Carboxylates and Thiocarboxylates

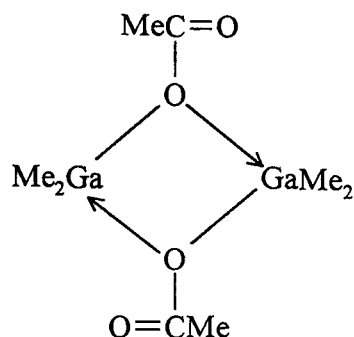
These derivatives are of interest because they contain an example of ligands which are isoelectronic with the amidines. This section is concerned with the reactions of simple organic groups (RCE_2H , $\text{R} = \text{alkyl, aryl}$; $\text{E} = \text{O, S}$) with organometallic compounds and concentrates on the structures formed by this type of metal complex.

Acetic acid reacts with one equivalent of Me_3M ($\text{M} = \text{Al, Ga, In}$) to eliminate methane and generate $[\{\text{Me}_2\text{M}(\text{OAc})\}_n]$. For dimethylaluminium acetate, a number of forms of association have been suggested. The infra-red and Raman spectroscopic data reported by Weidlein are consistent with dimer, trimer and tetramer forms with three-atom AlOCOAl bridges, rather than one-atom $\text{AlO}(\text{CO})\text{Al}$ bridges.¹⁶⁶ Also, the structure of $[\text{Et}_2\text{In}(\text{OAc})]$ has been shown to be polymeric.¹⁶⁷

The reaction of trimethylgallium with acetic acid in benzene proceeds with the elimination of methane forming dimethylgallium acetate. Molecular weight determinations in acetone solution indicate that the product is formulated as a dimer.¹⁵² Once again, infra-red and Raman spectroscopic data are consistent with three atom bridge groups as in structure (9) and not with structure (10).¹¹⁹



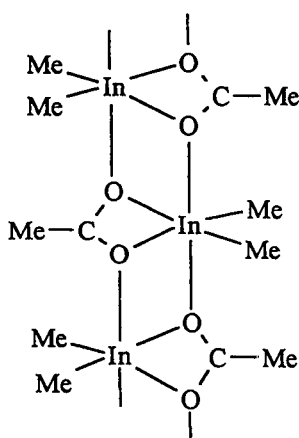
(9)



(10)

Treatment of trimethylgallium in diethylether with excess acetic acid gives $[\text{MeGa}(\text{OAc})_2]_n$, which is associated in benzene solution ($n \approx 2 - 3.3$).¹⁶⁸ X-ray crystallographic studies on the solid show it to be polymeric with bridging $\text{OC}(\text{Me})\text{O}$ groups. Two different gallium co-ordination sites are found, one which has a distorted trigonal bipyramidal, GaO_4C , environment and a second which has a distorted tetrahedral, GaO_3C , environment around the metal.

The analogous indium derivatives have been studied in more detail. Dimethylindium acetate, prepared from Me_3In and acetic acid in diethyl ether,^{145,169} is polymeric in the solid state, in which the indium attains a co-ordination number of six, as indicated below.¹⁷⁰



Upon the addition of a Lewis base such as DMSO or pyridine the polymeric structure is broken to give the adducts $[\text{Me}_2\text{In}(\text{OAc})\text{L}]$ ($\text{L} = \text{DMSO}, \text{pyridine}$).¹⁷¹

The reactions of the related dithioacetic acid with R_3M ($M = Al, R = Me; M = Ga, In, R = Me, Et$) proceed in a similar manner.¹⁷² The structure of dimethylaluminium dithioacetate is assigned as dimeric in the solid state, with bridging SCS units, on the basis of vibrational spectroscopic studies. The structures of the equivalent gallium and indium complexes are assigned as monomeric, with bidentate chelate co-ordination of this ligand. The solid state structure of the thioacetate complex, $[Et_2InO(S)CMe]$ is polymeric, containing five co-ordinate indium, with only the oxygen atom participating in bridging.¹⁷³

Reaction of two equivalents of Me_3Ga with oxalic acid yields bis(dimethylgallium)oxalato¹⁷⁴ and is structurally similar to the oxamidato derivatives mentioned earlier.

(c) Other Compounds Containing Metal–Oxygen Bonds

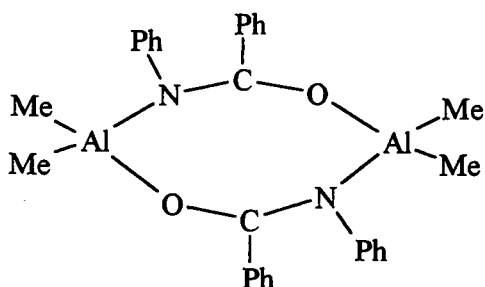
Dialkylmetal acetylacetonates of aluminium, gallium and indium are readily prepared and are monomeric with bidentate chelation of the metal.^{38,161,175} The solid state structure of gallium–tris(hexafluoroacetylacetonato) consists of a six co-ordinate metal centre, bonded to the oxygen atoms of the three hexafluoroacetylacetonato ligands, giving a slightly distorted octahedral co-ordination environment around the metal.¹⁷⁶

A range of phosphinates and arsinates $[(Me_2MO_2EMe_2)_2]$ ($M = Al, Ga, In; E = P, As$) are known and a dimeric structure based on a puckered eight-membered ring is postulated.¹⁷⁷

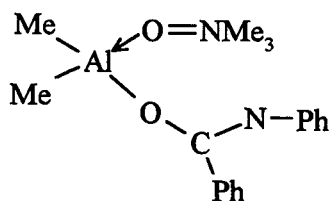
(iii) Compounds Containing Metal–Nitrogen and –Oxygen Bonds

The reactions of R_3M with amides are relevant to this discussion because of the similarity of this class of ligand to the amidines. The dialkyl–gallium and –indium derivatives of N–methylacetamide (alkyl = methyl, ethyl) have been prepared and their vibrational spectra support a dimeric structure with an eight-membered ring.¹⁷⁸ Cryoscopic measurements made on a range of dialkylaluminium amide compounds in benzene solution are in agreement with a dimeric formulation, which is also suggested

from spectroscopic results for these derivatives.¹⁷⁹ The solid state structure of dimethylaluminium N-phenylbenzamido (11), as determined by X-ray crystallography, confirms a dimeric arrangement with bridging NCO groups.¹⁸⁰ Addition of trimethylamine oxide to this latter compound yields a 1:1 complex. The reported X-ray crystallographic structural characterisation of the product shows that formation of the adduct results in cleavage of the Al-N amido bond and the additional ligand bonds via the oxygen atom (12).¹⁷⁹ Both structures are depicted below.

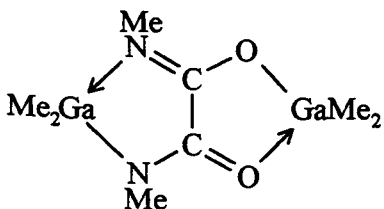


(11)

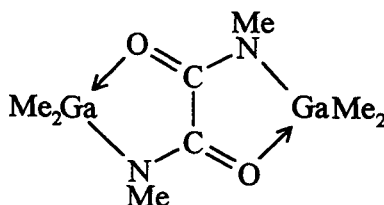


(12)

Oxamide derivatives of dimethyl- and diethyl-aluminium, -gallium and -indium are known.¹⁸¹ Their basic structure is similar to the oxamidinato and oxalato derivatives already mentioned, but in the gallium and indium compounds, the N.M.R. data suggests the presence of *cis* and *trans* isomers. In the *cis* isomer, (13), the two Me_2Ga units are inequivalent, attached to either two nitrogen atoms or two oxygen atoms, whereas in the *trans* isomer, (14), both units are identical, with each gallium attached to one nitrogen and one oxygen. The crystal structures of the *trans*-dimethylaluminium and the *cis*-dimethylgallium compounds are known.¹⁸²



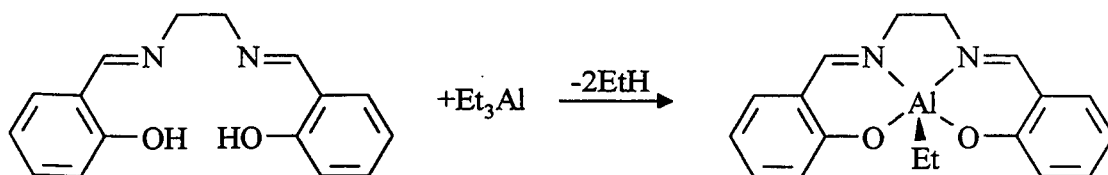
(13)



(14)

Lastly, triethylaluminium has been shown to react with the Schiff base shown overleaf, with the elimination of two mole equivalents of ethane to give a five co-

ordinate metal species.¹⁸³ This type of pseudo-macrocycle is more flexible than macrocycles such as the aromatic porphyrin and related tetraazamacrocycles discussed in Chapter 4, allowing subtle differences in the co-ordination environment of the metal. The analogous reaction using Me_3Ga has been investigated and the complex formed appears to be isostructural.¹⁸⁴



CHAPTER 2

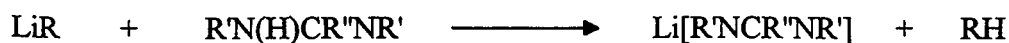
A Study of Some Organometallic N,N'-Diarylamidinato Derivatives of Aluminium, Gallium and Indium

CHAPTER 2

A Study of Some Organometallic N,N'-Diarylamidinato Derivatives of Aluminium, Gallium and Indium.

Introduction

Amidines, which may be regarded as the imino analogues of amides, are of the general formula shown in Figure 2.1(a). Comprehensive reviews cover the synthesis and properties of these ligands.^{185,186} While they may act as two electron donor ligands via the imino lone pair, a more synthetically versatile ligand is obtained when the R group is removed to form the amidinato group $[R'NCR''NR']^-$ ($R, R', R'' = H, \text{alkyl, aryl, etc.}$). The N,N'-disubstituted amidines $[R'N(H)CR''NR']$ are most useful in this respect, containing an acidic proton which is readily lost. For example, this is easily achieved using lithium alkyl reagents to form the lithium salt of the amidine which can be reacted further with a metal halide.¹⁸⁷



The amidinato ligand is isoelectronic with a number of better known species, such as the carboxylate $[\text{O}_2\text{CR}]^-$ and triazenido $[\text{RNNNR}]^-$ ions and the allyl radical $[\text{R}_2\text{CCCR}_2]^\cdot$, and as with these ligands a number of co-ordination modes are possible. The co-ordination chemistry of this ligand with the transition metals is well established and is the subject of a recent review.¹⁸⁸ The two most common amidinato bonding modes with transition metal species are the chelating mode, shown in Figure 2.1(b), in which the relatively small size of the four-membered $\text{M}(\text{NCN})$ ring introduces steric strain and distortion of the valence angles, and the bridging mode, shown in Figure 2.1(c), which often leads to metal-metal interactions.

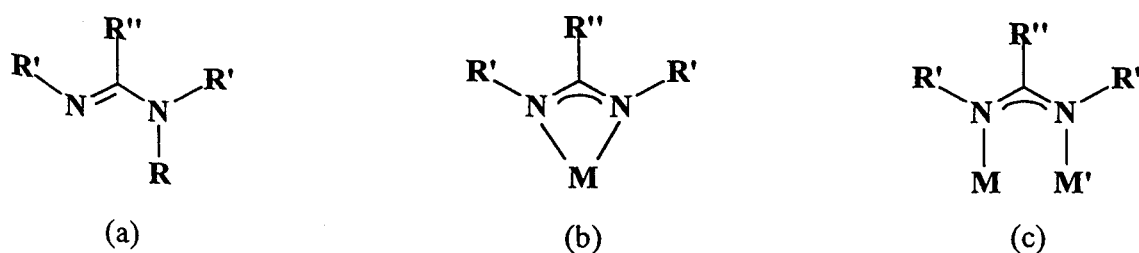


Figure 2.1 The amidine group and common amidinato co-ordination modes

In contrast, there are relatively few studies of this ligand involving main group elements and much less is known about the types of bonding modes encountered in these complexes. For the group 13 metals in particular there are only five definitive structures reported and these will be discussed later in this chapter.

This study was initiated to explore the general reactions of group 13 compounds with amidines and to investigate the structures and properties of these complexes. It is also of interest to compare these structures with known structures of other related complexes with nitrogen-containing ligands. Most of the previously reported complexes obtained from the reactions between the trialkyl derivatives of these metals with disubstituted amine ligands, R_2NH , are amido-bridged dimers of the type $[(R_2MNR'_2)_2]$.^{38,56,126-129} For example, the well known reactions between the secondary amine, $NHMe_2$, and the trimethyl compounds of aluminium, gallium and indium at room temperature terminate with adduct formation of the type $Me_3M.NHMe_2$. These eliminate methane only on heating to relatively high temperatures to form dimeric species based on a four-membered $(MN)_2$ ring.^{38,128}

The reactions of R_3M with the triazene ligand $[ArN(H)NNAr]$ lead to the elimination of 1, 2 or 3 mole equivalents of alkane and the formation of mono-, bi- or tri-substituted complexes. These reactions will also be discussed further later in this chapter. The unsaturated nature of these R_2NH ligand systems is comparable to that found in the amidine ligand, and by using this similarity, a reaction with further equivalents of amidine than 1:1 mole ratio reactions may be expected.

A further area to be explored is whether the amidine complexes prepared show any potential for use as precursors to the fabrication of the III/V semi-conductor materials, the group 13 metal nitrides, MN ($M = Al, Ga, In$). This topic is of particular interest to our collaborating body, The Associated Octel Company, in this CASE Award. These complexes are often appreciably volatile and, unlike conventional group 13 metal sources, such as the trialkyls, are non-pyrophoric and therefore more easily handled. Their thermal decomposition products have been studied and the results are discussed in Appendix 1.

Previous studies of the reactions of amidine ligands with group 13 compounds have concentrated mainly on two derivatives of amidine, namely the N,N' -dimethyl substituted acetamidinato ligand, $[\text{MeNCMeNMe}]^-$ which gave dimeric products,¹⁰⁹ and the N,N' -di(trimethylsilyl) substituted amidinato derivatives, $[(\text{Me}_3\text{Si})\text{NCXN}(\text{SiMe}_3)]^-$ ($X = \text{Ph}, \text{Me}$), which produced monomeric species.^{189,190,191,192,193} A review of the chemistry of N -silylated benzamidines with main group elements has recently been published.¹⁹⁴ Other related studies have used the nitrogen analogue of the oxalate ligand, and were mentioned in Chapter 1 earlier.¹¹⁰

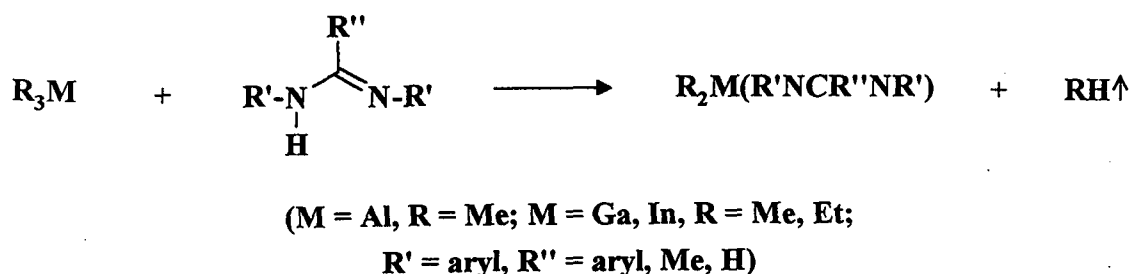
The work presented in this chapter is concerned with the reactions of N,N' -diaryl substituted amidines, of the general formulae $\text{RN}(\text{H})\text{CR}'\text{NR}$ ($\text{R} = \text{aryl}, \text{R}' = \text{aryl}, \text{Me}, \text{H}$), where the acidic proton is displaced to form the amidinato group. This type of ligand substitution was selected in order to compare the chemical reactivity and structural properties of the complexes prepared with those previously investigated by other researchers.

Amidines are named after the acid or amide obtained from it after hydrolysis. Thus the compound $\text{H}_2\text{N}-\text{C}(\text{H})=\text{NH}$ is named formamidine, $\text{H}_2\text{N}-\text{C}(\text{Me})=\text{NH}$ is acetamidine, and $\text{H}_2\text{N}-\text{C}(\text{Ph})=\text{NH}$ is benzamidine. Likewise, $\text{PhN}(\text{H})\text{CPhNPh}$ is known as N,N' -diphenylbenzamidine. The nomenclature used in Chemical Abstracts treats amidines as amides of the corresponding imidic acid. For example, formamidine is methanimidamide, acetamidine is ethanimidamide and benzamidine is benzenecarboximidamide. We adopt the older traditional name for convenience.

Preparation of the Dialkylmetal–Amidinato Complexes of Aluminium, Gallium, and Indium.

The reaction of equimolar quantities of the trimethyl derivatives of aluminium, gallium and indium with a series of amidines in toluene or hexane solution at low temperature leads to the elimination of one mole equivalent of methane and the formation of colourless or pale yellow solid products which hydrolyse in air. The reactions proceed in a clean, controlled manner with gas evolution commencing around -50°C , and usually being completed by the time the solution has warmed to room

temperature. A similar reaction was confirmed to occur for the triethyl derivatives of gallium and indium.



The synthesis of the gallium and indium complexes was also carried out at room temperature and control over the exothermic reaction was achieved by slow addition of the amidine to a hexane solution of the appropriate trialkylmetal derivative (Et₃Ga, Me₃In, Et₃In).

A series of dialkylmetal–amidinato complexes was synthesised in this work, as detailed in Table 2.1, in order to study the effect of changing the ligand substituents on the chemical and physical properties of the complexes formed. The nature of all the products was investigated by elemental analysis (C, H, N), ¹H and ¹³C N.M.R., I.R, and mass spectroscopy.

Table 2.1 Compounds of the type [R₂M(R'NCR''NR')] prepared in this study

R ₂ Al	R ₂ Ga	R ₂ In	R'	R''
Me ₂ Al	Me ₂ Ga, Et ₂ Ga	Me ₂ , Et ₂ In	Ph	Ph
Me ₂ Al	Me ₂ Ga	Et ₂ In	Ph	Me
Me ₂ Al	Me ₂ Ga	Et ₂ In	Ph	H
Me ₂ Al	Me ₂ Ga	Et ₂ In	4-Cl-C ₆ H ₄	Ph
-	Me ₂ Ga	-	4-NO ₂ -C ₆ H ₄	Ph
Me ₂ Al	-	-	4-Cl-C ₆ H ₄	Me
-	Me ₂ Ga	-	3,4-Cl ₂ -C ₆ H ₃	H

The products are highly soluble in moderately polar and co-ordinating solvents such as dichloromethane, chloroform, toluene, tetrahydrofuran and diethyl ether. They are slightly more soluble than their parent amidines in non-polar solvents such as pentane and hexane. As solids they decompose rapidly in air, and as solutions in organic solvents are very sensitive to hydrolysis, which produces the parent amidine ligand. Their hydrolysis reactions have been studied by N.M.R. and I.R. methods and the results are presented later in this chapter. However, the compounds can be conveniently handled in an inert atmosphere and manipulations were therefore carried out in a nitrogen filled glove box or by using a Schlenk-line equipped with dry argon.

The reactions were performed in toluene and hexane, although use of the latter proved to be more successful in three respects.

Firstly, the low solubility of the parent amidines in this solvent, compared to the generally greater solubility in toluene, minimises the amount of free ligand in solution available to react with the trialkyl metal, thereby effecting control over the exothermic reaction. For example, the reaction of trimethylaluminium and N,N'-diphenylbenzamidine in toluene solution in a 1:1 mole ratio gave the expected dimethylaluminium-N,N'-diphenylbenzamidinato product, along with a variable small quantity of the monomethylaluminium-bis(N,N'-diphenylbenzamidinato) derivative. This product presumably results from a rapid reaction of the dimethylaluminium derivative with the excess amidine still in solution. Repeated attempts to obtain solely this complex using toluene as solvent failed, even with the slow addition of the amidine to the reaction mixture. Changing the solvent to hexane gave more satisfactory results and the desired complex was obtained with both high purity and yield.

Secondly, removal of the toluene from a number of compounds proved difficult, particularly for the aluminium derivatives. Also because of the appreciable solubility of the dimethylmetal derivatives in non-co-ordinating solvents such as hexane, layering techniques with toluene-hexane mixtures proved unsatisfactory. Lower yields and impure products were obtained because of hydrolysis of the complexes. Free ligand was

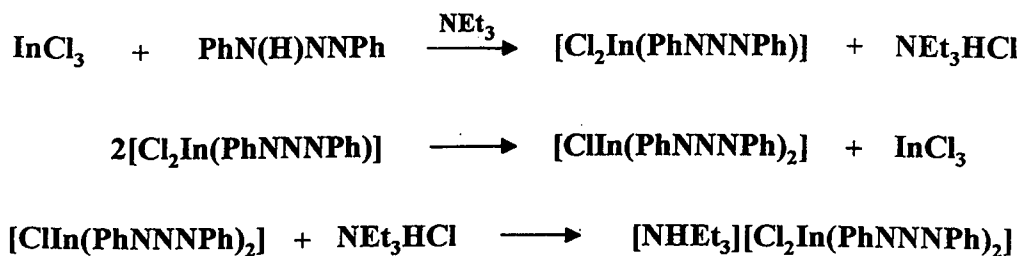
often detected from slight water contamination during the layering/recrystallisation process, despite rigorous precautions taken to exclude moisture.

Finally, when hexane was used as the reaction solvent, the products were generally sufficiently soluble in hexane to allow recrystallisation directly from the mother liquor, thereby minimising the chance of ingress of moisture, and the products were then obtained with both high purity and yield.

All the parent amidines used in this work were sublimed under vacuum before use and handled in the glove box to ensure the absence of impurities, such as water. This rather obvious procedure is worthy of further comment in two respects. Firstly, as mentioned above, solutions of these compounds in organic solvents are very sensitive to hydrolysis, and therefore the use of rigorously dry starting materials removes the need for repeated recrystallisation of the products. Secondly, it was found that removal of other trace impurities from the ligand greatly enhanced the potential for obtaining crystalline solids directly from the reaction mixture.

Two routes to the related class of dichlorometal–amidinato derivatives of gallium and indium were tried with limited success. The reaction between the trichlorides of gallium and indium and *N,N'*-diphenylbenzamidine in refluxing toluene for prolonged periods failed to liberate HCl and appeared to yield the respective metal(III)–chloride adducts of this ligand. This was indicated by the presence of an NH band in their I.R. spectra, although satisfactory elemental analysis for this formulation could not be obtained, despite repeated attempts to recrystallise a pure product. This result was disappointing in that this method would have provided a convenient route to this type of complex. A possible modification of it, which was not attempted because of shortage of time, would have been the addition of a Lewis base to the reaction mixture, such as triethylamine, whereupon two further possible reactions could occur. Firstly, the presence of the amine may allow isolation of the substitution product $[\text{MCl}_2(\text{PhNCPhNPh})]$ and HCl, the latter being trapped by the triethylamine. Secondly, an ionic complex of the type $[\text{NHEt}_3][\text{MCl}_2(\text{PhNCPhNPh})_2]$ could be obtained, similar to that obtained from the analogous reaction between indium trichloride and 1,3-

diphenyltriazene, namely $[\text{NEt}_3][\text{InCl}_2(\text{PhNNNPh})_2]$, reported by Barron and co-workers.¹⁹⁵ This is probably formed by a ligand disproportionation reaction to give the bis(triazenido) product, with subsequent re-association of the chloride to this complex.



The use of the lithium salt of *N,N'*-diphenylbenzamidine, formed by treatment of the free ligand with *n*-butyllithium in THF and subsequent reaction with InCl_3 gave a colourless solid, but characterisation of this product proved problematic. The elemental analysis results (C, H, N) were inconsistent with those required by a number of different reasonable formulations, and the ^1H and ^{13}C N.M.R. spectra indicated the presence of a number of different species. It is conceivable, in the light of the situation found for the triazenido derivative mentioned above, that these species could be formed by ligand exchange reactions yielding a mixture of products.

Spectroscopic Characterisation of the Dialkylmetal-Amidinato Complexes

Nuclear Magnetic Resonance Spectra

^1H N.M.R. spectra have been recorded routinely during the course of this work and have proved useful in verifying both the stoichiometry and purity of the reaction products. Details of the ^1H N.M.R. data for the individual compounds are given in the Experimental Section. All the spectra were recorded from CDCl_3 solutions, which allows comparisons to be made between the series of compounds, and all show a similar general appearance and therefore only the general features of the spectra will be discussed here. Some typical spectra of the dimethylaluminium-*N,N'*-diphenylacetamidinato, dimethylaluminium-*N,N'*-diphenylbenzamidinato and diethylmetal-*N,N'*-diphenylbenzamidinato (metal = gallium and indium) are reproduced in Figures 2.2 and 2.3, which show the relative positions of the resonances.

An important feature of the spectra of the dimethylmetal complexes is the presence of one sharp singlet resonance in the region expected for the organometallic protons. This is near -0.5 p.p.m. for the aluminium complexes, near 0.0 p.p.m. for the gallium complexes and near 0.2 p.p.m. for the indium complex $[\text{Me}_2\text{In}(\text{PhNCPPhNPh})]$. Similarly, the expected multiplets from the organometallic protons of the diethylmetal derivatives are well defined and occur further downfield, between 0.76 and 1.40 p.p.m. The sharp resonances attributed to the ligand protons indicate that the ligand is symmetrically co-ordinated to the metal centre, although some overlap of some of the aromatic proton multiplets is observed for the $\text{N,N}'$ -diphenylbenzamidinato derivatives, even in the high field 400MHz spectrum.

^{13}C N.M.R. spectra have been recorded for all the compounds prepared and the data are summarised in Tables 2.2 to 2.4. Assignments are based on ^1H - ^{13}C N.M.R. correlation experiments. The atom numbering scheme used in these assignments is given in the Experimental Section. The aryl carbon atoms that are bonded directly to the amidine nitrogen atoms consistently appear as a single sharp resonance around 144 to 147 p.p.m., and only three other peaks assigned to these aryl rings were found. These data are consistent with the ^1H N.M.R. results, showing that the two N -aryl rings are equivalent on the N.M.R. timescale. The ^{13}C N.M.R. signal corresponding to the skeletal amidinato carbon atom ($\text{N}\underline{\text{C}}\text{N}$) for the acetamidinato and benzamidinato derivatives occurs in the region 167.3 – 171.6 p.p.m. and for the formamidinato complexes in the region 154.7 – 157.3 p.p.m.

The position of the sharp organometallic carbon atom resonance is relatively unaffected by change of amidinato ligand, and is shifted further downfield on moving from aluminium through to indium. This resonance occurs near -11 p.p.m. for the dimethylaluminium complexes, near -6 p.p.m. for the dimethylgallium complexes and near -5 p.p.m. for the dimethylindium complex. The ^{13}C N.M.R. signals from the ethyl organometallic carbon atoms occur further downfield.

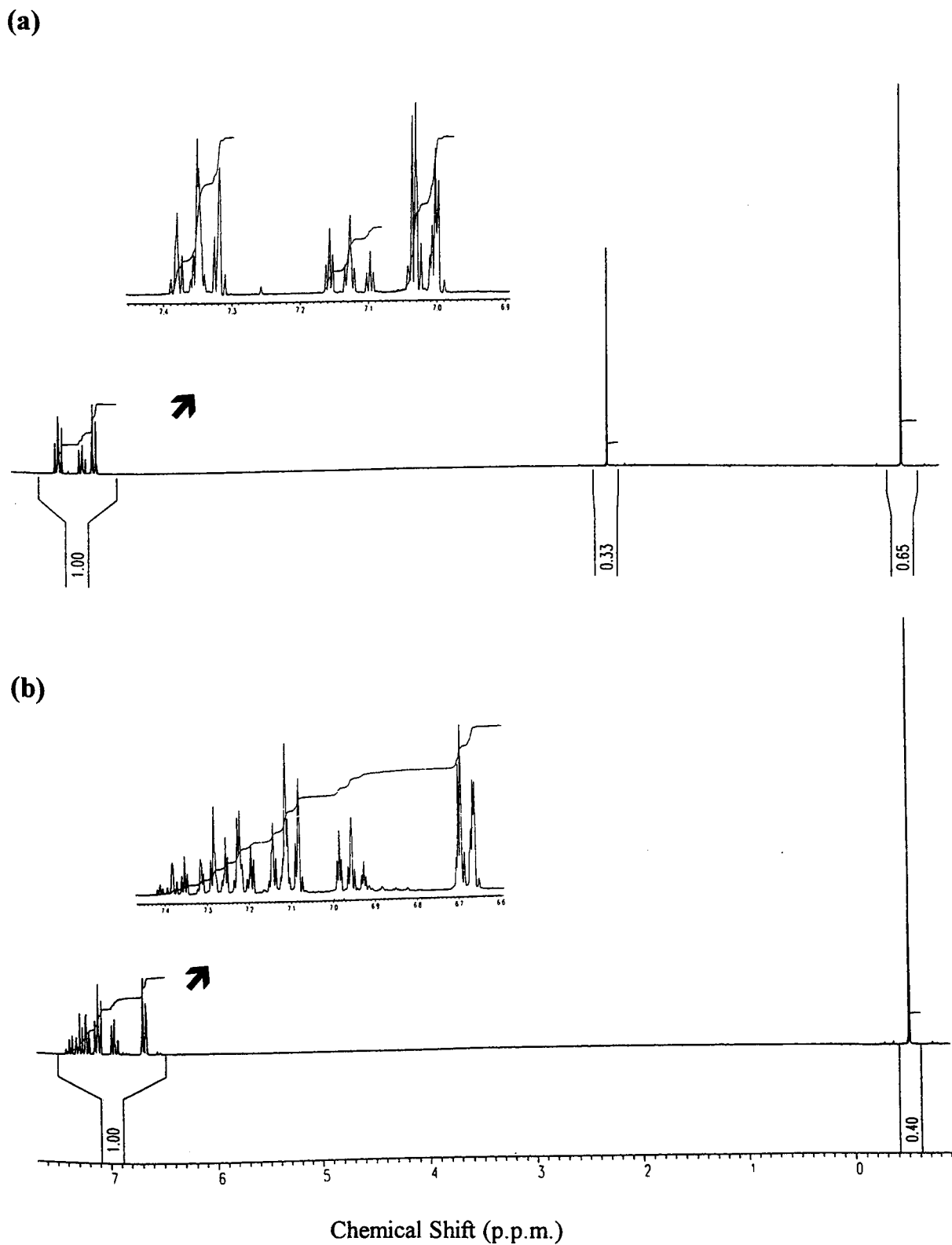
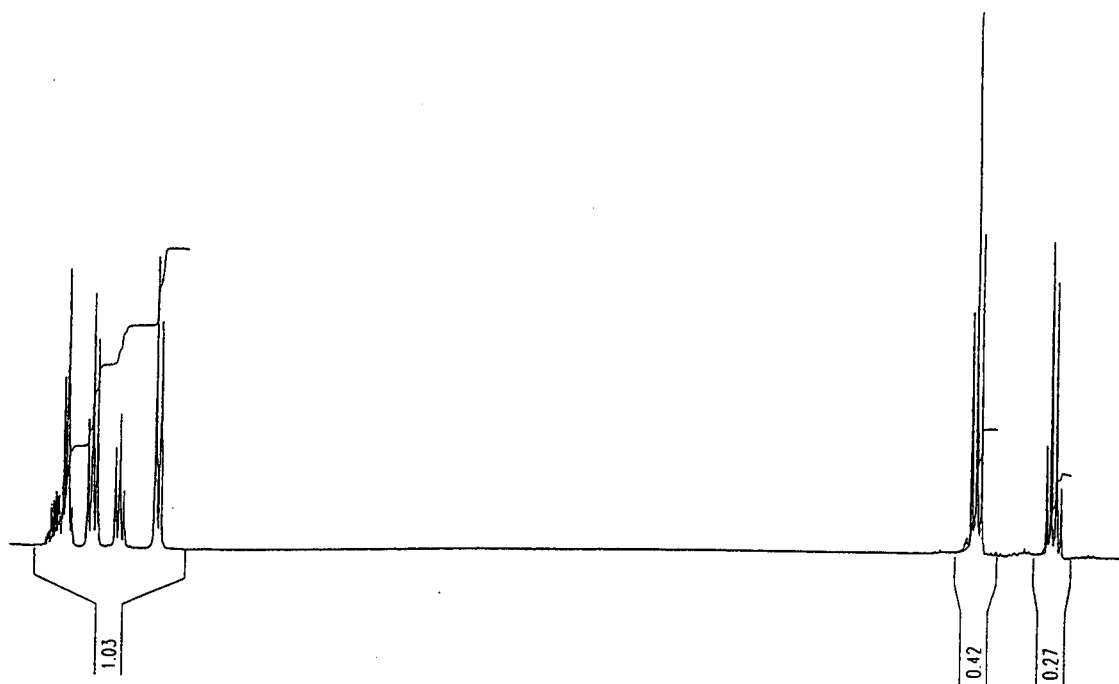


Figure 2.2 ^1H N.M.R. spectra of (a) dimethylaluminium- N,N' -diphenylacetamidinato, (b) dimethylaluminium- N,N' -diphenylbenzamidinato.

(a)



(b)

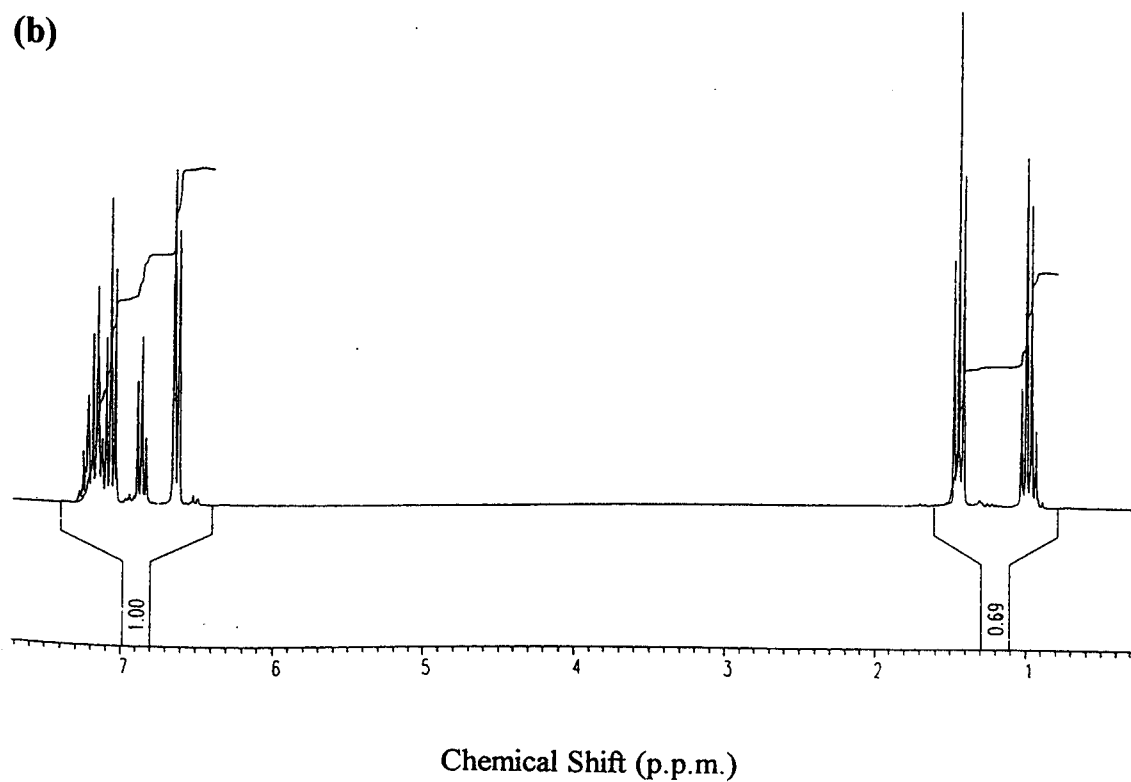


Figure 2.3 ^1H N.M.R. spectra of (a) diethylgallium- N,N' -diphenylbenzamidinato, (b) diethylindium- N,N' -diphenylbenzamidinato.

Table 2.2 Summary of Proton decoupled ^{13}C N.M.R. data (δ / p.p.m.) for dimethylaluminium-amidinato complexes.

Complex	Al-CH ₃	C-10	aromatic	C-6	C-1	C-5
[Me ₂ Al(PhNCPHPh)]	-11.23	-	123.19 (C4), 123.45 (C2) 128.63 (C3, C8) 129.10 (C7), 129.13 (C9)	130.43	142.67	170.26
[Me ₂ Al({4-ClC ₆ H ₄ })NCPHN- {4-Cl-C ₆ H ₄ })]	-11.34	-	124.56, 128.32, 128.68 128.76, 128.93, 129.01	130.89	141.08	170.36
[Me ₂ Al(PhNCMeNPh)]	-10.83	14.87	123.50 (C4), 123.77(C2) 129.07 (C3)	-	142.92	171.52
[Me ₂ Al({4-ClC ₆ H ₄ })NCMeN- {4-Cl-C ₆ H ₄ })]	-10.89	14.76	124.71, 129.20, 129.31	-	141.26	171.55
[Me ₂ Al(PhNCHNPh)]	-10.03	-	119.42 (C2), 122.85 (C4) 129.78 (C3)	-	143.65	158.66

Run as CDCl₃ solutions at 25°C

Table 2.3 Summary of Proton decoupled ^{13}C N.M.R. data (δ / p.p.m.) of dialkylgallium-amidinato complexes.

Complex	Ga-CR ₃	Ga-CH ₂ CH ₃	C-10	aromatic	C-6	C-1	C-5
[Me ₂ Ga(PhNCPPhNPh)]	-6.54	-	-	122.48 (C4), 123.23 (C2) 128.48 (C3), 128.54 (C8) 129.21 (C7), 129.85 (C9)	130.55	144.10	167.24
[Et ₂ Ga(PhNCPPhNPh)]	4.15	9.80	-	122.36 (C4), 123.33 (C2) 128.52 (C3), 128.65 (C8) 129.26 (C7), 129.84 (C9)	130.62	144.50	167.48
[Me ₂ Ga({4-Cl-C ₆ H ₄ })NCPPhN- {4-Cl-C ₆ H ₄ })]	-6.51	-	-	124.39, 127.87, 128.60 128.85, 129.18, 129.73	130.32	142.53	167.37
[Me ₂ Ga({4-NO ₂ Ph})NCPPhN- {4-NO ₂ -C ₆ H ₄ })]	-6.04	-	-	122.93, 124.33, 124.88 128.30, 128.70, 129.62	131.50	143.12	167.20
[Me ₂ Ga(PhNCMeNPh)]	-6.04	-	15.20	123.05 (C4), 123.30 (C2) 128.99 (C3)	-	144.42	167.46
[Me ₂ Ga(PhNCHNPh)]	-5.34	-	-	118.12 (C2), 122.75 (C4) 129.37 (C3)	-	143.88	154.68
[Me ₂ Ga({3,4-ClPh})NCHN- {3,4-Cl-C ₆ H ₃ })]	-5.56	-	-	117.90 (CH), 120.0 (CH) 126.48(C-Cl) 130.99 (CH) 133.21 (C-Cl)	-	143.20	155.13

Run as CDCl₃ solutions at 25°C

Table 2.4 Summary of Proton decoupled ^{13}C N.M.R. data (δ / p.p.m.) of dialkylindium-amidinato complexes.

Complex	In-CR ₃	In-CH ₂ CH ₃	C-10	aromatic	C-6	C-1	C-5
[Me ₂ In(PhNCPPhNPh)]	-5.21	-	-	121.90 (C4), 124.05 (C2) 128.15 (C7), 128.30 (C3) 128.99 (C9), 129.56 (C8)	132.48	146.21	168.32
[Et ₂ In(PhNCPPhNPh)]	9.02	11.63	-	121.65 (C4), 124.14 (C2) 128.15 (C7), 128.29 (C3) 128.87 (C9), 129.57 (C8)	132.70	146.69	168.76
[Et ₂ In({4-Cl-C ₆ H ₄ }NCPPhN- {4-Cl-C ₆ H ₄ })]	9.30	11.60	-	125.17, 126.93, 128.38 128.48, 129.34, 129.53	131.95	145.19	168.90
[Et ₂ In(PhNCMeNPh)]	9.33	11.45	15.35	122.97 (C4), 123.20 (C2) 128.69 (C3)	-	145.42	168.54
[Et ₂ In(PhNCHNPh)]	9.41	11.40	-	119.07 (C2), 122.20 (C4) 129.29 (C3)	-	146.80	157.29

Run as CDCl₃ solutions at 25°C

No deterioration of the complexes in solvents such as $\text{CD}_3\text{C}_6\text{D}_5$, CDCl_3 and CD_2Cl_2 was detected, provided the samples were kept well sealed. This confirms that these derivatives are stable to disproportionation, even after prolonged heating (48 hours) at temperatures of up to 60°C . However, the solutions are rapidly hydrolysed upon exposure to moist air, with the ^1H N.M.R. spectra showing splitting of the metal-alkyl resonance. In addition, new peaks corresponding to parent amidine resonances can be identified, along with the appearance of broad peaks assigned as NH or OH resonances. The ^1H N.M.R. spectrum obtained from a sample of $[\text{Me}_2\text{Ga}\{(4\text{-NO}_2\text{-C}_6\text{H}_4)\text{NCPH}(4\text{-NO}_2\text{-C}_6\text{H}_4)\}]$ (CDCl_3) which was reacted with approximately 0.5 mole equivalents of water is described below. A singlet found at 0.01 p.p.m. corresponds to unreacted complex, and a new singlet at -0.16 p.p.m. (with an integral value approximately equal to that for the previous resonance) is attributed to a gallium-containing species, such as $(\text{Me}_2\text{Ga})_2\text{O}$ or Me_2GaOH . The aromatic region is more complex, and peaks similar to those found in the spectrum of the parent ligand are present. A broad peak near 6.60 p.p.m. is assigned to the parent amidine NH proton.

Infra-Red Spectra

Infra-red spectroscopy has not been used routinely in this work because of the difficulty of detailed interpretation. Spectra for five dialkylmetal-amidinato complexes were recorded as Nujol mulls, and are summarised in detail in the Experimental Section.

The vibrational spectra of N,N'-disubstituted amidines have been studied in detail by Prevorsek¹⁹⁶ and the results are summarised as follows. Absorptions near 1640cm^{-1} are assigned to asymmetrical CN_2 stretching modes and those near 1588cm^{-1} to $\text{C}=\text{N}$ stretching modes. Both these bands are designated Amidine I bands. Bands in the region $1540\text{--}1390\text{cm}^{-1}$ are assigned as a complex mixture of $\text{C}-\text{N}$ stretching modes and $\text{N}-\text{H}$ deformation modes and are designated Amidine II bands. The complex series of absorptions in the region $1400\text{--}1240\text{cm}^{-1}$ are described as $\text{C}-\text{N}$ and $\text{C}-\text{C}$ stretching modes and $\text{N}-\text{H}$ deformation modes and are designated Amidine III bands.

The most notable features of the spectra of the complexes are the disappearance of the $\nu(\text{N-H})$ bands at ca 3250cm^{-1} as expected, a large shift in the position of the absorption band assigned to the $\nu_{\text{asym}}(\text{CN}_2)$ stretch in the Amidine I region to lower wavenumbers, and a reduction in the number and intensity of the absorptions in this region. The strong absorptions in the Amidine II region of the complexes remain essentially unchanged compared to those for the corresponding parent ligand, with many overlapping peaks. Since no consistent pattern emerges, only tentative assignment of the $\nu_{\text{sym}}(\text{CN}_2)$ can be made, although the band near 1500cm^{-1} in the spectra of the N,N'-diphenylbenzamidinato derivatives appears to be the prime candidate. The bands in the Amidine III region are also considerably reduced in intensity and are shifted to lower wavenumbers compared to those for the free ligand. The spectra clearly indicate co-ordination of the metal has occurred, with a weakening of the ligand C=N bond, and the relative simplicity of the spectra compared to that of the parent ligand suggests a symmetrical co-ordination of the ligand. The major differences between the spectra of the parent ligand N,N'-diphenylbenzamidine and the corresponding metal complexes are presented in Table 2.5.

A further important feature of the spectra of the complexes is the presence of medium intensity bands, though poorly defined, in the regions expected for the asymmetrical and symmetrical metal-carbon stretches (750 to 400 cm^{-1}), which overlap with weaker but sharper bands in the ligand spectrum. The positions of these bands are consistent with the corresponding values reported for the dimethylmetal-oxamidinato derivatives of aluminium, gallium and indium, which are shown in parenthesis in Table 2.5.

The use of infra-red spectroscopy as a technique for assigning the amidinato co-ordination mode in a particular complex is limited by the lack of data associated with complexes which have also been structurally characterised by X-ray crystallography. The spectrum reported for the dimeric complex $[\text{Me}_2\text{Ga}(\text{MeNCMeNMe})]_2$, with bridging amidinato ligands, shows $\nu_{\text{asym}}(\text{CN}_2)$ and $\nu_{\text{sym}}(\text{CN}_2)$ bands at 1552 and 1475cm^{-1} respectively,¹⁰⁹ whereas these bands occur at 1565 and 1400cm^{-1} respectively for the

bidentate chelate amidinato ligand in $[\text{AlCl}_2(\text{SiMe}_3\text{NCPPhNSiMe}_3)]$.¹⁹⁷ It is likely that these frequencies are also affected by the substituents on the amidine group, as analogously found for the carboxylates,¹⁹⁸ and it is therefore more useful to compare data from complexes with the same amidinato ligand. Thus the bidentate chelating amidinato ligand in the complex $[\text{Pt}(\text{PhNCPPhNPh})_2]$ shows a strong absorption band at 1589cm^{-1} , which was assigned to the $\nu_{\text{asym}}(\text{CN}_2)$ stretching mode.¹⁸⁷ Likewise, the molecular structure of the complex $[\text{Cu}_2(\text{PhNCPPhNPh})_4]$ contains bridging amidinato ligands, and bands at 1568 and 1463cm^{-1} were assigned as $\nu_{\text{asym}}(\text{CN}_2)$ and $\nu_{\text{sym}}(\text{CN}_2)$ stretching modes respectively for the CN_2 unit.¹⁹⁹ A symmetrical bidentate chelating bonding mode has been previously confirmed by an X-ray crystallographic study of the complex $[\text{Me}_2\text{Ga}(\text{PhNCPPhNPh})]$ in this laboratory,²⁰⁰ and the indium analogue has been shown to be isostructural in this work. Both molecular structures will be discussed later in this chapter. Therefore the positions of the band assignments presented in Table 2.5 refer to this mode of co-ordination, with the $\nu_{\text{sym}}(\text{CN}_2)$ and $\nu_{\text{asym}}(\text{CN}_2)$ stretching modes for both complexes occurring around 1595 and 1500cm^{-1} respectively. The aluminium derivative $[\text{Me}_2\text{Al}(\text{PhNCPPhNPh})]$ is suggested to have a similar structure based on the similar data for this complex.

Exposure of the Nujol samples to moist air causes hydrolysis of the complexes with the formation of the parent free or co-ordinated ligand being detected after five minutes. This is characterised by the appearance of bands attributed to $\nu(\text{N-H})$ absorptions near 3250cm^{-1} , and accordingly the remaining ligand bands revert to those found for the free ligand. The bands assigned to the dimethylmetal groups in the complex collapse, but additional weak and broad bands appear in this region, suggesting that the metal-carbon bond may remain intact. Interestingly, no broad peak is observed around 3600cm^{-1} as expected for metal hydroxy species, such as Me_2GaOH .¹⁴³

Table 2.5 The major differences between the I.R. spectra of N,N'-diphenylbenzamidine and the dimethylmetal complexes.

Region	I.R. Bands (cm^{-1})			
	[PhN(H)CPhNPh]	[Me ₂ Al(PhNCPPhNPh)]	[Me ₂ Ga(PhNCPPhNPh)]	[Me ₂ In(PhNCPPhNPh)]
Amidinium I	1627 (s)	—	—	—
	1588 (vs)	1595 (m)	1596 (m)	1594 (m)
	1578 (s)	1580 (m)	1580(m)	1581 (m)
Amidinium II	1532 (vs)	1497 (s)	1500 (s)	1495 (s)
	1485 (s)	1480 (m)	1463 (s)	1543 (m, br)
	1441 (vs)	1442 (m)		
Amidinium III	1333 (s)	1334 (w-m)	1317 (w-m)	1310 (w-m)
	1247 (s)	1210 (w)	1216 (w)	1212 (m)
	1223 (s)			
$\nu_{\text{asym}}(\text{M}-\text{C})$	—	675 (m) (665)	584 (br, m) (566)	505 (m) (503)
$\nu_{\text{sym}}(\text{M}-\text{C})$	—	625 (br, m) (—)	530 (br, m) (530)	465 (br, m) (473)

Recorded as Nujol mulls using CsI plates.

Numbers in parenthesis refer to reported values given in reference 110.

Mass Spectra

E.I. and C.I. mass spectra have been obtained for all the dialkylmetal compounds prepared and provide valuable evidence that the intended products have been formed. The E.I. spectra were obtained at source temperatures typically ranging from ca. (25 - 150)°C and showed weak peaks corresponding to monomeric molecular ions, with more intense peaks detected following the sequential loss of an alkyl radical and alkane. No evidence was found for ions corresponding to a dimeric structure in the vapour state, even in the spectra obtained at low temperature (ca. 25°C), although this does not exclude the possibility of weakly associated dimers in the solid state. Figures 2.4 to 2.6 show the significant ions of the E.I. spectra for the dialkylindium complexes with N,N'-diphenylbenzamidinato, N,N'-diphenylacetamidinato and N,N'-diphenylformamidinato, where the percentage relative intensities are given for the ^{115}In isotope (95.7% natural abundance). The E.I. spectra of the analogous aluminium and gallium complexes showed similar ions.

Fragmentation of the complexes involves loss of the amidinato groups as a whole and significant peaks corresponding to the dialkylmetal cation, $[\text{R}_2\text{M}]^+$ were detected, demonstrating the surprising stability of this 2 co-ordinate ion. The abundance of the $[\text{RM}]^{++}$ ion varied progressively from being barely detectable in the spectra of the aluminium complexes, to being significant in the spectra of the indium complexes. This variation is consistent with that observed in a mass spectroscopic study of the group 13 trimethyls and this study reports that the appearance of this ion involves a change of metal oxidation state to the +1 state.²⁰¹ In all cases, the abundance of the dimethylmetal cation was greater. The M^+ ion abundance generally showed a similar variation, reflecting the relative strengths of the metal-carbon bond.

The base peak in the N,N'-diphenyl substituted complexes is the same as that obtained for the parent amidines, ie. $[\text{PhNCR}]^+$ for the benzamidine and acetamidine, and $[\text{PhNH}_2]^+$ for the formamidine.²⁰²

At higher source temperatures (typically >250°C) additional peaks of higher mass units are seen, particularly for the aluminium complexes, which originate from ligand

Figure 2.5 Diethylindium-N,N'-diphenylacetamidinato fragmentation pattern

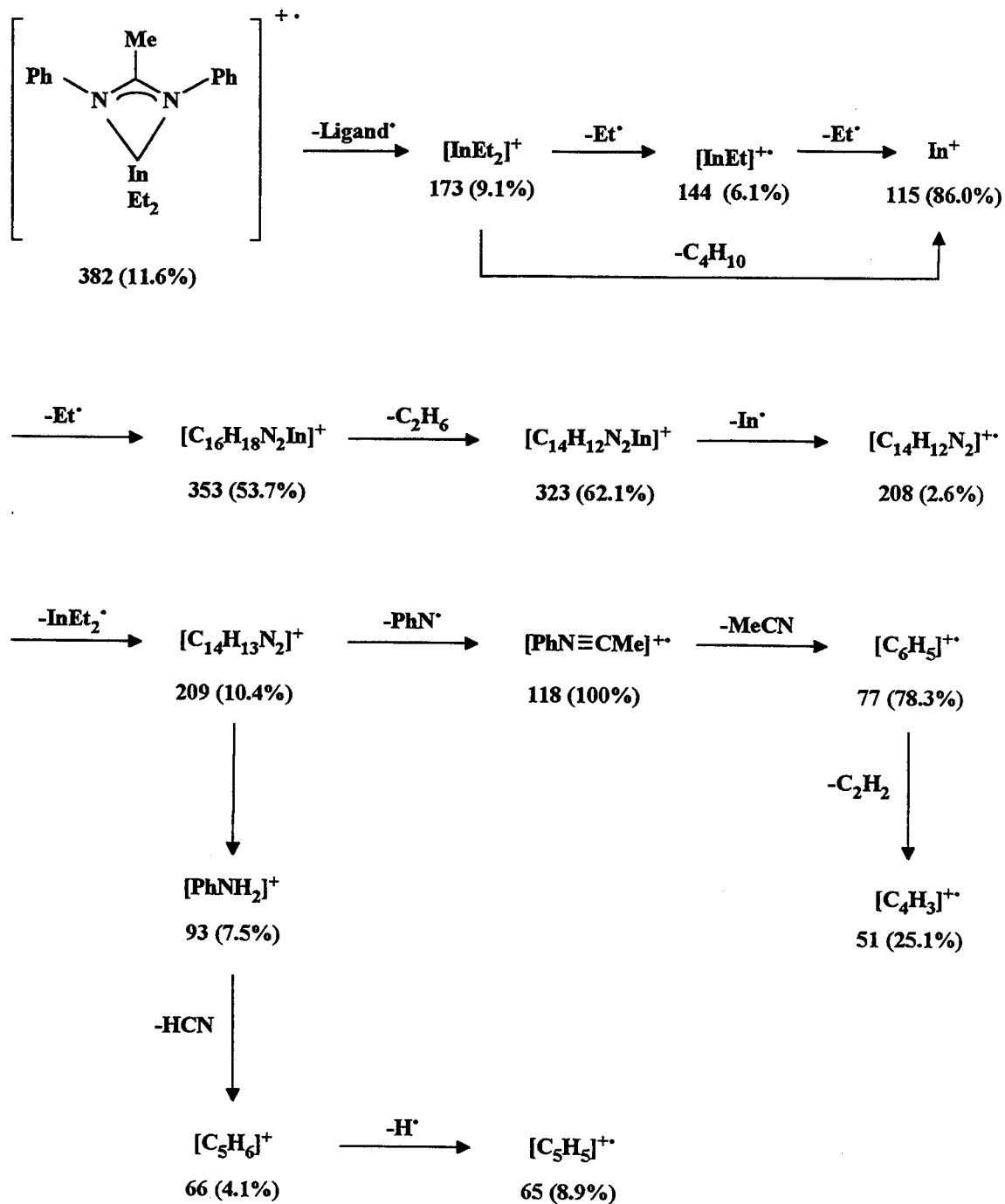
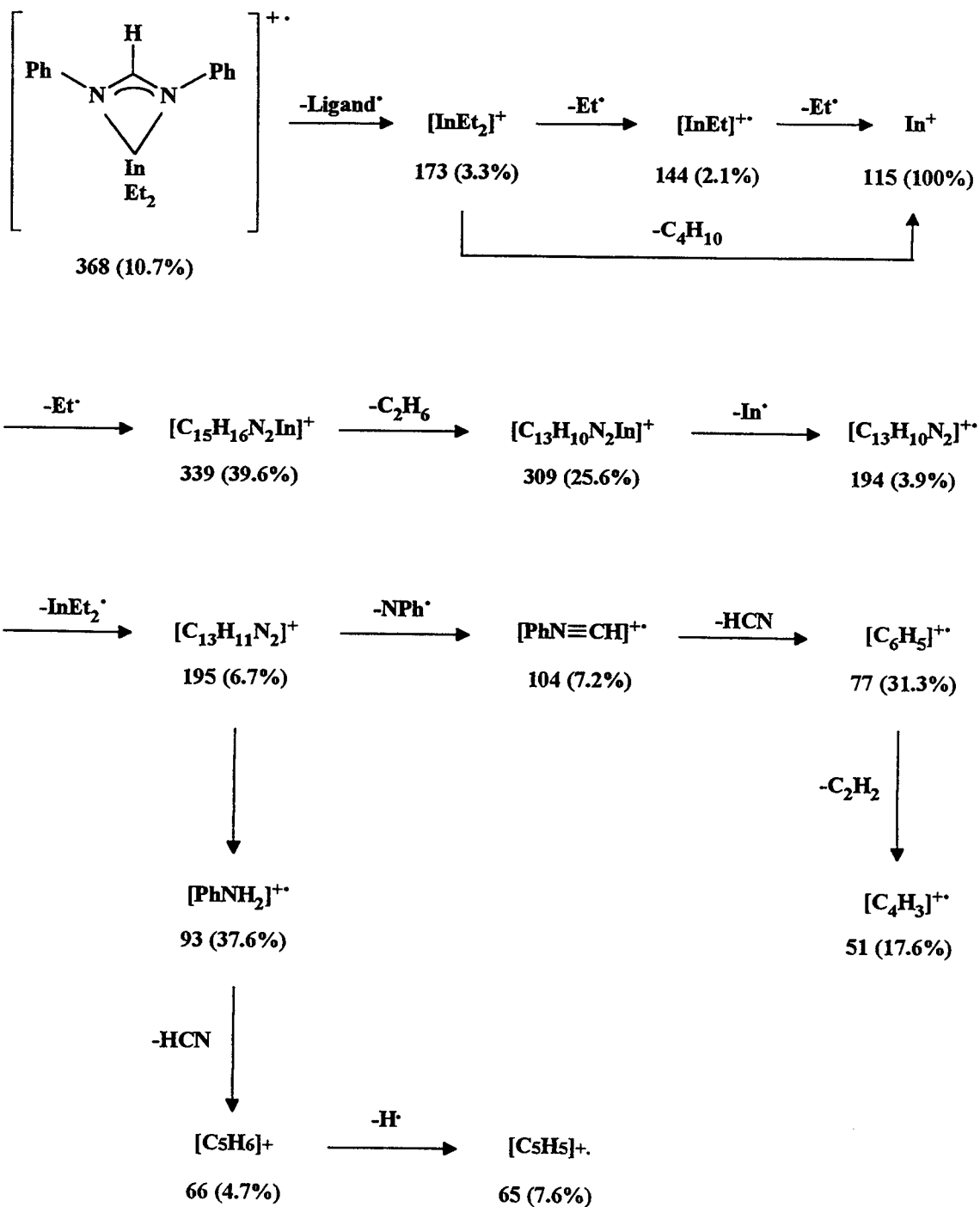


Figure 2.6 Diethylindium-N,N'-diphenylformamidinato fragmentation pattern



exchange reactions occurring in the source, producing species such as $[\text{MeAl}(\text{L})_2]^+$ and $[\text{Al}(\text{L})_3]^+$ ($\text{L} = \text{amidinato}$).

The C.I. spectra showed a more intense peak corresponding to the monomeric parent ion and gave a simplified fragmentation pattern compared to that obtained in the E.I. spectra, as expected. Fast atom bombardment (F.A.B.) spectra of the $\text{N}_2\text{N}'$ -diphenylbenzamidino complexes showed only amidino peaks, indicating hydrolysis of the complexes by the matrix nitrobenzylalcohol.

Additional peaks of low-medium relative intensity are found for the benzamidinato derivatives (i.e. when the central NCN carbon substituent is a phenyl ring), and are easily identified as corresponding to metal-containing species in the spectra of the gallium derivatives by the relative intensities of the two metal isotopes (^{69}Ga , 60.5%, ^{71}Ga , 39.5%). It is interesting to speculate that these peaks arise from a second less favoured fragmentation pathway, involving fragmentation of the ligand while still attached to the metal, as shown in Figure 2.7 below.

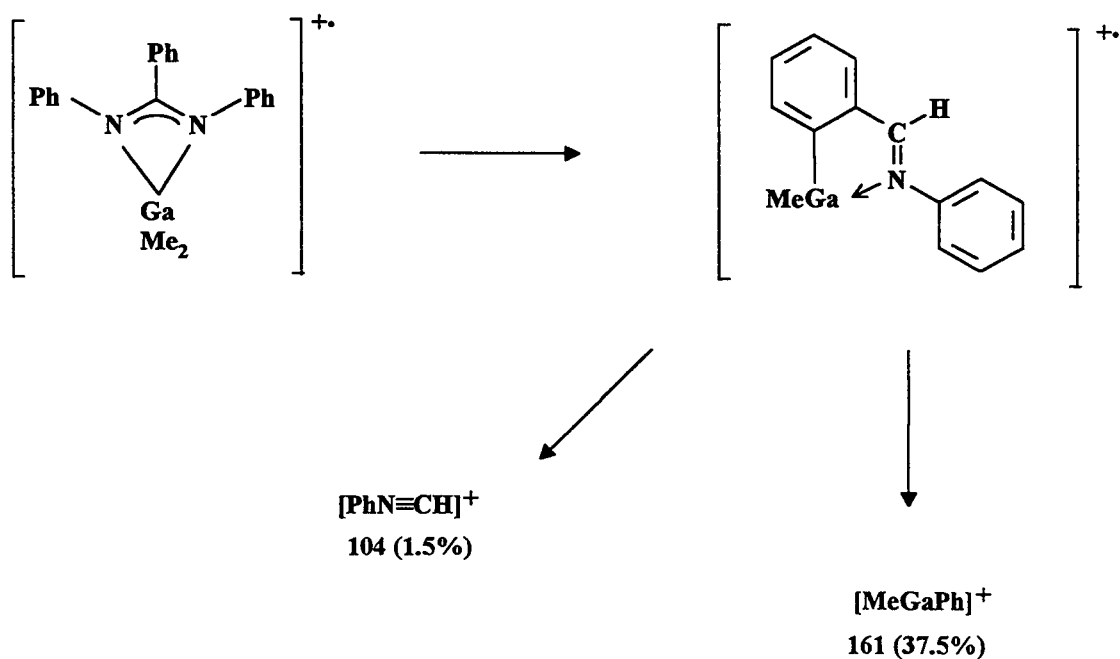


Figure 2.7 Proposed co-ordinated amidinato ligand fragmentation scheme

The peak corresponding to $[\text{MeGaPh}]^+$ is found in the spectra recorded for the substituted N-phenyl complexes, such as dimethylgallium-(N,N'-di-4-chlorophenylbenzamidinato), demonstrating that the phenyl group originates from the central C-phenyl substituent. The spectrum obtained for the diethylgallium-N,N'-diphenylbenzamidinato complex displays a peak corresponding to $[\text{EtGaPh}]^+$ ($m/z = 175$), but no peak at $m/z 161$, thus ruling out the possibility of it being assigned to $[\text{GaNHPH}]^+$ ($m/z 161$).

X-ray Crystallographic Studies

The spectroscopic data presented suggest that the N,N'-diaryl substituted amidines used in this study act as bidentate chelating ligands in the complexes of the general formula $[\text{R}_2\text{M}(\text{R}'\text{NCR}''\text{NR}''')]$. In order to obtain definitive structural evidence, considerable effort was put into attempts to grow X-ray quality single crystals of these complexes. However, this proved difficult for the following reasons. Firstly, the complexes were generally appreciably soluble in non-co-ordinating solvents such as hexane, so precluding the efficient use of layering techniques. In addition, hydrocarbon solutions of these complexes were found to be very sensitive over a period of time to trace quantities of moisture. Slow evaporation of solvent from hexane or toluene solutions kept in a nitrogen-filled glove box gave a crystalline material which, on analysis, proved to be parent ligand. Recrystallisation of the complexes directly from the concentrated mother liquor, using hexane as solvent, at -35°C for prolonged periods proved to be the most successful method for obtaining pure crystalline samples, but unfortunately these were frequently needle-like in appearance and unsuitable for X-ray diffraction work.

X-ray quality crystals of two complexes, $[\text{Et}_2\text{In}\{(4\text{-Cl-C}_6\text{H}_4)\text{CPhN}(4\text{-Cl-C}_6\text{H}_4)\}]$ and $[\text{Me}_2\text{In}(\text{PhNCPHNPh})]$ were eventually obtained by this method. Analysis of the X-ray data obtained for the former complex failed to reveal a refineable structure, probably because of crystal twinning. Finally, the X-ray diffraction study carried out on

the *N,N'*-diphenylbenzamidino derivative was successful and confirmed the monomeric form predicted for this complex. Two crystallographically independent indium molecules were found in the unit cell which differ slightly essentially in the orientation of the ligand phenyl rings, and two views of one of the molecules are shown in Figures 2.8 and 2.9. Principal bond lengths and angles are given in Table 2.6. The analogous gallium derivative $[\text{Me}_2\text{Ga}(\text{PhNCPhNPh})]$ has been shown to be isostructural by other studies in this laboratory,²⁰⁰ which allows useful comparisons to be made between the resulting geometries of these complexes.

As stated in the introduction, there are only five other definitive structures reported in the literature for the group 13 metal–amidino derivatives. The known structures are the monomeric aluminium $[\text{AlCl}_2(\text{Me}_3\text{SiNCPhNSiMe}_3)]$ and $[\text{Me}_2\text{Al}(\text{Me}_3\text{SiNCMeNSiMe}_3)]$ species,^{111,197} and the ionic thallium $[\text{Me}_3\text{SiN}(\text{H})\text{CPhN}(\text{H})\text{SiMe}_3][\text{TlCl}_3(\text{Me}_3\text{SiNCPhNSiMe}_3)]$ complex,²⁰³ all of which contain a chelating *N,N'*-trimethylsilyl–amidino group. The aluminium and gallium derivatives $[\text{Me}_2\text{M}(\text{MeNCMeNMe})]_2$ ($\text{M} = \text{Al}, \text{Ga}$) adopt a dimeric form with a puckered eight–membered ring with bridging *N,N'*-dimethylacetamidino ligands,¹⁰⁹ as shown for the gallium derivative in Figure 2.10, along with the relevant bond angles in Table 2.7.

In addition, Weidlein *et al*¹¹⁰ have found that the related di–amidino *N,N',N'',N'''*-tetramethyloxamidino reacts with two moles of Me_3M ($\text{M} = \text{Al}, \text{Ga}, \text{In}$) and the product has been shown by X–ray crystallography to form monomeric bis(dimethylmetal) complexes with this ligand. The molecular structure of the indium complex is shown in Figure 2.11 and the principal bond lengths and angles are given in Table 2.8.

The molecular structures of dimethylgallium–*N,N'*-dimethylacetamidino (Figure 2.10) and bis(dimethylindium)–*N,N',N'',N'''*-tetramethyloxamidino (Figure 2.11) will now be compared with that of dimethylindium–*N,N'*-diphenylbenzamidino under sections (a) and (b) below.

(a) The Metal Co-ordination Environment

The metal atom in all three complexes is in a distorted tetrahedral environment in which the dimethylmetal moiety is symmetrically bound to two amidinato-nitrogen atoms.

In the dimeric dimethylgallium-*N,N'*-dimethylacetamidinato complex, $[\{\text{Me}_2\text{Ga}(\text{MeNCMeNMe})\}_2]$, the co-ordination geometry around the gallium atom shows the least distortion from ideal tetrahedral geometry, with angles varying from around 105° to around 115° . This small distortion is a consequence of the two amidinato groups forming a puckered eight-membered ring arrangement.

In contrast, the bond angles around the indium atom in the oxamidinato complex are more distorted, because the metal atom is part of a five-membered chelate ring in which the mean *N-In-N* bite angle is decreased to only $76.2(2)^\circ$, with a concomitant increase in the *C-In-C* angle to $129.0(2)^\circ$. The indium-carbon bond lengths [aver. $2.175(6)\text{\AA}$] are essentially the same as those in $[(\text{Me}_2\text{InNMe}_2)_2]$.¹²⁹ The indium-nitrogen distances are fractionally longer, their average being $2.181(5)\text{\AA}$, which is significantly shorter than the mean *In-N* distance in $[(\text{Me}_2\text{InNMe}_2)_2]$, of $2.236(13)\text{\AA}$, perhaps because they are non-bridging. The *In-C* distances fall well within the expected ranges of $2.119(10)$ – $2.27(2)\text{\AA}$ whereas the *In-N* distances are short in comparison with the range $2.194(4)$ – $2.62(1)\text{\AA}$ found in previous studies of four co-ordinate organoindium species.^{108,204,205,206}

The metal co-ordination geometry found in dimethylindium-*N,N'*-diphenylbenzamidinato shows significant differences from the above two amidinato compounds, primarily because of the steric strain which results from formation of the four-membered *In(NCN)* ring. This leads to a further distortion of the tetrahedral arrangement around the metal, with the mean *N-In-N* bite angle decreasing to $58.9(2)^\circ$, whereas the mean *C-In-C* angle essentially remains unchanged at $128.1(3)^\circ$. The average *In-N* distance has increased to $2.253(4)\text{\AA}$, while the average *In-C* bond distance shortens to $2.144(6)\text{\AA}$, presumably to compensate for the longer *In-N* bonds.

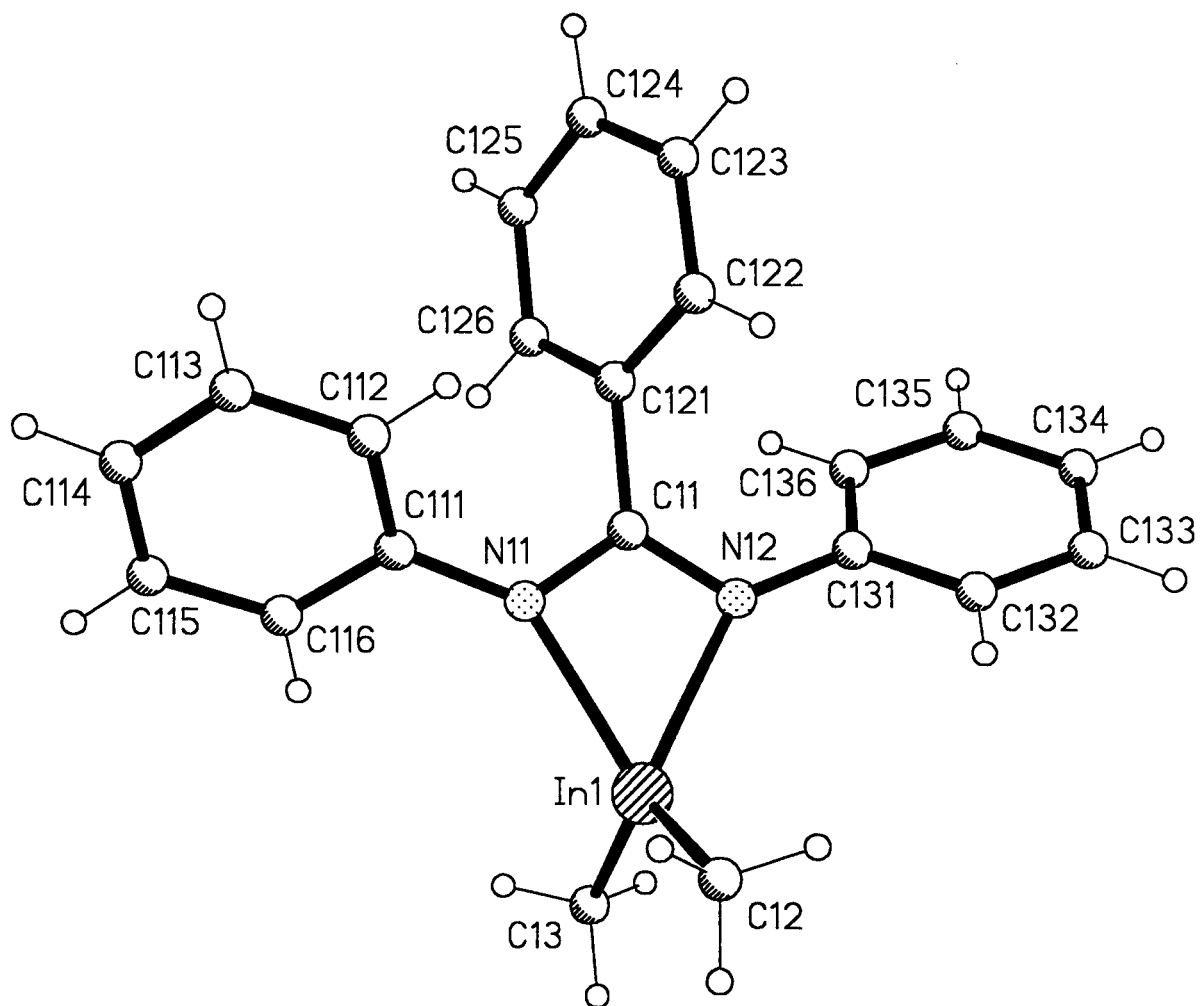


Figure 2.8 The molecular structure of dimethylindium-N,N'-diphenylbenzamidinato, as determined by a single crystal X-ray diffraction study.

Table 2.6 Principal bond lengths (Å) and angles (°) for [Me₂In(PhNCPhNPh)].

In(1)-C(12)	2.142(6)	In(1)-C(13)	2.138(7)
In(1)-N(11)	2.239(4)	In(1)-N(12)	2.265(4)
In(2)-C(22)	2.133(6)	In(2)-C(23)	2.143(6)
In(2)-N(22)	2.249(4)	In(2)-N(21)	2.258(5)
N(11)-C(11)	1.328(8)	N(11)-C(111)	1.404(8)
N(12)-C(11)	1.314(8)	N(12)-C(131)	1.416(8)
N(21)-C(21)	1.349(8)	N(21)-C(211)	1.420(8)
N(22)-C(21)	1.302(7)	N(22)-C(231)	1.436(7)
C(11)-C(121)	1.514(8)	C(21)-C(221)	1.487(8)
C(12)-In(1)-C(13)	125.2(3)	C(12)-In(1)-N(11)	116.8(3)
C(13)-In(1)-N(11)	111.6(3)	C(12)-In(1)-N(12)	112.5(2)
C(13)-In(1)-N(12)	113.6(3)	N(11)-In(1)-N(12)	58.8(2)
C(22)-In(2)-C(23)	130.9(3)	C(22)-In(2)-N(22)	107.7(2)
C(23)-In(2)-N(22)	113.3(3)	C(22)-In(2)-N(21)	112.4(2)
C(23)-In(2)-N(21)	111.4(2)	N(22)-In(2)-N(21)	58.9(2)
C(11)-N(11)-C(111)	125.2(5)	C(11)-N(11)-In(1)	94.2(4)
C(111)-N(11)-In(1)	140.3(4)	C(11)-N(12)-C(131)	125.2(5)
C(11)-N(12)-In(1)	93.5(4)	C(131)-N(12)-In(1)	141.1(4)
C(21)-N(21)-C(211)	123.4(5)	C(21)-N(21)-In(2)	93.0(4)
C(211)-N(21)-In(2)	140.6(4)	C(21)-N(22)-C(231)	126.5(5)
C(21)-N(22)-In(2)	94.7(4)	C(231)-N(22)-In(2)	138.5(4)
N(12)-C(11)-N(11)	113.6(5)	N(12)-C(11)-C(121)	124.9(6)
N(11)-C(11)-C(121)	121.5(6)	N(22)-C(21)-N(21)	113.3(5)
N(22)-C(21)-C(221)	125.4(6)	N(21)-C(21)-C(221)	121.3(6)

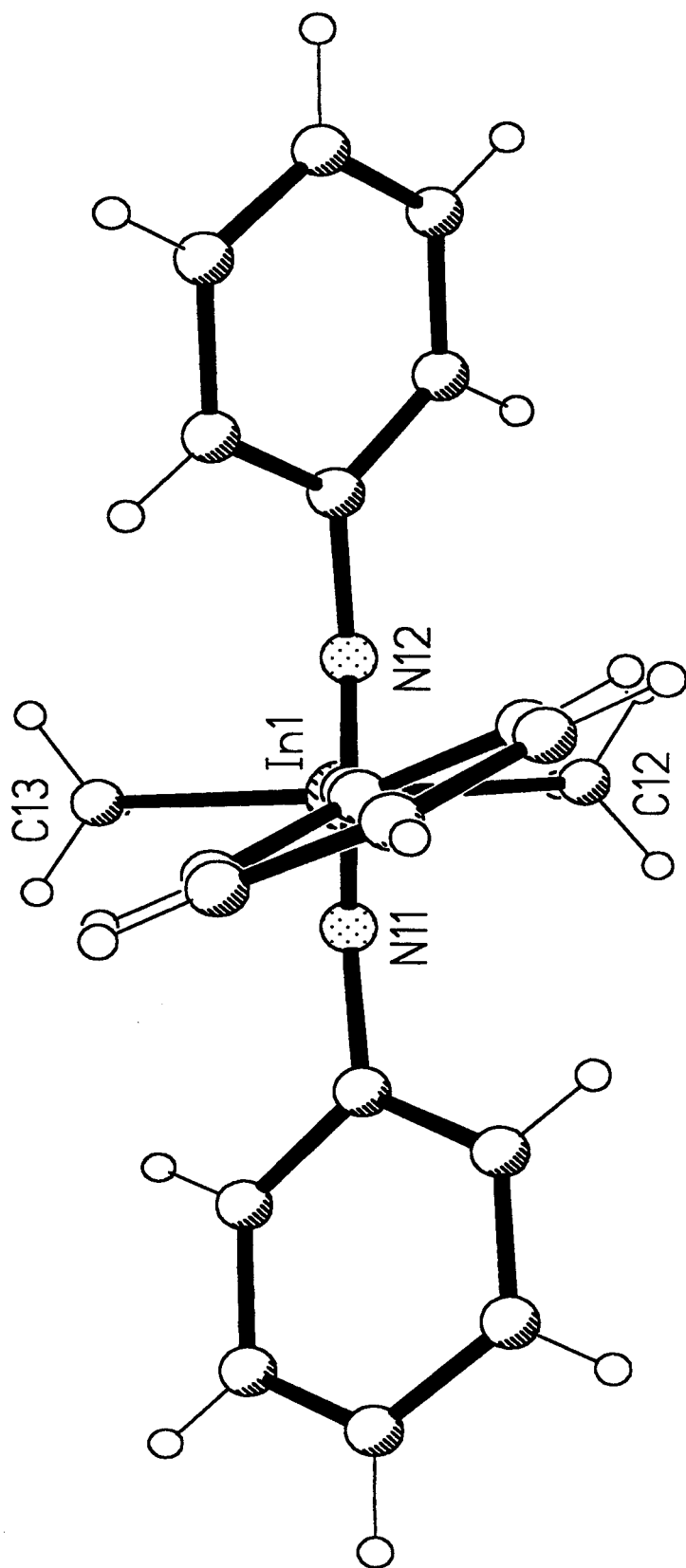


Figure 2.9 A further view of the molecular structure of dimethylindium-N,N'-diphenylbenzamidinato, showing the orientation of the phenyl rings.

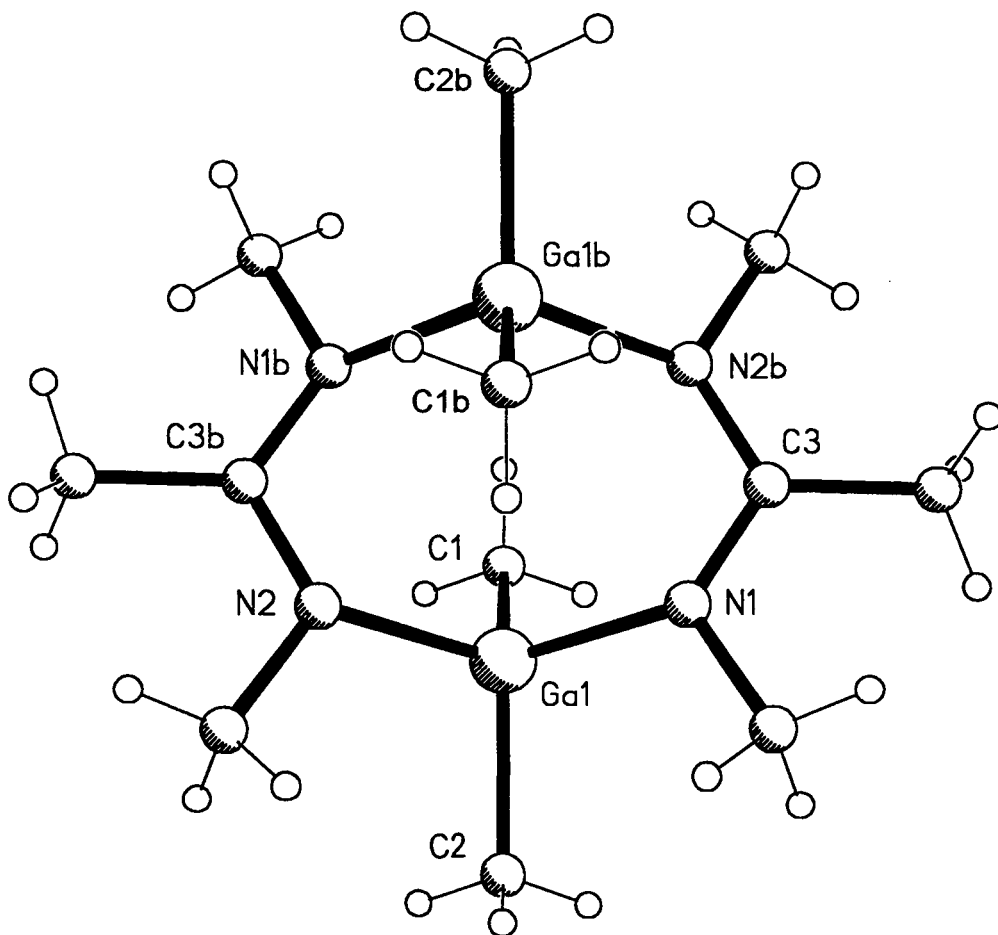


Figure 2.10 Molecular structure of dimethylgallium-*N,N'*-dimethylacetamidinato.¹⁰⁹

Table 2.7 Relevant bond angles (°) for dimethylgallium-*N,N'*-dimethylacetamidinato.

N(1)-Ga(1)-N(2)	110.0(2)	C(1)-Ga(1)-C(2)	114.7(2)
C(1)-Ga(1)-N(1)	110.0(2)	C(2)-Ga(1)-N(1)	106.1(2)
C(1)-Ga(1)-N(2)	110.7(2)	C(2)-Ga(1)-N(2)	105.1(2)
Ga(1)-N(1)-C(3)	122.4(3)	Ga(1)-N(1)-C(4)	116.4(3)
C(4)-N(1)-C(3)	117.4(4)	Ga(1)-N(2)-C(3)	120.7(3)
Ga(1)-N(2)-C(5)	117.9(3)	C(3)-N(2)-C(5)	117.2(4)
N(1)-C(3)-N(2)	117.4(4)	N(1)-C(3)-C(6)	121.6(4)
C(6)-C(3)-N(2)	121.0(4)		

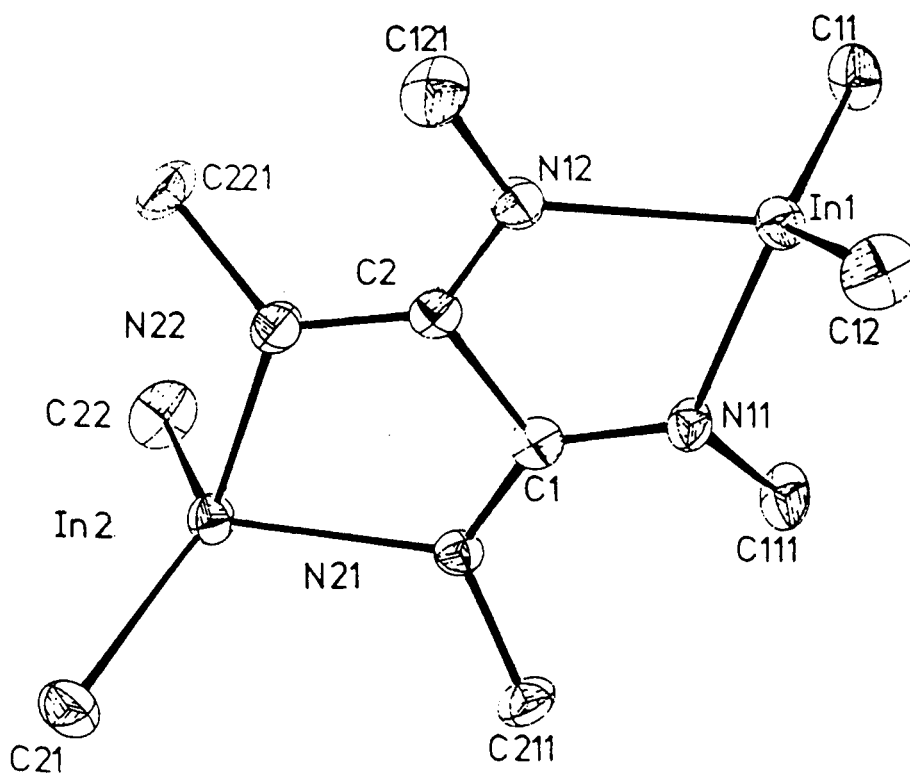


Figure 2.11 Molecular structure of bis(dimethylindium)-N,N',N'',N'''-tetramethyloxamidinato. Hydrogen atoms omitted for clarity.¹¹⁰

Table 2.8 Relevant bond lengths (Å) and angles (°) for bis(dimethylindium)-N,N',N'',N'''-tetramethyloxamidinato.

In(1)-N(11)	2.182(5)	In(1)-N(12)	2.183(5)
In(2)-N(21)	2.182(5)	In(2)-N(22)	2.178(5)
In(1)-C(11)	2.182(6)	In(1)-C(12)	2.173(6)
In(2)-C(21)	2.165(5)	In(2)-C(22)	2.181(6)
N(11)-C(1)	1.329(7)	N(12)-C(2)	1.326(7)
N(21)-C(1)	1.329(7)	N(22)-C(2)	1.342(7)
C(1)-C(2)	1.546(8)		
N(11)-In(1)-N(12)	76.0(2)	N(21)-In(2)-N(22)	76.4(2)
C(11)-In(1)-C(12)	131.8(2)	C(21)-In(2)-C(22)	126.1(2)
N(11)-C(1)-N(21)	128.8(5)	N(12)-C(2)-N(22)	129.5(5)

This complex has the same basic structure as the gallium analogue [Me₂Ga(PhNCPPhNPh)]. The extent of distortion of the tetrahedral geometry from the idealised 109° 28' is significantly less for this gallium derivative, as shown by the larger metal bite angle N–Ga–N of 65.0(3)° [c.f. 58.9(2)° for the indium complex]. This result is not unexpected considering the smaller covalent radius of Ga [1.26Å] compared to that of In [1.44Å]²⁰⁷ and the limited bite size of the ligand. In addition, the difference in the calculated radii between these two metals is comparable to the difference in the average metal–carbon and metal–nitrogen distances of 0.20 and 0.21Å respectively, suggesting similar metal–ligand interactions in both complexes.

b) Ligand Structure

The molecular and crystal structure of the parent amidine [PhN(H)CPhNPh] has been determined,²⁰⁸ which allows an examination of the change of structural parameters that occur on complexation to the metal entity. The ligand exists as an asymmetric dimer, linked by a single N–H···N interaction [2.46(5)Å], and the skeletal NCN bond lengths are differentiated into amine [1.360(8)Å aver.] and imine [1.302(7)Å aver.] carbon–nitrogen bond types and are comparable to those found in similar amidines.²⁰⁸ The NCN angle, [121.5(5)° aver.], indicates near ideal *sp*²–hybridisation of the central carbon and again is close to that found in other amidines.²⁰⁸ The mean N–C(phenyl) bond lengths [1.411(8)Å] are significantly shorter than expected for a pure single covalent N–C distance [1.47Å], and the mean central C–(phenyl) bond distance [1.485(8)Å] is intermediate between a normal single (C–C) and double (C=C) covalent bond distance, indicating some degree of conjugation of these substituents with the central NCN unit.

Complexation of the ligand in dimethylindium-*N,N'*-diphenylbenzamidinato causes significant structural changes in the NCN unit. The difference between the two skeletal C–N bond distances decreases [0.032(7)Å aver.], indicating that the π –electrons are further delocalised in the NCN skeletal framework, but these bonds do not show the symmetrical delocalised system found in the analogous dimethylgallium complex, in

which the two distances are 1.331(11) and 1.335(11)Å. There is little change in the mean N–C(phenyl) and C–C(phenyl) bond distances [1.419(8) and 1.500(8)Å aver. respectively], indicating that there is no further delocalisation of the NCN fragment to the rings.

The chelate NCN angle of 113.5(5)° aver. found in the complex shows a reduction of 8.0(5)° compared to the value in the free ligand. This departure from the ideal value is indicative of the inherent strain within the four-membered chelate ring, but is significantly larger than the chelate angle in the analogous gallium derivative of 110.8(7)°, and this is in line with the relative covalent radii of these two metals. Transition metal complexes with bidentate chelate co-ordination of this ligand have NCN angles in the range 106.7(5)–110.0(6)°. The data shown below suggest this angle is sensitive to the size of the metal, although the trend of bite angle with covalent radius is only approximate because of the imperfect nature of these radii values.

Table 2.9 Structural parameters in bidentate chelate N,N'-diphenylbenzamidinato groups

Complex	Average NCN Angle (°)	Average M-N (Å)	Covalent Radius (Å) ²⁰⁷	Reference
[Me ₂ In(PhNCPhNPh)]	113.5(5)	2.253(4)	1.44	This work
[Me ₂ Ga(PhNCPhNPh)]	110.8(7)	2.041(8)	1.26	199
[Rh(PhNCPhNPh)(C ₈ H ₁₂)]	110.0(6)	2.100(6)	1.35	209
[Pd ₂ (PhNCPhNPh) ₂ (μ-PhNC(Ph)NPh) ₂]	109.7(17)	2.06(1)	1.31	210
[Pt(PhNCPhNPh) ₂]	106.7(5)	2.033(5)	1.28	187

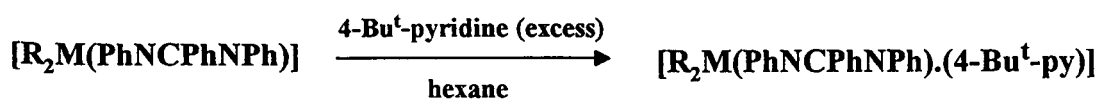
In all cases, this angle is considerably smaller than those found in bridging N,N'-diphenylbenzamidinato complexes (e.g. [Pd₂(PhNCPhNPh)₄], 123.2(13)° aver.).²¹⁰ Comparison of the NCN angles in the dimethylgallium and dimethylindium-N,N'-diphenylbenzamidinato derivatives, [Me₂M(PhNCPhNPh)] (M = Ga, In) [113.5(5) aver., 110.8(7)° respectively] with that found the dimeric dimethylgallium-N,N'-

dimethylacetamidinato derivative, [117.4(4)°], where the acetamidinato ligand acts in a bridging co-ordination manner, reveals the lower valency strain in the puckered eight-membered ring found for the acetamidinato derivative.

The structure of the ligand in bis(dimethylindium)-N,N',N'',N'''-tetramethyloxamidinato is not directly comparable because each indium atom is co-ordinated to one nitrogen atom of each amidine skeletal fragment, giving two fused five-membered chelate rings with a large N-C-N angle of 129.2(5)° (aver.). However, the skeletal C-N distances are equal, thus indicating complete delocalisation within the NCN units, although interestingly, the C-C bond distance linking the two amidinato groups of 1.546(8)Å suggests that delocalisation does not extend throughout the ligand. This five-membered chelate arrangement results in less distortion of the metal co-ordination geometry than the alternative four-membered chelate arrangement and the geometry may be considered as midway between the bridging and chelate geometries.

Reaction of the Dialkylmetal-N,N'-diphenylbenzamidinato Complexes of Aluminium, Gallium and Indium with Lewis Bases

Although the metal atom in these compounds is already four co-ordinate, it was of interest to see whether the metal centre would still act as a Lewis acid and either expand its co-ordination shell or displace one arm of the amidinato ligand on reaction with a Lewis base. Treatment of hexane solutions of the compounds dimethylgallium-N,N'-diphenylbenzamidinato and diethylindium-N,N'-diphenylbenzamidinato with the monodentate Lewis base, 4-*tert*-butyl-pyridine, at room temperature yields the 1:1 adducts shown below.



The nature of these compounds was investigated by elemental analysis (C, H, N), which gave results consistent with the formation of 1:1 adducts. The question as to whether the metal centre adopts a four- or five-co-ordination, or some other structural arrangement, was answered by an X-ray crystallographic study as outlined below.

Spectroscopic Properties of the Adducts

Nuclear Magnetic Resonance Spectra

The ^1H and ^{13}C N.M.R. data, recorded from CDCl_3 solution for both compounds, are presented in Tables 2.10 and 2.11 as is that obtained for the free Lewis base. These chemical shifts clearly show that a significant Lewis acid-base interaction occurs in solution. The ^1H N.M.R. spectra are also useful in determining the stoichiometry of the reaction products, in particular by integration of the sharp singlet at 1.3 p.p.m. assigned to the *tert*-butyl protons. Complexation moves the pyridine ligand proton resonances downfield by about 0.3 to 0.5 p.p.m. The position of the organometallic proton resonance in the adduct is essentially the same as the chemical shift found in the corresponding dialkylmetal-amidinato complex. This is slightly surprising in view of the expected change in the co-ordination number of the metal.

Table 2.10 ^1H N.M.R. data for the dimethylmetal-N,N'-diphenylbenzamidinato adducts and parent Lewis base.

Compound	$\delta/\text{p.p.m.}$ (multiplicity, integral)
4-Bu ^t -pyridine	0.78 (s, 9) 6.73 ("d", 2) 8.01 ("d", 2)
$[\text{Me}_2\text{Ga}(\text{PhNCPhNPh}).(4\text{-Bu}^t\text{-py})]$	0.03 (s, 6) 1.32 (s, 9) 6.64 (d, 4) 6.86-7.11 (m, 6) 7.24-7.30 (m, 7) 8.52 (d, 2)
$[\text{Et}_2\text{In}(\text{PhNCPhNPh}).(4\text{-Bu}^t\text{-py})]$	0.91 (q, 4) 1.30 (s, 9) 1.41 (t, 6) 6.53 (d, 4) 6.77 (t, 2) 6.93 (t, 4) 7.07-7.19 (m, 5) 7.22 (d, 2) 8.35 (d, 2)

Recorded as CDCl_3 solutions. Full assignments given in Experimental Section.

Conversely, the ^{13}C resonance of the metal-carbon atom in the gallium adduct shows a significant downfield shift of 1.03 p.p.m. compared to the corresponding value found in the spectrum of the dimethylgallium-amidinato complex, whereas in the indium adduct it is shifted upfield by 1.88 p.p.m. compared to the corresponding value found in the spectrum of the diethylindium-amidinato coimply. The similarity of the ^{13}C chemical shifts of the central NCN carbon atom with those found for the dialkylmetal complexes suggests that the mode of co-ordination of the amidinato ligand in these complexes is little changed.

Table 2.11 ^{13}C N.M.R. data for the dimethylmetal-N,N'-diphenylbenzamidinato adducts and parent Lewis base.

Compound	$\delta/\text{p.p.m.}$					
4-Bu ^t -pyridine	29.38	33.43	119.57	148.63	158.50	
[Me ₂ Ga(PhNCPhNPh).(4-Bu ^t -py)]	-5.51	30.41	34.50	120.65	123.28	124.78
	127.79	128.46	128.52	129.54	130.71	
	144.52	149.53	160.21	167.20		
[Et ₂ In(PhNCPhNPh).(4-Bu ^t -py)]	7.14	12.23	30.36	34.65	120.87	121.83
	124.67	127.66	127.98	128.09	129.95	
	132.65	146.25	148.80	160.78		
	168.61					

Recorded as CDCl₃ solutions.

Infra-red Spectra

Infra-red spectra of both compounds were recorded from Nujol mulls and are summarised in the Experimental Section. They show a similar general appearance to the spectra obtained for the dialkylmetal-N,N'-diphenylbenzamidinato counterparts. The most notable difference is the presence of extra bands attributable to the complexed 4-*tert*-butyl-pyridine ligand. In particular there is an additional band in the Amidine I region at 1616cm⁻¹ in the spectrum of the gallium complex and at 1607cm⁻¹ in the spectrum

of the indium complex. Both of these absorptions are of medium intensity and are assigned to a pyridine ring stretching vibration. The band assigned to the $\nu_{\text{asym}}(\text{CN}_2)$ stretching vibration in the spectra of both adducts is not significantly different to the value found for the corresponding dialkylamidinato complex, although the band which is tentatively assigned to the $\nu_{\text{sym}}(\text{CN}_2)$ stretching vibration is shifted to wavenumbers lower by ca. 10cm^{-1} , that is, to 1489cm^{-1} . These spectroscopic similarities also suggest a similar bidentate chelate amidinato co-ordination mode in these adducts to that established for the dialkylmetal complexes.

Mass Spectra

Only the C.I. mass spectra showed peaks corresponding to the molecular ion of the adducts, although of low relative intensity. The highest mass peaks under E.I. ionisation correspond to loss of the Lewis base, producing the ions $[\text{R}_2\text{M}(\text{PhNCPPhNPh})]^+$ (where $\text{M} = \text{Ga}$, $\text{R} = \text{Me}$; $\text{M} = \text{In}$, $\text{R} = \text{Et}$). This is presumably caused by the relatively high temperatures ($> 200^\circ\text{C}$) required to produce these spectra. Had time permitted, it would have been interesting to carry out a more thorough investigation using various ionisation potentials and source temperatures to find the optimum conditions in order to establish qualitatively the relative strength of the Lewis acid-base interaction in the gas phase. The remaining E.I. fragmentation patterns closely resemble those observed for the corresponding dialkylmetal-amidinato complexes.

X-ray Crystallographic Studies

Single crystals of the gallium adduct were grown from a hexane solution and an X-ray crystallographic study was carried out to determine the type of Lewis acid–base interaction and the effect of this ligand on the metal and amidinato ligand co-ordination geometry. Analysis of the X-ray data led to the molecular structure shown in Figures 2.12 and 2.13. The principal bond lengths and angles are given in Table 2.12. The structure consists of a monomeric five co-ordinate gallium atom with the amidinato ligand bound in a bidentate chelate manner.

Examples of crystal structures of five co-ordinate group 13 metals are relatively rare, and usually show a distorted trigonal bipyramidal metal geometry, unless the geometry is constrained by the configuration of the ligand, as in the alkylmetal-porphyrins and related tetraaza-macrocyclic compounds discussed in Chapter 4, where a square pyramidal metal geometry is observed.

(a) Metal Co-ordination Environment

The geometry around the metal is best described as highly distorted trigonal bipyramidal with the bidentate chelate amidinato nitrogen atoms in the pseudo-axial [N(2)] and equatorial [N(1)] positions and the Lewis base in the remaining pseudo-axial site [N(3)]. Departure from the ideal trigonal bipyramidal geometry can be seen in the axial N(2)–Ga(1)–N(3) bond angle of $148.8(12)^\circ$. This distortion is a consequence of the rigidity and small bite angle of the amidinato ligand. The gallium atom lies $0.171(3)\text{\AA}$ out of the equatorial plane defined by N(1), C(2) and C(3) in the direction of the axial pyridine substituent, thereby reducing the steric interactions between this ligand and the equatorial substituents.

The equatorial Ga–N amidinato distance of $2.010(3)\text{\AA}$ is significantly shorter than the Ga–N distances found in dimethylgallium-N,N'-diphenylbenzamidinato of $2.036(8)$ and $2.045(7)\text{\AA}$,²⁰⁰ though the corresponding axial bond length of $2.347(3)\text{\AA}$ is considerably longer. Several studies on five co-ordinate trigonal bipyramidal gallium

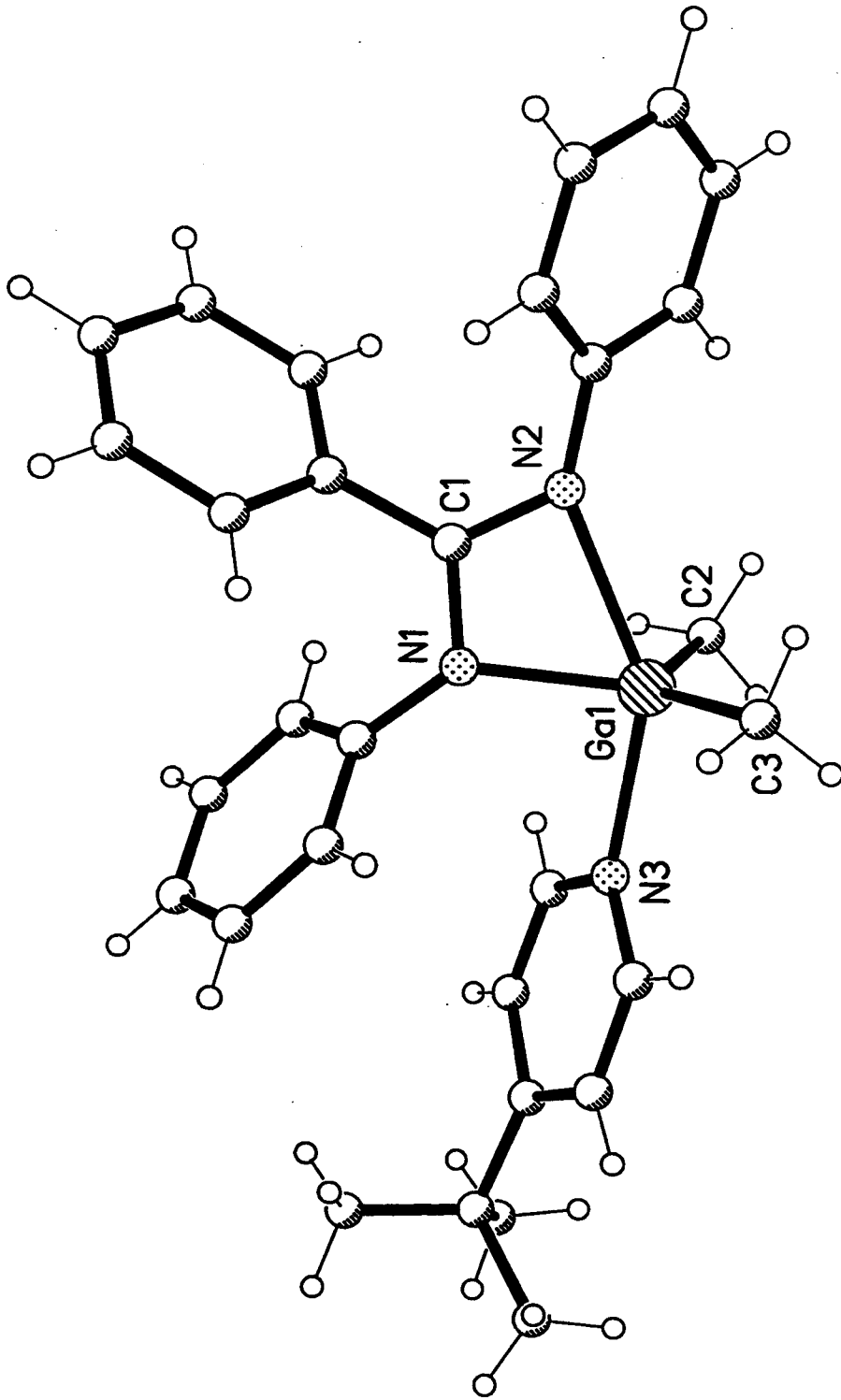


Figure 2.12 The molecular structure of dimethylgallium-N,N',N''-diphenylbenzamidinato.4-Bu¹-pyridine.

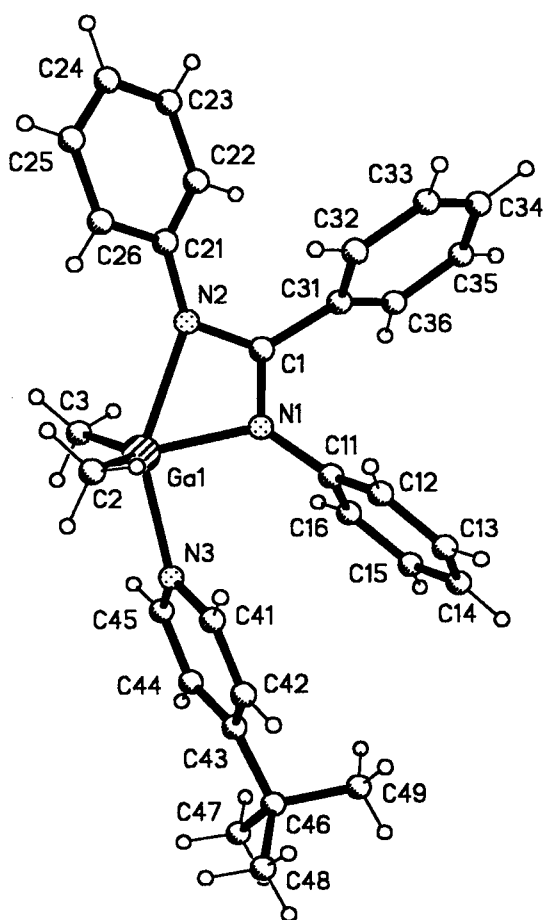


Figure 2.13 Another view of the molecular structure of $[\text{Me}_2\text{Ga}(\text{PhNCPhNPh}) \cdot (4\text{-Bu}^t\text{-pyridine})]$, showing the atomic numbering scheme.

Table 2.12 Principal bond angles (Å) and angles (°) for $[\text{Me}_2\text{Ga}(\text{PhNCPhNPh}) \cdot (4\text{-Bu}^t\text{-pyridine})]$.

Ga(1)-C(3)	1.950(4)	Ga(1)-C(2)	1.963(5)
Ga(1)-N(1)	2.010(3)	Ga(1)-N(3)	2.210(3)
Ga(1)-N(2)	2.347(3)	N(1)-C(1)	1.344(5)
N(1)-C(11)	1.414(5)	N(2)-C(1)	1.312(5)
N(2)-C(21)	1.394(5)	C(1)-C(31)	1.491(5)
C(3)-Ga(1)-C(2)	124.7(2)	C(3)-Ga(1)-N(1)	115.8(2)
C(2)-Ga(1)-N(1)	117.2(2)	C(3)-Ga(1)-N(3)	99.5(2)
C(2)-Ga(1)-N(3)	95.6(2)	N(1)-Ga(1)-N(3)	89.32(12)
C(3)-Ga(1)-N(2)	99.4(2)	C(2)-Ga(1)-N(2)	93.7(2)
N(1)-Ga(1)-N(2)	60.07(12)	N(3)-Ga(1)-N(2)	148.80(12)
N(2)-C(1)-N(1)	111.9(3)	C(1)-N(1)-Ga(1)	101.1(2)
C(11)-N(1)-Ga(1)	131.4(2)	C(1)-N(2)-C(21)	125.5(3)
C(1)-N(2)-Ga(1)	86.8(2)	C(21)-N(2)-Ga(1)	147.2(3)
C(1)-N(1)-C(11)	123.6(3)	N(1)-C(1)-C(31)	122.8(3)
N(2)-C(1)-C(31)	125.3(3)		

complexes have shown that the Ga–N_{ax} distance is greater than the Ga–N_{eq} distance, because of the relatively increased s-character of the Ga–N_{eq} bond compared to the predominant p-character of the Ga–N_{ax} bond expected for this geometry. The two distances found in these previous studies vary by 1.92–2.48 Å and 1.94–2.78 Å respectively.^{211,212,213} The gallium–Lewis base bond distance [Ga(1)–N(3)] of 2.210(3) Å suggests a strong interaction compared to the other axial Ga–N(amidinato) distance and this results from the increased steric freedom of this ligand which allows a better metal–ligand orbital overlap than that which can be achieved by the amidinato nitrogen atoms. The Ga–C bond distances of 1.950(4) and 1.963(5) Å lie well within the range found previously for other equatorially co-ordinated carbon in trigonal bipyramidal organogallium compounds of 1.924(4) to 2.080(4) Å.^{211,212,213} They are only slightly greater than the Ga–C bond lengths found in dimethylgallium–N,N'-diphenylbenzamidinato of 1.944(11) and 1.944(12) Å, which indicates that these bonds are less dependant on the type of co-ordination geometry.

(b) Ligand Structure

Unlike the bond lengths in the skeletal NCN unit in the dimethylgallium–N,N'-diphenylbenzamidinato complex [*viz* 1.331(11) and 1.335(11) Å], the skeletal C–N bond lengths in the adduct complex are N(1)–C(37) 1.344(5) and N(2)–C(1) 1.312(5) Å, that is, they are not equal. This is because of the different stereochemical environments of the two amidinato nitrogen atoms. They do however indicate further delocalisation of the skeletal NCN framework than found in the parent ligand.²⁰⁸ The two amidinato N–C(phenyl) bond lengths of 1.394(5) Å [N(2)–C(21)] and 1.414(5) Å [N(1)–C(11)] and the central C–C(phenyl) length of 1.491(5) Å [C(1)–C(31)] compare with mean lengths of 1.411(8) Å and 1.485(8) Å respectively in the parent ligand.²⁰⁸ The ligand bite angle of 111.89(35)° compares closely with the value obtained for the dimethylgallium complex of 110.8(7)°, though the remaining internal angles give an asymmetrical four-membered M(NCN) ring in contrast to the symmetrical ring present in the four co-ordinate dimethylgallium complex.

Since addition of excess 4-Bu¹-pyridine to either the dimethylgallium or diethylindium-N,N'-diphenylbenzamidinato complex failed to produce a bis-adduct, a similar reaction was attempted using the bidentate Lewis base, N,N,N',N'-tetramethylethylenediamine (TMEDA), to determine whether such a six co-ordinate species could be formed, albeit possibly with a weak interaction, or whether a five co-ordinate species would still result. Treatment of the dimethylindium complex, [Me₂In(PhNCPhNPh)], in hexane solution with TMEDA did not yield either of these postulated products, but instead, surprisingly, the bis-amidinato complex [MeIn(PhNCPhNPh)₂] was precipitated as a colourless solid in 39% yield according to the scheme shown in Figure 2.14. Although no direct evidence relating to the reaction pathway by which this complex is formed was obtained, two mechanisms may be proposed, both of which involve the initial formation of a five co-ordinate Lewis acid-base species, as illustrated in Figure 2.14. In the first reaction pathway, the bidentate TMEDA ligand bridges two metal species [2.14(a)] and the close proximity of these two metal centres enhances bridge formation of the alkyl and amidinato groups, with subsequent exchange of these ligands [2.14(b)–(d)], and precipitation of the bis-amidinato product. Alternatively, it is suggested that the TMEDA ligand co-ordinates to a metal centre through one nitrogen atom, leaving the second nitrogen atom unco-ordinated [2.14(e)]. The close proximity of this second nitrogen base atom promotes the formation of the alkyl/amidinato bridge intermediate and subsequent ligand exchange [2.14(f)(g)], and the vacant co-ordination site formed is rapidly occupied by this donor atom [2.14(h)].

The following observations support the above proposed reaction pathways:

(i) The fact that the addition of excess of the monodentate Lewis base 4-*tert*-butylpyridine to the dimethylgallium or diethylindium-N,N'-diphenylbenzamidinato derivatives did not yield the six co-ordinate bis-adduct is evidence for the initial formation of a five co-ordinate species. Given that the sterically similar triazenido complex [InCl₂(PhNNNPh)(3,5-Me-pyridine)₂] exists,¹⁹⁵ where the Lewis acidity of the

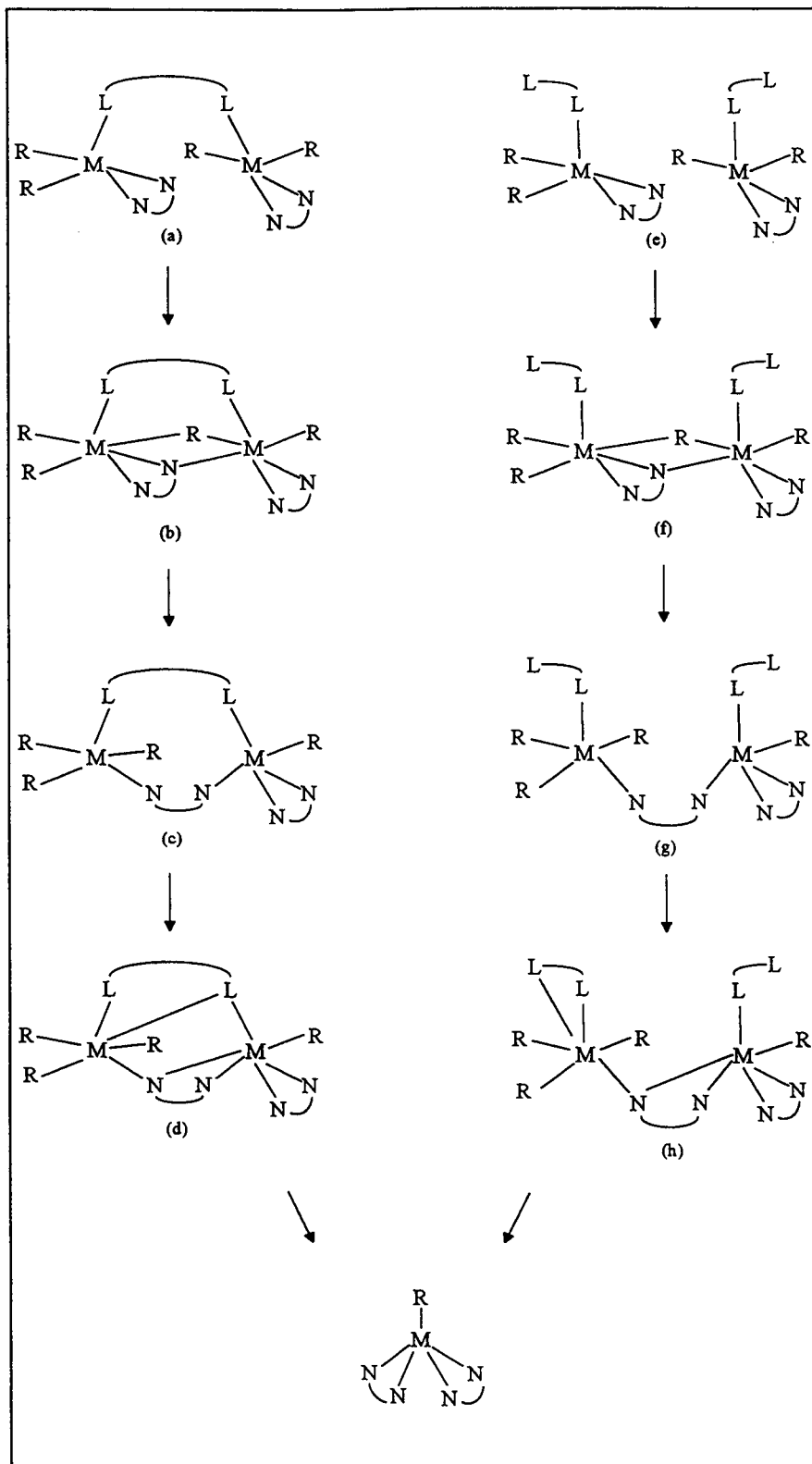


Figure 2.14 Proposed ligand exchange mechanism scheme for $[\text{Me}_2\text{In}(\text{PhNCPhNPh})]$.

indium centre is expected to be increased by the two chlorine atoms, it is unlikely that the failure to form six co-ordinate species such as $[\text{Me}_2\text{In}(\text{PhNCPhNPh})(\text{Bu}^t\text{-py})_2]$ is caused by steric factors.

(ii) Resonances in the ^1H N.M.R. spectrum of the crude reaction mixture correspond to species such as $\text{Me}_3\text{InN}(\text{Me}_2)\text{CH}_2\text{CH}_2\text{N}(\text{Me}_2)\text{InMe}_3$.

(iii) No adduct was formed by the addition of 4-*tert*-butylpyridine or TMEDA to $[\text{MeIn}(\text{PhNCPhNPh})_2]$ indicating that this complex is co-ordinatively saturated, and is stable to further disproportionation to the tris-amidinato complex.

(iv) A similar ligand exchange is thought to occur during the reaction between Me_3Al and 1,3-diphenyltriazene to yield the aluminium-tris(triazenido) complex as the sole product even when an excess of the trialkyl is used. However, the corresponding reaction with 1 or 2 moles of $\text{AlH}(\text{Bu}^i_2)$ allows isolation of the less highly substituted mono- and bis-triazenido complexes, $\text{AlBu}^i_x(\text{PhNNNPh})_{3-x}$ (where $x = 1$ or 2), suggesting the involvement of alkyl-bridged intermediates, the formation of which are known to be inhibited by increasing the alkyl steric bulk.¹¹⁷

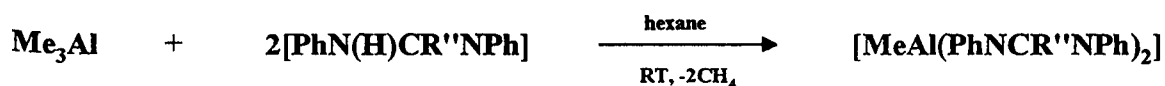
Treatment of dimethylaluminium-N,N'-diphenylbenzamidinato with 4-*tert*-butylpyridine in hexane solution did not lead to the isolation of an adduct, but resulted in a similar ligand exchange reaction, producing the aluminium-bis(amidinato) complex, $[\text{MeAl}(\text{PhNCPhNPh})_2]$ in almost quantitative yield. This may be explained in terms of the greater ability of aluminium to form bridge species which allows more facile ligand exchange.

The ^1H and ^{13}C N.M.R. spectra obtained from 1:1 mixtures of $[\text{Et}_2\text{In}(\text{PhNCPhNPh})]$ with each of the ligands THF, PPh_3 , AsPh_3 and $\text{Ph}_2\text{PCH}_2\text{CH}_2\text{PPh}_2$ showed no substantial chemical shift change of the ligand resonances compared to those found in the spectra of the free ligand, using the same solvent (CDCl_3). This suggests that no significant interaction occurs in solution.

Preparation of the Monoalkylmetal-bis(amidinato) Complexes of Aluminium, Gallium, and Indium.

The monoalkylmetal-bis(amidinato) derivatives of aluminium, gallium and indium mentioned above were also prepared by the direct addition of two moles of amidine to one mole of the appropriate trialkylmetal derivative. It was decided that only two amidine ligands would be used, namely N,N'-diphenylbenzamidine and N,N'-diphenylacetamidine, for the preparation of these complexes to establish a synthetic route to encompass the general type of N,N'-diaryl substituted amidines. These two ligands differ only in respect of the central carbon substituent of the NCN unit. It was hoped also to investigate the effect of variation of these central NCN groups on the structures of these complexes by X-ray diffraction for those complexes where suitable single crystals could be obtained.

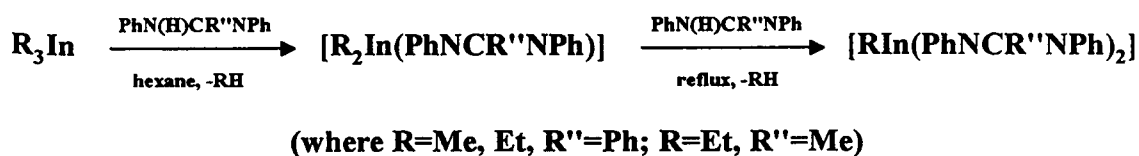
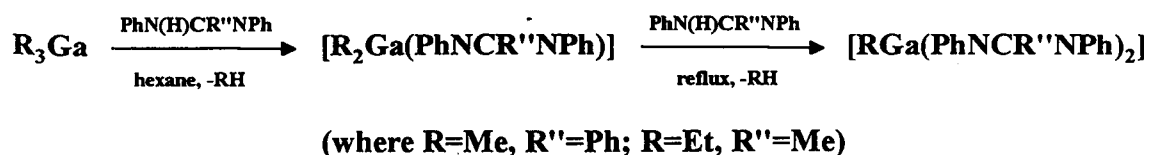
The methylaluminium complexes were prepared by the interaction of a hexane suspension of the amidine (2 moles) held at low temperature with a hexane solution of trimethylaluminium with the elimination of two moles of methane. Recrystallisation of the products from the reaction liquor gave microcrystalline solids in yields typically greater than 70%.



For example, the addition of Me_3Al to a hexane suspension of N,N'-diphenylbenzamidine chilled in liquid nitrogen, which was subsequently allowed to warm to room temperature, gave a colourless solution. Cooling of the reaction mixture to -35°C yielded a crop of colourless crystals in 75% yield. Repeating the reaction in toluene solution gave the same products, although recrystallisation of the product from the reaction liquor proved less satisfactory, as it produced a low yield.

The corresponding reaction using the trialkylgallium or trialkylindium reagents (where alkyl = methyl, ethyl) and hexane as solvent led to the evolution of 1 mole of

alkane at room temperature, but in these cases no further reaction occurred, and excess amidine remained in the reaction mixture. Heating under reflux for 12 hours led to the release of a further mole of alkane, and precipitation of colourless solid products in high yield. The preparation of the methylgallium derivative of *N,N'*-diphenylbenzamidine was initially carried out in refluxing toluene, but again recrystallisation of the product from this solvent gave a lower yield and thus hexane was the preferred solvent.



All the products prepared here are air sensitive to some extent, but less so than the dialkylmetal derivatives, and are soluble in hexane, chloroform, toluene and THF. The complexes were spectroscopically characterised by elemental analysis (C, H, N), ^1H and ^{13}C N.M.R., I.R., and mass spectroscopy.

Spectroscopic Properties of the Monoalkylmetal-bis(amidinato) Complexes.

Nuclear Magnetic Resonance Spectra

The ^1H N.M.R. spectra, recorded from CDCl_3 solution, are particularly informative and readily confirm the substitution by two amidinato ligands with one metal-alkyl group remaining. The data for the individual compounds are presented in the Experimental Section. The general appearance of the spectra of all the complexes is very similar and therefore only their more salient features will be discussed here.

The main feature of the spectra is that the organometallic proton region contains a sharp singlet resonance of integral value corresponding to three protons for the

metal–methyl derivatives and well defined triplet and doublet multiplets of total integral value corresponding to five protons for the metal–ethyl derivatives. The organometallic proton resonance in the methylaluminium complexes occurs near -0.3 p.p.m., in the methylgallium complex at 0.28 p.p.m., and in the methylindium complex at 0.38 p.p.m., and are shifted slightly downfield compared to their corresponding dimethylmetal–amidinato complexes. The sharp ligand proton resonances indicate that the environments of both the amidinato ligands and the N–phenyl substituents of each ligand are indistinguishable on the N.M.R. timescale at 25°C .

The ^{13}C N.M.R. spectra of the compounds have been recorded and are summarised in Table 2.13. Assignments are based on ^1H – ^{13}C N.M.R. correlation experiments. The atom numbering scheme is shown in the key given in the Experimental Section. The spectra are consistent with the ^1H N.M.R. data in showing the chemical equivalence and symmetrical nature of the co–ordination of the amidinato ligands. In particular, only one resonance is found corresponding to the aryl carbon atoms that are directly bonded to the amidine nitrogen atoms, which is consistently present around 144 to 146 p.p.m. The sharp metal–methyl ^{13}C N.M.R. resonance in the spectra of the methylaluminium complexes occurs near -12 p.p.m., at -7.80 p.p.m. in the methylgallium complex, and at -8.78 p.p.m. in the methylindium complex. In all cases they show upfield shifts compared to the ^{13}C N.M.R. shift of the metal–methyl obtained for the corresponding dimethylmetal compounds. These data suggest a possible correlation between the shift of this resonance and the metal co–ordination number of four in the dimethylmetal complexes and perhaps five in the methylmetal complexes. The corresponding resonances found in the spectra of the metal–ethyl derivatives occur further upfield, between 4.5 and 12 p.p.m.

Comparison of the position of the central NCN carbon resonance found near 171 p.p.m. in the aluminium complexes, and in the region 167.0 to 168.3 p.p.m. in the gallium and indium complexes, with the data previously presented for the dialkylmetal derivatives suggests that the amidinato ligands are co–ordinated to the metal in a similar manner.

Table 2.13 Summary of Proton decoupled ^{13}C N.M.R. data (δ / p.p.m.) of alkylmetal-bis(amidinato) complexes. Run as CDCl_3 solutions at 25°C .

Complex	M-CR ₃	M-CH ₂ CH ₃	C-10	aromatic	C-6	C-1	C-5
[MeAl(PhNCPhNPh) ₂]	-12.03	-	-	122.42 (C4), 124.85 (C2) 127.91 (C3), 128.10 (C8) 129.59 (C7), 129.67 (C9)	129.78	143.99	170.83
[MeAl(PhNCMeNPh) ₂]	-12.11	-	14.03	122.84 (C4), 124.36 (C2) 128.29 (C3)	-	144.19	170.94
[MeGa(PhNCPhNPh) ₂]	-7.70	-	-	122.22 (C4), 124.96 (C2) 127.96 (C3), 128.05 (C8) 129.31 (C7), 129.82 (C9)	130.70	144.90	167.96
[EtGa(PhNCMeNPh) ₂]	4.50	10.16	13.92	122.43 (C4), 124.31 (C2) 128.24 (C3)	-	145.15	167.05
[MeIn(PhNCPhNPh) ₂]	-8.78	-	-	121.92 (C4), 124.81 (C2) 128.09 (C3, C7), 129.04 (C9), 129.96 (C8)	132.03	145.97	168.23
[EtIn(PhNCPhNPh) ₂]	6.28	11.90	-	121.79 (C4), 124.85 (C2) 128.02 (C3, C7), 128.96 (C9), 129.96 (C8)	132.03	146.13	168.28
[EtIn(PhNCMeNPh) ₂]	5.86	11.93	15.26	122.37 (C4), 124.52 (C2) 128.52 (C3)	-	146.35	167.29

Barron *et al*¹¹⁷ have reported that the bis(triazenido) compounds $[\text{RAl}(\text{PhNNNPh})_2]$ ($\text{R} = \text{Me}, \text{Bu}^i$) decompose rapidly in solution to give the mono- and tris-substituted triazenido products, $[\text{R}_2\text{Al}(\text{PhNNNPh})]$ and $[\text{Al}(\text{PhNNNPh})_3]$. In contrast, heating the methylaluminium-bis(amidinato) samples (or analogous gallium/indium compounds) to 80°C in CDCl_3 solution causes no change in the ^1H and ^{13}C N.M.R. spectra, confirming that this type of disproportionation does not occur for these compounds within the temperature range used. Pure samples of the compounds are stable in CDCl_3 solution for at least 1 week if kept sealed under an inert atmosphere. However, these solutions do react with moisture and the susceptibility of $[\text{MeGa}(\text{PhNCPHNP})_2]$ in CDCl_3 to hydrolysis was investigated by ^1H N.M.R. spectroscopy. Exposure of the solution to air caused the Ga-Me resonance attributed to the complex to decrease by about 50% after two hours. Free ligand $[\text{PhN}(\text{H})\text{CPhNP}]$ formed as well as unidentified gallium species (which may be of the type $[\text{MeGaOH}(\text{PhNCPHNP})]$ and $[\text{MeGaO}]_n$). Small resonances from Ga-Me fragments occurred at δ 1.28 and -0.36 p.p.m. in the hydrolysed solution.

Infra-red Spectra

Infra-red spectra have been recorded for the N,N' -diphenylbenzamidinato complexes with aluminium, gallium and indium and a list of the significant bands in each spectrum is given in the Experimental Section.

Once again, the most distinctive features of the spectra are the absence of the NH bands present in the spectra of the free ligands around 3250cm^{-1} , and the close similarity of the changes in the Amidine I and III regions to those observed in the spectra of the dimethyl-amidinato complexes, in particular the band assigned to the asymmetrical CN_2 stretching vibration present at 1595cm^{-1} in all three spectra. These common features strongly suggest that a similar amidinato co-ordination mode exists in all these complexes, and this implication is consistent with a monomeric five co-ordinate bis-amidinato formulation.

Mass Spectra

E.I. mass spectra have been obtained for all the compounds prepared and Tables 2.14 to 2.19 show the major metal-containing ions present (where L = amidinato ligand). A more complete listing of the peaks produced for each compound is given in the Experimental Section.

The spectra show weak intensity peaks corresponding to the monomeric bis-chelate form $[\text{MR}(\text{L})_2]^+$ (where M = Al, R = Me; M = Ga, In, R = Me, Et) with a characteristic much more intense peak arising from the loss of the metal-alkyl group. The remaining metal-containing peaks are consistent with the loss of the amidinato ligand as a whole, which produces species such as $[\text{ML}]^+$ and $[\text{M}]^+$. Fragmentation of the co-ordinated N,N'-diphenylbenzamidinato ligand is again indicated by the presence of peaks assigned to the species $[\text{MRPh}(\text{L})]^+$, $[\text{MPh}_2]^+$ and $[\text{MRPh}]^+$ (where M = Al, R = Me; Ga, In, R = Me, Et; L = N,N'-diphenylbenzamidinato).

Table 2.14 Major aluminium-containing fragments from $[\text{MeAl}(\text{PhNCPPhNPh})_2]$

m/z	Rel. Int. (%)	Assignment
584	1.1	M^+
569	16.7	$[\text{Al}(\text{L})_2]^+$
375	10.6	$[\text{AlPh}(\text{L})]^+$
313	25.1	$[\text{AlMe}(\text{L})]^+$
181	24.9	$[\text{AlPh}_2]^+ *$

* also assigned to $[\text{PhNCPPh}+1]^+$

Table 2.15 Major aluminium-containing fragments from [MeAl(PhNCMeNPh)₂]

m/z	Rel. Int. (%)	Assignment
460	2.1	M ⁺
445	86.4	[Al(L) ₂] ⁺
251	19.5	[AlMe(L)] ⁺
236	23.4	[Al(L)] ⁺

Table 2.16 Major gallium-containing fragments from [MeGa(PhNCPPhNPh)₂]

m/z	Rel. Int. (%)	Assignment*
626	7.8	M ⁺
611	43.4	[Ga(L) ₂] ⁺
417	9.4	[GaPh(L)] ⁺
355	13.5	[GaMe(L)] ⁺
223	8.8	[GaPh ₂] ⁺
161	23.5	[GaMePh] ⁺
69	10.0	Ga ⁺

* based on ⁶⁹Ga**Table 2.17** Major gallium-containing fragments from [EtGa(PhNCMeNPh)₂]

m/z	Rel. Int. (%)	Assignment*
516	1.0	M ⁺
487	91.5	[Ga(L) ₂] ⁺
307	14.3	[GaEt(L)] ⁺
279	19.5	[Ga(L)+ 1] ⁺
69	68.4	Ga ⁺

* based on ⁶⁹Ga

Table 2.18 Major indium-containing fragments from [EtIn(PhNCPPhNPh)₂]

m/z	Rel. Int. (%)	Assignment*
686	0.4	M ⁺
657	26.9	[In(L) ₂] ⁺
463	1.5	[InPh(L)] ⁺
415	19.2	[InEt(L)] ⁺
385	16.0	[In(L)] ⁺
269	3.0	[InPh ₂] ⁺
115	100	In ⁺

* based on ¹¹⁵In**Table 2.19** Major indium-containing fragments from [EtIn(PhNCMeNPh)₂]

m/z	Rel. Int. (%)	Assignment*
562	0.6	M ⁺
533	57.9	[In(L) ₂] ⁺
353	7.3	[InEt(L)] ⁺
324	7.3	[In(L)] ⁺
115	100	In ⁺

* based on ¹¹⁵In

X-ray Crystallographic Studies

It was noted in the introduction to this section that one aim of this work was to characterise structurally a number of the complexes using X-ray diffraction in order to determine the type of metal co-ordination geometry found in these complexes and to examine any structural changes that may become apparent by varying either the metal atom or the central substituent of the amidinato ligand. The molecular structures of four compounds were determined, namely methylaluminium-bis(N,N'-diphenylbenzamidinato) (Figure 2.15), methyl-gallium-bis(N,N'-diphenylbenzamidinato) (Figure 2.16), ethylindium-bis(N,N'-diphenylbenzamidinato) (Figure 2.17) and ethylgallium-bis(N,N'-diphenylacetamidinato) (Figure 2.18). Further views of their molecular structures are shown in Figures 2.19 and 2.20. The major bond lengths and angles of the compounds are presented in Tables 2.20–2.22 and a complete listing is given in Appendix 2.

The central structural unit of all four compounds features a monomeric five co-ordinate metal atom which is bound to two bidentate chelate amidinato ligands and an alkyl ligand.

(a) The Metal Co-ordination Environment

The structures of the gallium and indium complexes will be discussed first, then that of the aluminium complex.

The metal co-ordination geometry in the alkylgallium and alkylindium-bis(amidinato) complexes is best described as a highly distorted trigonal bipyramid. The pseudo-axial sites are occupied by N(1) and N(4) and the equatorial plane is defined by N(2), N(3) and C(1), with the metal atom essentially coplanar.

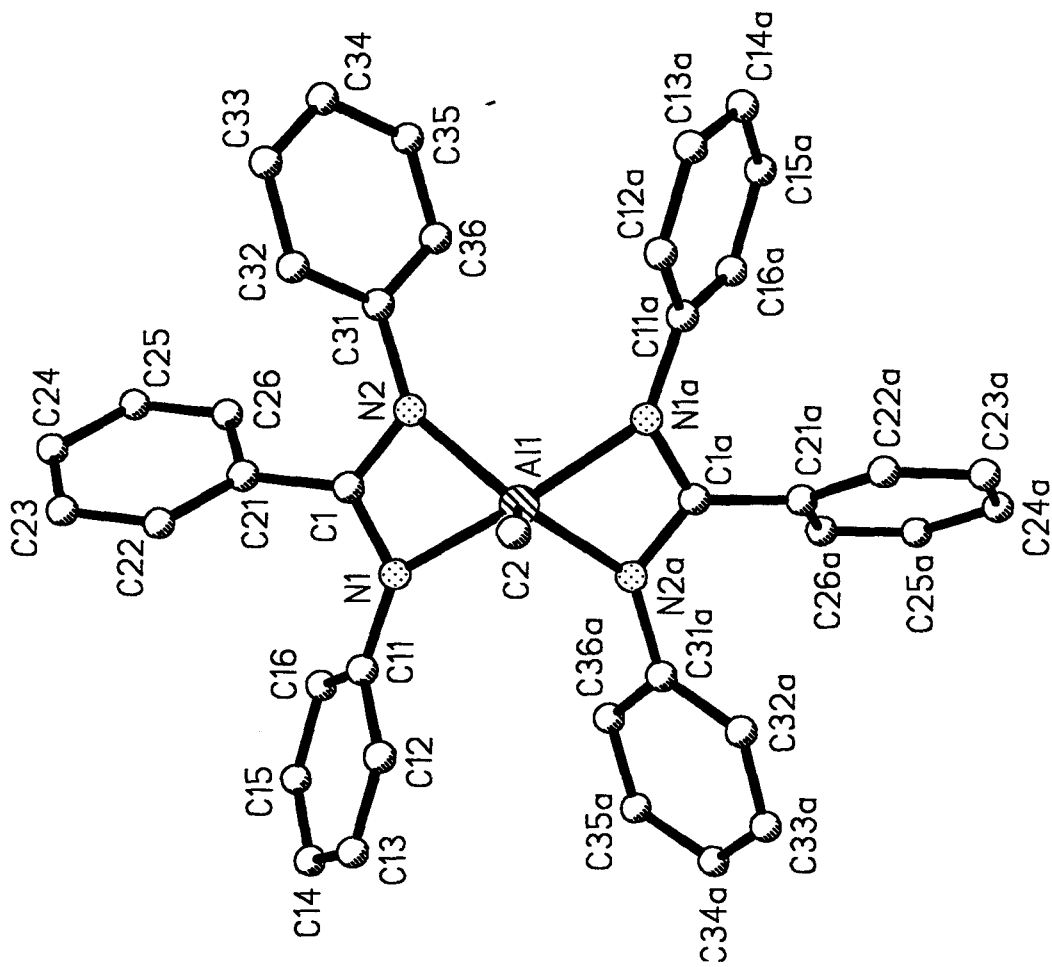


Figure 2.15 The molecular structure of methylaluminum-*N,N'*-diphenylbenzamidinato, showing the atomic numbering scheme used.

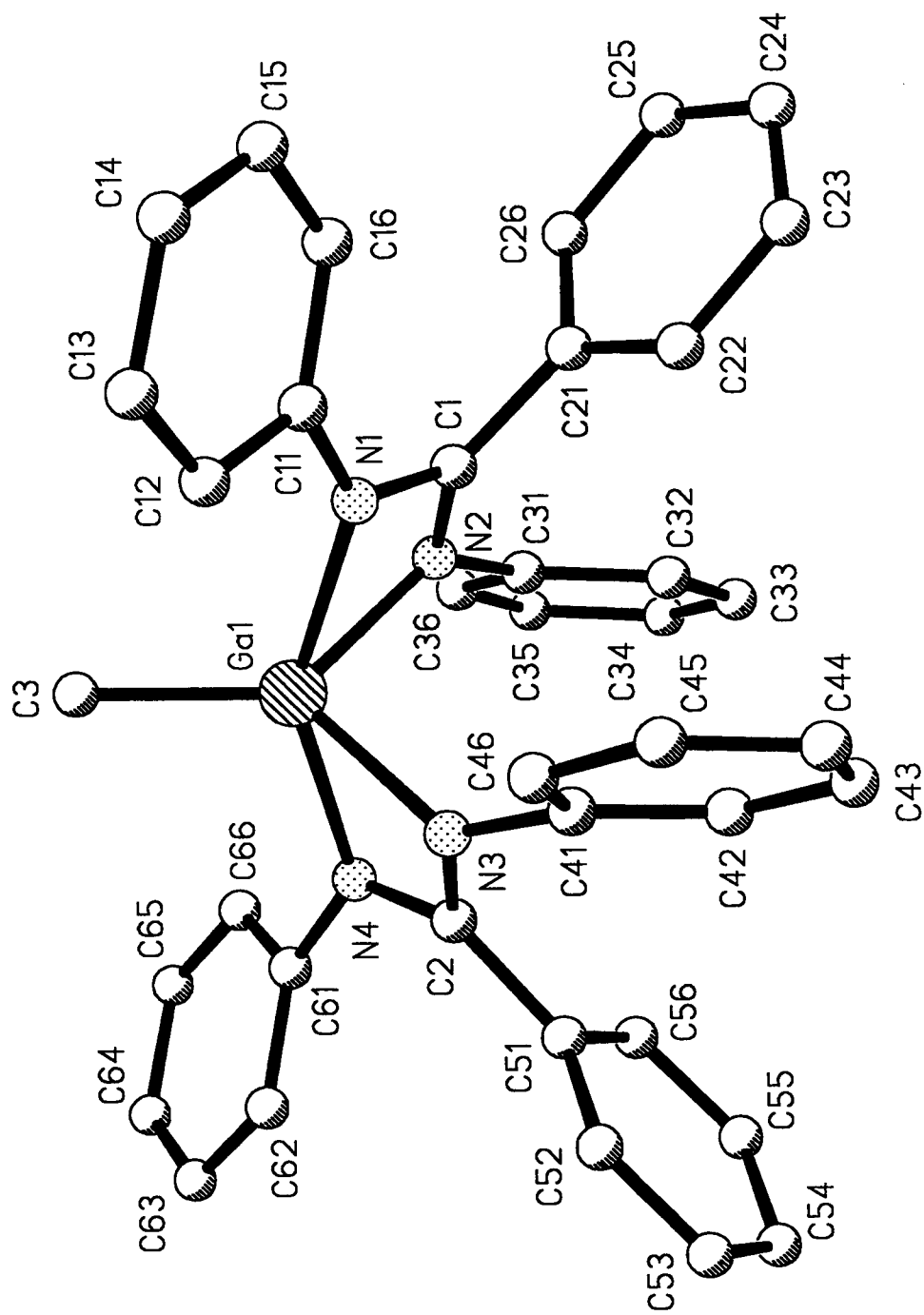


Figure 2.16 The molecular structure of methylgallium-N,N'-diphenylbenzamidinato, showing the atomic numbering scheme used.

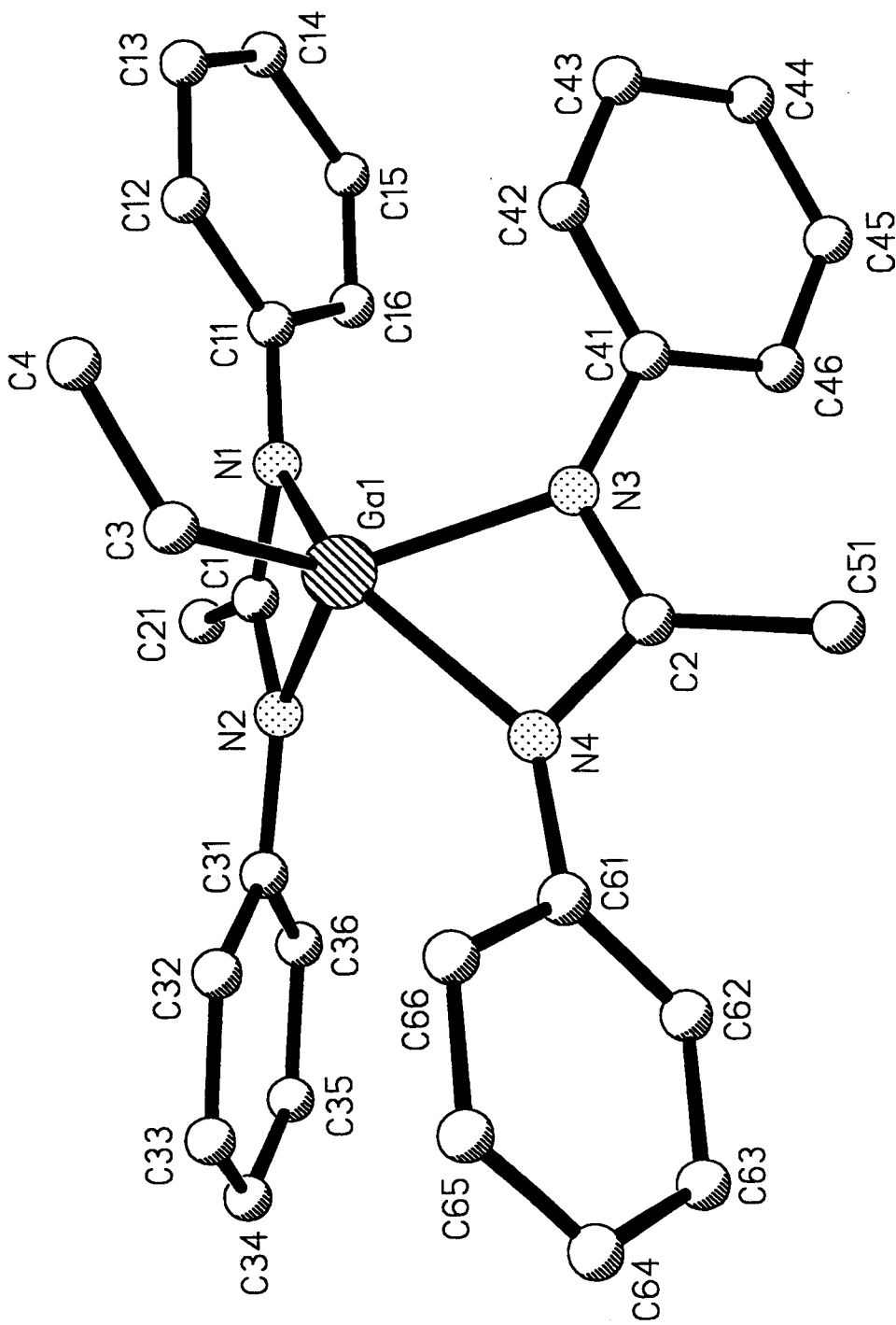


Figure 2.17 The molecular structure of ethylgallium-*N,N'*-diphenylacetamidinato, showing the atomic numbering scheme used.

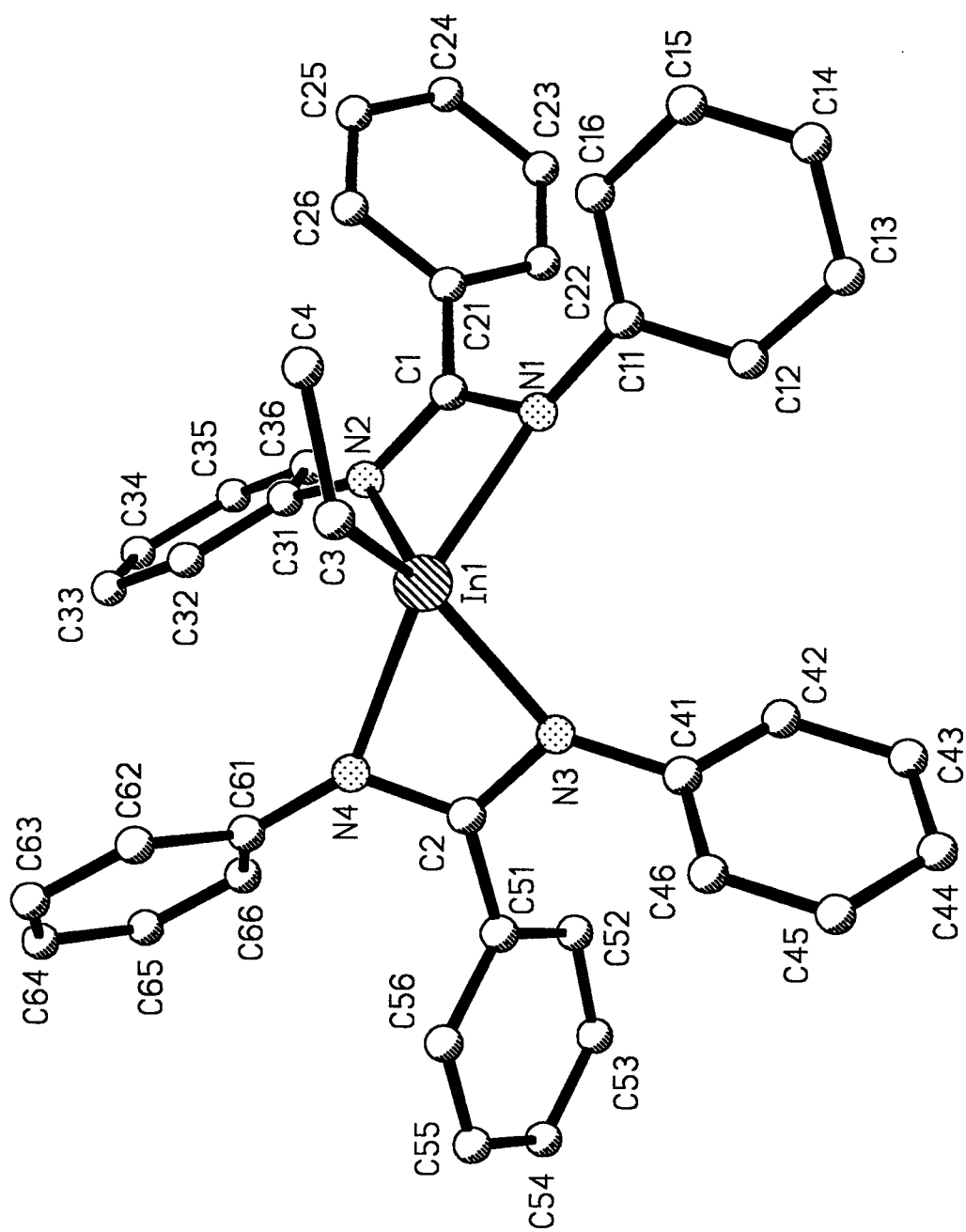


Figure 2.18 The molecular structure of ethylindium-*N,N'*-diphenylbenzamidinato, showing the atomic numbering scheme used.

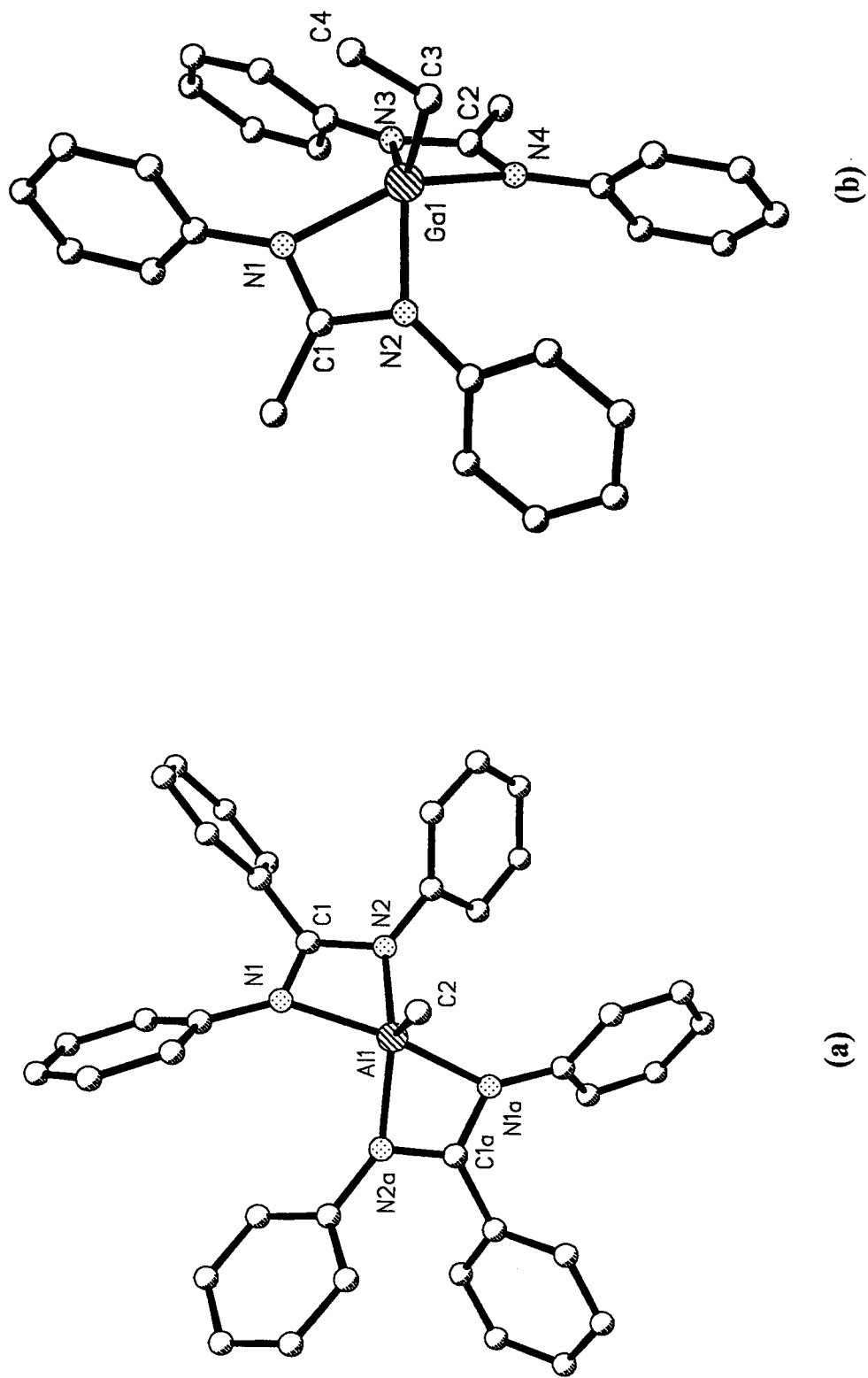


Figure 2.19 Molecular structures of (a) $[\text{MeAl}(\text{PhNCPPhNPPh})_2]$, and (b) $[\text{EtGa}(\text{PhNCMeNPh})_2]$, showing the distorted trigonal bipyramidal metal co-ordination geometry.

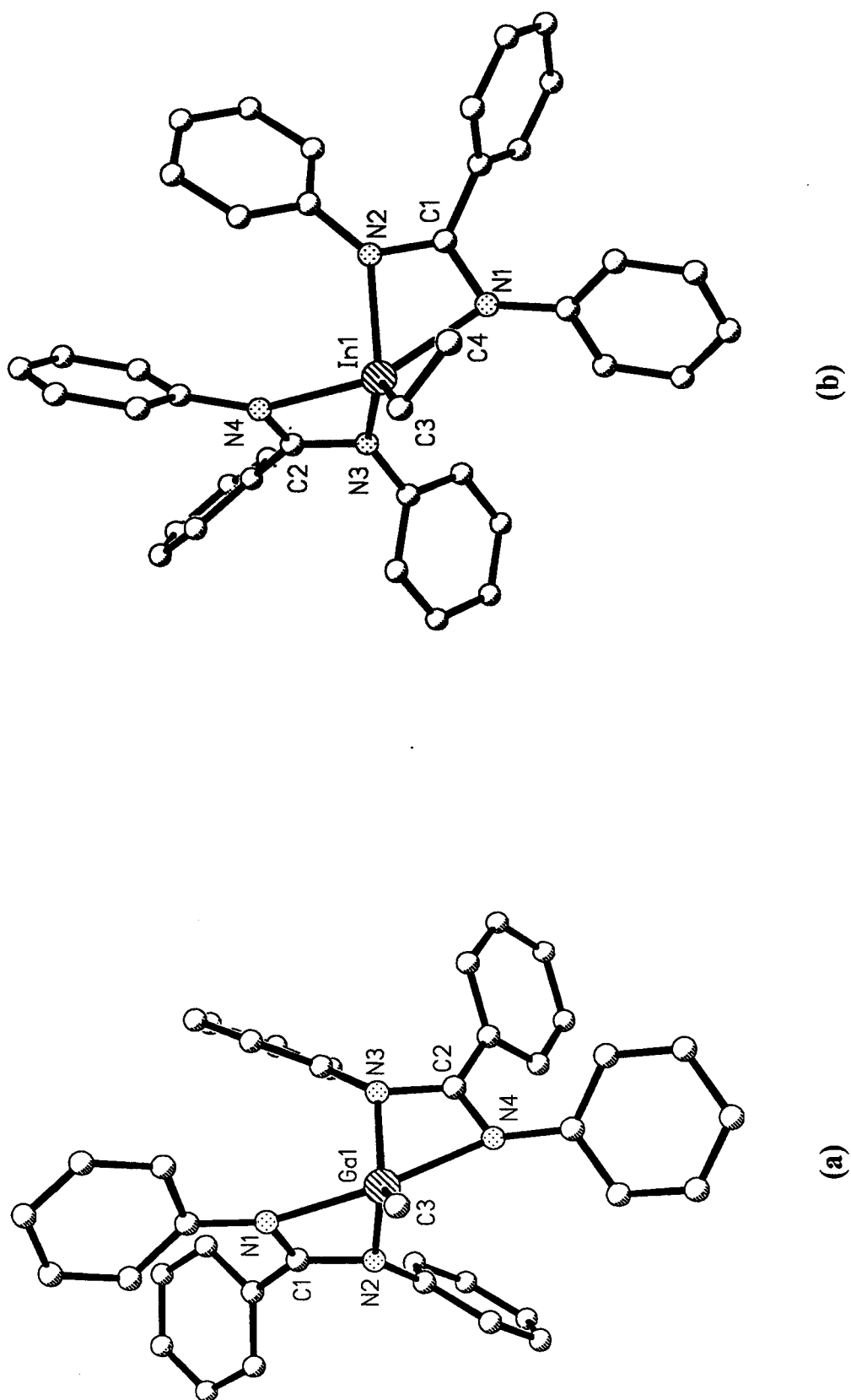


Figure 2.20 Molecular structures of (a) $[\text{MeGa}(\text{PhNCPhNPh})_2]$, and (b) $[\text{EtIn}(\text{PhNCPhNPh})_2]$, showing the distorted trigonal bipyramidal metal co-ordination geometry.

The axial and equatorial bond angles shown in Table 2.21 deviate considerably from the idealised values because of the steric constraints imposed by the rigidity and limited bite size of the two chelating amidinato ligands. Figure 2.21 defines the planes A, B, C and D which are each occupied by three atoms in the co-ordination polyhedron, and Table 2.23 shows the dihedral angles between the planes A and C (1), A and D (2), B and C (3), and B and D (4).

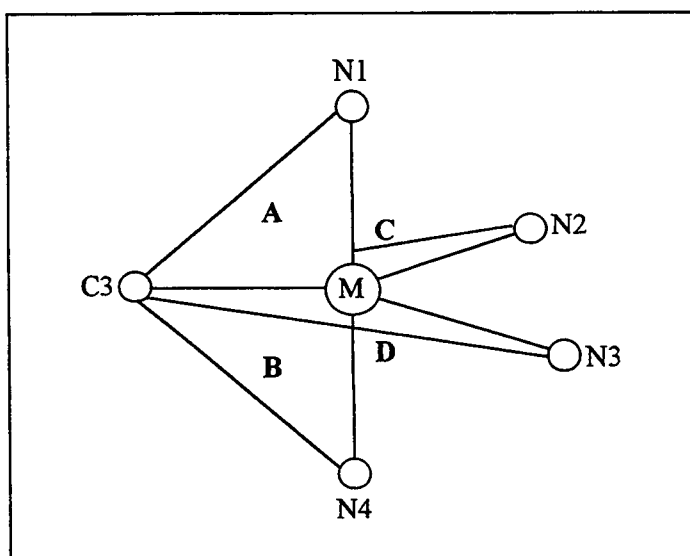


Figure 2.21 Schematic view of the co-ordination polyhedron around the metal in $[\text{RM}(\text{PhNCR}''\text{NPh})_2]$

Table 2.23 Dihedral angles between the planes defined in Figure 2.21

Dihedral Angle ($^\circ$)	1	2	3	4
$[\text{MeGa}(\text{PhNCPhNPh})_2]$	69.9	66.6	69.0	65.5
$[\text{EtGa}(\text{PhNCMeNPh})_2]$	72.3	66.3	73.0	67.0
$[\text{MeIn}(\text{PhNCPhNPh})_2]$	61.2	60.8	69.6	69.3

All these angles deviate considerably from 90° , as do the bond angles between the pseudo-axial and equatorial atoms, and illustrate that the extent of the distortion of the metal valency angles from a regular trigonal bipyramid is greatest for the indium complex.

The two metal–nitrogen distances within each chelate ring differ significantly as a consequence of each amidinato ligand spanning the axial and equatorial positions, which imply a weak axial and a stronger equatorial bond. This is also indicated by the ratio $M-N_{ax}:M-N_{eq}$ (Table 2.20) which is found to be in the range 1.059(2) to 1.082(3) for the gallium complexes and 1.067(4) for the indium complex.

Comparison of the gallium–nitrogen bond lengths shows that there is a significant variation in the two $Ga-N_{ax}$ distances, whereas the $Ga-N_{eq}$ distances remain essentially the same. In both cases, the values found fall well within the range of previously determined $Ga-N$ bond lengths of 1.92 to 2.48 Å for equatorial bond distances, and 1.94 to 2.78 Å for axial bond distances.^{211,212,213} The gallium–carbon bond lengths found here also lie within the range reported for other equatorial $Ga-C$ distances in five co-ordinate organogallium complexes of 1.924(4) to 2.080(4) Å,^{211,212,213} and the distance found in $[MeGa(PhNCPPhNPh)_2]$ of 1.940(3) Å is similar to those found in the four co-ordinate dimethylgallium- N,N' -diphenylbenzamidinato complex of 1.944 (11) and 1.944(12) Å.²⁰⁰

The molecular structure of the bis[2-(methylamino)pyridine]complex, $[MeIn\{MeNC(CH_3)_4N\}_2]$ reported by Bradley *et al*²¹⁴ is shown in Figure 2.22 and the important bond lengths and angles found in this complex are given in Table 2.24. Examination of the metal geometry in this complex reveals an almost identical metal co-ordination geometry to that found in $[MeIn(PhNCPPhNPh)_2]$. This comparison illustrates the sterically related nature of these two ligands.

The two $In-N_{ax}$ bond lengths of 2.314(4) [$In(1)-N(4)$] and 2.337(5) Å [$In(1)-N(1)$] also differ significantly, as do the $In-N_{eq}$ distances of 2.169(5) Å [$In(1)-N(3)$] and 2.190(4) [$In(1)-N(2)$]. Both bond types are slightly longer than the corresponding distances found in methylindium-bis[2-(methylamino)pyridine]. They contrast with the relatively narrow range found in the two crystallographically independent molecules of $[Me_2In(PhNCPPhNPh)]$ of 2.239(4) to 2.263(4) Å, whereas the equatorial $In-C$ bond length of 2.146(6) Å remains similar to the range observed in the four co-ordinate dialkylmetal derivative from 2.134(6) to 2.152(6) Å. The $In-C$ and $In-N$ distances fall well within the range found in previous studies of five co-ordinate organoindium complexes of 2.13(1) to 2.210(17) Å and of 2.158(4) to 2.711(5) Å respectively.^{214,215,216,217}

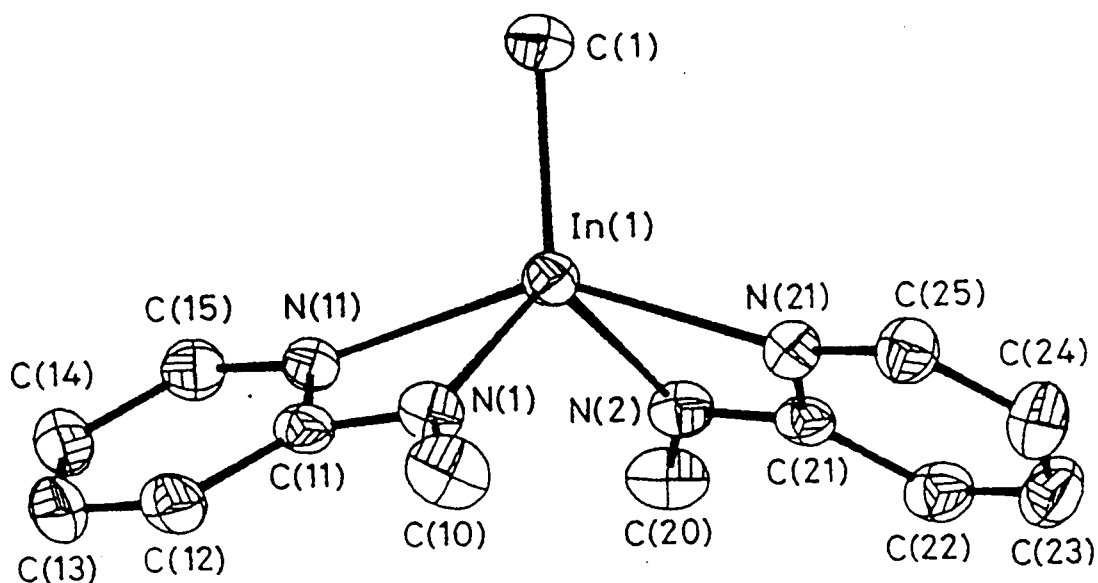


Figure 2.22 The molecular structure of $[\text{MeIn}\{\text{MeNC}(\text{CH})_4\text{N}\}_2]$. Hydrogen atoms omitted for clarity.²¹⁴

Table 2.24 Relevant bond lengths (Å) and angles (°) for $[\text{MeIn}\{\text{MeNC}(\text{CH})_4\text{N}\}_2]$.

In(1)-N(11)	2.351(5)	In(1)-N(1)	2.140(5)
In(1)-N(21)	2.334(5)	In(1)-N(2)	2.138(5)
In(1)-C(1)	2.137(7)	N(11)-In(1)-N(21)	144.8(1)
N(1)-In(1)-C(1)	123.6(3)	N(2)-In(1)-C(1)	123.4(3)
N(1)-In(1)-N(2)	113.0(2)	N(1)-In(1)-N(11)	59.4(2)
N(2)-In(1)-N(21)	59.6(2)	N(1)-C(11)-N(11)	111.6(4)
N(2)-C(21)-N(21)	110.7(5)	C(1)-In(1)-N(11)	106.5(3)

A useful comparison may also be made between the distances found in the indium-bis(amidinato) complex and those found in the five co-ordinate ethylindium macrocyclic complex [EtIn(tmtaa)], which contains a square-based pyramidal co-ordination geometry around the indium (reported in Chapter 4) with In-N distances in the range 2.193(4) to 2.216(4)Å, and an In-C distance of 2.158(6)Å.

The metal co-ordination environment found in the aluminium complex [MeAl(PhNCPPhNPh)₂], differs slightly from these above. The resulting metal geometry is midway between trigonal bipyramidal and square planar and closely resembles the C₈ "twisted wedge" geometry described by King.²¹⁸ The methyl group can be defined as being both apical and trigonal bipyramidal [with N(1) and N(4) occupying the "axial" sites]. In this geometry the difference between the two metal-nitrogen distances within each chelate ring [0.030(2)Å] is consistent with neither the expected large difference between the axial and equatorial distances occupying axial and equatorial sites for trigonal bipyramidal geometry nor the expected equality of the basal distances for square pyramidal geometry.

The aluminium-nitrogen distances of 1.963(2) and 1.993(2)Å are both shorter than those reported in [MeAl(salen)] of 2.033(8) and 2.041(8)Å.¹¹⁷ This complex shares a broadly similar metal co-ordination geometry with that found in the present complex. The Al-N(amidinato) bond distances are comparable to those observed in the square pyramidal aluminium complex, [EtAl(tmtaa)] which range from 1.963(3) to 1.973(3)Å.²¹⁹ The metal-carbon distance of 1.941(4)Å compares with that of 1.95(1)Å in [MeAl(salen)] and with that of 1.976(3)Å in [EtAl(tmtaa)]. It is the same as that found in the analogous gallium complex [MeGa(PhNCPPhNPh)₂] of 1.940(3)Å, and this suggests that the metal covalent radius in each complex is equal.

(b) Ligand Co-ordination Geometry

The molecular structure of the free ligand [PhN(H)CMeNPh] was determined during the course of this work and is included in Appendix 2 (pages 269 – 271) for completeness.

The carbon–nitrogen bond lengths within each NCN skeletal unit of the complexes do show some asymmetry because of the two distinct co–ordination sites. The N–C(phenyl) bond lengths are comparable to those found in their respective parent ligands, and the appropriate average values are given in tabular form below. The similarities of the respective bond distances show that the delocalised NCN system does not extend to any further significant extent into the phenyl rings, even though they contain a delocalised unit. Incidentally, the N_{ax} –C(phenyl) and N_{eq} –C(phenyl) bond lengths in [MeAl(PhNCPPhNPh)₂] differ significantly [1.400(3) and 1.431(4)Å respectively].

Compound	Average N–C(phenyl) (Å)	Average C–C(phenyl) (Å)
PhN(H)CMeNPh	1.412(3)	1.501(3)
PhN(H)CPhNPh ²⁰⁸	1.411(8)	1.485(8)
[RM(PhNCMeNPh) ₂]	1.406(5)	1.499(5)
[RM(PhNCPPhNPh) ₂]	1.414(5)	1.488(6)

The NCN angle of ca. 121.6° in both parent ligands is reduced considerably upon complexation, by ca. 11.8° in the aluminium complex, by ca. 11.5° in the gallium complexes and by ca. 9.2° in the indium complex. This reduction is in line with the increasing metal size. Examination of the remaining skeletal amidinato bond angles reveals that whereas the equatorial M–N–C bond angles are constant at around 90 to 92°, which is a severe distortion from the idealised angle of 120°, the distortion of the axial M–N–C valency angle varies with metal size, and decreases as expected on descending the group. Changing the central N₂C substituent from a phenyl group to a methyl group in the gallium complexes causes no significant change in the co–ordination geometry of the skeletal NCN unit.

It is likely that a significant factor in determining the different distortions from the idealised geometries for these five co–ordinate complexes in the solid state is attributed to crystal packing requirements as well as changing metal size and ligand constraints.

Table 2.20 Metal-Ligand Bond Lengths (Å) for the Complexes [RM(PhNCR''NPh)₂]

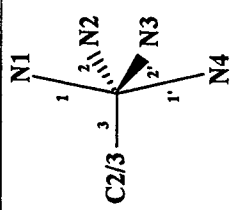
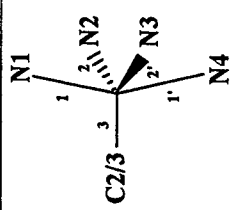
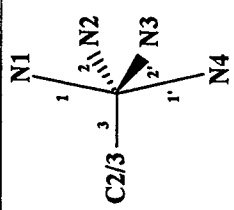
Complex																						
	M-N(1)	M-N(2)	M-N(4)	M-N(1)	M-N(2)	M-N(4)	M-N(1)	M-N(2)	M-N(4)	M-N(3)	M-C(2/3)	M-N(1)	M-N(2)	M-N(3)	M-N(4)	M-C(2/3)	M-N(1)	M-N(2)	M-N(3)	M-N(4)	M-C(2/3)	equatorial plane- metal distance
[MeAl(PhNCR''NPh) ₂]	1.993(2)	1.963(2)	1.993(2)	1.993(2)	1.963(2)	1.993(2)	1.993(2)	1.963(2)	1.993(2)	1.941(4)	1.015(2)	1.015(2)	1.015(2)	1.015(2)	1.015(2)	1.941(4)	1.015(2)	1.015(2)	1.015(2)	1.015(2)	0.0	1.18
[MeGa(PhNCR''NPh) ₂]	2.112(2)	1.995(2)	2.112(2)	2.112(2)	1.995(2)	2.112(2)	2.112(2)	1.995(2)	2.112(2)	1.940(3)	1.059(2)	1.059(2)	1.059(2)	1.059(2)	1.059(2)	1.940(3)	1.059(2)	1.059(2)	1.059(2)	1.059(2)	0.026(2)	1.26
[EtGa(PhNCMeNPh) ₂]	2.137(3)	2.009(2)	2.137(3)	2.137(3)	2.009(2)	2.137(3)	2.137(3)	2.009(2)	2.137(3)	1.983(5)	1.073(3)	1.073(3)	1.073(3)	1.073(3)	1.073(3)	1.983(5)	1.073(3)	1.073(3)	1.073(3)	0.059(3)	1.26	
[EtIn(PhNCR''NPh) ₂]	2.337(5)	2.190(4)	2.337(5)	2.337(5)	2.190(4)	2.337(5)	2.337(5)	2.190(4)	2.337(5)	2.146(6)	1.067(4)	1.067(4)	1.067(4)	1.067(4)	1.067(4)	2.146(6)	1.067(4)	1.067(4)	1.067(4)	0.004(4)	1.44	
	2.314(4)	2.169(5)	2.314(4)	2.314(4)	2.169(5)	2.314(4)	2.314(4)	2.169(5)	2.314(4)		1.067(4)	1.067(4)	1.067(4)	1.067(4)	1.067(4)		1.067(4)	1.067(4)	1.067(4)			

Table 2.21 Metal-Ligand Bond Angles (°) for the Complexes [RM(PhNCR^aNPh)₂]

Complex	N(1)-M-N(4)	N(2)-M-C(2/3)	N(3)-M-C(2/3)	d	e	e'
[MeAl(PhNCR ^a NPh) ₂]	148.23(13)	113.81(7)	113.81(7)	132.37(14)	66.13(10)	66.13(10)
[MeGa(PhNCR ^a NPh) ₂]	150.05(9)	129.10(13)	132.90(13)	97.94(10)	63.98(9)	63.43(9)
[EtGa(PhNCR ^a MeNPh) ₂]	140.91(12)	120.16(17)	123.17(17)	116.40(13)	63.39(12)	63.00(12)
[EtIn(PhNCR ^a NPh) ₂]	141.31(19)	114.09(22)	131.94(22)	113.97(19)	58.53(17)	58.94(16)

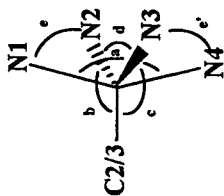
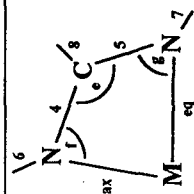


Table 2.22 Important Ligand Bond Lengths (Å) and Angles (°) for the Complexes [RM(PhNCRⁿNPh)₂]

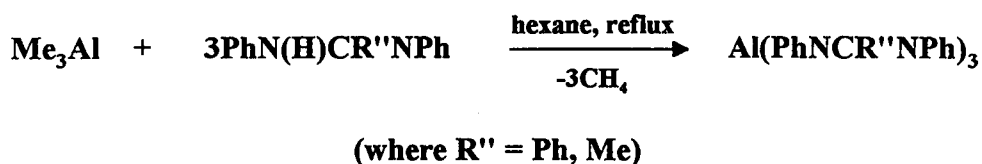


Complex	4	5	6	7	8	e	f	g
	N(1)-C(1)	N(2)-C(1)	N(1)-C(11)	N(2)-C(31)	C(1)-C(21)	N(1)-C(1)-N(2)	M-N(1)-C(1)	M-N(2)-C(1)
	N(1a/4)-C(1a/2)	N(2a/3)-C(1a/2)	N(1a/4)-C(11a/61)	N(2a/3)-C(31a/41)	C(1a/2)-C(21a/51)	N(2a/3)-C(1a/2)-N(1a/4)	M-N(1a/4)-C(1a/2)	M-N(2a/3)-C(1a/2)
[MeAl(PhNCR ⁿ NPh) ₂]	1.320(3)	1.318(3)	1.400(3)	1.431(4)	1.494(4)	109.82(23)	91.23(17)	92.61(17)
[MeGa(PhNCR ⁿ NPh) ₂]	1.326(3)	1.335(3)	1.399(3)	1.409(3)	1.481(4)	109.92(23)	90.21(16)	95.15(17)
[EtGa(PhNCR ⁿ NPh) ₂]	1.319(3)	1.338(3)	1.409(3)	1.410(3)	1.479(4)	110.61(23)	90.14(16)	95.44(16)
[EtGa(PhNCR ⁿ MeNPh) ₂]	1.316(4)	1.338(5)	1.412(5)	1.401(4)	1.505(5)	109.92(30)	90.43(22)	96.25(22)
[EtIn(PhNCR ⁿ NPh) ₂]	1.315(4)	1.343(5)	1.408(5)	1.403(4)	1.494(5)	109.87(30)	90.26(22)	96.76(21)
[EtIn(PhNCR ⁿ NPh) ₂]	1.332(7)	1.344(7)	1.415(7)	1.421(7)	1.497(9)	112.55(50)	90.80(33)	97.34(33)
[EtIn(PhNCR ⁿ NPh) ₂]	1.311(7)	1.350(7)	1.429(9)	1.416(7)	1.487(8)	112.17(47)	91.74(34)	97.14(34)

Preparation of Tris(Amidinato) Complexes of Aluminium, Gallium and Indium.

The evidence presented in the remainder of this chapter shows that the sequential substitution of the alkyl groups in the trialkyl derivatives of aluminium, gallium and indium can be continued with the amidine ligand to form complexes of the type $[M(L)_3]$ ($L =$ amidinato). It was again decided to use the two amidine ligands, N,N' -diphenylbenzamidine and N,N' -diphenylacetamidine, to establish a general preparatory route for this type of complex.

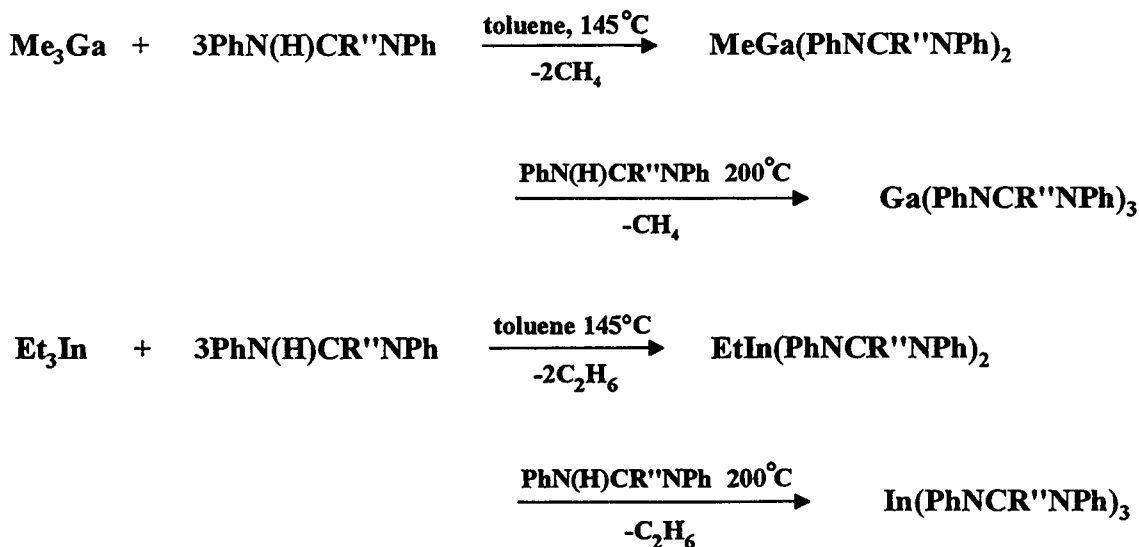
The aluminium-tris(amidinato) complexes are prepared at a relatively low temperature by the reaction of trimethylaluminium (1 mole) with amidine (3 moles) in refluxing hexane. Three moles of methane are eliminated and the complexes form as insoluble precipitates which can be isolated in high yield by filtration:



For example, the interaction of Me_3Al with three mole equivalents of a hexane suspension of N,N' -diphenylbenzamidine chilled in liquid nitrogen and, following the initial exothermic reaction, heating the mixture under reflux affords a flocculent pale green suspension. Cooling of the reaction mixture allows the isolation of the aluminium-tris(amidinato) derivative, $[\text{Al(PhNCPHNPh)}_3]$, in a yield of ca. 70%.

The synthesis of the corresponding gallium and indium complexes requires more extreme conditions. Thus when Me_3Ga or Et_3In (1 mole) and N,N' -diphenylbenzamidine (3 moles) in toluene solution are heated in a sealed tube at 145°C for 12 hours only two moles of alkane are evolved with the formation of the bis(amidinato) products $[\text{RM(PhNCPHNPh)}_2]$ ($M = \text{Ga, R = Me; M = In, R = Et}$), and 1 mole of unreacted free ligand. Removal of the solvent and further heating of the melt at 200°C for 0.5 hours leads to the further elimination of 1 mole of alkane, yielding the tris-substituted products

leads to the further elimination of 1 mole of alkane, yielding the tris-substituted products $[M(\text{PhNCR}''\text{NPh})_3]$ as pale yellow solids. The analogous N,N' -diphenylacetamidino derivatives are prepared in a similar manner.



(where $R'' = \text{Me, Ph}$)

These complexes are less soluble in chloroform than their mono- and dialkyl-metal counterparts, and recrystallisation from this solvent gives microcrystalline solids, which are only slightly air sensitive, and also soluble in toluene and THF. The nature of the complexes has been investigated by elemental analysis (C, H, N), ^1H and ^{13}C N.M.R., I.R., and mass spectroscopy and the solid state structure of $[\text{In}(\text{PhNCPHNP})_3]$ has been determined by a single crystal X-ray diffraction study.

Spectroscopic Properties of the Metal-tris(amidinato) Complexes

Nuclear Magnetic Resonance Spectra

Details of the ^1H N.M.R. spectra of the individual compounds are reported in the Experimental Section and only the general features of the spectra will be discussed here. The spectra of the N,N' -diphenylbenzamidinato and N,N' -diphenylacetamidinato compounds of aluminium, gallium and indium are all very similar and indicate a high

degree of symmetry in these compounds. All the N-phenyl aromatic protons appear as a set of three signals of multiplicity doublet, triplet and triplet with integral ratios of 4:4:2 respectively. The central C-phenyl ring protons in the benzamidinato compounds also appear as one set of doublet, triplet and triplet resonances with integral ratio of 2:2:1 respectively, and the methyl protons in the acetamidinato derivatives appear as a sharp singlet.

All the compounds were sufficiently soluble in deuteriochloroform to allow ^{13}C N.M.R. spectra to be obtained routinely and these are summarised in Table 2.25. Assignments of the resonances were made by ^1H - ^{13}C correlation experiments (see Experimental Section for the atom numbering scheme). The spectra are clearly consistent with the ^1H N.M.R. spectra; the N,N'-diphenylbenzamidinato derivatives show 8 signals in the aromatic carbon region and the N,N'-diphenylacetamidinato derivatives show 4 such signals and 1 additional signal corresponding to the methyl carbon atom. The remaining resonance, near 169 p.p.m. in the spectra of the aluminium compounds and in the region 166.5 to 167.5 p.p.m. for the gallium and indium compounds, is assigned to the skeletal NCN carbon atom. These shifts are similar to those found for the mono- and bis-(amidinato) derivatives already discussed, in which a bidentate chelate ligand co-ordination mode was established.

Infra-red Spectra

The infra-red spectra of the three N,N'-diphenylbenzamidinato derivatives were obtained from Nujol mulls. Although these spectra suffer from the usual problems associated with detailed interpretation because of complexity, they are useful for comparison with the data obtained from the related derivatives prepared with this ligand. A detailed listing of the spectra of the complexes is given in the Experimental Section.

Above ca. 750cm^{-1} , the overall appearance of each spectrum closely resembles that obtained for the corresponding dimethylmetal-N,N'-diphenylbenzamidinato complex. Most notably, the position and relative intensity of the band in the Amidine I region assigned to the $\nu_{\text{asym}}(\text{CN}_2)$ stretching vibration at ca. 1595cm^{-1} is not significantly

Table 2.25 Summary of Proton decoupled ^{13}C N.M.R. data (δ / p.p.m.) of metal-tris(aminato) complexes.

Complex	C-10	aromatic	C-6	C-1	C-5
$[\text{Al}(\text{PhNCPPhNPh})_3]$	-	121.75(C4), 124.78 (C2) 127.76 (C3), 128.24 (C8) 129.23 (C9), 129.29 (C7)	130.84	144.50	169.17
$[\text{Al}(\text{PhNCMeNPh})_3]$	13.71	122.40 (C4), 124.67 (C3) 128.27 (C2).	-	145.11	169.04
$[\text{Ga}(\text{PhNCPPhNPh})_3]$	-	121.78 (C4), 124.71 (C2) 127.83 (C3), 128.27 (C8) 129.23 (C9)	130.97	144.60	166.70
$[\text{Ga}(\text{PhNCMeNPh})_3]$	14.73	122.46 (C4), 124.80 (C2) 128.54 (C3)	-	146.23	166.50
$[\text{In}(\text{PhNCPPhNPh})_3]$	-	121.62 (C4), 124.63 (C2) 127.96 (C3), 128.23 (C7) 129.10 (C9), 129.96 (C8)	131.84	145.60	167.51
$[\text{In}(\text{PhNCMeNPh})_3]$	14.64	122.31 (C4), 124.65 (C2) 128.4 (C3)	-	146.07	166.58

Run as CDCl_3 solutions at 25°C

different. The similarity in this region of the spectra of these two types of complex suggests that a common amidinato co-ordination mode exists in the solid state.

Comparison of the spectra below ca. 750cm^{-1} reveals some differences, mainly that there are fewer bands in the spectra of the metal-tris(amidinato) complexes which is consistent with the absence of any metal-alkyl groups. Relatively weak but well defined bands at 592 and 523cm^{-1} in the spectrum of the aluminium complex, at 542 and 465cm^{-1} in the spectrum of the gallium complex, and at 465 and 375cm^{-1} in the spectrum of the indium complex are tentatively assigned to the MN_2 asymmetric and symmetric stretches respectively, and these are consistent with the values reported for the dimethylmetal- $\text{N,N}'$ -dimethylacetamidinato and bis(dimethylmetal)-oxamidinato compounds of aluminium, gallium and indium.^{109,110}

Upon exposure of the complexes to moist air over a period of ca. 15 minutes, the spectra show the presence of decomposition products. The region below 750cm^{-1} becomes more complex and the presence of free or co-ordinated amidine is indicated by the appearance of a broad band near 3250cm^{-1} assigned to $\nu(\text{N-H})$ stretching frequencies, and the remaining additional ligand bands are similar to those found in the parent ligand.

Mass Spectra

E.I. mass spectra were recorded for all the compounds and complete lists of the important peaks are given in the Experimental Section. Tables 2.26 to 2.31 detail the major metal-containing ions. For convenience, the appropriate amidinato ligand is abbreviated to L and, where applicable, assignments are based on ^{69}Ga and ^{115}In . The spectra show molecular ion peaks of low intensity corresponding to the presence of the monomeric species $[\text{M}(\text{L})_3]^+$ in the gas phase for all the complexes, so providing structural evidence consistent with that obtained in solution and the solid state from the N.M.R. and I.R. work respectively. No peaks at higher mass were found. More intense peaks corresponding to metal-containing ions arise from sequential loss of whole amidinato units producing the species $[\text{M}(\text{L})_2]^+$, $[\text{ML}]^+$ and $[\text{M}]^+$ ($\text{M} = \text{Al}, \text{Ga}, \text{In}$).

Additional metal-containing ions of low-medium relative intensity are found for the *N,N'*-diphenylbenzamidinato derivatives similar to those observed for the mono- and bis-amidinato compounds, where fragmentation and rearrangement of the ligand occurs while still attached to the metal. This alternative less favoured pathway produces peaks assigned to the species $[\text{MPh(L)}]^+$ and $[\text{MPh}_2]^+$, although, in fact, no peaks corresponding to the species $[\text{MPh(L)}_2]^+$ were observed ($\text{M} = \text{Al, Ga, In}$).

Molecular ion peaks from the ligand, with fragmentation products similar to those found previously, are prominent in all the spectra.

Table 2.26 Major aluminium-containing fragments from Al(PhNCPhNPh)_3

<i>m/z</i>	Rel. Int. (%)	Assignment
840	17.0	M^+
839	9.3	$[\text{M}-1]^+$
569	54.8	$[\text{Al(L)}_2]^+$
375	26.5	$[\text{AlPh(L)}]^+$
181	39.4	$[\text{Al(Ph)}_2]^+$

Table 2.27 Major aluminium-containing fragments from Al(PhNCMeNPh)_3

<i>m/z</i>	Rel. Int (%)	Assignment
654	11.9	M^+
445	6.8	$[\text{Al(L)}_2]^+$
236	3.9	$[\text{AlL}]^+$

Table 2.28 Major gallium-containing fragments from $\text{Ga}(\text{PhNCPHNP})_3$

m/z	Rel. Int. (%)	Assignment*
882	7.0	M^+
611	26.4	$[\text{Ga}(\text{L})_2]^+$
417	5.5	$[\text{GaPh}(\text{L})]^+$
340	1.4	$[\text{GaL}]^+$
223	20.1	$[\text{GaPh}_2]^+$
69	9.7	Ga^+

* based on ^{69}Ga **Table 2.29** Major gallium-containing fragments from $\text{Ga}(\text{PhNCMeNPh})_3$

m/z	Rel. Int. (%)	Assignment*
696	4.5	M^+
487	11.9	$[\text{Ga}(\text{L})_2]^+$
278	7.4	$[\text{GaL}]^+$
69	68.0	Ga^+

* based on ^{69}Ga **Table 2.30** Major indium-containing fragments from $\text{In}(\text{PhNCPHNP})_3$

m/z	Rel. Int. (%)	Assignment*
928	33.8	M^+
657	43.9	$[\text{In}(\text{L})_2]^+$
463	4.7	$[\text{InPh}(\text{L})]^+$
386	3.8	$[\text{InL}]^+$
269	9.7	$[\text{In}(\text{Ph})_2]^+$
115	48.6	In^+

* based on ^{115}In

Table 2.31 Major indium-containing fragments from $\text{In}(\text{PhNCMeNPh})_3$

m/z	Rel. Int. (%)	Assignment*
742	7.9	M^+
534	23.9	$[\text{In}(\text{L})_2 + \text{H}]^+$
324	2.2	$[\text{InL}]^+$
115	48.6	In^+

* based on ^{115}In

X-ray Crystallographic Studies

Single crystal X-ray diffraction studies have been conducted on the indium derivative of N,N'-diphenylbenzamidine in order to provide structural information on the nature of this type of complex, and in particular, to determine the effects of the ligand steric constraints upon the metal co-ordination geometry. The results of the X-ray study are discussed in this section and a view of the structure and atomic labelling scheme is shown in Figure 2.23. The structure consists of a monomeric six co-ordinate indium atom with three bidentate chelate amidinato ligands and is similar to that reported by Barron *et al* for the related indium-tris(triazenido) complex $[\text{In}(\text{PhNNNPh})_3]$.¹¹⁸ Both structures are shown together in Figure 2.24 and the bond lengths and bond angles of the two compounds are compared in Table 2.32.

(a) The Indium Co-ordination Environment

In both structures the indium atom is surrounded by six nitrogen donor atoms in a trigonally distorted octahedral co-ordination geometry, with the three bidentate ligands in a pseudo- C_3 propeller arrangement. In the tris(amidinato) complex, the *trans* N-In-N atoms are separated by 152.4° [N(1)-In(1)-N(5)], 149.3° [N(2)-In(1)-N(4)], and 136.0° [N(3)-In(1)-N(6)]. As all three ligands are chemically equivalent and there are no unusual intramolecular contacts, the larger distortion of the latter metal valency angle is

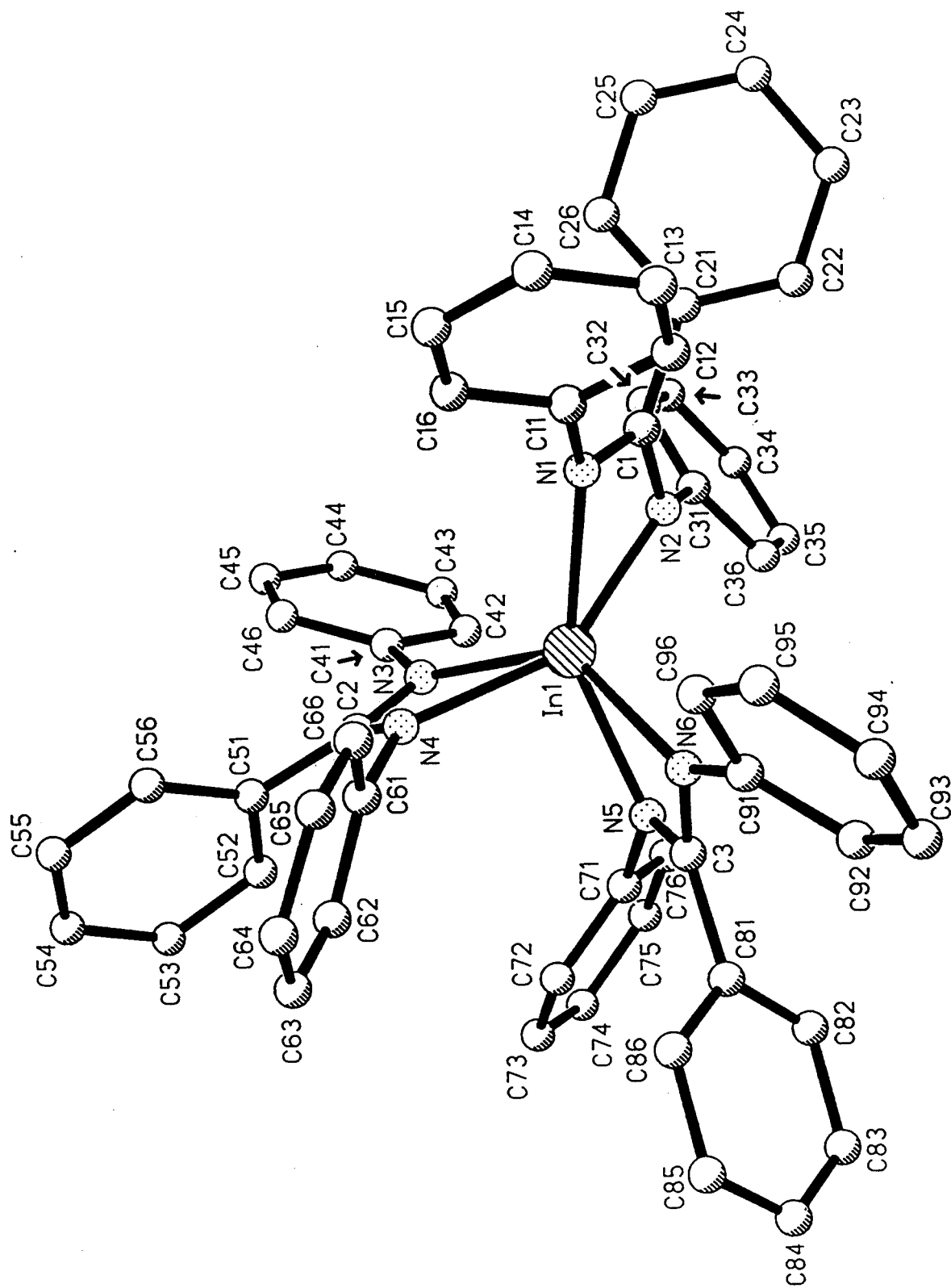


Figure 2.23 The molecular structure of indium-tris(*N,N'*-diphenylbenzamidinato), viewed along the C_3 axis.

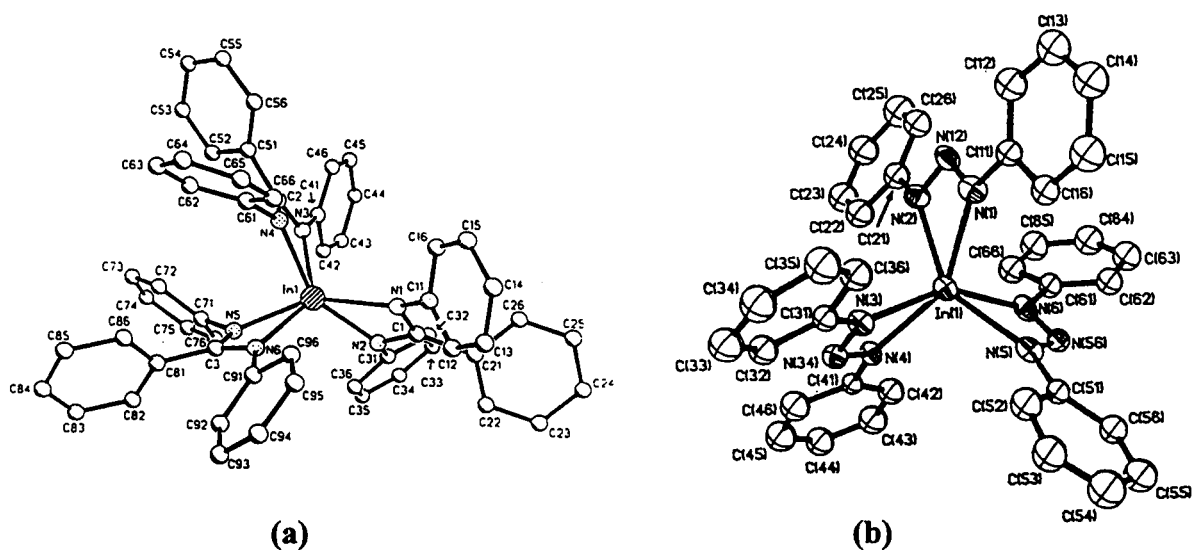


Figure 2.24 The molecular structures of (a) $[\text{In}(\text{PhNCPhNPh})_3]$ and (b) $[\text{In}(\text{PhNNNPh})_3]$.

Table 2.32 Principal bond lengths (Å) and angles ($^\circ$) in $[\text{In}(\text{PhNCPhNPh})_3]$ and $[\text{In}(\text{PhNNNPh})_3]$.

	$[\text{In}(\text{PhNCPhNPh})_3]$	$[\text{In}(\text{PhNNNPh})_3]$
In(1)-N(1)	2.26(6)	2.259(9)
In(1)-N(2)	2.217(5)	2.26(1)
In(1)-N(3)	2.278(7)	2.22(1)
In(1)-N(4)	2.221(6)	2.231(9)
In(1)-N(5)	2.252(8)	2.24(1)
In(1)-N(6)	2.242(7)	2.21(1)
N(1)-In(1)-N(2)	59.07(25)	55.2(4)
N(3)-In(1)-N(4)	58.92(26)	56.5(3)
N(5)-In(1)-N(6)	59.10(27)	56.3(4)
N(1)-In(1)-N(4)	104.19(25)	148.9(4)
N(2)-In(1)-N(5)	107.53(25)	144.1(4)
N(3)-In(1)-N(6)	135.99(25)	151.5(4)
N(1)-In(1)-N(3)	116.19(24)	105.6(4)
N(1)-In(1)-N(5)	152.41(26)	102.0(3)
N(1)-In(1)-N(6)	102.47(27)	99.7(4)
N(2)-In(1)-N(3)	103.05(26)	107.8(4)
N(2)-In(1)-N(4)	149.32(21)	102.9(4)
N(2)-In(1)-N(6)	114.88(25)	97.2(4)
N(3)-In(1)-N(5)	89.52(26)	105.0(4)
N(4)-In(1)-N(5)	97.54(25)	107.1(43)
N(4)-In(1)-N(6)	92.96(25)	105.4(3)

attributed to crystal packing requirements. These angles compare with the corresponding angles found in the tris(triazenido) complex of 144.1°, 148.9° and 151.5°.

The three metal–amidinato ligand bite angles are effectively equal with a mean value of 59.0° and show little variation from the values previously presented in the four and five co-ordinate indium complexes with this ligand, namely [Me₂In(PhNCPhNPh)] and [EtIn(PhNCPhNPh)₂], [58.9° (aver.) and 58.7°(aver.) respectively]. These angles compare with the smaller metal–triazenido bite angle of 56.0°(aver.).

The In–N distances show a significant variation, ranging from 2.217 to 2.278 Å and reveal that two of the amidinato ligands are substantially asymmetrically bound to the metal centre, with the remaining ligand more symmetrically co-ordinated. The mean In–N distance of 2.25 Å is very similar to that found in the tris(triazenido) complex of 2.24 Å, in which all three chelate ligands are symmetrically co-ordinated, and a similar variation in the In–N distances is found, ranging from 2.220 to 2.260 Å. Despite these variations, both mean values compare closely with the mean distance found in the four co-ordinate complex [Me₂In(PhNCPhNPh)] of 2.25 Å, as already discussed. The reason for these variations is unclear, particularly in the absence of any strong intramolecular interactions of hydrogen atoms with the nitrogen atoms. As mentioned above, these are probably as a result of packing forces on the ligand system, although distortions originating from electronic effects should also be considered for this heavier p-block element.

(b) Ligand Co-ordination Geometry

Once again, the bidentate chelation of the amidinato ligand leads to a high degree of delocalisation within the NCN framework. However, the asymmetrical co-ordination of two of the amidinato ligands, [N(1)–C(1)–N(2)] and [N(3)–C(2)–N(4)], is reflected in the two slightly different skeletal amidinato carbon–nitrogen bond distances from those in the symmetrically co-ordinated ligand [N(5)–C(3)–N(6)] where the two distances are effectively equal. The average distance of 1.328(11) Å is similar to the corresponding

values found in the complex $[\text{Me}_2\text{Ga}(\text{PhNCPhNPh})]$ of $1.333(11)\text{\AA}$, where the amidinato ligand is symmetrically co-ordinated to the gallium atom.

The ligand bond angles within each of the three four-membered chelate rings show little variation throughout the structure. The mean ligand N–C–N angle of 112.8° is similar to that found for $[\text{Me}_2\text{In}(\text{PhNCPhNPh})]$ of 113.5° . Both these angles are significantly larger than the mean value of 108.6° found in the tris(triazenido) complex. This difference may be accounted for by the skeletal C–N bond distances in the amidinato ligand being slightly longer than the N–N distances in the triazenido ligand. Comparison of the ligand and metal bite angles found in these complexes indicates that co-ordination of the triazenido ligand imposes greater steric strain in the four-membered chelate ring than in the amidinato chelate ring. It may therefore be concluded that the amidinato ligand, $[\text{PhNCPhNPh}]^-$ is a more effective chelating ligand than the triazenido ligand $[\text{PhNNNPh}]^-$ for this size of metal atom.

Discussion

Given the isoelectronic nature and structural similarities of the amidinato and triazenido anions, it is perhaps not surprising that their complexes with the alkyl derivatives of the group 13 metals of aluminium, gallium and indium also possess similar chemical and structural properties. However, there are some notable differences in the reactions involving the triazenes and the amidines. With the former, the compounds $[\text{M}(\text{L})_3]$ ($\text{M} = \text{Al}, \text{In}; \text{L} = [\text{PhNNNPh}]^-$), are obtained at room temperature and, as previously discussed for the aluminium compound, this is the only isolable product, even when an excess of Me_3Al is used, although the intermediates, $[\text{R}_2\text{Al}(\text{PhNNNPh})]$ and $[\text{RAl}(\text{PhNNNPh})_2]$, can be obtained for the bulky $\text{R} = \text{Bu}^t$ group.^{116,117,118} There is an earlier report of $[\text{Me}_2\text{Ga}(\text{PhNNNPh})]$ being formed when 1 mole of the triazene is added to a slight excess of Me_3Ga , but this type of intermediate has not been reported in the later work of Barron *et al.*¹¹⁹

With the amidines, controlled sequential alkyl substitution reactions occur for aluminium, gallium and indium, allowing isolation of the intermediates of the type

$[R_xM(L)_{3-x}]$ ($R = \text{Me, Et, L} = \text{ArNCR}''\text{NAr, R}'' = \text{Me, Ph; } x = 0, 1 \text{ and } 2$). Such complexes are indefinitely stable in an inert atmosphere in both the solid and in solution. However, it was also found in the present work that treatment of a hexane suspension of N,N' -diphenylbenzamidinium with an excess of the trimethylamine adduct of aluminium hydride, $\text{AlH}_3 \cdot \text{NMe}_3$, at -78°C , exclusively yields the tris(amidinato) complex, $[\text{Al}(\text{PhNCPhNPh})_3]$, on warming to room temperature.

These observations suggest that alkyl (or hydride)–ligand exchange reactions are responsible for the formation of further aluminium–ligand substituted products, presumably via bridged intermediates, and are consistent with the inhibition of such exchange with the increasing steric bulk of the R groups on the metal. Furthermore, the points noted above demonstrate the greater tendency of the aluminium–triazenido complexes, compared to the amidinato complexes, to form the tris–substituted product. Such ligand exchange necessarily involves opening of the chelate ring, which presumably occurs more readily for the triazenido derivatives, and may be explained in terms of the greater inherent strain within the triazenido chelate ring (see previous section), which may promote these exchange reactions.

The N,N' -diphenylbenzamidinato and N,N' -diphenylacetamidinato anions have been shown to act as chelating or bridging ligands with transition metal species,¹⁸⁸ indicating the co–ordinative versatility of these ligands. In all the amidinato complexes structurally characterised by X–ray crystallography in this work, these amidinato ligands bind exclusively in a bidentate chelate manner in which the metal valency and ligand bond angles are considerably distorted from their ideal values. This is in contrast to the bonding situation found in the dimethylaluminium and dimethylgallium derivatives of the dimethylacetamidinato ligand, in which a dimeric structure with bridging ligands is obtained,¹⁰⁹ presumably because the nitrogen and central carbon atoms in this ligand can not accommodate the required extent of distortion from their ideal valency angles for bidentate chelation.

CHAPTER 3

Reactions of Trimethylgallium with Two N,N'-Unsubstituted Amidine Ligands

CHAPTER 3

Reactions of Trimethylgallium with Two N,N'-Unsubstituted Amidine Ligands.

Introduction

There now exists a significant number of studies reported in the chemical literature on N,N'-disubstituted amidine complexes with metal species. A variety of synthetic routes to these types of complexes is known and a substantial amount of X-ray crystallographic data is available. This stands in contrast to the comparatively few studies involving N,N'-unsubstituted amidine-metal complexes. This is evident from the small number of X-ray crystal structures known for metal complexes with these ligands, and these are confined to eight examples of transition metal salt complexes with these amidine derivatives. The reader is referred to the review by Barker and Kilner for further information on these complexes.¹⁸⁸

This paucity of previous study of the co-ordination chemistry of these ligands may be in part attributed to synthetic difficulties in obtaining and handling them because of their generally highly hygroscopic nature. For example, it was not until relatively recently (1981) that a satisfactory synthetic procedure was reported in the chemical literature for the preparation of crystalline acetamidine, $[\text{H}_2\text{NCMeNH}]$, which reacts rapidly in air to give a clear liquid.²²⁰

An early example of an acetamidine complex was that involving the reaction between $[\text{Pt}(\text{MeCN})_2\text{Cl}_2]$ and ammonia. The product of this reaction was initially reported in 1915 to be formulated as $[\text{Pt}(\text{NH}_3)_4(\text{MeCN})_2]\text{Cl}_2 \cdot \text{H}_2\text{O}$.²²¹ However, the X-ray structural determination of the complex, reported later (1962) revealed it to be $[\text{Pt}(\text{NH}_3)_2(\text{H}_2\text{NCMeNH})_2]\text{Cl}_2 \cdot \text{H}_2\text{O}$, containing the acetamidine ligand (co-ordinated via the imino-N lone pair) which is formed via nucleophilic attack of ammonia on the co-ordinated nitrile ligand.²²²

Similar reactions between a series of dialkylaluminium and alkyl(chloro)aluminium amides with nitriles to produce aluminium–amidinato complexes have also been investigated.^{223,224,225} For example, insertion of $\text{MeAl}(\text{Cl})\text{NH}_2$ into benzonitrile yielded the aluminium complex, $[\text{Me}(\text{Cl})\text{Al}(\text{HNCPhNH})]$.²²⁵ The application of this type of reaction for the preparation of the corresponding free amidine ligand was demonstrated in this work. Hydrolysis of the above complex produced the free benzamidine ligand.

In this Chapter the results of the reactions between trimethylgallium and two $\text{N,N}'$ -unsubstituted ligands, namely *tert*-butyramidine, $[\text{H}_2\text{NCBu}^t\text{NH}]$ and trifluoroacetamidine, $[\text{H}_2\text{NCCF}_3\text{NH}]$ are reported. These ligands have been chosen in order to evaluate the contrasting electronic character of the central carbon atom substituent on the chemical reactivity of the amidine functional group.

(1) Reaction of trimethylgallium with *tert*-butyramidine, $[\text{H}_2\text{NCBu}^t\text{NH}]$.

This reaction was performed by mixing equimolar quantities of *tert*-butyramidine and trimethylgallium in hexane solution. Me_3Ga was condensed under vacuum onto the amidine suspension which was held at -196°C . A reaction occurred readily, with the evolution of methane commencing at around -70°C , and was complete by the time the mixture had warmed to room temperature. Using a calibrated portion of the vacuum line, the amount of methane evolved was shown to be one mole equivalent. The result was a colourless solution, which, after concentrating and cooling at -35°C , gave a low yield (ca. 10%) of small irregularly shaped colourless crystals. These were found to be very sensitive to air and moisture, becoming opaque in appearance after exposure to air for approximately ten seconds. Removal of the remaining solvent gave a white solid, which was shown by its ^1H N.M.R. and I.R. spectra to contain a number of species, including free ligand. Attempts to recrystallise a pure complex failed, primarily because of the appreciable solubility in the most preferable solvents, including hexane and toluene, and the extreme sensitivity of the product to traces of moisture which resulted in the formation of free ligand.

The reaction was repeated using the same general method except that no solvent was used in order to eliminate the presumed source of moisture contamination. Care was taken to ensure that the reaction mixture was warmed slowly to room temperature, thus allowing it to be completed at low temperatures (ca. -40°C). The resultant white solid sublimed rapidly under vacuum at 80°C onto a water cooled cold finger, and produced regular-shaped colourless crystals in an essentially quantitative yield with no detectable decomposition of the product. Unfortunately, these were too small for single crystal X-ray diffraction work. Because of the high moisture sensitivity of the product, this purification method was preferable to attempting multiple recrystallisation from hexane or toluene solution.

The ^1H and ^{13}C N.M.R. spectra of the sublimed product were recorded from C_6D_6 solution and are summarised in the Experimental Section. The ^1H spectrum shows a sharp singlet at 0.08 p.p.m. (rel. intens. 6) which is assigned to two organometallic gallium-methyl groups. The protons of the *tert*-butyl group appear as one sharp singlet at 0.79 p.p.m. (rel. intens. 9), and the remaining broad resonance, centred near 4.7 p.p.m., is attributed to two NH protons, confirming the loss of one proton by methane elimination. The overall simplicity of the spectrum implies that the gallium atom is either in a symmetrical co-ordination site or is in rapid motion on the N.M.R. timescale between chemically different co-ordination environments.

A similar pattern is repeated in the ^{13}C spectrum which shows only three sharp resonances for the ligand carbon atoms and one well defined resonance in the region expected for the organometallic carbon atoms. The most interesting feature to note is the position of the resonance attributed to the skeletal NCN carbon atom at 184.19 p.p.m. This shift is significantly further downfield compared to those found for the dialkylgallium-N,N'-diaryl substituted amidinato derivatives between 154 and 168 p.p.m. While this comparison may justify an explanation in terms of a change in amidinato bonding mode for the butyramidinato derivative from the bidentate chelate mode seen in the complexes reported in Chapter 2, the N.M.R. frequency of this atom is also expected

to be affected by the change in the electronic properties of the amidinato substituents found in this derivative.

The E.I. mass spectrum was recorded and the significant gallium-containing ions found are summarised in Table 3.1. The spectrum shows peaks that correspond to both monomer and dimer units, and each is clearly identified by the peak patterns derived from the isotopes ^{69}Ga (60.5%) and ^{71}Ga (39.5%). These results show that associated species exist in the gas phase, and an associated solid state structure is proposed, such as dimeric or trimeric (or higher oligomeric) species, as discussed further below.

Table 3.1 Significant gallium-containing ions in the E.I. mass spectrum of $[\text{Me}_2\text{Ga}(\text{HNCBu}^t\text{NH})]$. (D = dimer, M = monomer, L = amidinato).

m/z	Relative Intensity (%)	Assignment
397, 399, 401	2.4 : 3.1 : 1.1	$[\text{DH}]^+$
381, 383, 385	4.7 : 6.2 : 2.0	$[\text{D-Me}]^+$
298, 300, 302	9.7 : 12.0 : 4.1	$[\text{D-L}]^+$
198, 200	2.5 : 1.5	M^+
183, 185	84.0 : 53.6	$[\text{M-Me}]^+$
168, 170	12.0 : 7.7	$[\text{M-2Me}]^+ / [\text{M-Me-NH}]^+$
153, 155	8.5 : 5.9	$[\text{M-2Me-NH}]^+$
99, 101	28.7 : 22.0	$[\text{GaMe}_2]^+$
69, 71	24.6 : 15.3	Ga^+

Ions derived from the amidinato ligand include the base peak at m/z 85 $[\text{Bu}^t\text{CNH}_2]^+$, m/z 57 $[\text{Bu}^t]^+$ (23.5%), m/z 43 $[\text{H}_2\text{NCNH}]^+$ (81.6%) and m/z 42 $[\text{HNCNH}]^+$ (59.0%).

The infra-red spectrum was recorded as a Nujol mull and a summary of the important peaks is given in the Experimental Section. The spectrum displays some similarity with that reported for the dimethylgallium-N,N'-dimethylacetamidinato

complex.¹⁰⁹ The spectrum of this latter complex was reported to show strong bands assigned to the asymmetrical and symmetrical stretching modes of the CN_2 skeletal unit at 1552 and 1475cm^{-1} respectively. In the spectrum of the butyramidinato complex, these modes are assigned to the bands observed at 1562 and 1514cm^{-1} respectively. The strong bands at 574 and 531cm^{-1} can be assigned as the $\nu_{\text{asym}}(\text{GaC}_2)$ and $\nu_{\text{sym}}(\text{GaC}_2)$ modes respectively and the weak band at 409cm^{-1} can be assigned to the $\nu_{\text{symm}}(\text{GaN}_2)$ mode. These values are consistent with the corresponding values reported for the C_2GaN_2 unit in the acetamidinato complex of 557 , 518 and 414cm^{-1} . As expected, the most notable difference between the spectra is the sharp band of medium intensity centred near 3409cm^{-1} in the spectrum of the butyramidinato complex, which is assigned to the remaining NH groups of this ligand.

The similarity of the I.R. spectra of these compounds, particularly in the position and intensity of the band assigned to the $\nu_{\text{asym}}(\text{CN}_2)$ mode, may warrant speculation that the butyramidinato complex shares a structure similar to that found for the $\text{N,N}'$ -dimethylacetamidinato complex, namely, a puckered eight-membered ring arrangement, see (A) below. Importantly, this evidence suggests that an alternative oligomeric arrangement, such as a dimeric four-membered ring arrangement, with bridging amido groups, (B), is unlikely. This type of arrangement would reasonably be expected to give rise to a strong band from the $\nu(\text{C}=\text{N})$ or $\nu_{\text{asym}}(\text{CN}_2)$ mode at above 1600cm^{-1} , and thus is improbable.

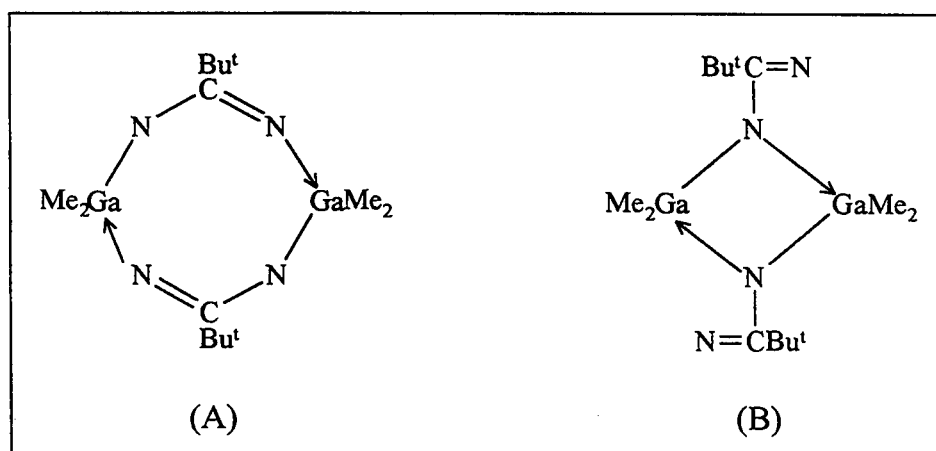


Figure 3.1 Possible amidinato co-ordination modes in $[\{\text{Me}_2\text{Ga}(\text{HNCBu}^t\text{NH})\}_2]$

Discussion

Two other related dimethylgallium-N,N'-unsubstituted amidinato complexes have been previously prepared in this laboratory using the ligands acetamidine and benzamidine.²⁰⁰ The mass spectroscopic data obtained for these compounds also suggests that dimeric species are present in the vapour phase. In the solid state, these compounds are assigned a dimeric or higher oligomeric formulation, $[\{\text{Me}_2\text{Ga}(\text{HNCRNH})\}_n]$ (R = Me, Ph). In the light of this previous and the present work, it would appear that when the amidinato ligand contains N-Ph (or substituted phenyl groups), only ions corresponding to monomer species are observed, whereas when NH groups are present in the amidinato ligand, there is clear evidence for the existence of higher oligomeric species similar to that observed for $[\{\text{Me}_2\text{Ga}(\text{MeNCMeNMe})\}_2]$.¹⁰⁹ It is noted that the data do not exclude the possibility of weakly bound oligomers for the "N-Ph" class of amidinato ligand, but the mass spectroscopic data are compatible with the X-ray data obtained for dimethylgallium-N,N'-diphenylbenzamidinato.²⁰⁰

(2) Reaction of trimethylgallium with trifluoroacetamidine, $[\text{H}_2\text{NCCF}_3\text{NH}]$.

This reaction was also carried out in the absence of solvent, and Me_3Ga was manipulated using a high-vacuum line. Thus Me_3Ga was condensed onto 1 mole equivalent of degassed $[\text{H}_2\text{NCCF}_3\text{NH}]$ held at -196°C . On allowing the mixture to warm slowly to room temperature, a gas started to evolve at around -70°C , and this gas elimination ceased by the time the mixture had reached room temperature. By using a calibrated portion of the vacuum line, the amount of gas evolved was shown to be 1 mole equivalent. The infra-red spectrum of the gas proved that it was methane. The reaction mixture contained a colourless viscous liquid and a colourless crystalline material. Upon heating to 70°C under a static vacuum, this solid rapidly sublimed onto the cold sides of the reaction vessel as well formed, colourless, and approximately cube-shaped air stable crystals, which were easily removed in the glove box, leaving the colourless viscous liquid at the bottom of the vessel. This solid was isolated in a yield (by weight) of typically around 35 – 40%.

The crystals were of a suitable quality to permit a single crystal X-ray diffraction study to be carried out in order to determine the nature of this compound. It is more convenient to introduce the results of this study first, and subsequently to explain the experimental and spectroscopic data obtained by using the X-ray structure. Figure 3.2 shows the molecular structure of the complex and the atomic labelling scheme used. The bond lengths and angles are shown in Figure 3.3 and Table 3.2. The molecular structure consists of a planar six-membered metallocycle containing the N,N'-chelating trifluoroacetimidoyltrifluoroacetamidinato ligand, $[\text{HNC}(\text{CF}_3)\text{NC}(\text{CF}_3)\text{NH}]$.

(a) The Gallium Co-ordination Environment

The dimethylgallium unit is symmetrically co-ordinated to both terminal nitrogen atoms of the imidoamidinato ligand, which results in a distorted tetrahedral environment, C_2GaN_2 , around the metal. The distortion from ideal metal co-ordination geometry arises from the steric constraints imposed by the rigid planar nature of the bidentate chelating ligand and gives a bite angle, $[\text{N}(1)\text{--Ga}(1)\text{--N}(3)]$ of $86.7(4)^\circ$, and a separation of the carbon atoms of $125.5(7)^\circ$.

The two gallium-nitrogen bond lengths of $1.992(9)$ and $2.012(9)\text{\AA}$ are both similar to the mean value reported in bis(dimethylgallium)-N,N',N'',N'''-tetramethyloxamidinato of $1.98(10)\text{\AA}$.¹¹⁰ The gallium atom in this latter complex is incorporated into a five-membered chelate ring and the complex is isostructural with the analogous indium derivative discussed in Chapter 2. The gallium centre exhibits a substantially similar co-ordination geometry, with N-Ga-N and C-Ga-C bond angles of $84.0(4)$ and $122.5(6)^\circ$ respectively. In comparison, the mean Ga-N distance observed in dimethylgallium-N,N'-diphenylbenzamidinato is slightly longer at $2.041(8)\text{\AA}$.²⁰⁰

The two gallium-carbon bond lengths, $1.900(12)$ and $1.931(15)\text{\AA}$, are considerably shorter than the average distance found in the oxamidinato derivative of $2.004(13)\text{\AA}$, but are comparable in length to the mean distance found in the amidinato complex of $1.944(12)\text{\AA}$. Comparison of the distances found in the present structure with values summarised by Tuck^{6c} for a number of four co-ordinate organogallium species,

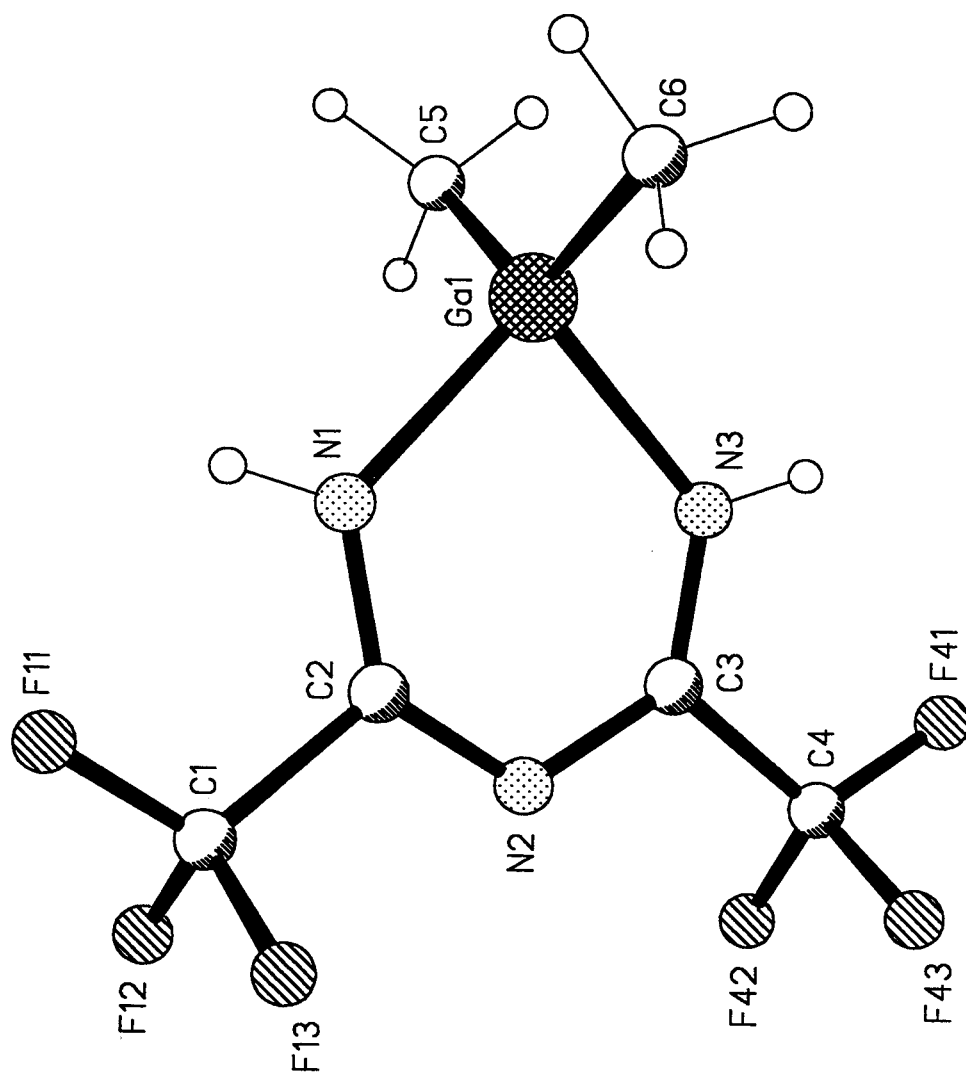


Figure 3.2 The molecular structure of $[\text{Me}_2\text{Ga}\{\text{HNC}(\text{CF}_3)\text{NC}(\text{CF}_3)\text{NH}\}] \cdot$.

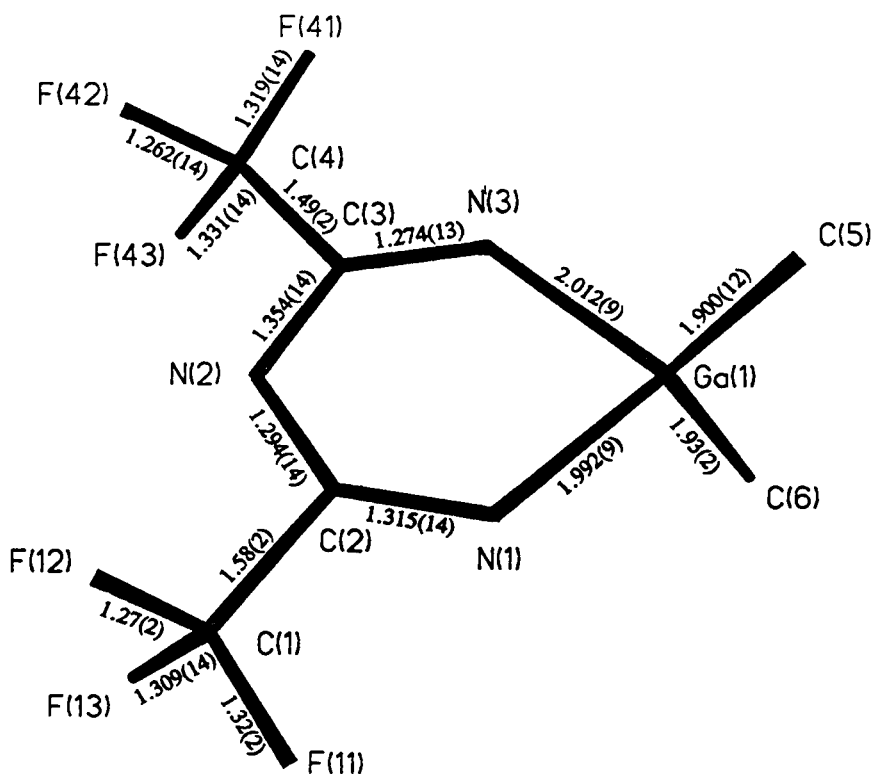


Figure 3.3 The molecular structure of $[\text{Me}_2\text{Ga}\{\text{HNC}(\text{CF}_3)\text{NC}(\text{CF}_3)\text{NH}\}]$, showing bond lengths (Å).

Table 3.2 Bond angles ($^\circ$) in $[\text{Me}_2\text{Ga}\{\text{HNC}(\text{CF}_3)\text{NC}(\text{CF}_3)\text{NH}\}]$.

C(5)-Ga(1)-C(6)	125.5(7)	C(5)-Ga(1)-N(1)	111.0(5)
C(6)-Ga(1)-N(1)	108.1(5)	C(5)-Ga(1)-N(3)	108.8(5)
C(6)-Ga(1)-N(3)	109.9(5)	N(1)-Ga(1)-N(3)	86.7(4)
C(2)-N(1)-Ga(1)	125.2(7)	C(2)-N(2)-C(3)	118.7(10)
C(3)-N(3)-Ga(1)	127.2(8)	F(12)-C(1)-F(13)	108.5(13)
F(12)-C(1)-F(11)	109.4(13)	F(13)-C(1)-F(11)	108.1(12)
F(12)-C(1)-C(2)	110.5(11)	F(13)-C(1)-C(2)	108.6(11)
F(11)-C(1)-C(2)	111.7(11)	N(2)-C(2)-N(1)	132.4(10)
N(2)-C(2)-C(1)	111.8(11)	N(1)-C(2)-C(1)	115.8(10)
N(3)-C(3)-N(2)	129.8(10)	N(3)-C(3)-C(4)	118.9(12)
N(2)-C(3)-C(4)	111.2(10)	F(42)-C(4)-F(41)	107.9(11)
F(42)-C(4)-F(43)	103.9(13)	F(41)-C(4)-F(43)	105.3(11)
F(42)-C(4)-C(3)	113.4(11)	F(41)-C(4)-C(3)	113.3(12)
F(43)-C(4)-C(3)	112.3(10)		

reveals that the Ga–N distances lie well within the range of 1.976(10) to 2.078(3)Å, whereas both Ga–C distances are amongst the shortest reported for the range 1.936(5) to 2.006(13)Å.

(b) Ligand Geometry

The structure of the ligand causes it to be planar, with a rigid bidentate chelating angle. All six atoms of the ring are coplanar within 0.010(7)Å. Furthermore, the CF₃ groups are symmetrically orientated in relation to each other, with the carbon and one fluorine atom from each group [F(1) and F(4)] lying approximately in the ring plane. This configuration is shown in Figure 3.4. The NH hydrogen atoms are not clearly visible on difference Fourier maps, but the orientation of the CF₃ groups suggests that the hydrogen atoms are associated with the terminal nitrogen atoms. This orientation maximises the interaction between the in-plane fluorine atoms and the hydrogen atoms. These hydrogen atoms are placed in calculated positions on N(1) and N(3). The calculated hydrogen–fluorine interactions have lengths of 2.217Å [H(1)–F(1)] and 2.231Å [H(3)–F(4)] compared with the sum of their van der Waals radii of 2.67Å.

The two internal ring N–C–N bond angles of 129.8(10)° [N(2)–C(3)–N(3)] and 132.4(10)° [N(1)–C(2)–N(2)] are significantly larger than the 110.8(7)° and 117.4(4)° observed in the bidentate chelating and bridging gallium–amidinato complexes respectively, discussed in Chapter 2.^{109,200} The internal bond angle at the central nitrogen atom, [C(2)–N(2)–C(3)] of 118.7(10)° indicates near ideal *sp*² hybridisation at this atom, while those at the two terminal nitrogen atoms have angles of 125.2(7)° [Ga(1)–N(1)–C(2)] and 127.2(8)° [Ga(1)–N(3)–C(3)]. These ring angles extend from the idealised value of 120° in order to compensate for the small ring angle at the metal.

The ring carbon–nitrogen bond distances indicate extensive delocalisation throughout the skeletal π -system. The ring comprises three short C–N distances, which vary from 1.274(13) to 1.315(14)Å, and one longer distance of 1.354(14)Å, and have a mean distance of 1.309(14)Å. This distance is significantly shorter than the corresponding average distance of 1.333(11)Å found in the strained four-membered

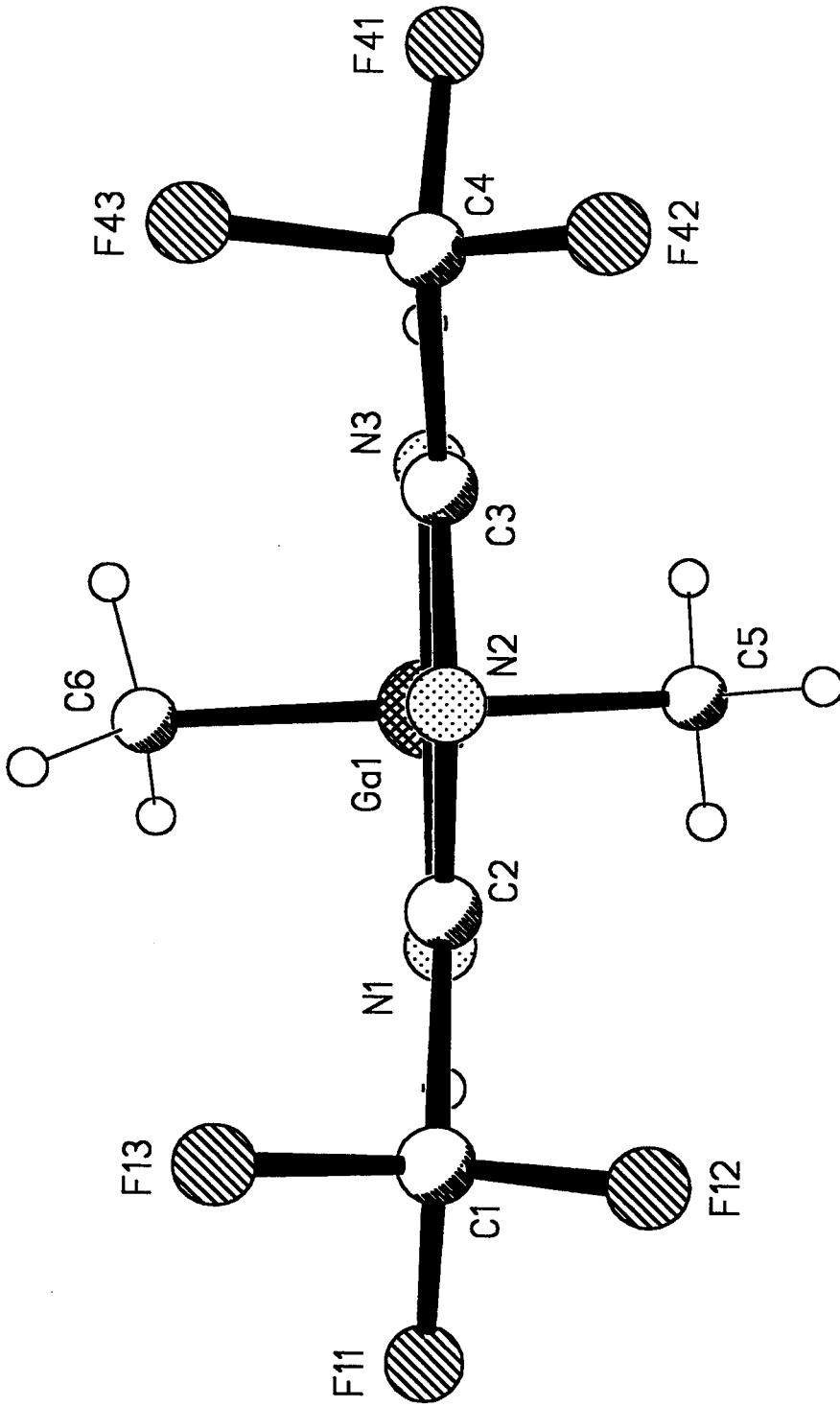
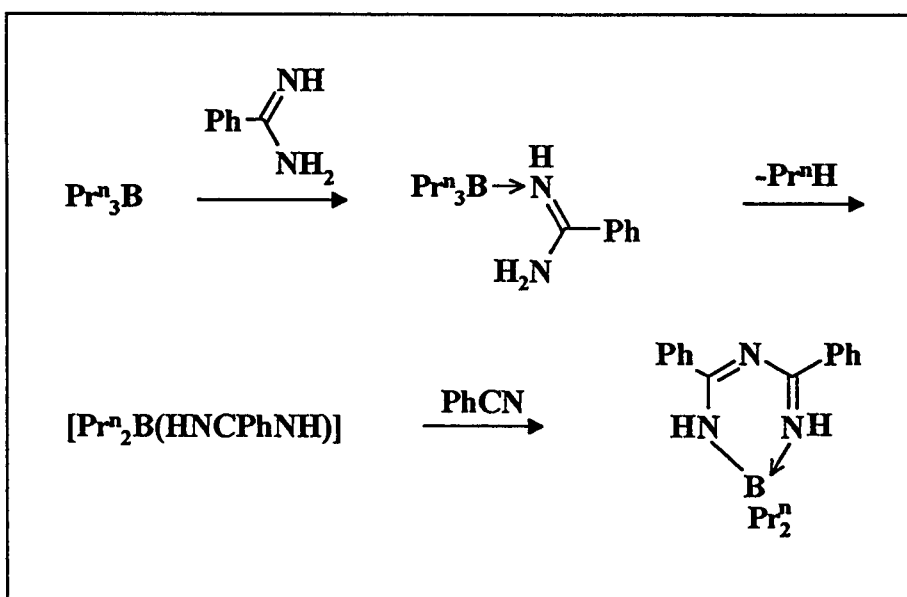


Figure 3.4 Molecular structure of $[\text{Me}_2\text{Ga}\{\text{HNC}(\text{CF}_3)\text{NC}(\text{CF}_3)\text{NH}\}]$, illustrating the orientation of the CF_3 groups.

GaNCN ring in $[\text{Me}_2\text{Ga}(\text{PhNCPhNPh})]$, and that of $1.336(6)\text{\AA}$ reported for the dimeric complex $[\{\text{Me}_2\text{Ga}(\text{MeNCMeNMe})\}_2]$, in which the metal and ligand valency angles suffer much less distortion from their ideal values.

The $[\text{HNC}(\text{CF}_3)\text{NC}(\text{CF}_3)\text{NH}]^-$ ligand (L) has been previously encountered in the complexes $[\text{Ir}(\text{L})(\text{CO})(\text{PPh}_3)_2]$ ²²⁶ and $[\text{Ru}(\text{L})\text{PPh}_3(\text{C}_5\text{H}_5)]$,²²⁷ and is formed by the reaction of $[\text{Ir}(\text{C}_5\text{H}_5)(\text{CO})(\text{PPh}_3)_2]$ and $[\text{RuCl}(\text{PPh}_3)_2(\text{C}_5\text{H}_5)]$ respectively with trifluoroacetonitrile in the presence of traces of water. Treatment of the ruthenium complex with $\text{P}(\text{OMe})_3$ produces $[\text{Ru}(\text{L})\{\text{P}(\text{OMe})_3\}(\text{C}_5\text{H}_5)]$, and the solid state structure of this compound, determined by X-ray crystallography, has been reported in the same paper.²²⁷ The related dianionic ligand, $[\text{NC}(\text{CF}_3)\text{NC}(\text{CF}_3)\text{NH}]^{2-}$ is formed by the reaction of $\text{F}_3\text{C-CN}$ and $[\text{Pt}(\text{PPh}_3)_4]$ which gives the Pt(II) complex $[\text{Pt}\{\text{NC}(\text{CF}_3)\text{NC}(\text{CF}_3)\text{NH}\}(\text{PPh}_3)_2]$.²²⁸ Treatment of $[\text{Pt}(\text{PhCN})_2\text{Cl}_2]$ with $[\text{Li}(\text{HNCPhNH})]$ yields the bis(benzimidoylbenzamidinato) complex, $[\text{Pt}\{\text{HNC}(\text{Ph})\text{NC}(\text{Ph})\text{NH}\}_2]$, which is formed by nucleophilic attack of the lithiobenzamidine on the co-ordinated benzonitrile.²²⁹ Similarly, the reaction between di-n-propylborane(benzamidinato), $[\text{Pr}^n_2\text{B}(\text{HNCPhNH})]$ and benzonitrile has been reported to yield $[\text{Pr}^n_2\text{B}\{\text{HNC}(\text{Ph})\text{NC}(\text{Ph})\text{NH}\}]$ as shown below.²³⁰



It was realised that the trifluoroacetamide reagent may contain trifluoroacetonitrile as an impurity or as part of an equilibrium with ammonia, and that the imidoamidinato ligand could be formed by nucleophilic attack of free F_3C-CN on the co-ordinated amidinato ligand. Gas chromatography mass spectrometry analysis of the ligand detected no nitrile, which thus eliminated this possible route of formation. Therefore, it is most likely that this complex is formed from an amidine condensation reaction between an amidinato ligand molecule and a free parent ligand molecule, which results in the elimination of ammonia.

Repeating the reaction using a 1:2 (trimethylgallium:trifluoroacetamide) mole ratio under similar conditions leads to the elimination of 1 mole equivalent of methane and the production of the complex in 46% yield (based on Me_3Ga). This yield is a significant improvement over the typical 25 – 30% yield (35 – 40% by weight) obtained from the 1:1 reaction. No release of ammonia is detected, and it is suggested that this gas is readily trapped by a further dimethylgallium–amidinato molecule, which produces the viscous colourless oil as a by-product. The exact identity of this product has not been established conclusively. Its 1H N.M.R. spectrum ($CDCl_3$) showed a complex series of resonances in the region 0.1 to -0.8 p.p.m., indicating the presence of a number of different Ga–Me containing species/environments. It is noteworthy that the dimethylgallium–amidinato complex $[Me_2Ga(PhNCPhNPh)]$ acts as a Lewis acid which results in the formation of a stable adduct with the pyridine ligand as described in Chapter 2. This finding provides evidence to support the above suggestion.

During the course of this work, this type of ligand condensation reaction has been reported by Robinson *et al*²³¹ to occur between a series of ruthenium, osmium and iridium hydrides with 2 mole equivalents of trifluoroacetamide, to yield products containing the chelate imidoamidinato ligand, and eliminate ammonia gas. The X-ray crystal structure of $[Ru\{HNC(CF_3)NC(CF_3)NH\}(CO)(PPh_3)_2]$ shows that the ligand co-ordinates to the metal in a manner similar to that reported above.

The imidoamidinato ligand is isoelectronic with the β -diketonate anion, $[OC(R)CH(O)C(R)]^-$, which is also known to form isostructural metallocyclic rings,

such as found in $[\text{Ga}(\text{acac})_3]$ ²³² and $[\text{Ga}(\text{hfac})_3]$ ¹⁷⁶ [$\text{acac} = \text{OC}(\text{CH}_3)\text{CH}(\text{O})\text{C}(\text{CH}_3)$; $\text{hfac} = \text{OC}(\text{CF}_3)\text{CH}(\text{O})\text{C}(\text{CF}_3)$]. Upon co-ordination to gallium in these complexes, the β -diketonate bite angle varies from ca. 90 to 92°, which is similar to the range from ca. 83 to 90° found for the imidoylamidinato ligand.^{227,231} Both types of ring systems are delocalised, but the internal ring angles in the former ligands are found to be consistently close to 125°, whereas in the latter, these angles vary considerably from ca. 119 to 133°.

Spectroscopic Properties of $[\text{Me}_2\text{Ga}\{\text{HNC}(\text{CF}_3)\text{NC}(\text{CF}_3)\text{NH}\}]$

The infra-red spectrum of the complex has been recorded as a KBr disc and is shown in Figure 3.5. A list of the peak positions is provided in the Experimental Section. The most notable feature of the spectrum is the presence of two $\nu(\text{N-H})$ stretching frequencies, both of medium intensity centred at 3331 and 3307 cm^{-1} . By making the assumption that the NH protons are associated with the terminal nitrogen atoms of the ligand, the presence of two distinct NH bands may be explained by the existence of hydrogen bonding interactions in the solid state. As mentioned during the discussion of the X-ray crystal structure of the complex, the positions of the hydrogen atoms used in the refinement are estimated, and not located from the difference map. Therefore, an accurate identification and evaluation of any such interactions can not be made with confidence. However, the symmetrical nature of the molecule, in particular in relation to the orientation of the two CF_3 groups, suggests that any intramolecular H-bonded interactions between the fluorine atoms F(1) and F(4) and hydrogen atoms H(1) and H(3) are substantially the same. This assumption implies that intermolecular H-bonds are responsible for the presence of two $\nu(\text{N-H})$ stretching vibrations.

The strong absorptions in the region 1630 – 1150 cm^{-1} are assigned to ligand $\nu(\text{CN})$ and $\nu(\text{CF})$ modes. This region shows a similar general appearance to that found in the spectrum of the free trifluoroacetamide ligand, recorded as a thin film (see Experimental Section), with the exception of the presence of an intense band near 1680 cm^{-1} in the spectrum of the ligand which is assigned to the $\nu(\text{C=N})$ stretching vibration.

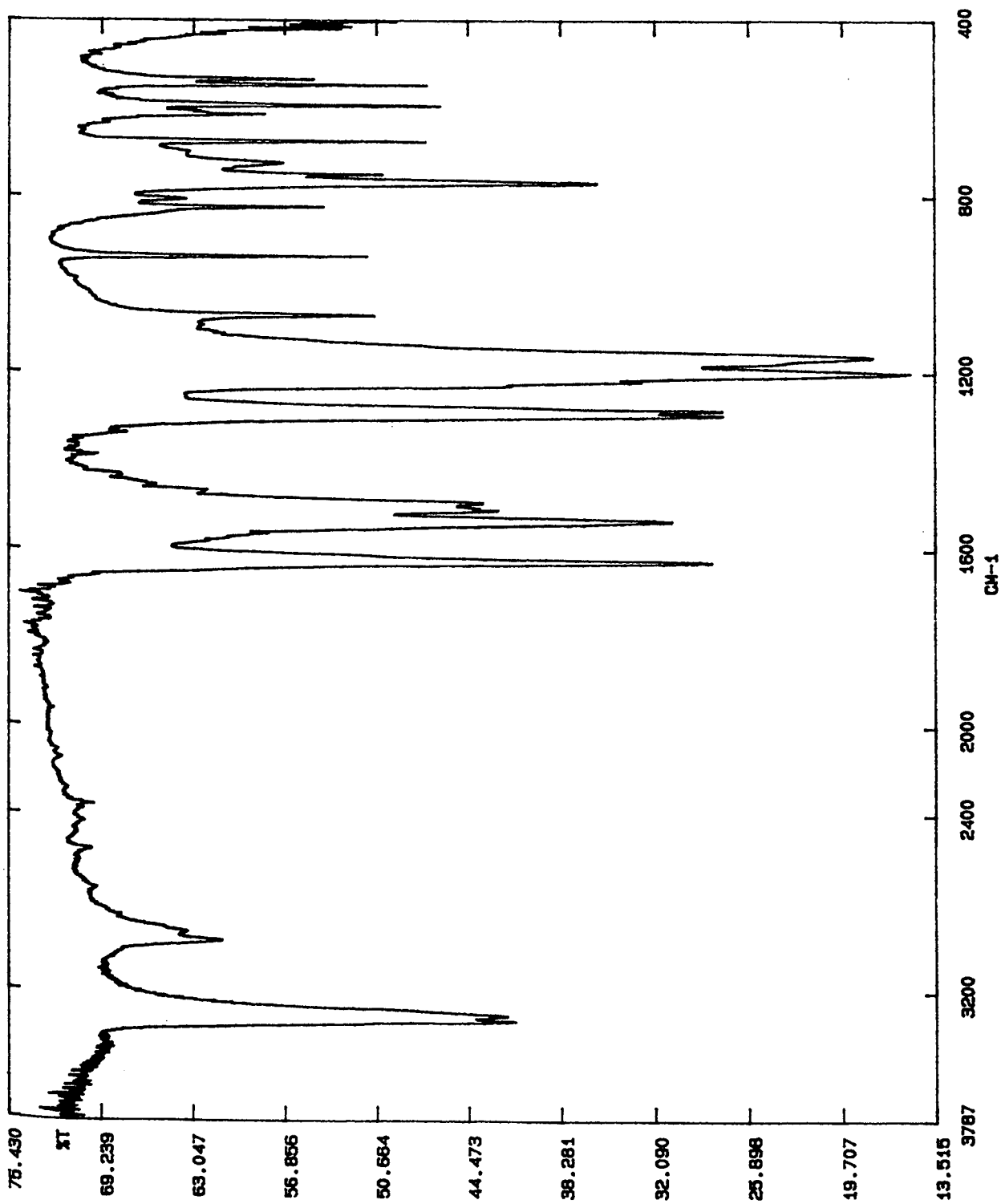


Figure 3.5 Infra-red spectrum of $[\text{Me}_2\text{Ga}\{\text{HNC}(\text{CF}_3)\text{NC}(\text{CF}_3)\text{NH}\}]$, recorded as a KBr disc.

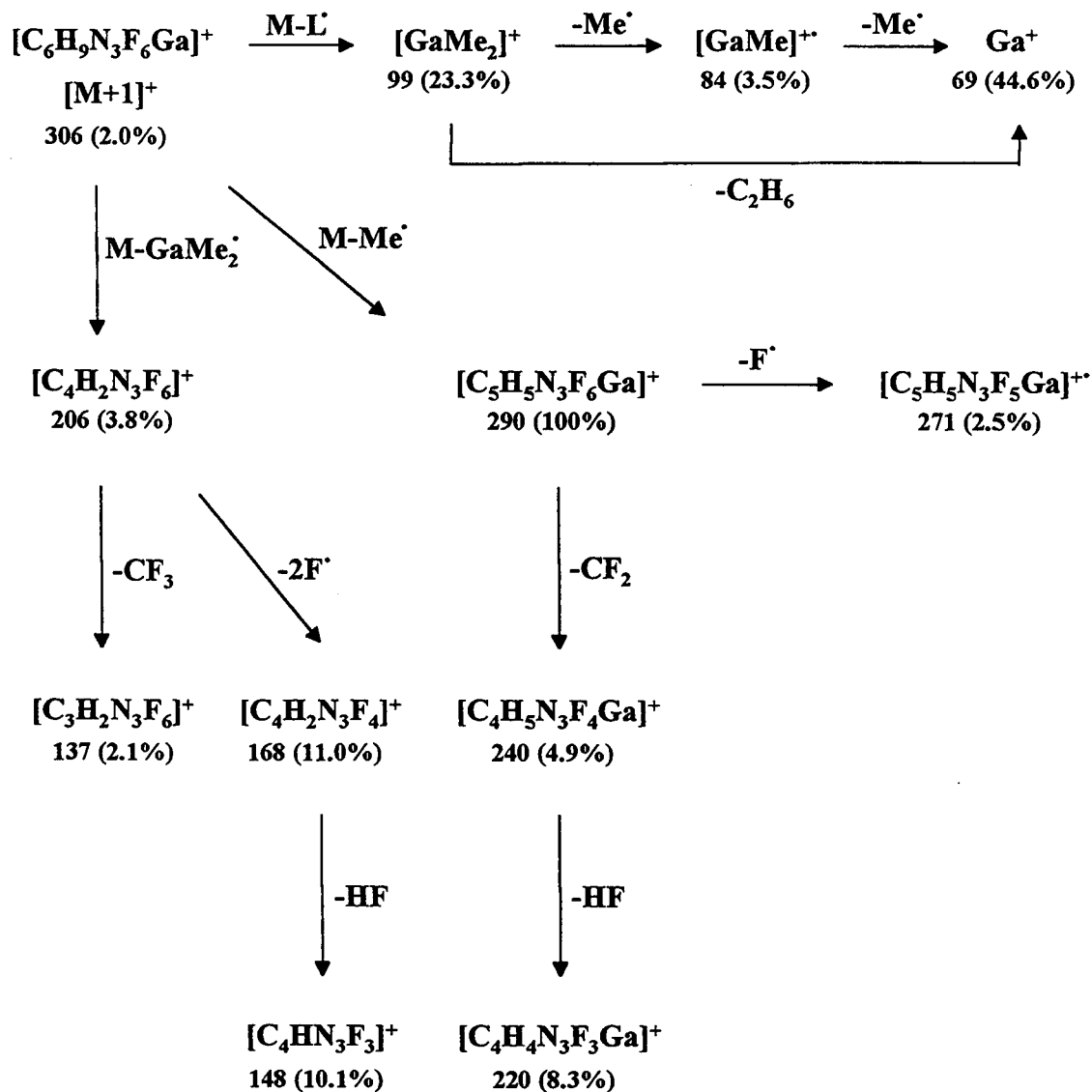
A further notable difference between these spectra is the presence of four additional sharp weak–medium intensity bands in the region below 600cm^{-1} in the spectrum of the complex. These bands are within the region expected for the asymmetrical and symmetrical GaC_2 and GaN_2 stretches. An exact assignment of these bands cannot be made with certainty, but the bands near 614 and 547cm^{-1} are tentatively assigned to the $\nu_{\text{asym}}(\text{GaC}_2)$ and $\nu_{\text{sym}}(\text{GaC}_2)$ stretches respectively, and the two remaining bands at 594 and 533cm^{-1} are attributed to the $\nu_{\text{asym}}(\text{GaN}_2)$ and $\nu_{\text{sym}}(\text{GaN}_2)$ stretches respectively.

The E.I. mass spectrum of the complex obtained is useful not only for giving evidence confirming the identity of the complex, but also for providing valuable information about the ease of ligand dissociation and further decomposition behaviour. The important ions of the spectrum are shown in Figure 3.6 and the appropriate assignments are based on ^{69}Ga . Three primary decomposition pathways are proposed which involve loss of $[\text{Me}]^+$, $[\text{GaMe}_2]^+$, and $[\text{L}]^+$, [where $\text{L} = \{\text{HNC}(\text{CF}_3)\text{NC}(\text{CF}_3)\text{NH}\}$], and produce ions at m/z 290, 206 and 99 respectively. This behaviour is analogous to the fragmentation process found for the dialkylmetal-amidinato complexes reported in Chapter 2. The ion at m/z 290 $[\text{MeGa}(\text{L})]^+$ undergoes further fragmentation by the loss of the F^\cdot radical and the neutral CF_2 and HF species. The loss of HF presumably involves the NH protons. The ions Ga^+ (m/z 69, 44.6%) and $[\text{GaMe}_2]^+$ (m/z 99, 23.3) are prominent, but $[\text{MeGa}]^{2+}$ (m/z 84, 3.5%) is not.

One notable feature of the spectrum is the absence of metal–containing ions which result from fragmentation of the ring. This is in contrast to the primary fragmentation pathway reported for the related complex, $[\text{Pt}\{\text{HNC}(\text{Ph})\text{N}(\text{Ph})\text{NH}\}_2]$, which involves rupture of the metallocyclic rings, and results in the loss of benzonitrile and formation of a bis(amidinato) complex ion.²²⁹

The base peak in the C.I. mass spectrum corresponds to the protonated molecular ion. An accurate mass determination of this ion confirms the formulation used in the X–ray crystallographic study. The remaining peaks correspond to the protonated free imidolyamidine ligand and to the free parent amidine ligand.

Figure 3.6 Fragmentation Scheme for the E.I. Mass Spectrum of $[\text{Me}_2\text{Ga}\{\text{HNC}(\text{CF}_3)\text{NC}(\text{CF}_3)\text{NH}\}]^+$.



The solution behaviour of the complex was characterised by ^1H , ^{13}C and ^{19}F N.M.R. spectroscopy. These data are summarised in the Experimental Section, together with that obtained for the parent amidine ligand.

The ^1H spectrum (CDCl_3) clearly establishes the presence of the Ga–Me groups, showing a sharp singlet at -0.27 p.p.m. (rel. intens. 6). The broad resonance centred near 7.4 p.p.m. corresponds to the two NH protons. The simplicity of the spectrum implies that the position of the Me_2Ga unit in CDCl_3 solution is similar to that found in the solid state.

The ^{13}C spectrum provides further structural information and consists of three types of resonance. The resonance assigned to the organometallic carbon atoms appears as a sharp singlet at -4.70 p.p.m., and the two remaining resonances, centred at 115.15 and 162.04 p.p.m., are each split into a 1:3:3:1 quartet. These can be easily assigned to the CF_3 and $\text{C}-\text{CF}_3$ carbon atoms respectively of the imidoamidinato ligand. The appearance of only one signal for each group is consistent with the singlet obtained in the ^{19}F spectrum and this suggests a symmetrical species.

Although these exploratory experiments can not establish a mechanism for the formation of the complex, they can be used to suggest the nature of the process and allow the following steps to be proposed. The first stage of the reaction probably involves formation of a dimethylgallium–amidinato complex, $[\text{Me}_2\text{Ga}(\text{HNCCF}_3\text{NH})]$ and the elimination of methane. Although no direct evidence has been obtained to show that this type of complex is involved, by analogy with the reaction between Me_3Ga and butyramidine discussed earlier, it appears to be a probable intermediate. Complexation of the amidinato ligand causes the carbon atom of the NCN unit to be more electrophilic than in the free amidine ligand. The subsequent steps involve nucleophilic attack of free amidine on the activated amidinato carbon centre and expulsion of ammonia, as shown below. Note that for the purposes of simplicity, the dimethylgallium–amidinato intermediate is written as monomeric.

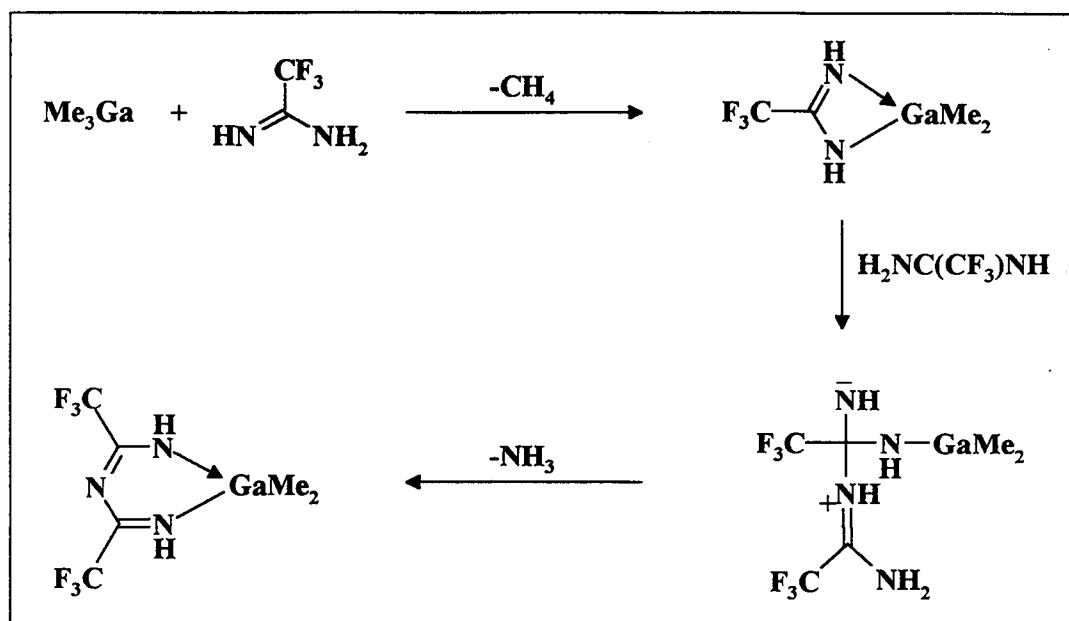


Figure 3.7 Proposed mechanism of formation of $[\text{Me}_2\text{Ga}\{\text{HNC}(\text{CF}_3)\text{NC}(\text{CF}_3)\text{NH}\}]$.

In contrast, the reaction between Me_3Ga and each of the amidine ligands acetamidine, benzamidine and butyramidine, discussed earlier, under similar conditions gives the appropriate dimethylgallium–amidinato complex in good yield. This contrasting reactivity can be explained by consideration of the influences of the group (R) attached to the central NCN carbon atom. Strongly electronegative R groups will enhance the electrophilicity of the NCN carbon centre and thereby favour nucleophilic attack. Replacement of the R group by a relatively neutral group will result in a decrease in the reactivity of this centre. Additionally, an increase in the steric size of the substituent would be expected to inhibit this type of reaction.

In summary, the trifluoroacetamide ligand shows a different type of reaction with Me_3Ga than found for the other N,N'–unsubstituted amidine ligands mentioned. The synthesis of the imidoamidinato ligand occurs by mixing trifluoroacetamide and Me_3Ga . In order to prepare other examples of this type of complex, an obvious extension to this work, which was not attempted because of shortage of time, involves the addition of suitable nitrile to a dimethylgallium–amidinato complex of the type mentioned above. It seems likely that this would provide a convenient route to other examples of imidoamidinato complexes.

CHAPTER 4

Tetraazamacrocyclic Complexes of Indium(III)

CHAPTER 4

Tetraazamacrocyclic Complexes of Indium(III).

Introduction

It was mentioned in Chapter 1 that the investigation of the reactions of organometallic derivatives of group 13 with macrocyclic ligands has attracted significant interest only during the last decade. The lack of previous interest is rather surprising in view of the ability of this class of ligand to stabilise unusual metal co-ordination geometries and oxidation states. Consequently, it is anticipated that incorporation of metal entities, such as group 13 metal-alkyls, into this type of ligand environment may result in unusual reactivity of these functionalities.

Organometallic complexes of group 13 compounds with porphyrins are well documented^{122,123,124,233} and are of interest because of the unusual co-ordination environment imposed on the metal centre and the application of such compounds as photoactive polymerisation catalysts. The work of Inoue and co-workers²³⁴ has shown that organoaluminium porphyrin compounds have an important application as catalysts for the polymerisation of methacrylates and other related compounds.

A survey of the Cambridge Crystallographic Database for organoaluminium and organogallium complexes with nitrogen- or oxygen-based macrocycle ligands (excluding porphyrin and phthalocyanine complexes) revealed the crystal structures detailed in Figures 4.1 and 4.2, which are presented in the order in which they were reported. Much of this work has been carried out by Robinson and co-workers.

In relation to organoindium compounds, previous work with macrocyclic ligands is sparse. Tuck *et al*²³⁵ have reported some preliminary work on the reactions of the organoindium halides, MeInCl_2 and MeInI_2 , with cyclam ($[\text{14}] \text{aneN}_4$) and dibenzo-18-crown-6. The nature of the products was investigated by infra-red and N.M.R. spectroscopic techniques. The results obtained from the reactions with cyclam failed to identify a possible product, but the complexes formed with the crown were assigned to be ionic of the form $[\text{In}(\text{Me}_2)(\text{crown})][\text{InX}_4]$ or $[\text{In}(\text{Me})\text{X}(\text{crown})][\text{In}(\text{Me})\text{X}_3]$.

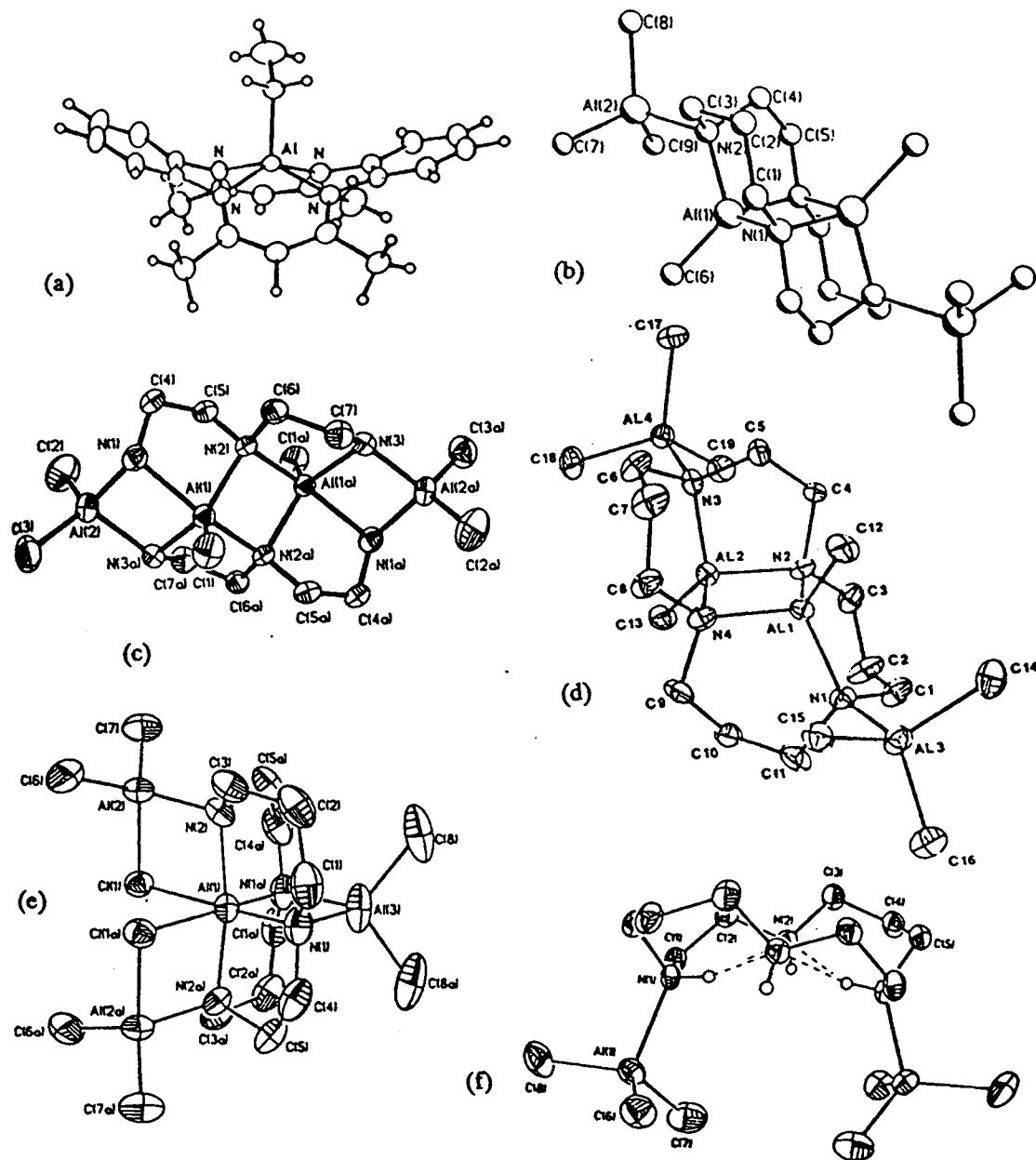


Figure 4.1 Reported organoaluminium–macrocyclic complexes

Compound	Formula	Reference
(a) [EtAl(tmtaa)]	$C_{24}H_{27}N_4Al$	219
(b) $(MeAl)_2([14]aneN_4)(AlMe_3)_2$	$C_{18}H_{44}N_4Al_4$	236
(c) $(MeAl)_2(C_8H_{20}N_6)(Me_2Al)_2$	$C_{14}H_{38}N_6Al_4$	237
(d) $(MeAl)_2([15]aneN_4)(Me_3Al)_2$	$C_{19}H_{46}N_4Al_4$	238
(e) $(Me_2AlCl)_2(Al.[14]aneN_4)(Me_2Al)$	$C_{16}H_{38}N_4Al_4Cl_2$	239
(f) $(Me_3Al)_2([14]aneN_4)$. The equivalent gallium compound is isostructural.	$C_{16}H_{42}N_4Al_2$	240

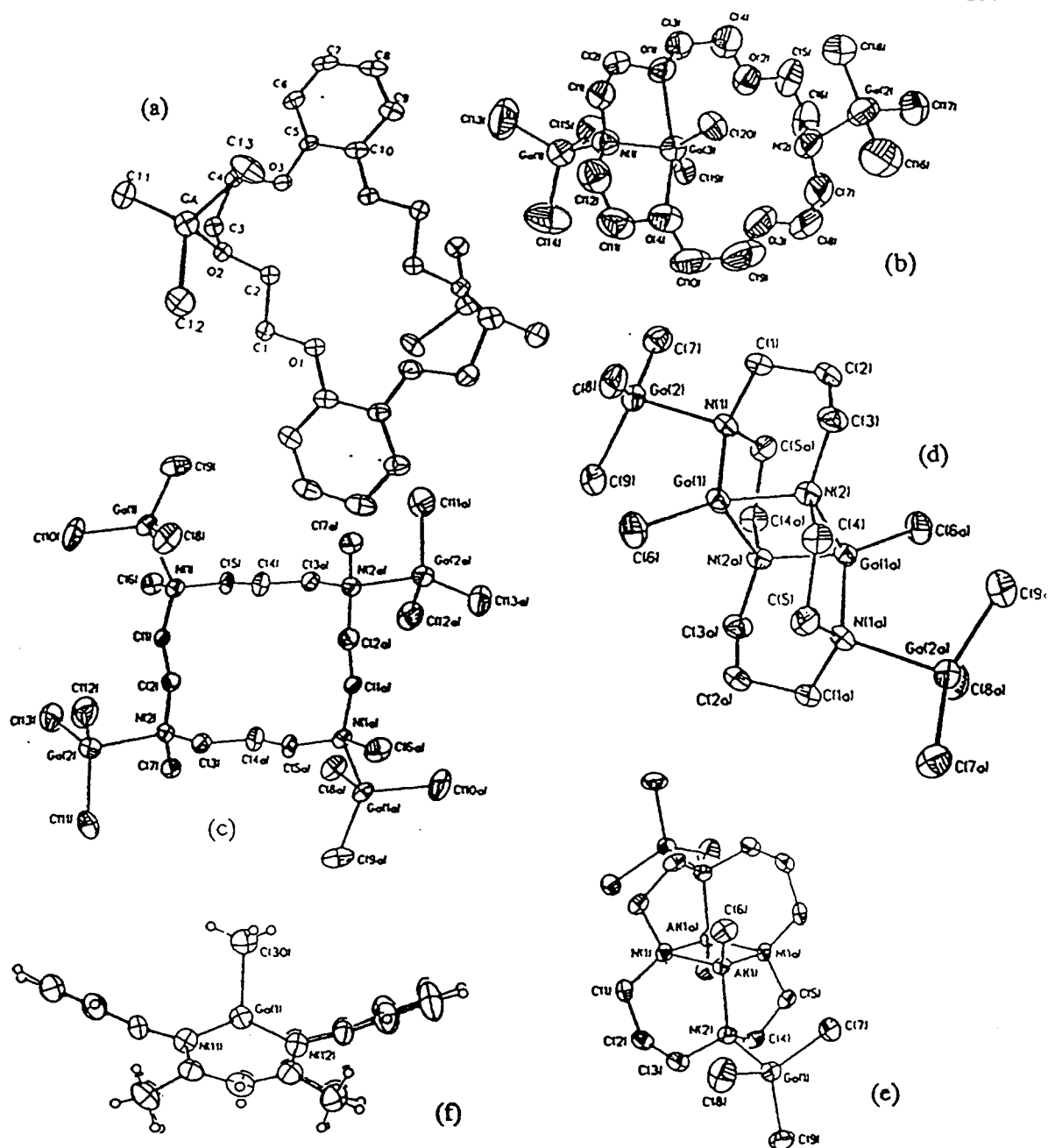


Figure 4.2 Reported organogallium–macrocyclic complexes

Compound	Formula	Reference
(a) $(\text{Me}_3\text{Ga})_2[\text{dibenzo-18-crown-6}]$	$\text{C}_{26}\text{H}_{42}\text{O}_6\text{Ga}$	96
(b) $(\text{Me}_2\text{Ga})[4,13\text{-diaza-18-crown-6}](\text{Me}_3\text{Ga})_2$	$\text{C}_{20}\text{H}_{49}\text{N}_2\text{O}_4\text{Ga}_3$	241
(c) $(\text{Me}_3\text{Ga})_4[\text{Me}_4[14]\text{aneN}_4]$	$\text{C}_{26}\text{H}_{69}\text{N}_4\text{Ga}_4$	242
(d) $(\text{MeGa})_2[14]\text{aneN}_4(\text{Me}_3\text{Ga})_2$	$\text{C}_{18}\text{H}_{44}\text{N}_4\text{Ga}_4$	242
(e) $(\text{MeAl})_2[14]\text{aneN}_4(\text{Me}_3\text{Ga})_2$	$\text{C}_{18}\text{H}_{44}\text{N}_4\text{Al}_2\text{Ga}_2$	240
(f) $[\text{MeGa}(\text{tmtaa})]$	$\text{C}_{23}\text{H}_{25}\text{N}_4\text{Ga}$	200

The adduct of trimethylindium with N,N',N'' -tri-*iso*-propyl-1,3,5-triazacyclohexane was mentioned in Chapter 1.¹⁰⁵ The solid state structure of this complex reveals an unusual property of the complex of donation of three lone pairs to the metal centre, rather than the more commonly found situation with adducts of Me_3In of one lone pair donation.

In view of the lack of previous study of organoindium-macrocylic complexes, it was decided to investigate the reactions of triethylindium with the tetraazamacrocycle, 5,7,12,14-tetramethyldibenzo[b,i][1,4,8,11]tetraazacyclotetradecine, usually abbreviated to H_2tmtaa . This macrocycle was chosen for the following reasons. Firstly, the reactions of triethylaluminium and trimethylgallium have been reported (in the case of the latter by other workers in our group)^{200,219} and therefore comparisons between the derivatives obtained can be made. In particular, the crystal structures of the compounds $[RM(tmtaa)]$ ($M = Al, R = Et; M = Ga, R = Me$) are known, and if the analogous indium complex could be prepared, it was hoped to determine its crystal structure in order to ascertain the influence that the increasing metal size has on these complexes. These aforementioned studies have shown that the metal atom in the complex $[RM(tmtaa)]$ ($M = Al, R = Et; M = Ga, R = Me$) is co-ordinated to all four nitrogen atoms out of the plane of the macrocycle N_4 cavity. Secondly, the conjugated structure of this ligand is of interest because it can be considered as midway between completely aliphatic macrocyclic ligands, such as cyclam, and the aromatic porphyrin systems. Unlike aliphatic macrocycles, the rigidity of the ligand imposes constraints on the type and geometry of metal co-ordination possible, but it is more flexible than porphyrin systems. Finally, this macrocycle is relatively easily prepared in reasonable quantities.

The first section of this Chapter describes the preparation and spectroscopic properties of two complexes obtained from the reaction between Et_3In and H_2tmtaa , and the molecular structure of one of the complexes. The second section likewise describes the incorporation of a range of other indium functionalities with this macrocycle, which give complexes of the general type $[XIn(tmtaa)]$ ($X =$ axial substituent).

(1) Preparation of the Complexes

The treatment of a hexane suspension of H_2tmtaa chilled at -78°C with triethylindium led to the elimination of 1 mole of ethane on warming to room temperature and the formation of the diethylindium compound, $[Et_2In(Htmtaa)]$ ($tmtaa = [C_{22}H_{22}N_4]^{2-}$) as a bright yellow precipitate, which was partially soluble in the reaction solvent. This product was highly soluble in chloroform, dichloromethane and toluene, but slightly less soluble in THF. It showed considerable thermal stability in relation to further alkane elimination involving the second NH group. Heating a solid sample to 100°C for 1 hour caused only negligible decomposition, but on further heating, the solid melted at 145°C , just prior to the elimination at around 155°C of gas (1 mole equivalent), which was presumed to be ethane, and the production of a bright orange solid. Thermogravimetric analysis (T.G.A.) and differential thermal analysis (D.T.A.) experiments were performed on $[Et_2In(Htmtaa)]$ under a stream of dry nitrogen, and the plots obtained are given in Figure 4.3. They show the initial melting point (ca. 145°C) and alkane elimination reaction (ca. 155°C) and decomposition or vaporisation around 275°C .

The bright orange solid is the monoethylindium derivative, $[EtIn(tmtaa)]$. This product was also obtained by heating a hexane solution of $[Et_2In(Htmtaa)]$ under reflux for 12 hours. The orange solution produced deposited orange crystals on cooling to room temperature, and these were suitable for single crystal X-ray diffraction studies. Removal of the solvent gave the product in a near quantitative yield.

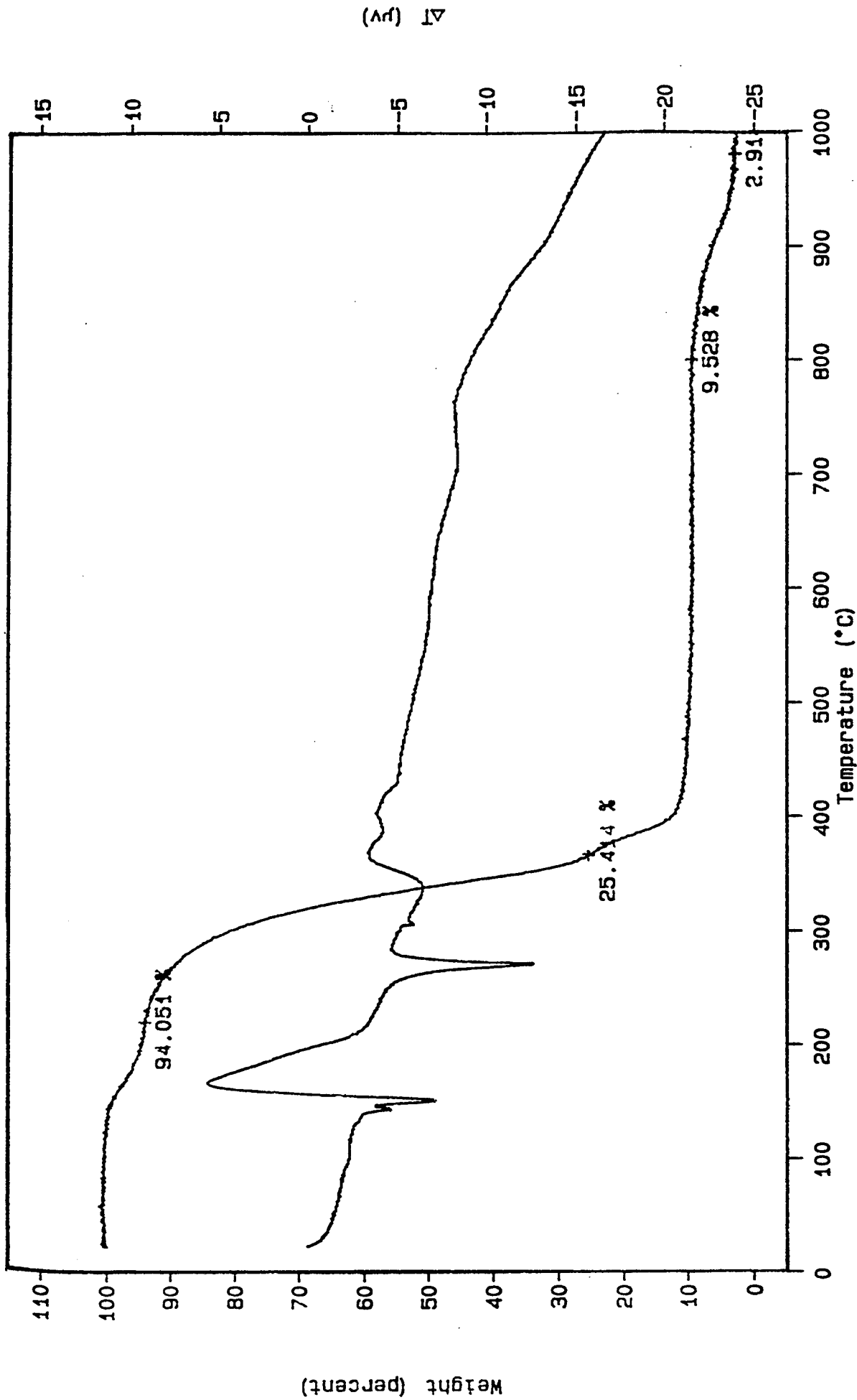


Figure 4.3 Combined T.G.A. and D.T.A. plot obtained for $[\text{Et}_2\text{In}(\text{Htmtaa})]$.

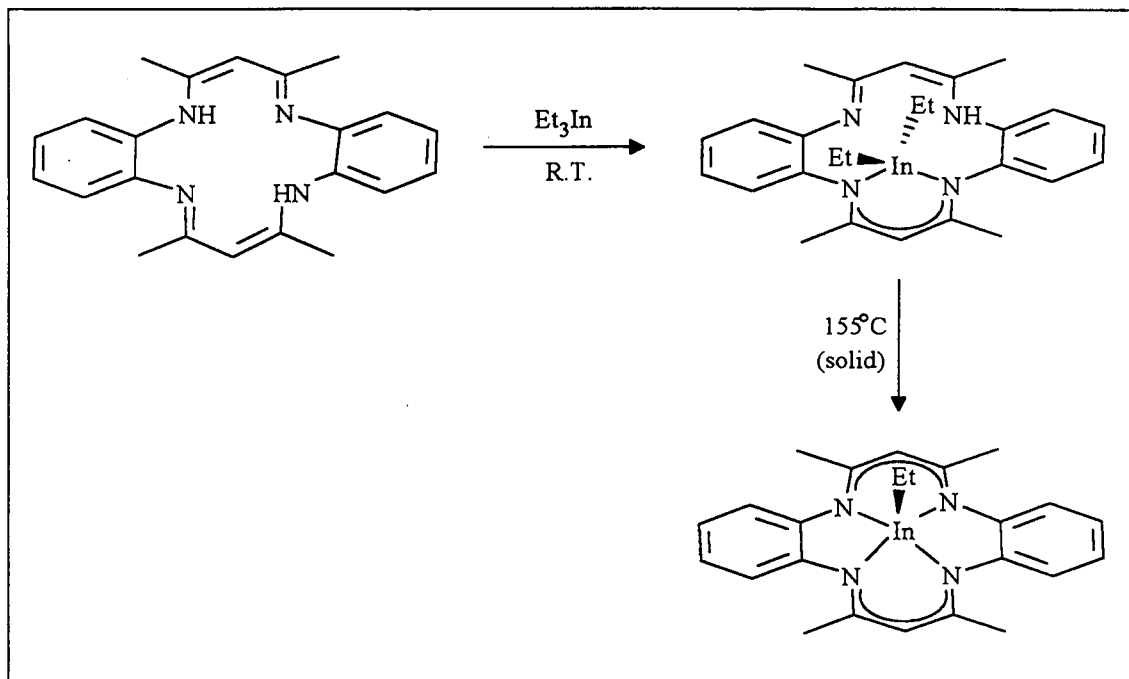


Figure 4.4 Two-step insertion reactions of Et_3In with H_2tmtaa

This reaction scheme is very similar to those reported for the analogous ethylaluminium²¹⁹ and methylgallium²⁰⁰ compounds, although the diethylindium compound evolves its second mole of alkane at a lower temperature than $[\text{Me}_2\text{Ga}(\text{Htmtaa})]$ (225°C), but at a higher temperature than $[\text{Me}_2\text{Al}(\text{Htmtaa})]$ (100°C). This is consistent with both the expected higher reactivity of aluminium carbon bonds and the lower metal carbon bond strength on descending the group.

Although the monoethylindium derivative is indefinitely stable in dry chloroform solution, exposure of the solution to air results in slow decomposition. This type of reaction was followed by the appearance of new resonances of gradually increasing relative intensity in the ^1H N.M.R. spectrum of a CDCl_3 solution of the compound exposed to air for a period of 3 hours over time intervals each of 30 minutes. These resonances are attributed to free ligand, H_2tmtaa . These results contrast with those reported for the monoethylaluminium compound $[\text{EtAl}(\text{tmtaa})]$, which remained intact in wet organic solvents, whereas irradiation of a chloroform solution resulted in the formation of the monochloroaluminium compound, $[\text{ClAl}(\text{tmtaa})]$. The greater resistance to demetallation of the aluminium versus the indium compound may reflect the better fit

of the aluminium into this macrocycle (discussed in more detail later in this chapter), which in turn may activate photochemical cleavage of the Al–C bond.

The observation that the initial alkane elimination reaction between Et_3In and H_2tmtaa occurs at room temperature, which is similar to the reactions found to occur with the amidine ligand discussed in Chapter 2, is expected on consideration of the acidic nature of the NH proton in both ligands. In contrast, reactions with secondary amines, such as Ph_2NH , usually lead to a Lewis adduct complex at room temperature, and these require elevated temperatures, often around 100°C , to eliminate alkane.⁵⁶ The reported reaction between 2 molar equivalents of Me_3M and the tetradentate secondary amine, cyclam, yields the adducts, $[(\text{Me}_3\text{M})_2[14]\text{aneN}_4]$ ($\text{M} = \text{Al}, \text{Ga}$) [Figure 4.1(f)] at room temperature,²⁴⁰ but in the presence of four equivalents of Me_3M with this ligand in refluxing toluene all four NH groups are cleaved.^{236,242} It might be expected that this product would be formulated as $[(\text{Me}_2\text{M})_4[14]\text{aneN}_4]$. However, in fact, condensation occurs only at two of the Me_3M moieties, yielding $[(\text{MeM})_2[14]\text{aneN}_4(\text{Me}_3\text{M})]$, which possesses the familiar $(\text{MN})_2$ fragment [Figures 4.1(b) and 4.2(d)]. This structure demonstrates the flexibility of this ligand and presumably the conformation of the intermediates favours intramolecular condensation. The reaction between diaza-18-crown-6 and excess Me_3Ga under similar conditions results in the elimination of only one mole of methane, with the dimethylgallium unit bound in the macrocycle cavity and the second NH group remaining intact [Figure 4.2(b)].²⁴¹ In these respects, this complex can be compared to $[\text{Et}_2\text{In}(\text{Htmtaa})]$, even though in the former complex two additional trimethylgallium groups are co-ordinated to the nitrogen lone pairs. No reaction between $[\text{Et}_2\text{In}(\text{Htmtaa})]$ and excess Et_3In was observed, and this may be in part explained by the orientation of the lone pairs and the remaining NH group which point toward the diethylindium unit. Although they are too far away to co-ordinate or react with the Et_2In fragment, reaction with further equivalents of triethylindium is blocked. Furthermore, the acidity of the remaining NH group is probably reduced in this complex because of electronic effects of metal complexation.

Spectroscopic Properties

N.M.R. Spectra

The ^1H and ^{13}C N.M.R. spectra of both metal complexes provide clear information regarding the symmetry of the molecular geometry within each complex. The ^1H and ^{13}C spectra of H_2tmtaa , $[\text{Et}_2\text{In}(\text{Htmtaa})]$ and $[\text{EtIn}(\text{tmtaa})]$ are shown in Figures 4.5 and 4.6. Summaries of the resonances and assignments are given in Tables 4.1 and 4.2.

Table 4.1 Summary of the ^1H N.M.R. data (400MHz) for H_2tmtaa , $[\text{Et}_2\text{In}(\text{Htmtaa})]$ and $[\text{EtIn}(\text{tmtaa})]$. Integrals are given in parenthesis.

Compound	δ (p.p.m.)				
	NH	ArH	CH	CH_3	In- CH_2CH_3
H_2tmtaa	12.58(2H)	6.99(8H)	4.87(2H)	2.13(12H)	–
$[\text{Et}_2\text{In}(\text{Htmtaa})]$	12.24(1H)	7.10 – 6.97(8H)	4.84(1H) 4.82(1H)	2.11(6H) 1.65(6H)	1.38(3H), 0.72(2H) 0.47(3H), –0.02(2H)
$[\text{EtIn}(\text{tmtaa})]$	–	7.10 – 6.90(8H)	4.66(2H)	2.17(12H)	0.76(3H), 0.34(2H)

The ^1H spectrum of the diethylindium derivative shows a single broad resonance at 12.24 p.p.m. of integral one, which is assigned to the remaining NH proton. The presence of the complex series of resonances in the aromatic region of the spectrum is explained by considering the expected reduced symmetry of this molecule compared to the parent ligand. All the remaining signals consist of pairs of resonances, including two sets of inequivalent organometallic ethyl proton resonances. The similarity of this spectrum to that obtained for the analogous gallium complex, $[\text{Me}_2\text{Ga}(\text{Htmtaa})]$, indicates that the position and orientation of the diethylindium unit is likely to be very similar to that found for the dimethylgallium unit both in CDCl_3 solution and in the solid state as shown below:

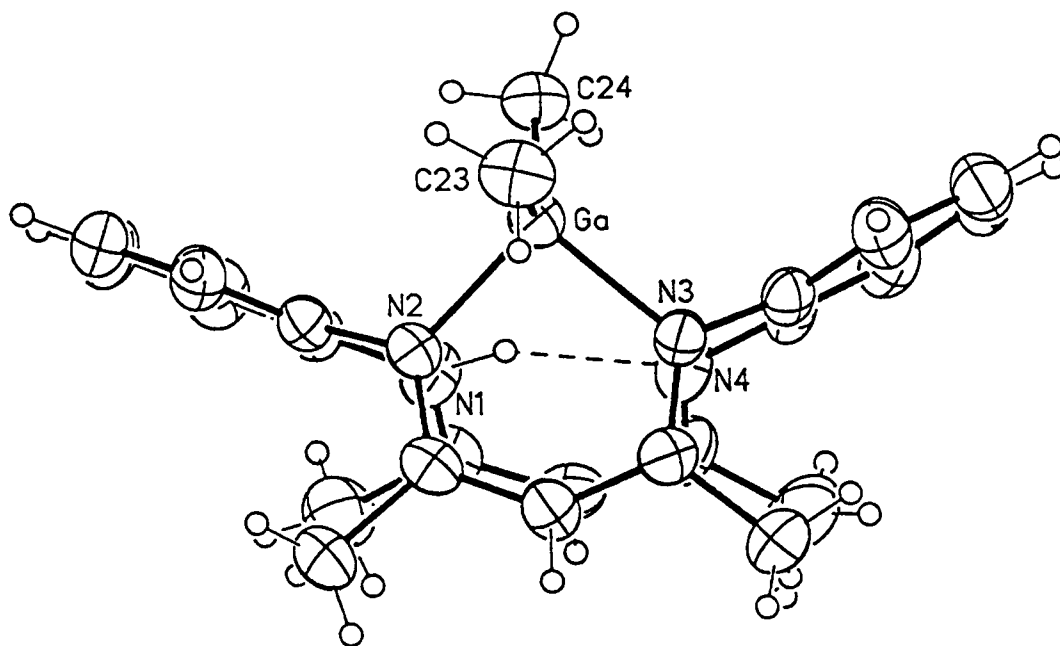


Figure 4.7 The molecular structure of $[\text{Me}_2\text{Ga}(\text{Htmtaa})]$.²⁰⁰

The dimethylgallium unit is symmetrically bound to two nitrogen atoms of one of the pentanediiiminate units, giving a distorted tetrahedral co-ordination geometry around the metal.

The ^1H spectrum obtained for the monoethylindium derivative reveals that the molecular symmetry is increased and the pattern of ligand resonances resembles those obtained for the parent ligand, except for the lack of an NH resonance. In addition, the spectrum shows only one set of resonances attributable to a single In–Et group. The relative simplicity of this spectrum implies that the indium atom is either co-ordinated in a central position with an axial ethyl ligand, or is in rapid rotation.

Figure 4.5 ^1H N.M.R. (400MHz) spectra of (a) H_2tmtaa , (b) $[\text{Et}_2\text{In}(\text{Htmtaa})]$, and (c) $[\text{EtIn}(\text{tmtaa})]$.

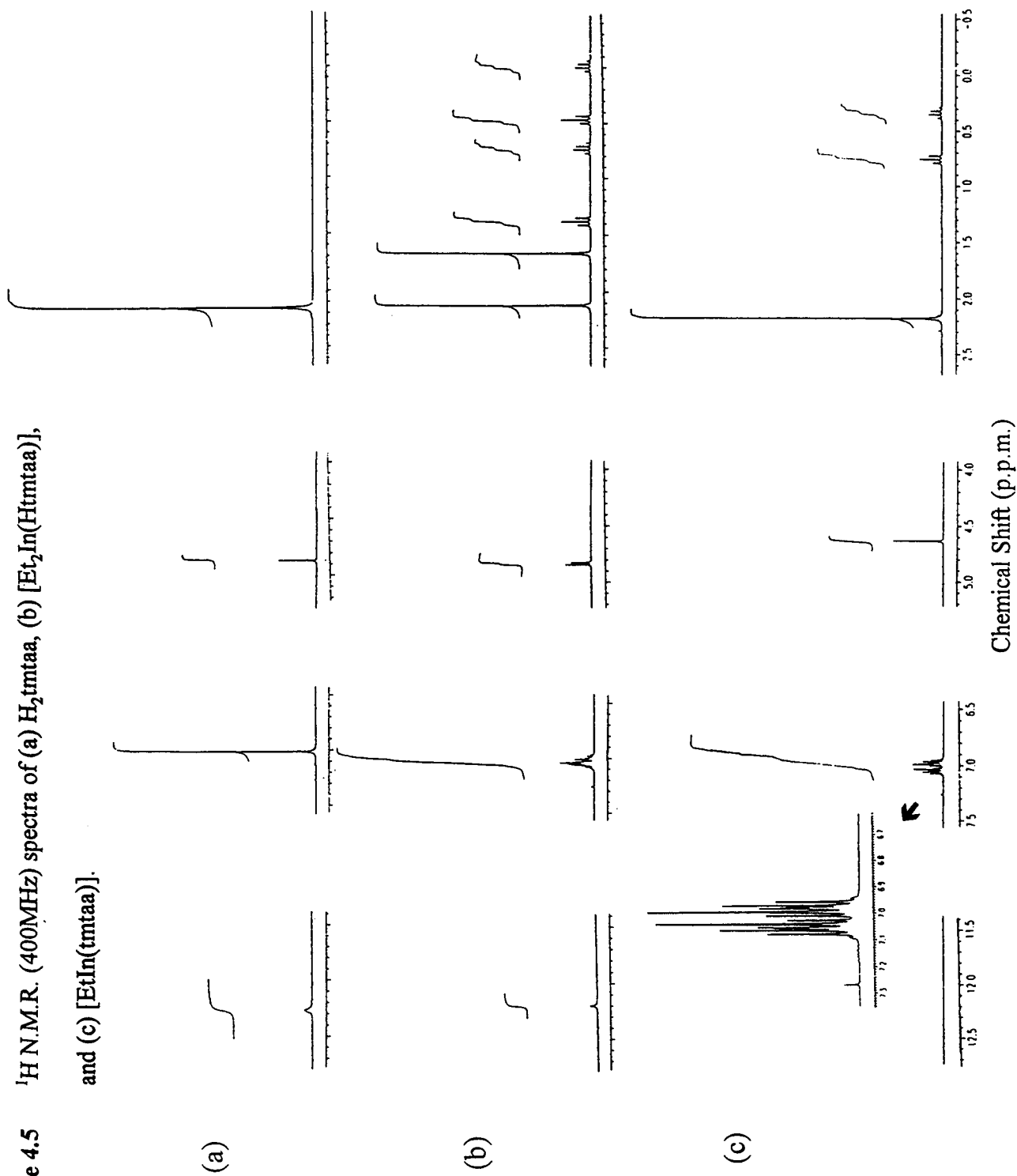
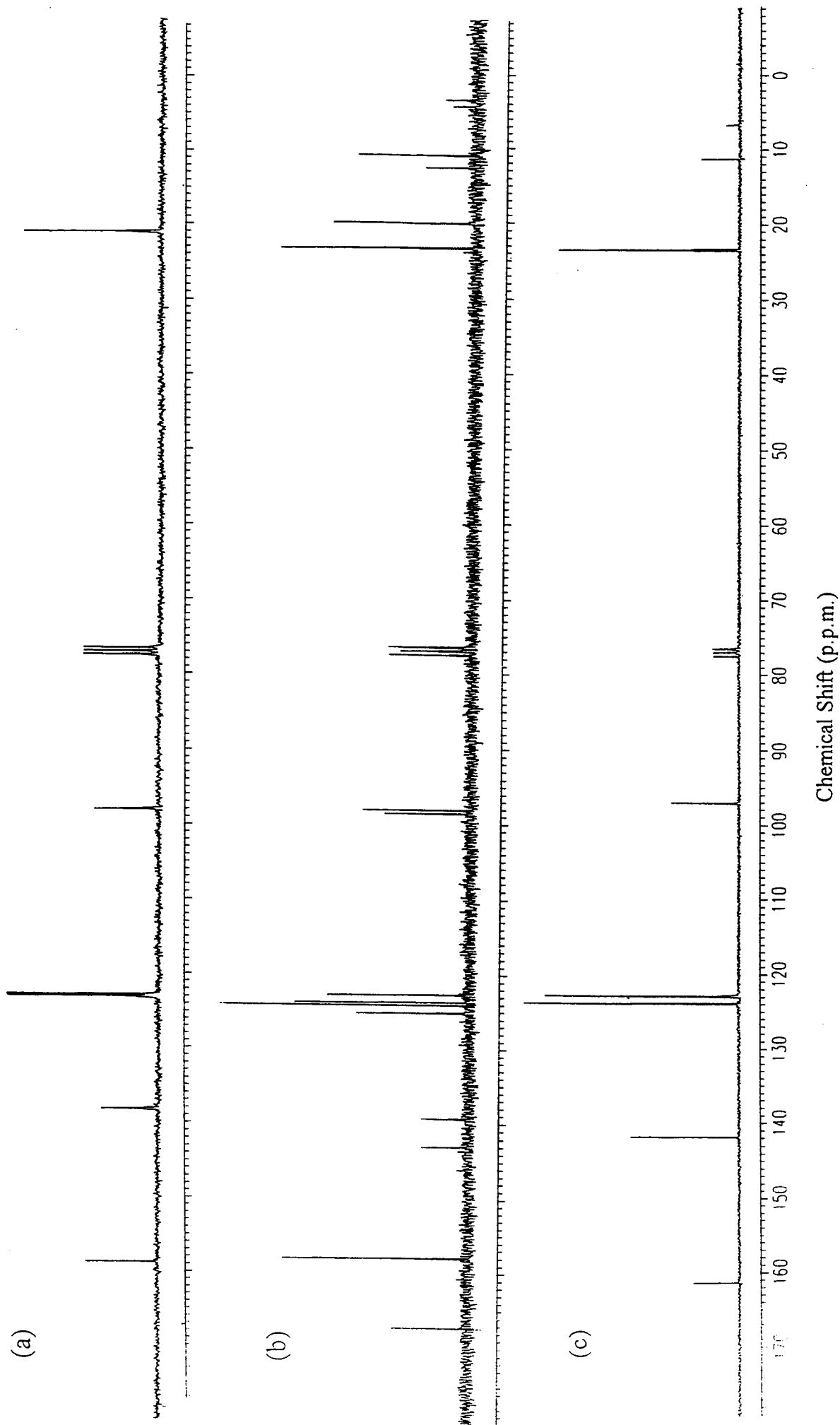


Figure 4.6 ^{13}C N.M.R. (400MHz) spectra of (a) H_2tmtaa , (b) $[\text{Et}_2\text{In}(\text{Htmtaa})]$, and (c) $[\text{EtIn}(\text{tmtaa})]$.



Chemical Shift (p.p.m.)

Table 4.2 Summary of the ^{13}C N.M.R. data (400MHz) for H_2tmtaa , $[\text{Et}_2\text{In}(\text{Htmtaa})]$, and $[\text{EtIn}(\text{tmtaa})]$.

δ (p.p.m.)			
H_2tmtaa	$[\text{Et}_2\text{In}(\text{Htmtaa})]$	$[\text{EtIn}(\text{tmtaa})]$	Assignment
158.84	167.24	161.39	methyl-C
	157.96		
138.00	139.31	141.80	aromatic-CN
	142.98		
122.79	122.65, 123.66	122.84	aromatic-CH
123.00	124.02, 125.07	123.80	
97.84	98.04	97.02	methine-CH
	98.57		
20.81	20.00	23.38	methyl-C
	23.31		
-	3.43, 10.96	6.67 11.22	In- CH_2CH_3
	4.48, 12.63		

The ^{13}C spectra display a similar pattern. The spectrum of the diethylindium compound has double the number of ligand resonances found in the spectra of both the parent ligand and the monoethylindium compound. This doubling is consistent with the lower symmetry anticipated within the molecular geometry of this compound. A further important feature in the spectra of the metal complexes is the presence of the sharp resonances assigned to the metal-ethyl organometallic carbon atoms.

Infra-red Spectra

The infra-red spectra of H_2tmtaa , $[Et_2In(Htmtaa)]$ and $[EtIn(tmtaa)]$ have been recorded as Nujol mulls and the important peaks are listed in the Experimental Section. The complexity of the spectra excludes detailed assignments, but several features become apparent upon comparison through the series of spectra. The NH bands of the free ligand and the diethylindium complex, expected around 3300cm^{-1} , were not detected, probably because of hydrogen-bonding involving the nitrogen atoms. The overall appearance of the spectrum of $[Et_2In(Htmtaa)]$ is more complex, as compared to those of H_2tmtaa and $[EtIn(tmtaa)]$. This is most likely to be a consequence of the reduced symmetry assigned to this molecule. The spectra of both the free ligand and the diethylindium complex contain strong absorptions near 1620 and 1595cm^{-1} . The most distinctive feature of the spectrum of the monoethylindium complex is that it contains no bands in the "finger-print" region at a higher frequency than 1553cm^{-1} . These bands are assigned to C=N and C=C stretching frequencies, and the shift to lower wavenumbers found in the spectrum of the monoethylindium compound is attributable to increased π -delocalisation within both pentanediiiminato units on metal co-ordination.

In contrast with the spectrum of the free ligand, the spectra of the indium derivatives show additional weak low frequency bands, which are likely to be In-C and In-N stretching frequencies. For $[Et_2In(Htmtaa)]$, sharp bands occur at 573 , 534 , 486 and 459cm^{-1} . For $[EtIn(tmtaa)]$, the bands are broad and centred close to 520 and 480cm^{-1} .

Mass Spectra

The mass spectra of the compounds are informative, not only by providing clear evidence for the identification of the compounds, but also for showing how readily the diethylindium compound is thermally decomposed to the monoethylindium compound. Table 4.3 below summarises the important high mass peaks recorded in the E.I. mass spectra of the free ligand and the complexes.

Table 4.3 Summary of the E.I. Mass Spectra of H_2tmtaa , $[Et_2In(Htmtaa)]$ and $[EtIn(tmtaa)]$.

Compound	m/z	Relative Intensity (%)	Assignment
H_2tmtaa	344	100	M^+
	343	5.8	$[M-H]^+$
	329	86.3	$[M-CH_3]^+$
$[Et_2In(Htmtaa)]$	516	1.2	M^+
	486	35.2	$[M-C_2H_6]^+$
	457	100	$[M-C_2H_6-C_2H_5]^+$
$[EtIn(tmtaa)]$	486	20.5	M^+
	457	60.8	$[M-C_2H_5]^+$

In all cases, a molecular ion was detected. The low intensity of the molecular ion of $[Et_2In(Htmtaa)]$ is not surprising because, at the source temperature required to volatilise this compound (ca. 150°C), the sample had partially decomposed to give $[EtIn(tmtaa)]$ by the elimination of ethane.

Further fragmentation of the indium complexes occurs with loss of the metal, as shown by a prominent molecular ion from the free ligand, and numerous lower mass peaks arise from fragmentation of the macrocyclic ring. This produces similar peaks to those obtained in the spectrum of the parent ligand. Important fragments in the spectrum of the ligand were recorded at m/z 211 (31.2%), 197 (98.9%), 173 (38.8%), 172 (36.4%), 157 (28.4%) and 133 (68.9%).

The metal ion, In^+ is prominent in the spectra of $[Et_2In(Htmtaa)]$ and $[EtIn(tmtaa)]$ (87.3 and 49.8% respectively), whereas peaks corresponding to $[Et_2In]^+$ (m/z 173) and $[EtIn]^+$ (m/z 144) are not significant.

X-ray Crystallographic Studies

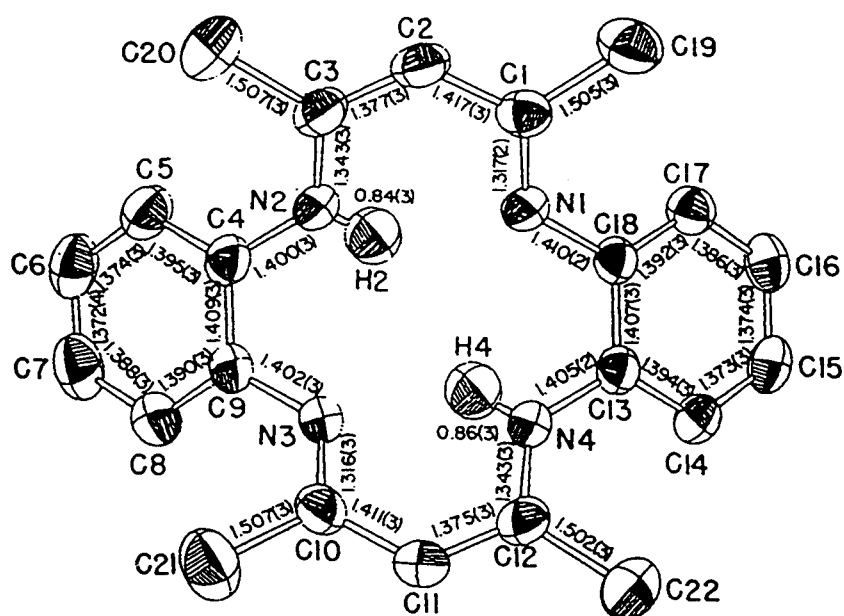
The molecular and crystal structure of the monoethylindium derivative was determined by a single crystal X-ray diffraction study. The atomic labelling scheme and the bond distances of the neutral parent ligand, H_2tmtaa ²⁴³ and the complex, $[EtIn(tmtaa)]$ are shown in Figure 4.8. Two further views of the indium complex are shown in Figures 4.9 and 4.10.

(a) Effects on Ligand Structure Upon Complexation

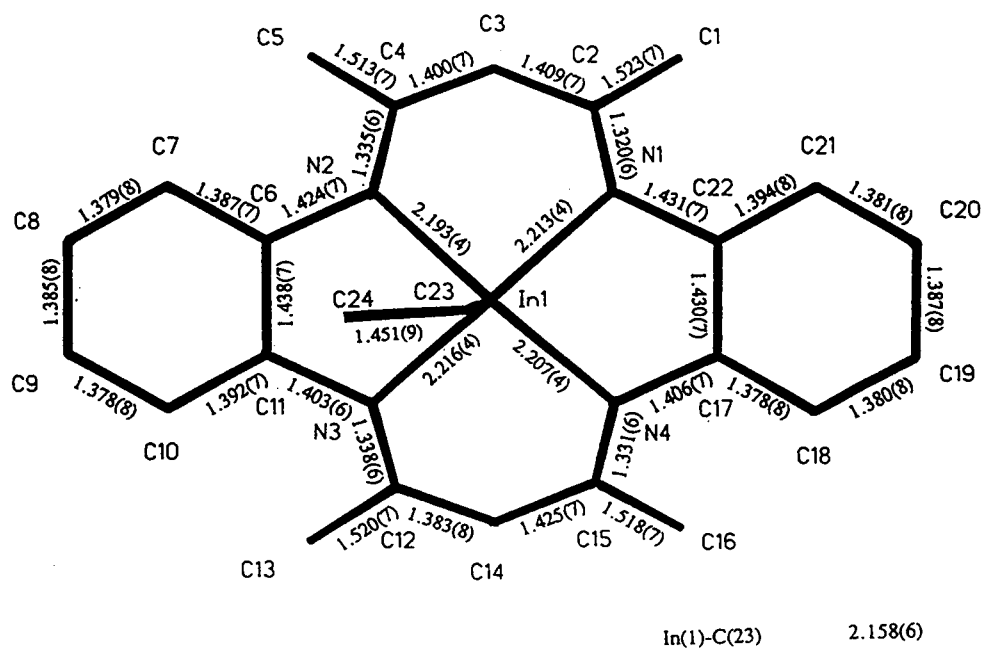
The known solid state structure of the neutral ligand, H_2tmtaa allows direct comparison of the structural parameters in the free ligand with those in its complexes. The effects of complexation of the dianion of this macrocycle with transition metal species on the conformation of the ligand has been the subject of a number studies^{243,244} and is covered by a recent review.²⁴⁵ Although the present discussion is concerned with main group complexes, many of the structural features noted with the transition metal complexes will be relevant.

The conjugated structure of this ligand makes it much more rigid than aliphatic macrocycles. It shares a number of features in common with porphyrins and phthalocyanine ligands, but possesses some important differences. The principal similarities and differences between these two systems have been summarised.^{243,245} The similarities are: (1) The four nitrogen atoms of H_2tmtaa are confined to a planar arrangement. (2) Upon metal complexation, the ligand usually loses two protons to form a dianion. (3) This dianion possesses a completely conjugated system of double bonds. The differences are: (1) The 14-membered ring of H_2tmtaa , as compared to the larger 16-membered porphyrin ring, leads to a shorter ideal metal–nitrogen distance. The N–Ct distance (defined as half the average distance between two diagonally opposite N atoms) for the neutral ligand is about 1.902 Å,²⁴³ and for the dianion is expected to lie in the range 1.85–1.87 Å.²⁴⁴ These values compare with a corresponding distance of about 2.01 Å in porphyrins.²⁴⁶ (2) In contrast to the porphyrins, the anionic charges are not delocalised over the entire ligand framework, but are essentially localised within the two

(a)



(b)



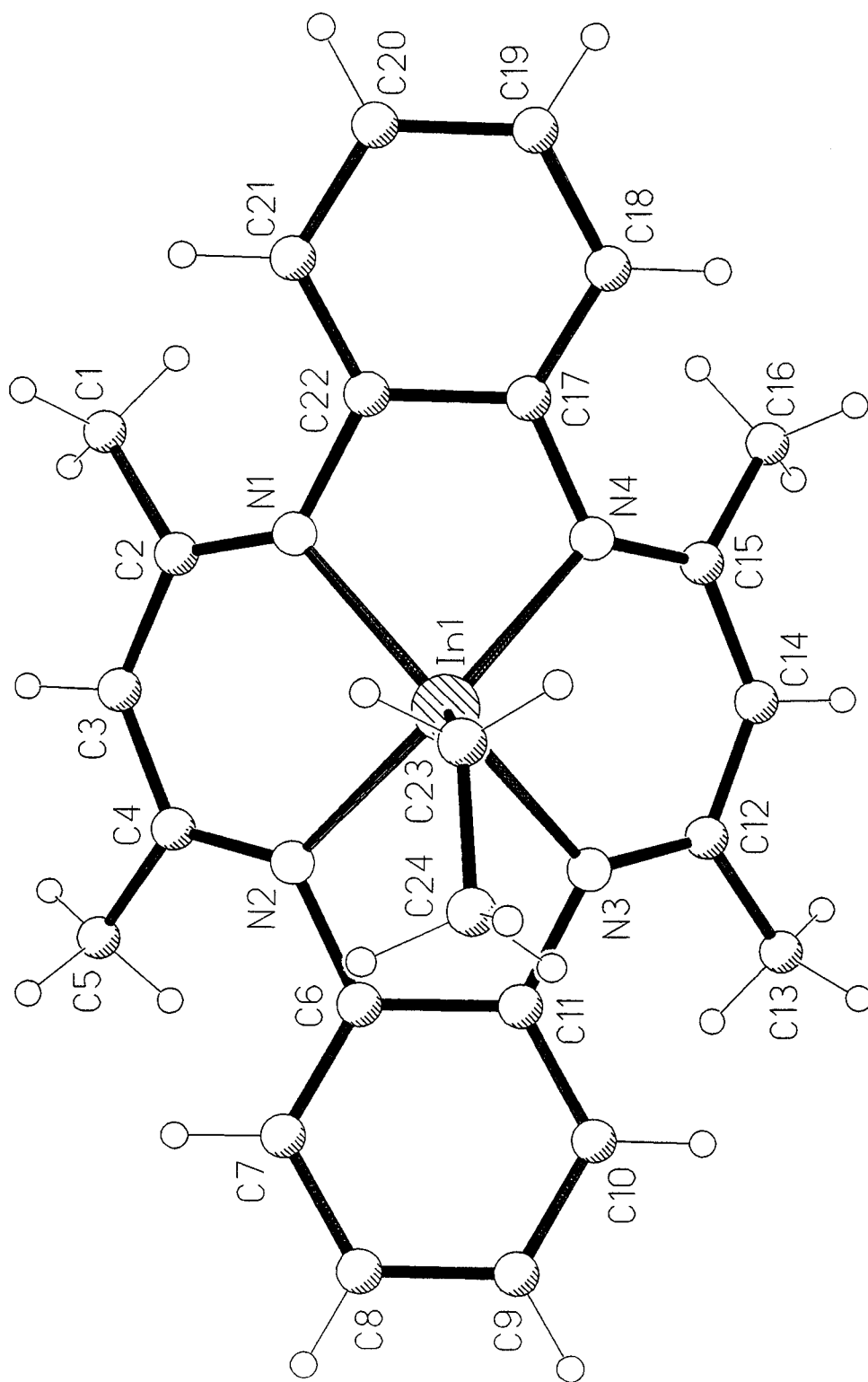


Figure 4.9 The molecular structure of [EtIn(tmtaa)], illustrating the atom numbering scheme.

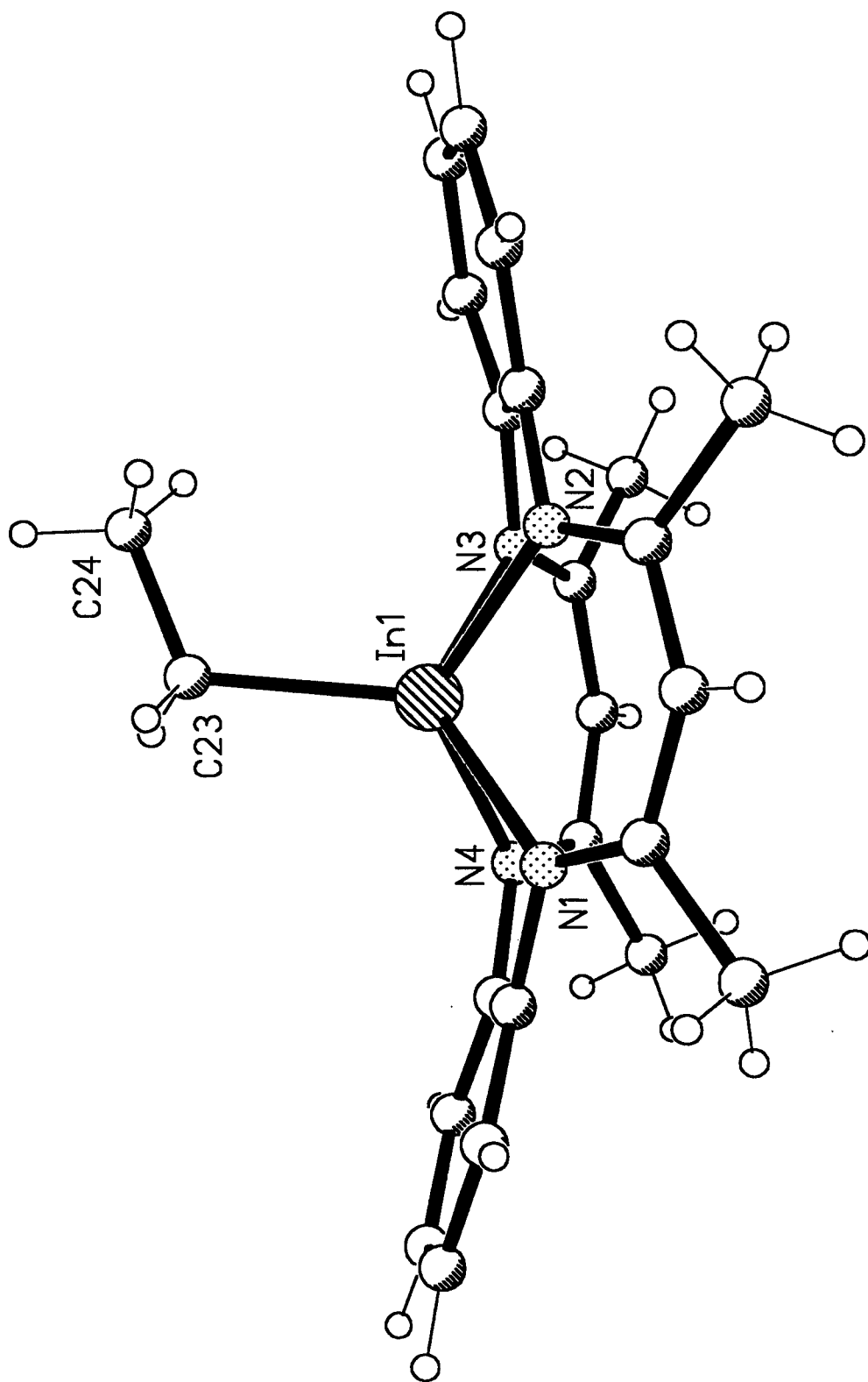


Figure 4.10 Side-view of the molecular structure of [EtIn(tmtaa)], showing the pronounced saddle shape of the ligand.

six-membered 2,4-pentanediiiminato chelate rings. (3) Although the ligand framework of the dianion is completely conjugated, the π -system is an antiaromatic ($4n$) and not, as in the porphyrins, an aromatic ($4n+2$) π electron system.

The rigid structure of this ligand imposes a number of interesting steric features which dictate the structure of these complexes. Firstly, unlike many aliphatic macrocyclic complexes, the conformation of the ligand in its complexes is predetermined to be very similar to that in the free ligand, which therefore justifies detailed comparisons. An important feature is the ability of the ligand to favour five co-ordinate, square-based pyramidal metal co-ordination because of the pronounced saddle-shape of the ligand. This conformation is caused by intramolecular steric interactions between the methyl groups and the benzenoid rings and results in the nitrogen lone pairs pointing out on the same side of the macrocycle as the benzenoid rings. Consequently, a metal atom is usually bound to this side of the N_4 plane, and the axial co-ordination positions are not chemically equivalent. This effect increases with metal size and is also dependant on the number and type of ligands occupying the remaining metal co-ordination sites, but to a lesser extent. A small metal ion, such as Co(III)^{244} can even flatten the ligand conformation from that found in the parent ligand, by pulling the lone pairs into the N_4 plane.

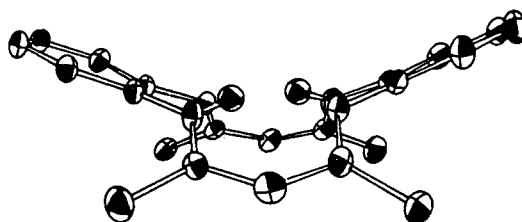


Figure 4.11 Side view of the free ligand, illustrating its saddle-shape.

The main features to note from the structure of the indium complex shown in Figure 4.8 are summarised below. Formation of the dianion causes increased delocalisation within each 2,4-pentanediiiminato unit. This is demonstrated by comparison

of the differences in the formally C–N and the C=N distances within each NCCCN unit in the free ligand of 0.026(3) and 0.027(3) Å²⁴³ with the equivalent, almost negligible differences found in the complex of 0.015(6) and 0.007(6) Å. The carbon–nitrogen bonds which link the 2,4–pentanediiminato units with the benzenoid rings show the greatest single bond character and are therefore most easily deformed upon complexation. The distances found in the free ligand range from 1.400(3) to 1.410(3) Å, with an average distance of 1.404(3) Å and compare with the range found in the complex of 1.403(6) to 1.431(6) Å, and a mean distance of 1.416(7) Å.

Figure 4.10 illustrates that the saddle–shape conformation found in the free ligand is retained in the complex. This structure is similar to those previously reported for the analogous ethylaluminium²¹⁹ and methylgallium²⁰⁰ derivatives, all of which possess a five co–ordinate metal centre which is symmetrically co–ordinated above the N₄ plane. The following analysis of the structures of these three group 13 complexes is similar to that previously used for the complexes [XM(tmtaa)] [M = Co(III), Fe(III), Mn(III); X = I, Cl, N(Et)₃ respectively] by Goedken *et al.*²⁴⁴ Table 4.4 compares some important structural parameters found in the structures of the group 13 metal complexes.

A most marked variation between the three structures is seen in the increasing distance of the metal from the N₄ plane from 0.57 Å in the aluminium complex, 0.65 Å in the gallium complex and to 0.91 Å in the indium complex, and a concomitant small increase in the N–Ct distance of the macrocycle core. These variations are caused by the increasing size of the metal on descending the group. The respective parameters in the cobalt(III), iron(III) and manganese(III) complexes range from 0.24 to 0.73 Å and 1.893 to 1.988 Å.²⁴⁴ In order to accommodate this increasing metal ion size, torsional distortions and angle deformations occur within the ring so as to re–direct the nitrogen lone pairs out of the ring and increase the core size of the ring. The conformation of each molecule can be initially described by the dihedral angles formed between the N₄ plane and the two planes defined by the pentanediiminato and benzenoid chelate rings. These planes are shown diagrammatically in Figure 4.12, and the average dihedral angles of these planes are given in Table 4.4.

Table 4.4 Summary of important structural parameters for the three [RM(tmtaa)] structures.

Distance (Å)	[EtAl(tmtaa)] ²¹⁹	[MeGa(tmtaa)] ²⁰⁰	[EtIn(tmtaa)]
Aver. M–N distance	1.967	2.016(5)	2.207(4)
Aver. N–Ct distance	1.88	1.908(5)	2.011(4)
M–N ₄ –plane distance	0.57	0.650(5)	0.910(2)
Aver. C–N distance (six–membered chelate ring)	1.336	1.336(7)	1.331(6)
Aver. C–C distance (six–membered chelate ring)	1.393	1.393(9)	1.404(7)
Aver. C–N distance (five–membered chelate ring)	1.418	1.404(9)	1.416(7)
		Average Dihedral Angles (°)^a	
1–2 ^b	32.6	34.7	33.0
1–3	15.9	14.9	8.4
1–4	21.6	21.9	14.0
5–6	43.4	47.5	46.3
6–7	4.7	2.3	1.5
		Average Bond Angles (°)^a	
α	128.0	129.9	131.8
β	121.7	121.8	123.5
γ	124.2	124.8	125.4
δ	113.9	114.2	115.7

^a See Figure 4.12 for Key. ^b Plane 2 calculated as the average of the 4 (methine C omitted) and 5 membered planes.

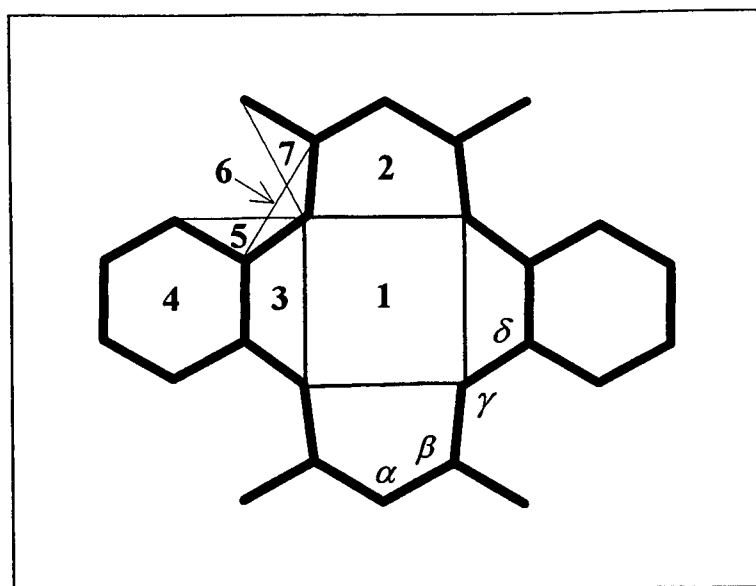


Figure 4.12 Diagrammatic key of the structural parameters introduced in Table 4.4

While the dihedral angles between planes 1 and 2 in all three molecules do not vary significantly from around 33 to 35°, the dihedral angles between planes 1 and 3 are not only substantially smaller and in an opposite direction, but also do vary considerably from 15.9° in the aluminium complex to 8.4° in the indium complex. The analogous values for the benzenoid rings (dihedral angles between planes 1 and 4) show a similar trend and these rings are bent further upwards by around 5 to 7°. This situation is similar to that previously reported for the Co(III), Fe(III) and Mn(II) complexes with this ligand, except that the dihedral angles between planes 1 and 2 in the solid state structures of these complexes also increase with a larger metal ion.

The unequal bending of the two types of chelate rings accounts for the direction of the lone pairs out of the N_4 plane on the side of the benzenoid rings in each of the complexes. Compared to this, the analogous average angles in the free ligand are 34.6 and 20.1° respectively,²⁴³ and indicate that complexation of these metals tends to flatten the conformation of the ligand. The average dihedral angles between the planes 5 and 6, 6 and 7 show a slight increase as the metal size increases, because of the re-direction of the lone pairs.

The small increase in the core size of the ligand arises from either (1) a slight lengthening of the bonds in the 14-membered ring or (2) an increase in the appropriate

bond angles within the ring (denoted α , β , γ , δ in Figure 4.12) or both factors. The level of the estimated standard deviations associated with the bond distances prevents an accurate evaluation of the extent of contribution (if any) from the first possibility. However, tabulation of the bond angles around the ring does reveal a trend to support the second possibility. The average bond angles given in Table 4.4 show a progressive increase as the metal size increases, thereby enlarging the core size. The sum of these angles in the indium complex is 19.0° larger than the sum of those in the gallium complex, and this latter total is 7.8° larger than the total in the aluminium complex.

(b) The Co-ordination Environment of the Indium Atom

The metal atom in [EtIn(tmtaa)] is in a distorted square-based pyramidal environment, CInN_4 , with the ethyl group in the axial site. The metal co-ordination geometry is similar to that found for the related organoindium macrocyclic complex, methylindium-(tetraphenylporphinato), [MeIn(TPP)].¹²⁵ This complex contains a monomethylindium unit which is co-ordinated to four basal N sites of the porphyrin ligand and an axial metal-methyl bond as illustrated below.

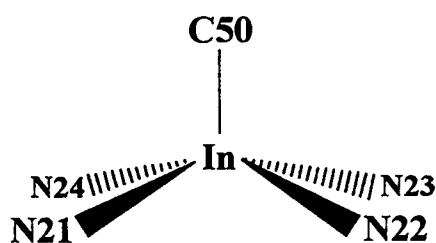


Figure 4.13 The co-ordination geometry of indium in [MeIn(TPP)]

Relevant bond lengths are: In-N(21) 2.20(1); In-N(22) 2.21(1); In-N(23) 2.20(1);
In-N(24) 2.21(1); In-C(50) 2.13(1).

The principal bond angles in both complexes are given below and demonstrate the similar indium co-ordination geometry in the complexes.

Table 4.5 Comparison of the indium co-ordination environments in [EtIn(tmtaa)] and [MeIn(TPP)].

[EtIn(tmtaa)]		[MeIn(TPP)] ¹²⁵	
Bonds	Angle (°)	Bonds	Angle(°)
N(1)–In(1)–N(2)	85.86(16)	N(21)–In–N(22)	83.1(5)
N(2)–In(1)–N(3)	74.51(15)	N(22)–In–N(23)	82.7(6)
N(3)–In(1)–N(4)	86.43(15)	N(23)–In–N(24)	81.6(5)
N(4)–In(1)–N(1)	73.86(15)	N(24)–In–N(21)	83.8(5)
N(1)–In(1)–N(3)	131.47(16)	N(21)–In–N(23)	137.6(6)
N(2)–In(1)–N(4)	131.15(16)	N(22)–In–N(24)	139.7(6)
N(1)–In(1)–C(23)	118.5(2)	N(21)–In–C(50)	109.4(7)
N(2)–In(1)–C(23)	112.72(21)	N(22)–In–C(50)	108.6(6)
N(3)–In(1)–C(23)	110.02(20)	N(23)–In–C(50)	113.0(6)
N(4)–In(1)–C(23)	116.04(21)	N(24)–In–C(50)	111.7(6)

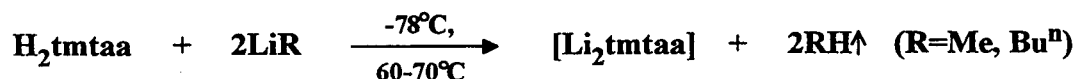
The indium atom in [MeIn(TPP)] is co-ordinated 0.78Å from the N₄ plane and the N–Ct distance is 2.06(1)Å (c.f. 0.91Å and 2.011(4)Å respectively for [EtIn(tmtaa)]). Despite the similarity of the N–Ct distances, the displacement of the metal from the N₄ plane is smaller in the porphyrin complex as a result of the larger available core size in the essentially flat porphyrin ligand.

The average indium–nitrogen bond distances in these two compounds are similar, at 2.207(4)Å in [EtIn(tmtaa)] and 2.205(1)Å in [MeIn(TPP)]. The axial indium–carbon bond length in the former complex of 2.158(6)Å is slightly greater than the corresponding value in the latter of 2.13(1)Å. As a comparison, the In–C distance found in the five co-ordinate distorted trigonal bipyramidal structure of [EtIn(DPBA)₂] (discussed in Chapter 2) of 2.146(6)Å falls within these two distances.

(2) The Synthesis of Further Indium Functionalities

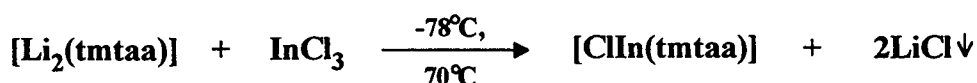
(i) Preparation of [ClIn(tmtaa)]

A second synthetic approach was used to prepare complexes of the type [XIn(tmtaa)]. This route involved the deprotonation of H₂tmtaa and the formation of the dilithium salt of the ligand, [Li₂tmtaa]. Using this method, it is then possible to react the salt with indium trichloride to form the monochloroindium complex, [ClIn(tmtaa)]. Several procedures were used for the lithiation of the free ligand, all of which involved the addition of two mole equivalents of lithium alkyl to the ligand in a suitable solvent held at -78°C.



The reaction was carried out using either a diethyl ether solution of LiMe, or a hexane solution of LiBuⁿ. The main reaction solvent used was either THF or toluene. A rapid colour change occurred even at this temperature from yellow/orange to deep red as the ligand was lithiated. To ensure the completion of the reaction, the mixture was heated (60–70°C) for 1–2 hours. These solutions were extremely air and moisture sensitive, reforming the free ligand, H₂tmtaa on exposure to air.

For the purposes of this work, it was not necessary to isolate this salt. Addition of the deep red solution to a toluene or THF suspension of indium trichloride, chilled at -78°C, followed by heating at 70°C for 2–3 hours gave an orange suspension, which was cooled to room temperature and filtered to leave a deep red solution.



A dark orange microcrystalline solid was precipitated on the addition of hexane to this concentrated solution. Elemental analysis (C, H, N) of the solid obtained from using toluene as solvent gave results consistent with the composition required for the

monochloroindium complex, [ClIn(tmtaa)], which showed it to be free of lithium chloride. Much less satisfactory results were obtained when the reaction was carried out using THF as solvent, presumably because of the difficulty of removal of all traces of LiCl from the product using this solvent. The complex was spectroscopically characterised by ^1H , ^{13}C N.M.R. and mass spectrometry. The ^1H N.M.R. data is given in the Experimental Section. The spectrum shows an overall appearance similar to that obtained for the monoethylindium complex, (except for the absence of resonances attributed to In–Et), and therefore suggests that the indium–chloride moiety is symmetrically co–ordinated to the four nitrogen atoms of the macrocycle, leading to an expected five co–ordinate, distorted square–based pyramidal metal geometry. The ^{13}C N.M.R. data are given at the end of this chapter and are clearly consistent with this interpretation.

The complex is apparently air stable – single crystals, suitable for an X–ray diffraction study, were grown from a chloroform/hexane solution of the compound which had been exposed to air for a prolonged period (several weeks). Analysis of the X–ray diffraction data led to the molecular structure shown in Figures 4.14 and 4.15 overleaf. Bond lengths are given in Figure 4.16 and the bond angles around the metal are given in Table 4.6. A complete list of the bond angles is given in Appendix 2. This study confirmed the anticipated metal co–ordination mode and the familiar saddle–shape of the ligand. The most salient aspect of this structure is the significantly smaller displacement of the metal atom from the plane of the four nitrogen atoms of $0.738(3)\text{Å}$, compared with the displacement of $0.910(2)\text{Å}$ for the monoethylindium derivative. Comparison of these structures will be discussed in detail later in this chapter.

The fact that this compound could be obtained by a relatively straight forward synthetic procedure in high purity and yield was of further synthetic importance. The availability of this compound provided an opportunity to investigate the nucleophilicity of the In–Cl bond in this unusual co–ordination environment and the possible production of further axial functionalities.

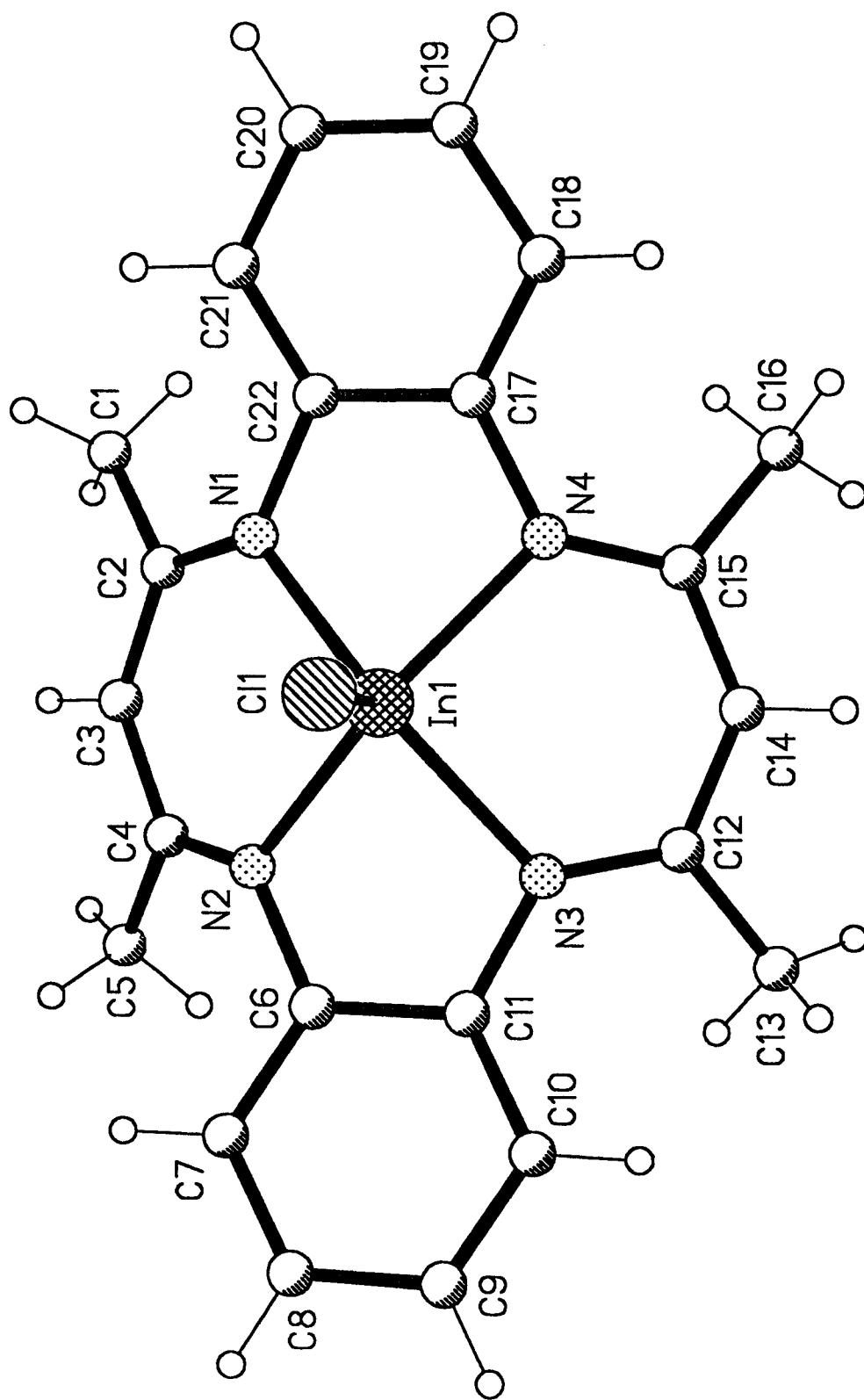


Figure 4.14 The molecular structure of $[ClIn(tmtaa)]$, illustrating the atom numbering scheme.

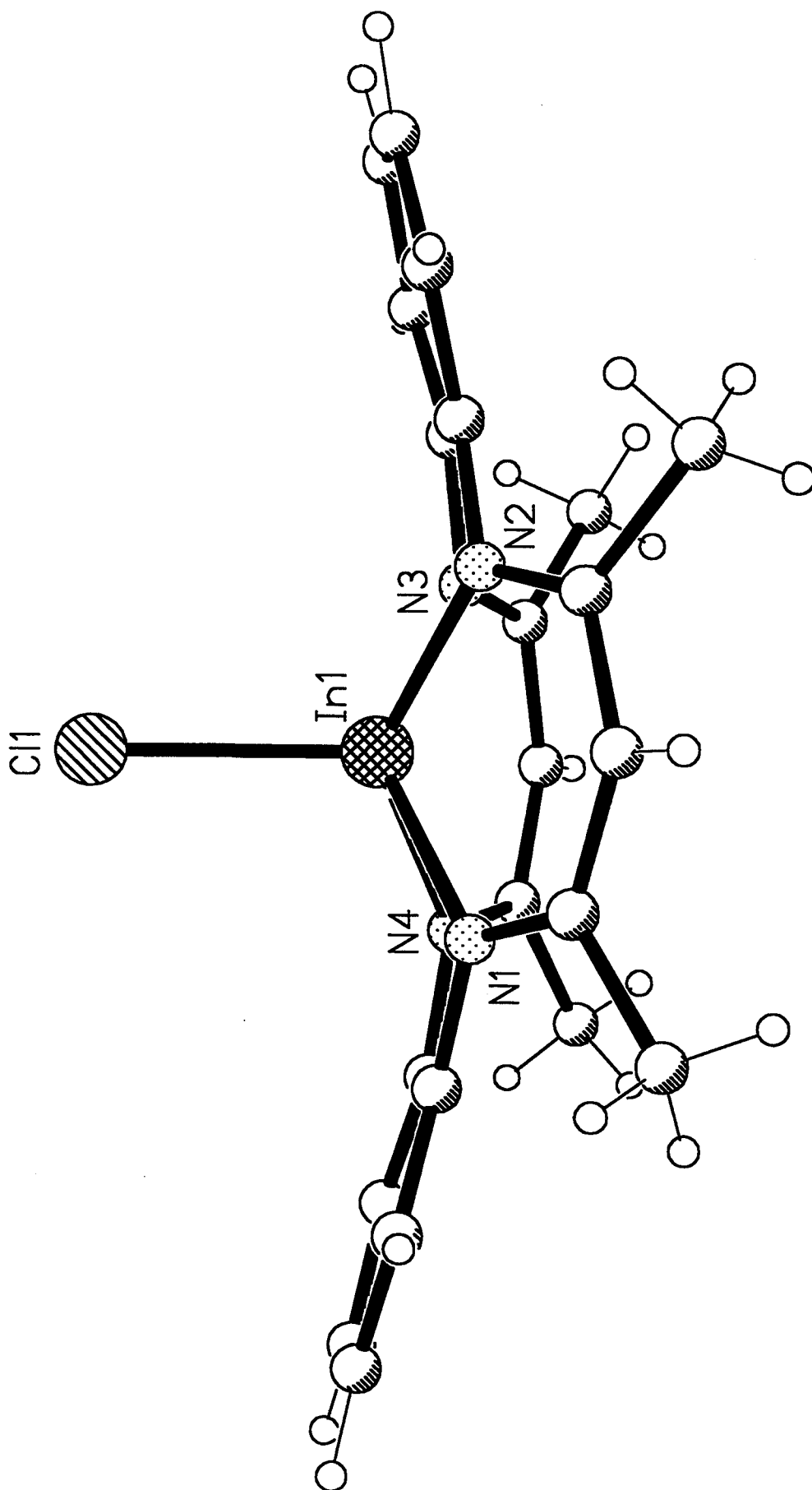


Figure 4.15 Side-view of the molecular structure of [ClIn(tmtaa)]

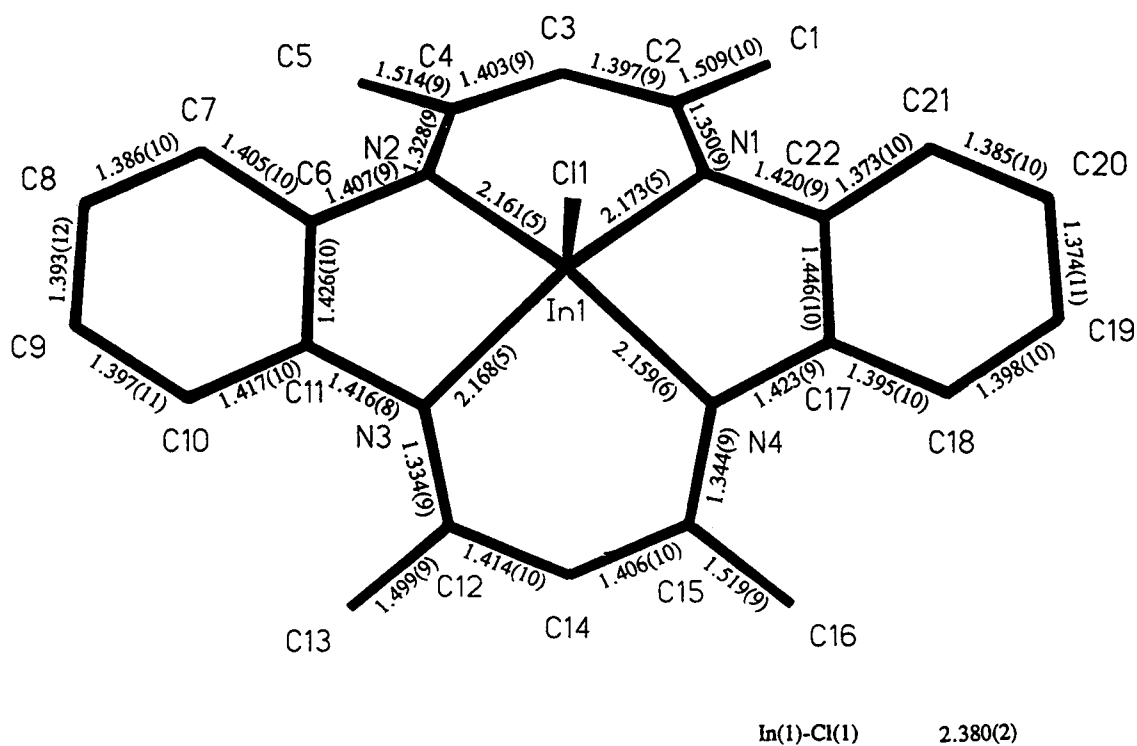


Figure 4.16 The molecular structure of $[\text{ClIn}(\text{tmtaa})]$, showing the bond lengths (Å).

Table 4.6 Bond angles ($^\circ$) around the indium atom in $[\text{ClIn}(\text{tmtaa})]$.

N(1)-In(1)-N(2)	89.47(21)	N(3)-In(1)-N(4)	90.55(21)
N(2)-In(1)-N(3)	76.74(21)	N(4)-In(1)-N(1)	76.45(21)
N(1)-In(1)-N(3)	140.10(21)	N(2)-In(1)-N(4)	140.31(22)
N(1)-In(1)-Cl(1)	110.17(15)	N(2)-In(1)-Cl(1)	112.23(16)
N(3)-In(1)-Cl(1)	109.71(15)	N(4)-In(1)-Cl(1)	107.45(16)

During the course of this work Cowley *et al*²⁴⁷ also reported the preparation of $[\text{ClM}(\text{tmtaa})]$ ($\text{M}=\text{Ga}, \text{In}$) using the same synthetic route, and investigated the reactivity of the $\text{M}-\text{Cl}$ bond. In summary, this group reports that the $\text{Ga}-\text{Cl}$ bond in $[\text{ClGa}(\text{tmtaa})]$ does not react with LiH , $\text{Li}(\text{BEt}_4\text{H})$, LiMe , or $[\text{Na}\{\text{Co}(\text{CO})_4\}]$. Furthermore, they claim that the monochlorogallium complex does not undergo reductive coupling with Na/K or $[\text{Na}(\text{naphthalenide})]$. However, the monochloroindium complex, $[\text{ClIn}(\text{tmtaa})]$ is reported to react slowly with LiMe to yield the corresponding monomethylindium complex. These authors conclude that the incorporation of the $\text{M}-\text{Cl}$ moiety into this ligand results in a significantly reduced reactivity of this bond.

The work presented here, however, shows that the $\text{In}-\text{Cl}$ bond is very susceptible to nucleophilic attack by the reagents LiCp , LiMe , $\text{LiN}(\text{SiMe}_3)_2$, and LiOSiMe_3 , to produce the complexes shown in the scheme below, and the elimination of LiCl .

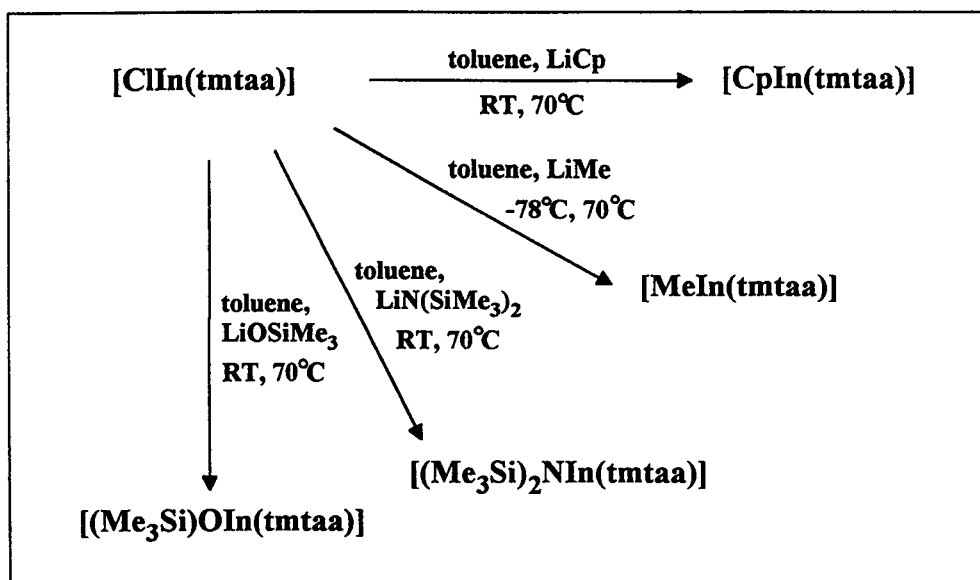


Figure 4.17 Reactions of $[\text{ClIn}(\text{tmtaa})]$.

(ii) Reaction of $[\text{ClIn}(\text{tmtaa})]$ with LiCp

This reaction was found to occur readily on heating a 1:1 mixture of $[\text{ClIn}(\text{tmtaa})]$ and lithium cyclopentadienide in toluene at 70°C , and an orange suspension was obtained. Filtration of the cooled suspension gave a deep red solution. Recrystallisation from this concentrated solution produced dark red, brick-shaped, single

crystals. The nature of this compound was initially investigated by microanalysis (C, H, N) and ^1H and ^{13}C N.M.R. spectroscopy (discussed in detail below), and these gave results compatible with the formulation $[\text{CpIn}(\text{tmtaa})]$. The compound is stable in air and insoluble in cold water. Consequently, product was also recovered from the filtered solid, which mainly consisted of LiCl , by washing with water and filtration of the remaining red solid. The compound is also soluble in dichloromethane, chloroform and THF.

In order to ascertain the effect of this axial group on the structure of this compound, and the nature of the bonding scheme of the indium–cyclopentadienyl moiety, the solid state structure of this compound was determined by X–ray crystallography. The structure was initially solved using data which were collected at -33°C . However, refinement of the structure solution using these data proved unsatisfactory, in particular in relation to the parameters of the cyclopentadienyl ring. This was presumed to be caused by the high thermal motion of the carbon atoms of this ring. The data were re–collected at -133°C in order to minimise thermal motion, and subsequent refinement of the model proved slightly more successful and gave a more precise location of the Cp carbon atoms. Two views of the molecular structure are presented. Figure 4.18 shows the atomic labelling scheme used and atomic vibration ellipsoids (excluding H atoms), and Figure 4.19 illustrates the familiar saddle–shape conformation of the ligand and also the orientation of the cyclopentadienyl group in relation to the ligand. The important bond lengths are given in Figure 4.20 and metal–bond angles are given in Table 4.7 and a complete list is given in Appendix 2.

The indium atom is once again in a distorted five co–ordinate, square–based pyramidal co–ordination environment, and is bound to the essentially planar four nitrogen atoms of the macrocyclic ligand and to one carbon atom of the cyclopentadienyl ring. Three of the four indium–nitrogen bond distances are identical, at $2.191(4)\text{\AA}$ [$\text{In}(1)\text{--N}(2)$] and $2.191(5)\text{\AA}$ [$\text{In}(1)\text{--N}(1)$, $\text{In}(1)\text{--N}(3)$], while the fourth, which is eclipsed by the Cp ring when viewed along the axial In–C bond, is significantly shorter at $2.171(4)\text{\AA}$.

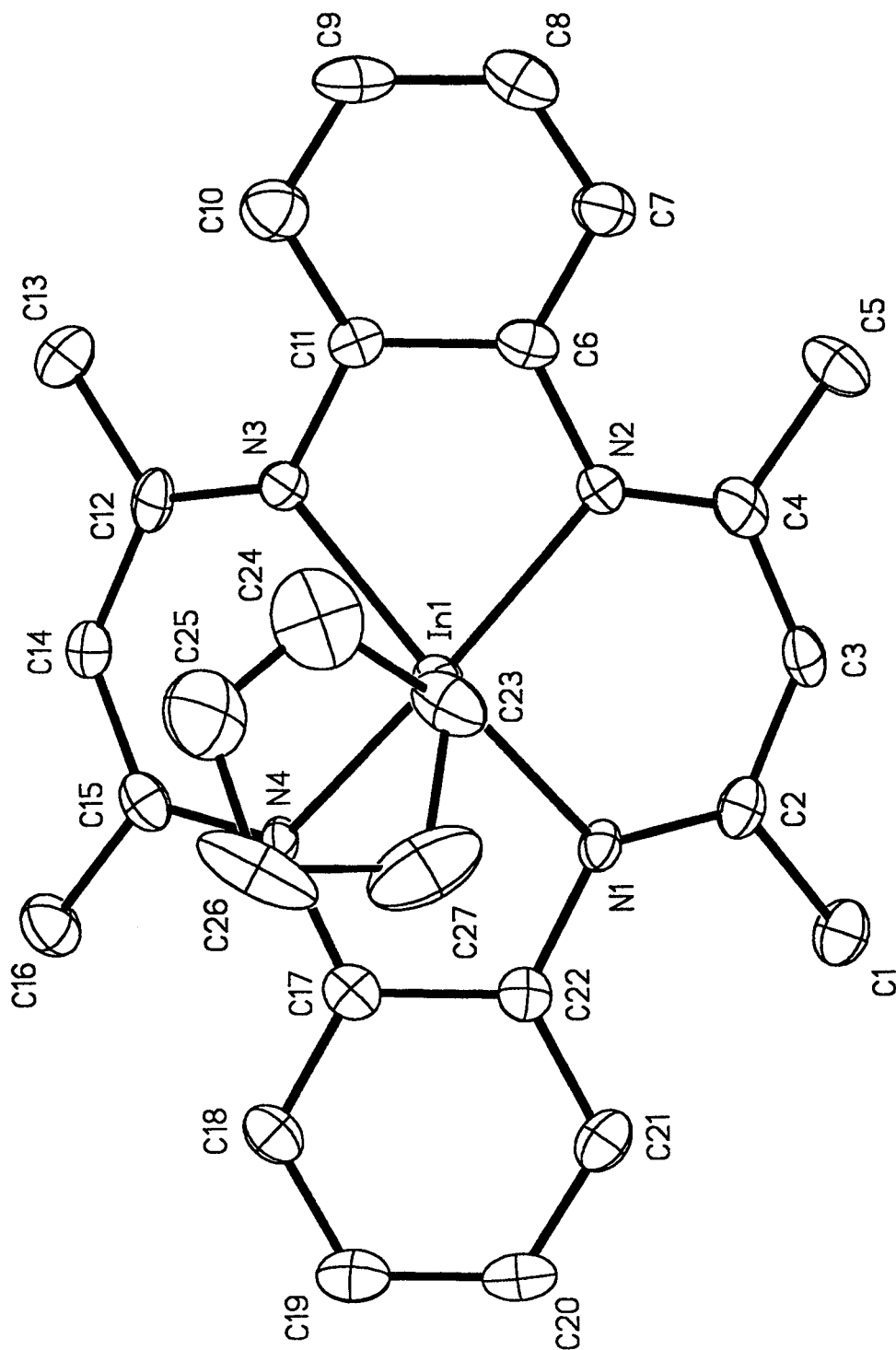


Figure 4.18 The molecular structure (ORTEP plot, showing 50% probability ellipsoids) of [CpIn(tmtaa)] and atom numbering scheme. H atoms excluded for clarity.

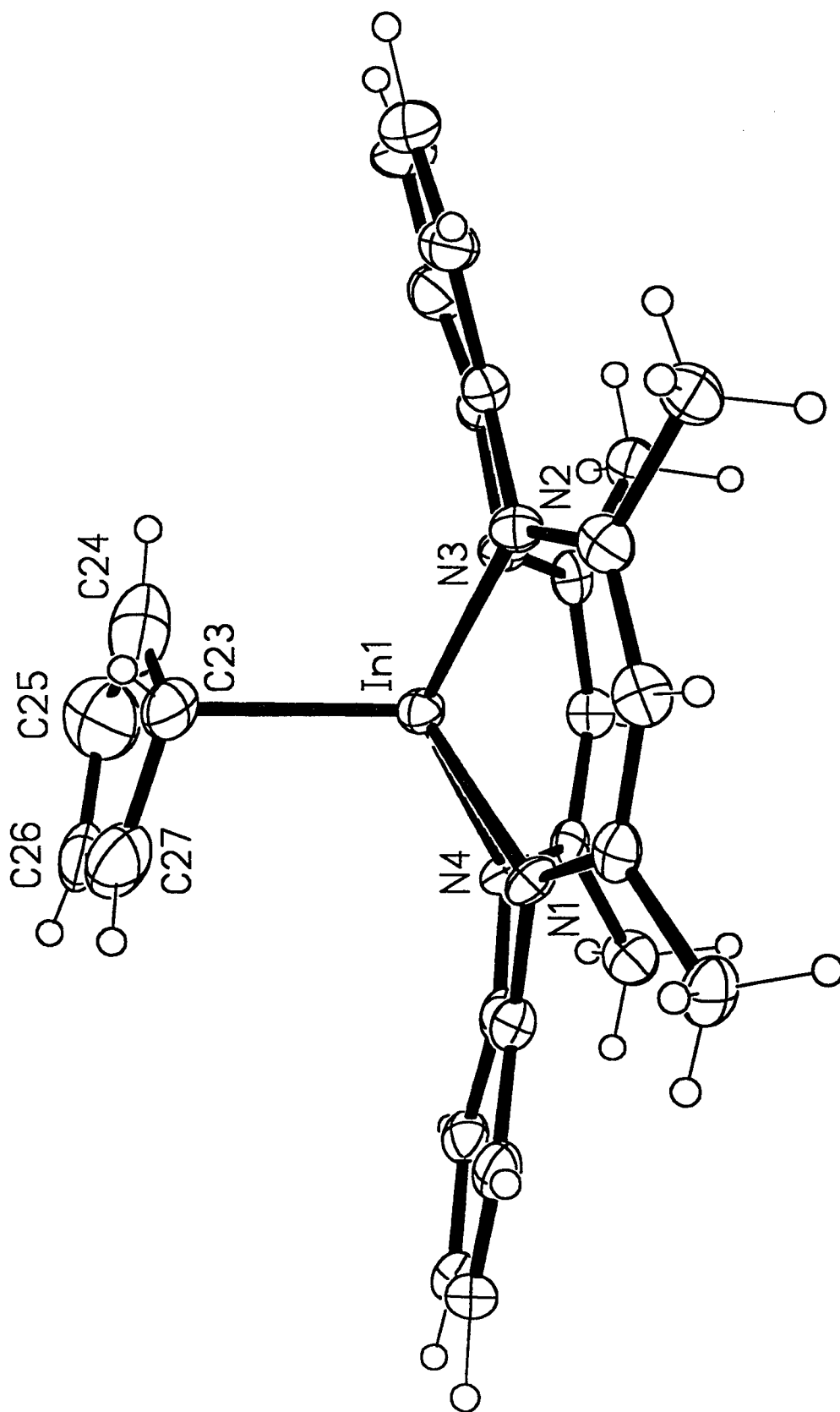


Figure 4.19 Side-view of the molecular structure (ORTEP plot, showing 50% probability ellipsoids) of [CpIn(tmtaa)].

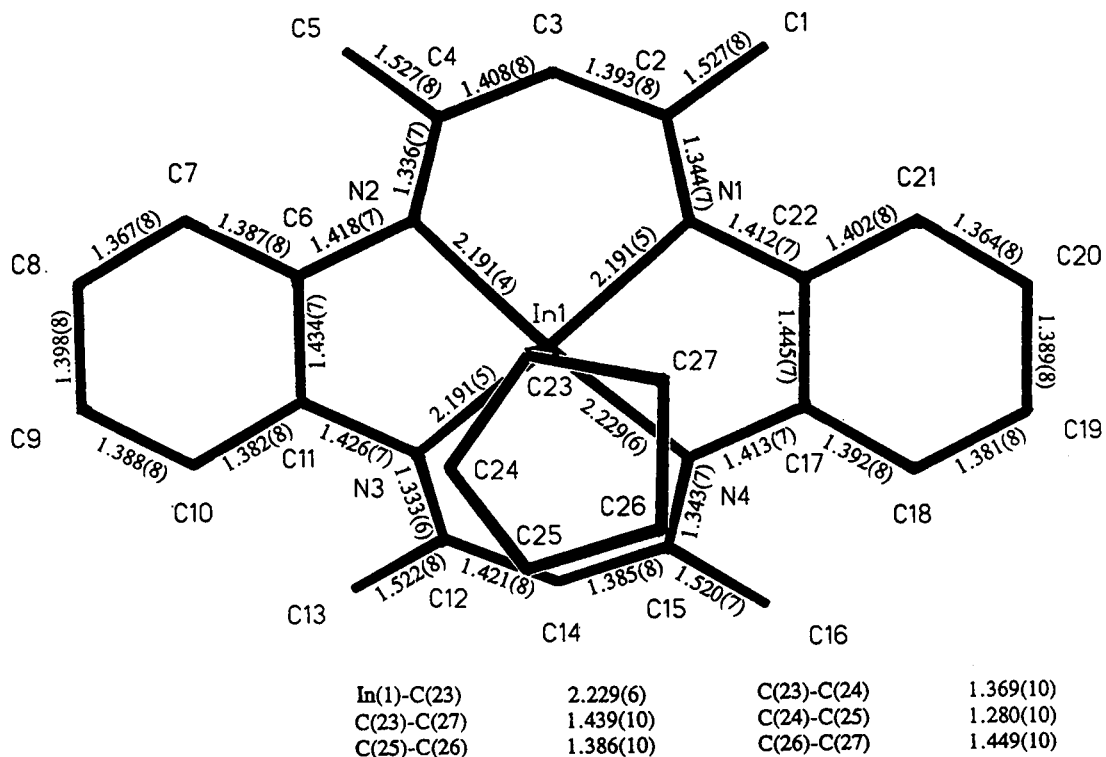


Figure 4.20 The molecular structure of [CpIn(tmtaa)], showing the bond lengths (Å).

Table 4.7 Bond angles around the indium atom in [CpIn(tmtaa)].

N(1)-In(1)-N(2)	88.49(17)	N(3)-In(1)-N(4)	88.05(16)
N(2)-In(1)-N(3)	74.60(16)	N(4)-In(1)-N(1)	75.68(16)
N(1)-In(1)-N(3)	134.39(17)	N(2)-In(1)-N(4)	136.58(17)
N(1)-In(1)-C(23)	111.34(21)	N(2)-In(1)-C(23)	107.97(20)
N(3)-In(1)-C(23)	114.13(21)	N(4)-In(1)-C(23)	115.44(20)

The indium–carbon bond distance, [In(1)–C(23)] of 2.229(6)Å is longer than the corresponding distance found in [EtIn(tmtaa)] of 2.158(6)Å, but is comparable with the range 2.237(9) to 2.466(8)Å found in tris(cyclopentadienyl)indium, which possesses a slightly distorted tetrahedral indium (III) centre.²⁴⁸

The displacement of the indium atom from the macrocyclic N₄ plane is 0.828(3)Å and the N–Ct distance of the macrocycle is 2.023Å. Table 4.8 shows the corresponding parameters for the other gallium– and indium–tmtaa complexes which have been structurally characterised by X–ray crystallography.

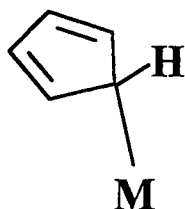
Table 4.8 Comparison of the important M–N distances in [XM(tmtaa)]

Complex	Distance (Å)			Reference
	M–N ₄	N–Ct (aver.)	M–N (aver.)	
[ClGa(tmtaa)]	0.480(4)	1.929(4)	1.988(4)	247
[MeGa(tmtaa)]	0.650(5)	1.908(5)	2.016(5)	200
[ClIn(tmtaa)]	0.737(3)	2.036(5)	2.165(5)	This work
[CpIn(tmtaa)]	0.828(3)	2.023(5)	2.186(5)	This work
[EtIn(tmtaa)]	0.910(2)	2.011(4)	2.207(4)	This work

These parameters demonstrate that the displacement distance of the metal from the N₄ plane shows a strong dependence on the type of axial group attached to the metal. For the three indium complexes, there is a progression in this distance from 0.737(3)Å for the monochloroindium complex, to 0.828(3)Å for the cyclopentadienylindium complex, and to a maximum of 0.910(2)Å for the monoethylindium complex. A similar progression exists for the two gallium complexes. These trends follow the expected sequence of the electron acceptor properties of these axial ligands. An axial ligand with strong electron acceptor properties, such as the chloride ligand, will reduce the electron density on the metal and therefore the metal will move closer to the N₄ donor plane and will be accompanied by a small increase in the N–Ct distance.

The Cyclopentadienyl Ring

The structure clearly demonstrates that the cyclopentadienyl ring is η^1 -bonded to the indium [In(1)–C(23)], with no other important indium–carbon contacts since the next nearest carbon atom [In(1)–C(24)] is 2.808(10)Å away. This type of bonding scheme normally leads to the occurrence of two formally distinct types of carbon–carbon bonds in the cyclopentadienyl ring, namely two short double bonds and three longer single bonds, as shown below:



The solid state structure reported for $\text{In}(\text{Cp})_3$ reveals that there are two types of cyclopentadienyl rings in this compound, two monodentate σ -bonded and one bridging, which give rise to infinite polymeric chains.²⁴⁸ The structure of the monodentate rings is compatible with the type of Cp bonding scheme shown above, with an average C–C bond distance of 1.418(14)Å and an average C=C bond distance of 1.348(14)Å. The internal ring angles at the olefinic carbon atoms vary from 108–110°, while those at the σ -bonded carbon atoms are significantly smaller and are within the range 105–106°.

The ring in the present structure is less easily described. The bond distances around the ring, given in Figure 4.21 (page 174), show a different pattern of formal bond types. The internal ring angles vary considerably, from 102–113°. This large variation is reflected in the significant non-planarity of the ring, and C(23) lies 0.137(11)Å out of the plane defined as a best-fit through C(24)–C(25)–C(26)–C(27). The dihedral angle between this plane and the plane C(23)–C(24)–C(27) is 9.9(10)°. This compares with the corresponding angles found in the monodentate rings in $\text{In}(\text{Cp})_3$ of 2.5 and 3.2°.

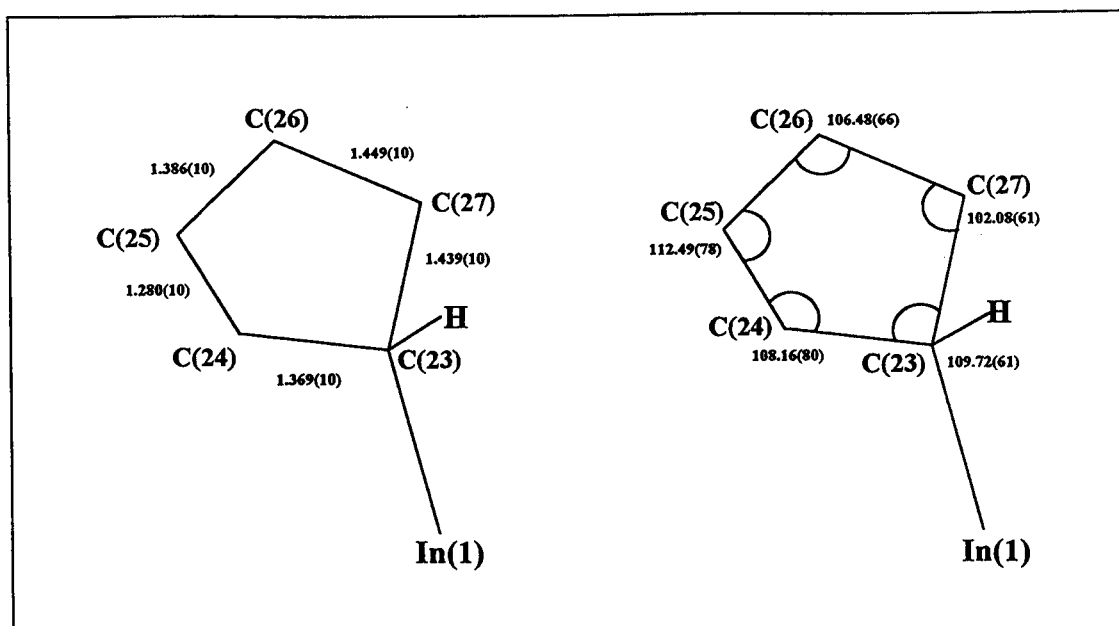


Figure 4.21 Important Bond Lengths (Å) and Angles (°) in the Cyclopentadienyl Ring in [CpIn(tmtaa)].

The three accurately measured angles around C(23) of 99.80(48), 107.80(46) and 109.72(61)° are close to the values expected for ideal sp^3 hybridisation of the carbon atom, with a hydrogen atom placed in a calculated fourth position.

The reported crystal structure of the indium(I) compound, InCp, displays a bonding scheme different from those above in that it involves a η^5 -cyclopentadienyl ring.²⁴⁹ This structure consists of polymeric zigzag chains based on [In(η^5 -Cp)] units, where each indium atom interacts with two cyclopentadienyl rings and each cyclopentadienyl ring interacts with two indium atoms. The indium carbon distances are substantially longer than the In(1)-C(23) distance of 2.229(6) Å in [CpIn(tmtaa)], and range from 2.853(22) to 3.091(21) Å, with a shorter indium to ring centre distance of 2.726 Å. In the gas phase it has a half-sandwich structure.²⁵⁰

Even though these crystallographic results do not demonstrate accurately the expected bonding scheme within the cyclopentadienyl ring for η^1 bonded type, it is most likely that true η^1 bonding does exist and that the occurrence of rotational disorder or other crystallographic complications is responsible for deviations from such a neat model.

The E.I. mass spectrum of the complex shows a weak molecular ion, with a much more intense peak corresponding to loss of $[\text{C}_5\text{H}_5]^\cdot$ (55.5%) (see Table 4.9). Other intense peaks correspond to $[\text{In}]^+$ (58.1), $[\text{C}_5\text{H}_6]^+$ (base peak) and $[\text{C}_5\text{H}_5]^+$ (55.3%).

The infra-red spectrum of the complex, recorded as a Nujol mull, has several weak bands in the region $3100\text{--}3000\text{cm}^{-1}$, which are assigned to C-H stretching vibrations of the Cp ring. The remaining appearance of the spectrum closely resembles that obtained for $[\text{EtIn}(\text{tmtaa})]$, although it shows additional bands in the region $1566\text{--}1500\text{cm}^{-1}$ attributable to C-C(Cp ring) stretching vibrations. Furthermore, it has a weak but well defined peak at 326cm^{-1} , which is in the $\nu(\text{In-C})$ region and compares with 339 and 316cm^{-1} reported for this mode in InCp_3 by Tuck and Poland.²⁵¹

The ^1H N.M.R. spectrum was recorded from CDCl_3 , or CD_2Cl_2 , or $\text{CD}_3\text{C}_6\text{D}_5$ solutions and the data are summarised in the Experimental Section. In each case the cyclopentadienyl protons appear as a sharp singlet, implying that a rapid "ring-whizzing" process was occurring. Cooling of the CD_2Cl_2 solution to -80°C showed no significant effect on the 400MHz ^1H spectrum, showing that the fluxional process was still rapid compared to the N.M.R. timescale, even at this temperature. Evidence for movement of the Cp ring even in the solid state is also shown by the thermal ellipsoids of the carbon atoms, indicating motion in the plane of the ring about the ring axis.

The complex in CDCl_3 solution at room temperature was unstable, and significant decomposition occurred over a period of several days, as evidenced by the appearance of new resonances in the ^1H and ^{13}C spectra. The decomposition was sufficiently slow to allow N.M.R. spectra to be recorded provided the samples were stored at -35°C . Warming such solutions to $50\text{--}60^\circ\text{C}$ caused rapid decomposition. The identity of the new indium product was confirmed to be $[\text{ClIn}(\text{tmtaa})]$ by comparing the ^1H and ^{13}C N.M.R. spectra with those obtained for the chloro compound, and further resonances attributable to dicyclopentadiene were located.

The remaining reactions shown in Figure 4.17 (page 167) were performed in a similar manner to that outlined above. Thus the reactants were heated to 70°C in toluene

solution for 2–3 hours. The lithium chloride suspension formed was cooled to room temperature and the deep red solutions separated by filtration. The liquor was concentrated until the onset of precipitation, then re-heated to re-dissolve the product and finally allowed to cool slowly back to room temperature. The products were deposited in high purity as microcrystalline solids. As solids, they are air stable and also soluble in chloroform and THF, but not to any significant extent in hexane. The identity of each product was initially investigated by mass spectroscopy and N.M.R. spectroscopy. Elemental analysis (C, H, N) results are consistent with the formulations given in Figure 4.17.

The E.I. mass spectrum of each compound shows a molecular ion peak, confirming that the intended axial substitution has been effected. Each spectrum also shows a peak corresponding to loss of the axial group, producing the ion $[\text{In}(\text{tmtaa})]^+$. Peaks corresponding to the important metal containing ions are summarised in Table 4.9. More complete listings are given in Appendix 3 (pages 280 - 281).

Table 4.9 Summary of the E.I. Mass Spectra of Complexes of the Type $[\text{XIn}(\text{tmtaa})]$

Compound	m/z	Relative Intensity (%)	Assignment
[MeIn(tmtaa)]	472	80.3	M^+
	457	100	$[\text{M}-\text{Me}]^+$
[CpIn(tmtaa)]	522	5.9	M^+
	457	55.5	$[\text{M}-\text{Cp}]^+$
[(Me ₃ Si) ₂ NIn(tmtaa)]	617	1.4	M^+
	457	39.3	$[\text{M}-(\text{Me}_3\text{Si})_2\text{N}]^+$
[(Me ₃ Si)OIn(tmtaa)]	546	5.0	M^+
	457	6.5	$[\text{M}-\text{O}(\text{SiMe}_3)]^+$
[ClIn(tmtaa)]	492	89.5	$\text{M}^+ *$
	457	4.5	$[\text{M}-\text{Cl}]^+$

* M^+ based on ³⁵Cl

The high solubility of each product in CDCl_3 allowed both the ^1H and ^{13}C N.M.R. spectra to be recorded routinely. The ^1H N.M.R. data are summarised in the Experimental Section and the ^{13}C N.M.R. data are given in Table 4.10. All the spectra show the predicted signals (in the expected integral ratios for the ^1H spectra), confirming the presence of the axial substituents, and also suggest that the indium is bonded symmetrically to the four nitrogen atoms of the macrocycle.

Closer examination of the series of ^{13}C data shown in Table 4.10 {and those recorded for $[\text{EtIn}(\text{tmtaa})]$ presented earlier in Table 4.2} reveals that there is a clear progression in the shift of the methine-C, C-N carbon atoms of the pentanediiminato rings and the aromatic C-N carbon atoms, with the predicted (and experimentally determined) variation of the metal- N_4 plane distance in these complexes. Using this postulated relationship and the similarity of the spectrum of $[(\text{Me}_3\text{Si})_2\text{NIn}(\text{tmtaa})]$ to that of $[\text{CpIn}(\text{tmtaa})]$, it is suggested that the conformation of the ligand and the M- N_4 distance in the solid state structure of the former is very similar to that found for the latter.

Table 4.10 Summary of proton decoupled ^{13}C N.M.R. data (δ / p.p.m.) of indium-(III)-tmtaa compounds.

Compound	methyl-C	methine-C	aromatic		C-N	In-axial group
			C-H	C-N		
H_2tmtaa	20.81	97.84	122.79 123.00	138.00	158.84	-
$[\text{MeIn}(\text{tmtaa})]$	23.43	97.14	122.84 123.84	141.48	161.42	*
$[\text{CpIn}(\text{tmtaa})]$	23.87	97.55	123.20 124.00	140.61	162.13	109.84
$[\text{CpIn}(\text{tmtaa})]$ (CD_2Cl_2)	24.46	98.20	124.04 124.86	141.09	163.29	110.53
$[\text{CpIn}(\text{tmtaa})]$ ($\text{CD}_3\text{C}_6\text{D}_5$)	23.56	98.34	123.52 124.41	137.42	162.22	110.58
$[(\text{SiMe}_3)_2\text{NIn}(\text{tmtaa})]$	23.76	97.33	123.09 124.02	140.67	161.95	4.15
$[(\text{SiMe}_3)\text{OIn}(\text{tmtaa})]$	24.23	98.51	123.25 124.14	139.84	162.95	2.51
$[\text{ClIn}(\text{tmtaa})]$	24.33	98.97	123.71 124.06	139.26	163.55	-

Run as CDCl_3 solutions (unless otherwise stated) at 25°C . * not located.

CHAPTER 5

Preliminary Investigation of the Photoreactivity of Some Group 13 Metal–Alkyl Bonds

CHAPTER 5

Preliminary Investigation of the Photoreactivity of Some Group 13 Metal–Alkyl Bonds.

Introduction

Activation of the group 13 metal–alkyl bond is of interest in view of the known ability of alkyl–aluminium porphyrin derivatives to catalyse under photolysis the polymerisation of a range of organic functional unsaturated compounds, such as methacrylates and acrylates. Much of the development of this type of catalyst system has been carried out by Inoue and co-workers at the University of Tokyo.^{234,252} These initial studies were carried out using the methylaluminium–porphyrin [MeAl(TPP)] (TPP is the dianion of the tetraphenylporphyrin) and this compound was shown to initiate the polymerisation of alkyl methacrylate upon irradiation with visible light and give a polymer of narrow molecular weight distribution.^{234,253} The polymerisation was shown to be living with each aluminoporphyrin molecule producing a polymer chain.

Goedkin *et al* have postulated that the Al–C bond in the complex [EtAl(TPP)] is homolytically cleaved upon photolysis in benzene solution.²⁵⁴ In the presence of a spin trapping agent an intense E.S.R. spectrum was obtained and attributed to an overlap of two signals from an ethyl radical and an aluminium–containing radical.

The photoreactivity of the Al–C bond in the complex [EtAl(tmtaa)] has been similarly investigated.²⁵⁵ Ito and co-workers reported the intense E.S.R. signal obtained upon irradiation of a benzene solution of the complex in the presence of a spin trap, which has been assigned to the ethyl radical. The photoreactivity of this complex will be discussed in further detail later in this chapter.

The results of several investigations into the photochemical behaviour of the metal–alkyl bond in the alkyl–metal–amidinato compounds (discussed in Chapter 2) of the formula $[R_xM(\text{PhNCPhNPh})_{3-x}]$ ($x = 1, 2$) using E.S.R. spectroscopy are presented in this chapter.

E.S.R Experiments

Irradiation of methylaluminium-*N,N'*-diphenylbenzamidinato (I) in degassed benzene solution with visible light ($\lambda > 435\text{nm}$) in the presence of a ca. ten fold excess of the spin trapping agent 2,4,6-tri-*tert*-butylnitrosobenzene (TBN) produced the E.S.R. spectrum shown below in Figure 5.1(a).

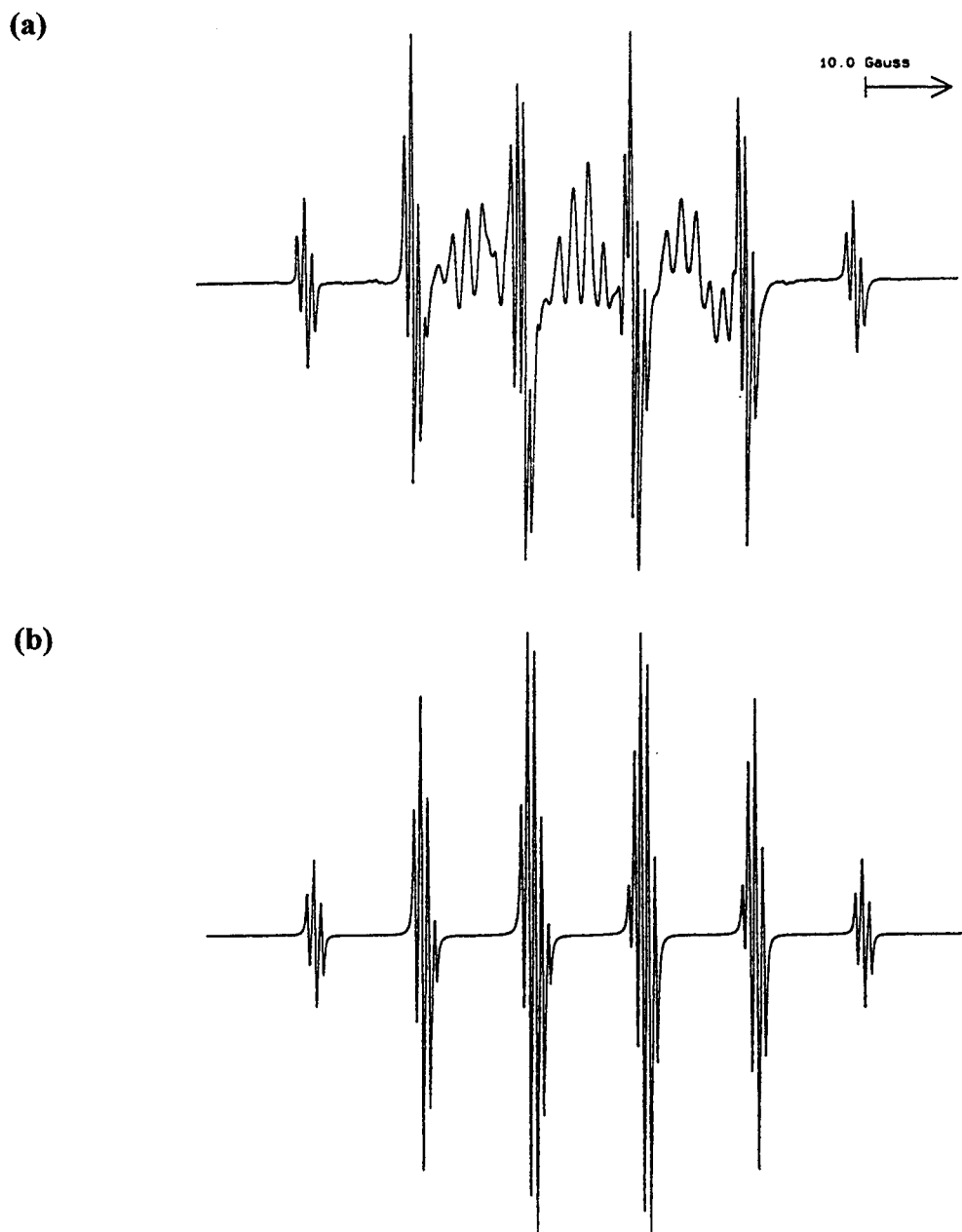


Figure 5.1 (a) E.S.R. spectrum of a benzene solution of $[\text{MeAl}(\text{PhNCPhNPh})_2]$ with added TBN upon irradiation ($\lambda > 435\text{nm}$). (b) E.S.R. simulation spectrum of TBN- CH_3 .

Although the spectrum appears rather complex, it can be assigned as an overlap of two signals from the nitroxyl methyl, $\text{RN}(\dot{\text{O}})\text{Me}$ (II) radical, and the anilino aluminium, $\text{R}\dot{\text{N}}\text{OAl}(\text{L})_2$ [$\text{R} = 2,4,6\text{-Bu}^t_3\text{C}_6\text{H}_2$; $\text{L} = (\text{PhNCPhNPh})$] (III) radical.

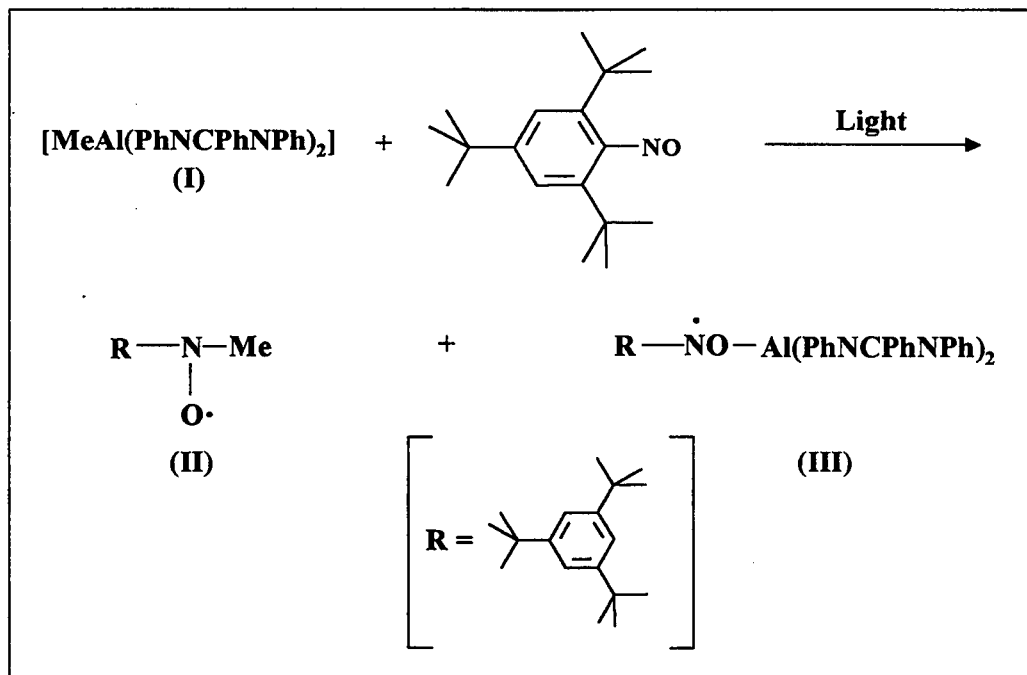


Figure 5.2 Spin trap adducts of TBN from irradiation of $[\text{MeAl}(\text{PhNCPhNPh})_2]$.

The former radical gives a triplet of quartets, from coupling of the unpaired electron with the nitrogen nucleus (spin = 1) of the spin trap, and the CH_3 protons, with hyperfine splitting constants of $a^{\text{N}} = 13.05$, $a^{\text{H}}(\text{CH}_3) = 12.30$ Gauss, and a g value of 2.0060. Extra fine splitting is also seen from the two protons on the aryl ring of the spin trap [$a^{\text{H}}(\text{meta}) = 0.80$ Gauss]. The signal assigned to the aluminium-containing radical produces a less well defined spectrum, but it is best described as a triplet of sextets (Al, spin = $\frac{5}{2}$). It is proposed that the aluminium is bound to the O atom of the spin trap to form the anilino radical, rather than the N atom of the spin trap, owing to the steric hindrance of the *tert*-butyl groups at the 2 and 6 positions. The spectrum clearly establishes the presence of a methyl-based radical. The simulated spectrum of the methyl-TBN radical is shown in Figure 5.1(b) and is based on parameters taken from the literature.²⁵⁶ This spectrum shows close agreement with the signal attributed to a methyl-TBN radical shown in Figure 5.1(a).

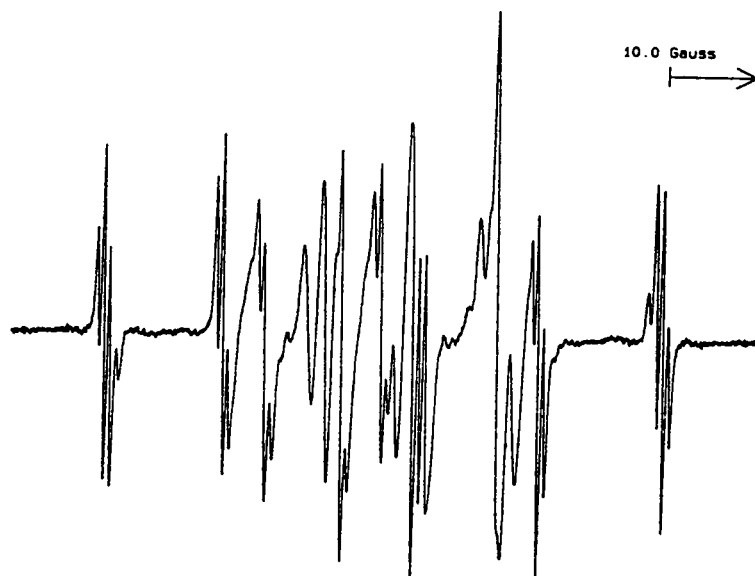
It should be noted that prior to irradiation of this sample, no E.S.R. signal was detected.

These results are related to those obtained previously for the ethylaluminium tetraaza-macrocyclic complex, [EtAl(tmtaa)]. Under similar experimental conditions, this complex produces an E.S.R. signal which is based on the ethyl radical adduct of TBN and a triplet of triplets is obtained. In the absence of a spin trap, no E.S.R. signal is obtained.

The co-ordination geometry around the metal in the amidinato complex [MeAl(PhNCPhNPh)₂] was shown in Chapter 2 to be similar to that found for [EtAl(tmtaa)], and in both cases the aluminium is bonded to four nitrogen atoms and one carbon atom. The most obvious structural difference between these derivatives is as follows. In the macrocyclic complex, all four nitrogen atoms are linked by a conjugated π -system of double bonds, whereas the amidinato complex comprises two separate delocalised ligand systems. However, as discussed in Chapter 4, complexation of the dianion [tmtaa]²⁻ does not lead to the delocalisation of charge throughout the ligand framework, but results in localisation of charge within the two pentanediiminate units. This fact can be used to further extend the similarity of the structural and electronic properties of these two types of ligand systems.

A similar study to that outlined for the methylaluminium amidinato complex was carried out using [EtGa(PhNCPhNPh)₂], which produced the spectrum shown in Figure 5.3(a). This spectrum indicates that the Ga-Et bond is cleaved under photolysis to yield the ethyl radical. This radical gives a triplet of triplets from coupling of the unpaired electron with the nitrogen nucleus of the spin trap, and the CH₂ protons, with hyperfine splitting constants of $a^N = 13.50$, $a^H(\text{CH}_3) = 18.00$ Gauss, and a g value of 2.0060. Extra fine splitting is again seen from the two aryl ring protons [$a^H(\text{meta}) = 0.85$ Gauss]. The gallium radical produces a complicated pattern owing to the presence of two gallium isotopes [⁶⁹Ga (60.5%), ⁷¹Ga (39.5%); both spin = $\frac{3}{2}$] which give two different hyperfine splitting constants. However, there is little doubt as to the presence of the ethyl based radical. The simulated spectrum of the ethyl-TBN radical is shown in Figure 5.3(b) and is based on parameters taken from the literature.²⁵⁶

(a)



(b)

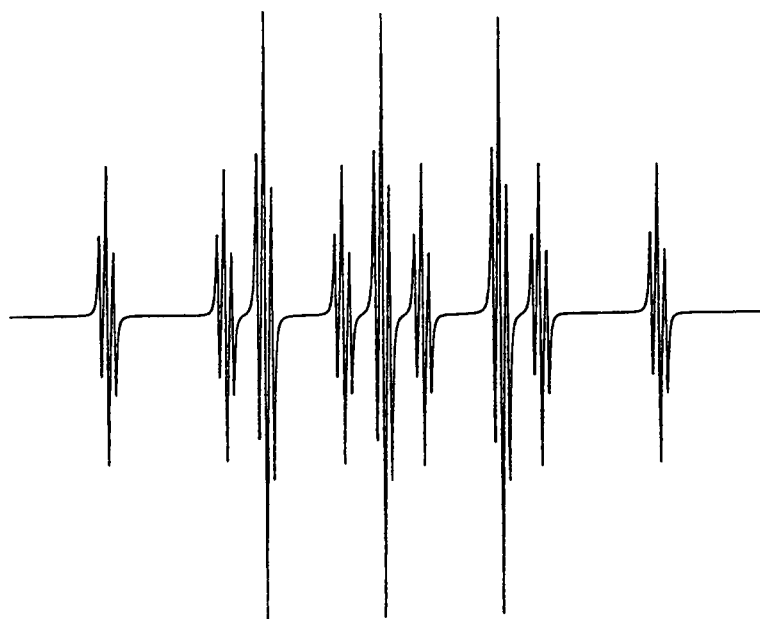


Figure 5.3 (a) E.S.R. spectrum of a benzene solution of $[\text{EtGa}(\text{PhNCPhNPh})_2]$ with added TBN upon irradiation ($\lambda > 435\text{nm}$). (b) E.S.R. simulation spectrum of $\text{TBN-C}_2\text{H}_5$.

The E.S.R. spectrum obtained from a benzene solution of $[\text{MeIn}(\text{PhNCPhNPh})_2]$ in the presence of TBN prior to any irradiation and kept at room temperature is shown in Figure 5.4(a). This shows a weak signal that is clearly mainly attributed to the spin trap adduct of the methyl radical. This indicates that the dissociation of the In–Me bond also proceeds thermally, albeit slowly, for this complex. When this sample was irradiated in the usual manner for 5 minutes, this E.S.R. signal intensified, but to a much smaller extent than that found for the aluminium analogue. The much greater relative intensity of the signal attributed to the methyl radical compared to that of the expected signal from an indium-containing radical suggests that the ease of adduct formation with the ethyl radical is greater than adduct formation with the indium radical. After standing at room temperature overnight, a new E.S.R. signal was observed and is shown in Figure 5.4(b). This spectrum still shows an intense signal attributed to a methyl radical, and additionally shows a series of broad, ill-defined signals between and superimposed on the former signal. These new signals are assigned an indium-containing radical. Such a radical would be expected to give rise to a triplet of decets (In, spin = $\frac{1}{2}$), although the lack of an obvious pattern to the new signals may suggest that a number of different indium-based radicals were present.

(a)



(b)

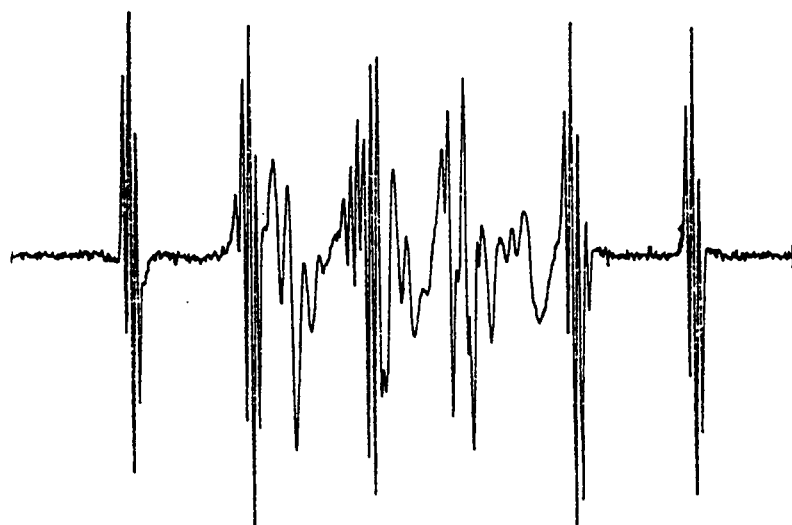


Figure 5.4 (a) E.S.R. spectrum of a benzene solution of $[\text{MeIn}(\text{PhNCPPhNPh})_2]$ with added TBN. (b) E.S.R. spectrum obtained after standing at room temperature overnight.

The dialkylmetal–amidinato complexes $[\text{Me}_2\text{Al}(\text{PhNCPhNPh})]$ and $[\text{R}_2\text{Ga}(\text{PhNCPhNPh})]$ ($\text{R} = \text{Me}, \text{Et}$) were shown to behave in a similar manner to the analogous bis–amidinato complexes. These complexes produce spectra that are identical to those obtained from the bis–amidinato derivatives.

A control experiment was performed whereby the reaction was repeated under the same conditions without the addition of the alkyl–metal derivative. No E.S.R. signal was detected. Only after prolonged irradiation for 24 hours were weak signals detected resulting from decomposition of the spin trap agent.

Although the above results indicate that homolytic cleavage of the M–R bond can be achieved by visible light, irradiation of the complexes $[\text{MeM}(\text{PhNCPhNPh})_2]$ ($\text{M} = \text{Al}, \text{Ga}, \text{In}$) under the same conditions except for the absence of the spin trap TBN produced no E.S.R. signal. This is presumably because of the rapid recombination of any radicals produced.

Kadish *et al*²⁵⁷ have investigated the photoreactivity of gallium and indium porphyrins of the type $[(\text{R})\text{M}(\text{P})]$ (e.g. $\text{R} = \text{methyl}, \text{ethyl}$; $\text{M} = \text{Ga}, \text{In}$; $\text{P} = \text{TPP}$) in THF (without the addition of a spin trap), to establish the nature of the photochemical process and products. This work suggests that the photochemical cleavage of the metal alkyl bond in these systems produces zwitterionic $\text{M}^+(\text{P})^-$ species from an intramolecular electron transfer.



The reported homolysis of the $\text{Co}^{\text{III}}\text{--C}$ bond in the analogous cobalt complex results in the reduction of the metal centre and generates $[(\text{P})\text{Co}^{\text{II}}]$ species.^{258,259}



Although the preliminary experiments presented in this chapter give little evidence regarding the nature of the photochemical behaviour of the group 13 metal amidinato complexes in the absence of a spin trap, it is unlikely that the latter type of metal species could be a photoproduct. The zwitterionic formulation would appear to be a more likely possibility for these complexes, particularly in electron donating solvents such as THF. However, it is also likely that this type of zwitterionic species may not be stable in solvents with low dielectric constants such as benzene.

In summary, the results from the E.S.R. experiments demonstrate that photochemical cleavage of the metal-alkyl bond in the monoalkyl- and dialkyl-aluminium, gallium and indium derivatives of *N,N'*-diphenylbenzamidinato can be achieved and the alkyl radicals produced can be successfully trapped using a spin trapping agent. The metal-alkyl bond in these systems appears to possess similar photochemical properties to those shown by the metal-alkyl bond in the related macrocyclic derivatives, namely with the porphyrin and *tmtaa* ligands. In view of these similarities, it would be of significant interest to establish whether the amidinato systems show utility for the polymerisation of organic monomers, thereby forming a direct parallel to the work carried out in this area using the class of macrocyclic ligands.

CHAPTER 6

Experimental

CHAPTER 6

Experimental

General Experimental

The air-reactive compounds were handled using a conventional Schlenk or high-vacuum line, and in a dry nitrogen-filled Miller-Howe glove box fitted with a gas circulating system. Glassware was oven dried or heated under vacuum before use.

Solvents were dried and distilled under dry nitrogen prior to use. Benzene, toluene, diethyl ether and tetrahydrofuran were dried using potassium or sodium, and dichloromethane, chloroform and hexane were dried using calcium hydride. Hexane was pre-dried using sodium wire. N.M.R. solvents were dried over 4Å molecular sieves before use.

Routine ^1H and ^{13}C N.M.R. spectra were recorded using a Bruker Associates ACF250 (250MHz) instrument connected to a personal computer running WIN-NMR. Additional ^1H , ^{13}C , and ^{19}F N.M.R. spectra were recorded using a Bruker Associates ACP400 (400MHz) spectrometer. ^1H and ^{13}C N.M.R. chemical shifts are quoted relative to tetramethylsilane, with upfield shifts being assigned negative values. ^{19}F N.M.R. chemical shifts are quoted relative to an external standard (CFCl_3). N.M.R. frequencies (MHz) used were as follows: ^1H , 250.136 (ACF250), 400.134 (ACP400), ^{13}C , 62.896 (ACF250), 100.614 (ACP400), ^{19}F , 376.503 (ACP400). Unless otherwise stated, all ^1H and ^{13}C N.M.R. data quoted in this thesis were obtained using the ACF250 instrument.

Infra-red spectra were recorded from Nujol mulls using either a Perkin Elmer 580B ($4000\text{--}200\text{cm}^{-1}$), or Perkin Elmer 1720X ($4000\text{--}400\text{cm}^{-1}$) spectrophotometer, using caesium iodide plates. Nujol was dried over sodium wire and stored in a glove box.

E.S.R. measurements were recorded using a Bruker ER200tt instrument operating at 9.77 GHz, with 100kHz field modulation. Calibration of g values was based on 1,1-diphenyl-2-picrylhydrazyl (dpph, $g=2.0036$) and potassium nitrosyldisulphonate (Fremy's salt, $g=2.0070$). Photochemical reactions were carried out in a quartz tube using a 250W medium-pressure mercury arc lamp. The spin trapping agent 2,4,6-tri-*tert*-

butylnitrosobenzene (TBN) was purchased from Aldrich Chemical Company. The E.S.R spectrum simulation program was obtained from Dr. Adrian Whitwood of the Department of Chemistry, University of York.

Elemental analysis was carried out by the Analytical Department at the Associated Octel Company (A.O.C). Carbon, hydrogen and nitrogen analytical data were obtained using a Perkin Elmer 2400 elemental analyser. The thermogravimetric analysis measurements were made at A.O.C. using a Stanton Redcroft STA 1000 instrument.

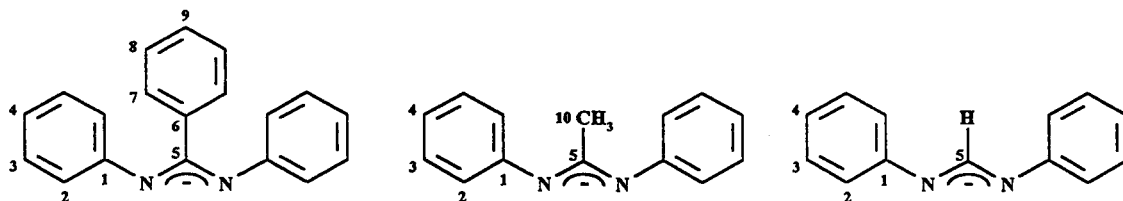
Energy dispersive X-ray measurements were carried out at the Department of Physics, University of Warwick and were obtained using a 5keV electron beam with a Cambridge S250 instrument with a link analytical X-ray system using an LZ5 Windowless detector.

Trimethylaluminium was obtained from Aldrich and used as a hexane (2.0M) solution. Trimethylgallium (b.p. 56°C) was supplied from Johnson Matthey, and Strem, and stored in a metal cylinder. Manipulations were carried out using a high-vacuum line. Triethylgallium (b.p. 143°C), trimethylindium (m.p. 88°C) and triethylindium (b.p. 184°C) were supplied by Strem. These reagents were kept in metal containers and handled in the glove box. Anhydrous indium (III) chloride was obtained from Aldrich.

EXPERIMENTAL (Chapter 2)

N,N'-Diphenylbenzamidine was obtained from Lancaster Synthesis. *N,N'*-Diphenylformamidine was purchased from Aldrich. All other amidine ligands were supplied by our collaborating body, A.O.C. (via Aldrich). The amidine ligands were purified by sublimation under vacuum before use. They were handled in the glove box and their purity checked by elemental analysis (C, H, N) and ^1H and ^{13}C N.M.R. before use. 4-*Tert*-butylpyridine and *N,N,N',N'*-tetramethylethylenediamine were supplied by Aldrich and both were dried using 4Å molecular sieves prior to use.

The numbering schemes used in the assignment of the ^1H and ^{13}C N.M.R. data obtained for the *N,N'*-diphenylbenzamidinato, *N,N'*-diphenylacetamidinato and *N,N'*-diphenylformamidinato derivatives are shown below:



The following dimethylaluminium-amidinato complexes, of formula $[\text{Me}_2\text{Al}(\text{L})]$ (L =amidinato ligand), were all prepared by the same general method. The procedure for the synthesis of dimethylaluminium-*N,N'*-diphenylbenzamidinato is given as a standard preparative method.

Preparation of Dimethylaluminium-*N,N'*-diphenylbenzamidinato

The free ligand, *N,N'*-diphenylbenzamidine (0.85g, 3.12mmol) was placed in a Schlenk tube charged with a magnetic stirring bar, and partially dissolved in hexane (40cm³). This suspension was chilled in a liquid nitrogen bath and a slight excess of a solution of trimethylaluminium in hexanes (1.70cm³, 3.40mmol) was added via a syringe through a Suba-seal. The mixture was allowed to warm to room temperature with stirring and vented to allow the methane evolved to escape. The pale green suspension

which was formed initially gave a pale yellow solution after stirring at room temperature for 1 hour. The solution was concentrated under reduced pressure to a volume of ca. 20cm³ and the product was crystallised by cooling the reaction liquor to -35°C for 2 hours. The pale green solid was isolated by filtration and dried *in vacuo* for 2 hours. Yield: 0.74g (72%). Melting point (sealed tube): 110.0–110.5°C. Analysis, calculated for C₂₁H₂₁N₂Al (M.W. 328.39): C, 76.81; H, 6.45; N, 8.53%. Found: C, 76.43; H, 6.39; N, 8.52%. ¹H N.M.R. (CDCl₃): δ/p.p.m. -0.48 (s, 6H, AlCH₃), 6.70 (d, 4H, H-2), 6.97 (t, 2H, H-4), 7.13 (t, 4H, H-3), 7.21-7.34 (m, 4H, H-7, H-8) 7.40 (t, 1H, H-9). The product can be sublimed rapidly under vacuum (0.003mm Hg) at 103°C.

Preparation of Dimethylaluminium-N,N'-di(4-chlorophenyl)benzamidinato

The preparation used was similar to that used for the dimethylaluminium-N,N'-diphenylbenzamidinato complex. The product was crystallised from hexane as pale green needle-shaped irregular crystals. Yield: 0.45g (71%). Analysis, calculated for C₂₁H₁₉N₂AlCl₂ (M.W. 397.28): C, 63.49; H, 4.82; N, 7.05%. Found: C, 63.79; H, 4.55; N, 6.84%. ¹H N.M.R. (CDCl₃): δ/p.p.m. -0.53 (s, 6H, AlCH₃), 6.59 (d, 4H, H-3), 7.07 (d, 4H, H-2), 7.18 (d, 2H, H-7), 7.32 (t, 2H, H-8), 7.42 (t, 1H, H-9).

Preparation of Dimethylaluminium-N,N'-diphenylacetamidinato

The product was crystallised from hexane as a colourless microcrystalline solid. Yield: 0.86g (77%). Analysis, calculated for C₁₆H₁₉N₂Al (M.W. 266.32): C, 72.16; H, 7.19; N, 10.52%. Found: C, 71.41; H, 7.16; N, 10.46%. ¹H N.M.R. (CDCl₃): δ/p.p.m. -0.54 (s, 6H, AlCH₃), 2.21 (s, 3H, CH₃), 7.02 (d, 4H, H-2), 7.12 (t, 2H, H-4), 7.35 (t, 4H, H-3).

Preparation of Dimethylaluminium-N,N'-di(p-chlorophenyl)acetamidinato

Crystallisation from hexane yielded a colourless microcrystalline solid. Yield: 0.54g (60%). Analysis, calculated for C₁₆H₁₇N₂AlCl₂ (M.W. 335.21): C, 57.33; H, 5.11;

N, 8.36%. Found: C, 56.75; H, 5.18; N, 8.34%. ^1H N.M.R. (CDCl_3): $\delta/\text{p.p.m.}$ -0.56 (s, 6H, AlCH_3), 2.16 (s, 3H, CH_3), 6.92 (d, 4H, ArH), 7.29 (d, 4H, ArH).

Preparation of Dimethylaluminium-N,N'-diphenylformamidinato

The product was crystallised from hexane as a colourless powder. Yield: 0.44g (56%). Analysis, calculated for $\text{C}_{15}\text{H}_{17}\text{N}_2\text{Al}$ (M.W. 252.29): C, 71.41; H, 6.79; N, 11.10%. Found: C, 70.82; H, 6.79; N, 10.77%. ^1H N.M.R. (CDCl_3): $\delta/\text{p.p.m.}$ -1.02 (s, 6H, AlCH_3), 6.23 (d, 4H, H-2), 6.68-6.76 (m, 6H, H-3, H-4), 7.36 (s, 1H, CH).

The following dimethylgallium-amidinato complexes, of the general formula $[\text{Me}_2\text{Ga}(\text{L})]$ (L=amidinato ligand) were all prepared by the same method. The procedure for the synthesis of dimethylgallium-N,N'-diphenylbenzamidinato is given as a standard preparative method.

Preparation of Dimethylgallium-N,N'-diphenylbenzamidinato

All preparations involving the handling of trimethylgallium were carried out using a high-vacuum line. Trimethylgallium (0.44g, 3.83mmol) was condensed into a weighed detachable cold finger device held at -196°C . N,N'-diphenylbenzamidino (1.0g, 3.67mmol) was partially dissolved in hexane (30cm^3) and the mixture was degassed by repeat freeze-pump-thaw cycles. The slight excess of trimethylgallium was condensed onto the solution at -196°C and the mixture allowed to warm to room temperature, over which time, methane was evolved. The approximate volume of methane evolved was measured using a calibrated portion of the vacuum-line. This volume was shown to be 1 mole equivalent. After stirring at room temperature for 2 hours a clear pale yellow solution was obtained. This solution was reduced in volume to ca. 15cm^3 by distillation under reduced pressure, and cooled to -35°C overnight. A crop of yellow crystals were obtained, and these were isolated by filtration and dried *in vacuo* for 1 hour. The product sublimes rapidly under vacuum (0.005mm Hg) at 120°C . Yield: 1.0g (72%). Analysis, calculated for $\text{C}_{21}\text{H}_{21}\text{N}_2\text{Ga}$ (M.W. 371.13): C, 67.95; H, 5.70; N,

7.55%. Found: C, 67.96; H, 5.70; N, 7.55%. ^1H N.M.R. (CDCl_3): δ /p.p.m. 0.01 (s, 6H, GaCH_3), 6.67 (d, 4H, H-2), 6.93 (t, 2H, H-4), 7.10 (d, 4H, H-3), 7.31-7.23 (m, 4H, H-7, H-8), 7.36 (t, 1H, H-9).

Preparation of Dimethylgallium-N,N'-di(4-chlorophenyl)benzamidinato

N,N'-Di(4-chlorophenyl)benzamidine (0.95g, 2.79mmol) was reacted with Me_3Ga (0.33g, 2.93mmol) in hexane (30cm^3). The product is a yellow solid. Yield: 1.14g (93%). Analysis, calculated for $\text{C}_{21}\text{H}_{19}\text{N}_2\text{Cl}_2\text{Ga}$ (M.W. 440.02): C, 57.32; H, 4.35; N, 6.37%. Found: C, 57.37; H, 4.61; N, 6.17%. ^1H N.M.R. (CDCl_3): δ /p.p.m. -0.01 (s, 6H, GaCH_3), 6.53 (d, 4H, H-2), 7.02 (d, 4H, H-3), 7.18 (d, 2H, H-7), 7.29 (t, 2H, H-8), 7.38 (t, 1H, H-9).

Preparation of Dimethylgallium-N,N'-di(4-nitrophenyl)benzamidinato

N,N'-Di(4-nitrophenyl)benzamidine (0.90g, 2.48mmol) was reacted with Me_3Ga (0.30g, 2.61mmol) in hexane (40cm^3). The product is a bright yellow solid. Yield: 1.02g (89%). Analysis, calculated for $\text{C}_{21}\text{H}_{19}\text{N}_4\text{GaO}_4$ (M.W. 461.13): C, 54.70; H, 4.15; N, 12.15%. Found: C, 54.78; H, 4.07; N, 11.99%. ^1H N.M.R. (CDCl_3): δ /p.p.m. 0.07 (s, 6H, GaCH_3), 6.65 (d, 4H, ArH), 7.22 (d, 2H, ArH), 7.39 (t, 2H, ArH), 7.50 (t, 1H, ArH), 7.99 (d, 4H, ArH).

Preparation of Dimethylgallium-N,N'-diphenylacetamidinato

N,N'-Diphenylacetamidine (0.80g, 3.81mmol) was reacted with Me_3Ga (0.46g, 4.0mmol) in hexane (30cm^3). The product is a colourless solid. Yield: 1.08g (92%). Analysis, calculated for $\text{C}_{16}\text{H}_{19}\text{N}_2\text{Ga}$ (M.W. 309.06): C, 62.18; H, 6.20; N, 9.06%. Found: C, 62.43; H, 6.02; N, 8.92%. ^1H N.M.R. (CDCl_3): δ /p.p.m. 0.03 (s, 6H, GaCH_3), 2.20, (s, 3H, CH_3), 7.01 (d, 4H, H-2), 7.11 (t, 2H, H-4), 7.36 (t, 4H, H-3).

Preparation of Dimethylgallium-N,N'-diphenylformamidinato

N,N'-Diphenylformamidine (0.31g, 1.58mmol) was reacted with Me₃Ga (0.19g, 1.66mmol) in hexane (40cm³). The product is a colourless solid. Yield: 0.38g (82%). Analysis, calculated for C₁₅H₁₇N₂Ga (M.W. 295.03): C, 61.07; H, 5.81; N, 9.50%. Found: 60.56; H, 5.76; N, 9.35%. ¹H N.M.R. (CDCl₃): δ/p.p.m. 0.03 (s, 6H, GaCH₃), 6.97-7.08 (m, 6H, H-2, H-4), 7.30 (t, 4H, H-3), 8.75 (s, 1H, CH).

Preparation of Dimethylgallium-N,N'-di(3,4-dichlorophenyl)formamidinato

N,N'-Di(3,4-dichlorophenyl)formamidine (0.78g, 2.34mmol) was reacted with Me₃Ga (0.30g, 2.62mmol) in hexane (30cm³). The product is a pale green solid. Yield: 0.74g (73%). Analysis, calculated for C₁₅H₁₃N₂Cl₄Ga (M.W. 432.81): C, 41.63; H, 3.03; N, 6.47%. Found: C, 41.79; H, 3.18; N, 6.15%. ¹H N.M.R. (CDCl₃): δ/p.p.m. 0.03 (s, 6H, GaCH₃), 6.80 (dd, J 8.5, 2.5Hz, ArH), 7.05 (d, J 2.5Hz, 2H, ArH), 7.32 (d, 2H, ArH), 8.60 (s, 1H, CH).

The following dialkylmetal-amidinato complexes, of the general formula [R₂M(L)] (L=amidinato; M=Ga, R=Et; M=In, R=Me, Et) were all prepared by the same general method. The procedure for the synthesis of diethylgallium-N,N'-diphenylbenzamidinato is given as a standard preparative method.

Preparation of Diethylgallium-N,N'-diphenylbenzamidinato

N,N'-Diphenylbenzamidine (0.71g, 2.60mmol) was added slowly to a stirred solution of a slight excess of Et₃Ga (0.41g, 2.62mmol) in hexane (30cm³) at room temperature in the glove box. The reaction proceeded immediately with the evolution of bubbles of gas. After stirring the reaction mixture for 2 hours at room temperature, the resulting pale yellow solution was concentrated under reduced pressure to a volume of ca. 15cm³ and cooled to -35°C for 12 hours. This produced pale yellow, irregular-shaped crystals which were collected by filtration and dried *in vacuo*. Yield: 0.71g (68%). Analysis, calculated for C₂₃H₂₅N₂Ga (M.W. 399.18): C, 69.20; H, 6.31; N,

7.02%. Found: C, 69.39; H, 6.47; N, 6.98%. ^1H N.M.R. (CDCl_3): δ /p.p.m. 0.76 (q, 4H, GaCH_2CH_3), 1.26 (t, 6H, GaCH_2CH_3), 6.67 (d, 4H, H-2), 6.93 (t, 2H, H-4), 7.12 (t, 4H, H-3), 7.25-7.40 (m, 5H, H-7, H-8, H-9).

Preparation of Dimethylindium-N,N'-diphenylbenzamidinato

N,N'-Diphenylbenzamidine (1.58g, 5.80mmol) was added slowly to a solution of Me_3In (1.17g, 5.81mmol) in hexane (40cm^3) at room temperature. An immediate reaction occurred as indicated by the evolution of gas bubbles, and a pale yellow solution was produced. After stirring for 2 hours the solution was concentrated to a volume of ca. 20cm^3 and cooled to -35°C . This caused the precipitation of a colourless microcrystalline solid that was isolated by filtration and dried *in vacuo*. Yield: 1.62g (67%). The complex sublimed at 107°C and 0.003mm Hg. Melting point (sealed tube): 102.0 - 103.5°C . Analysis, calculated for $\text{C}_{21}\text{H}_{21}\text{N}_2\text{In}$ (M.W. 416.23): C, 60.60; H, 5.09; N, 6.73%. Found: C, 60.59; H, 4.96; N, 6.83%. ^1H N.M.R. (CDCl_3): δ /p.p.m. 0.18 (s, 6H, InCH_3), 6.63 (d, 4H, H-2), 6.87 (t, 2H, H-4), 7.07 (t, 4H, H-3), 7.13-7.22 (m, 4H, H-7, H-8), 7.26 (t, 1H, H-9).

Crystals suitable for the X-ray structural analysis were grown from a toluene solution of the product which was cooled to -35°C .

Preparation of Diethylindium-N,N'-diphenylbenzamidinato

N,N'-Diphenylbenzamidine (0.91g, 3.34mmol) was reacted with Et_3In (0.68g, 3.36mmol) in hexane (40cm^3). Cooling of the hexane solution to -35°C overnight gave pale yellow, irregularly-shaped crystals. Yield: 0.85g (57%). Analysis, calculated for $\text{C}_{23}\text{H}_{25}\text{N}_2\text{In}$ (M.W. 444.28): C, 62.18; H, 5.67; N, 6.31%. Found: C, 61.80; H, 5.72; N, 6.29%. ^1H N.M.R. (CDCl_3): δ /p.p.m. 0.98 (q, 4H, InCH_2CH_3), 1.45 (t, 6H, InCH_2CH_3), 6.63 (d, 4H, H-2), 6.86 (t, 2H, H-4), 7.03-7.29 (m, 9H, H-3, H-7, H-8, H-9).

Preparation of Diethylindium-N,N'-di(4-chlorophenyl)benzamidinato

N,N'-Di-(4-chlorophenyl)benzamidine (0.72g, 2.11mmol) was reacted with Et₃In (0.43g, 2.13mmol) in hexane (30cm³). Cooling of the hexane solution to -35°C overnight gave pale yellow-green, needle-shaped crystals. Yield: 0.69g (64%). The complex sublimed at 115°C and 0.01mm Hg. Melting point (sealed tube): 150.0–152.0°C. Analysis, calculated for C₂₃H₂₃N₂Cl₂In (M.W. 513.18): C, 53.83; H, 4.52; N, 5.46%. Found: 53.87; H, 4.57; N, 5.50%. ¹H N.M.R. (CDCl₃): δ/p.p.m. 0.98 (q, 4H, InCH₂CH₃), 1.41 (t, 6H, InCH₂CH₃), 6.52 (d, 4H, H-2), 7.01 (d, 4H, H-3), 7.10 (d, 2H, H-7), 7.19-7.33 (m, 3H, H-8, H-9).

Preparation of Diethylindium-N,N'-diphenylacetamidinato

N,N'-Diphenylacetamidine (0.82g, 3.90mmol) was reacted with Et₃In (0.79g, 3.91mmol) in hexane (40cm³). The product is a colourless solid. Yield: 1.02g (68%). Analysis, calculated for C₁₈H₂₃N₂In (M.W. 382.21): C, 56.56; H, 6.07; N, 7.33%. Found: C, 56.79; H, 5.79; N, 6.87%. ¹H N.M.R. (CDCl₃): δ/p.p.m. 0.92 (q, 4H, InCH₂CH₃), 1.40 (t, 6H, InCH₂CH₃), 2.15, (s, 3H, CH₃), 6.99 (d, 4H, H-2), 7.15 (t, 2H, H-4), 7.30 (t, 4H, H-3).

Preparation of Diethylindium-N,N'-diphenylformamidinato

N,N'-Diphenylformamidine (0.75g, 3.82mmol) was reacted with Et₃In (0.78g, 3.86mmol) in hexane (30cm³). The product is a yellow microcrystalline solid. Yield: 0.76g (54%). Analysis, calculated for C₁₇H₂₁N₂In (M.W. 368.19): C, 55.46; H, 5.75; N, 7.61%. Found: C, 54.46; H, 5.81; N, 7.24%. ¹H N.M.R. (CDCl₃): δ/p.p.m. 1.03 (q, 4H, InCH₂CH₃), 1.39 (t, 6H, InCH₂CH₃), 7.01 (d, 4H, H-2), 7.06 (t, 2H, H-4), 7.34 (t, 4H, H-3), 9.07 (s, 1H, CH).

Preparation of the adduct Dimethylgallium-(N,N'-diphenylbenzamidinato).(4-tert-butyl-pyridine)

Me₃Ga (0.45g, 3.92mmol) was condensed onto a degassed solution of 4-tert-butyl-pyridine (0.53g, 3.92mmol) in hexane (30cm³) held at -196°C. The reaction mixture was allowed to warm to room temperature and stirred for 1 hour to give a clear solution. This was pumped to dryness *in vacuo* to give a colourless microcrystalline solid. Analysis, calculated for C₁₂H₂₂NGa (M.W. 250.03): C, 57.65; H, 8.87; N, 5.60%. Found: C, 58.09; H, 8.46; N, 5.73%. ¹H N.M.R. (CDCl₃): δ/p.p.m. -0.43 (s, 9H, GaCH₃), 1.35 (s, 9H, C(CH₃)₃), 7.47 (d, 2H, ArH), 8.41 (d, 2H, ArH).

Me₃Ga.(4-Bu^t-pyridine) (0.55g, 2.20mmol) was dissolved in hexane (30cm³) and to this stirred solution was added N,N'-diphenylbenzamidine (0.60g, 2.20mmol) at room temperature. After 24 hours, the pale green suspension was collected by filtration and dried *in vacuo*. Yield: 0.62g (56%). Analysis, calculated for C₃₀H₃₄N₃Ga (M.W. 506.34): C, 71.16; H, 8.30; N, 6.77%. Found: C, 72.15; H, 6.53; N, 8.43%. ¹H N.M.R. (CDCl₃): δ/p.p.m. 0.03 (s, 6H, GaCH₃), 1.32 (s, 9H, C(CH₃)₃), 6.64 (d, 4H, ArH), 6.86-7.11 (m, 6H, ArH), 7.24-7.30 (m, 7H, ArH), 8.52 (d, 2H, ArH).

Removal of a small amount of solvent from the filtrate followed by cooling in a freezer at -35°C for 24 hours gave crystals suitable for single crystal X-ray diffraction.

A similar product to that obtained above was prepared by the direct addition of 4-Bu^t-pyridine (0.35g, 2.59mmol) to a hexane solution (30cm³) of [Me₂Ga(PhNCPPhNPh)] (0.96g, 2.59mmol). This product gave elemental analysis and ¹H and ¹³C N.M.R. data consistent with that found above.

Preparation of the adduct Diethylindium-(N,N'-diphenylbenzamidinato).(4-tert-butyl-pyridine)

4-Tert-butyl-pyridine (0.35g, 2.59mmol) was added directly to a stirred solution of [Et₂In(PhNCPPhNPh)] (1.15g, 2.59mmol) in hexane (30cm³). After 1 hour some solvent was removed (ca. 15cm³) and the clear pale green solution was placed in the freezer (-35°C) from which a colourless microcrystalline solid was deposited. This was collected by filtration, washed with hexane (2 x 10cm³) and dried *in vacuo*. Yield 0.57g

(38%). Analysis, calculated for $C_{32}H_{38}N_3In$ (M.W. 579.49): C, 66.33; H, 6.61; N, 7.25%. Found: 66.86; H, 6.18; N, 6.95%. 1H N.M.R. ($CDCl_3$): 0.91 (q, 4H, $InCH_2CH_3$), 1.30 (s, 9H, $C(CH_3)_3$), 1.41 (t, 6H, $InCH_2CH_3$), 6.53 (d, 4H, ArH), 6.77 (t, 2H, ArH), 6.93 (t, 4H, ArH), 7.07-7.19 (m, 5H, ArH), 7.22 (d, 2H, ArH), 8.35 (d, 2H, ArH).

Preparation of Methylaluminium-bis(N,N' -diphenylbenzamidinato)

N,N' -Diphenylbenzamidine (1.18g, 4.33mmol) was partially dissolved in hexane ($40cm^3$) and the mixture chilled in a liquid nitrogen bath. A hexane solution of Me_3Al ($1.08cm^3$, 2.16mmol) was added to the mixture via a syringe through a Suba-seal. The reaction vessel was allowed to warm to room temperature and vented to allow escape of the evolved methane. After stirring at room temperature for 1 hour, the white suspension was cooled on an ice bath at $0^\circ C$ for 1 hour, separated by filtration and dried *in vacuo*. Removal of a small amount of solvent from the filtrate followed by cooling in a freezer at $-35^\circ C$ gave large plate-like crystals. Overall yield: 0.95g (75%). Analysis, calculated for $C_{39}H_{33}N_4Al$ (M.W. 584.70): C, 80.11; H, 5.69; N, 9.58. Found: C, 80.13; H, 5.90; N, 9.55. 1H N.M.R. ($CDCl_3$): $\delta/p.p.m.$ -0.36 (s, 3H, $AlCH_3$), 6.53 (d, 8H, H-2), 6.79-6.96 (m, 12H, H-3, H-4), 7.10-7.21, (m, 8H, H-7, H-8), 7.25 (t, 2H, H-9).

Colourless, block-shaped crystals of this complex, suitable for the X-ray diffraction study, were grown from a chloroform solution.

Preparation of Methylaluminium-bis(N,N' -diphenylacetamidinato)

This complex was prepared by the same procedure as used for methylaluminium-bis(N,N' -diphenylbenzamidinato). A hexane solution of Me_3Al ($1.38cm^3$, 2.76mmol) was added to a suspension of N,N' -diphenylacetamidine (1.16g, 5.52mmol) in hexane ($40cm^3$). The product is a colourless crystalline solid. Yield: 0.87g (69%). Analysis, calculated for $C_{29}H_{29}N_4Al$ (M.W. 460.56): C, 75.63; H, 6.35; N, 12.16%. Found: C, 75.89; H, 6.43; N, 12.10%. 1H N.M.R. ($CDCl_3$): $\delta/p.p.m.$ -0.26 (s, 3H, $AlCH_3$), 2.05 (s, 6H, CH_3), 6.80 (d, 8H, H-2), 6.96 (t, 4H, H-4), 7.11 (t, 8H, H-3).

Preparation of Methylgallium-bis(N,N'-diphenylbenzamidinato)

N,N'-Diphenylbenzamidine (2.28g, 8.4mmol) was partially dissolved in hexane (30cm³), and Me₃Ga (0.49g, 4.25mmol) was condensed onto the degassed mixture under vacuum at -196°C. The stirred solution was allowed to warm to room temperature, over which time one mole equivalent of methane was produced. The pale yellow solution was heated under reflux for 12 hours and a further mole of methane was evolved. The pale yellow suspension was placed at -35°C for 24 hours. The pale yellow solid was isolated by filtration and recrystallised from chloroform, producing yellow, block-shaped crystals suitable for single crystal X-ray analysis. Yield: 1.8g (68%). Analysis, calculated for C₃₉H₃₃N₄Ga (M.W. 627.44): C, 74.66; H, 5.30; N, 8.93%. Found: C, 74.62; H, 5.35; N, 8.93%. ¹H N.M.R. (CDCl₃): 0.28 (s, 3H, GaCH₃), 6.57 (d, 8H, H-2), 6.83 (t, 4H, H-4), 6.95 (t, 8H, H-3), 7.07-7.15 (m, 8H, H-7, H-8), 7.19 (t, 2H, H-9).

Preparation of Ethylgallium-bis(N,N'-diphenylacetamidinato)

N,N'-Diphenylacetamidine (0.90g, 4.28mmol) was added slowly to a stirred solution of Et₃Ga (0.34g, 2.16mmol) in hexane (40cm³) at room temperature, whereupon gas was immediately evolved and the reaction mixture was left to stir for 1 hour. After this time the white suspension was heated at 70°C for 12 hours and allowed to cool to room temperature. The colourless solution was concentrated under reduced pressure until the onset of the precipitation of a white microcrystalline solid occurred. The mixture was re-heated to re-dissolve the product. On allowing to cool slowly to room temperature, large, colourless, block-shaped X-ray diffraction quality crystals were deposited and these were isolated by filtration and dried *in vacuo*. Yield: 0.82g (74%). Analysis, calculated for C₃₀H₃₁N₄Ga (M.W. 517.32): C, 69.65; H, 6.04; N, 10.83%. Found: C, 67.99; H, 6.01; N, 10.58%. ¹H N.M.R. (CDCl₃): δ/p.p.m. 1.12 (q, 2H, GaCH₂CH₃), 1.42 (t, 3H, GaCH₂CH₃), 2.08 (s, 6H, CH₃), 6.82 (d, 8H, H-2), 7.00 (t, 4H, H-4), 7.17 (t, 8H, H-3).

Preparation of Methylindium-bis(N,N'-diphenylbenzamidinato)

This complex was prepared using a similar procedure to that used for the ethylgallium-bis(N,N'-diphenylacetamidinato) complex above. N,N'-Diphenylbenzamidine (1.50g, 5.51mmol) was added a solution of Me₃In (0.45g, 2.82mmol) in hexane (30cm³) at room temperature. After heating at 80°C for 4 hours, a white suspension was obtained, which was isolated by filtration and dried *in vacuo*. Yield: 1.26g (68%). Analysis, calculated for C₃₉H₃₃N₄In (M.W. 672.54): C, 69.65; H, 4.95; N, 8.33%. Found: C, 69.87; H, 5.06; N, 8.18%. ¹H N.M.R. (CDCl₃): δ/p.p.m. 0.38 (s, 3H, InCH₃), 6.55 (d, 8H, H-2), 6.85 (t, 4H, H-4), 6.98 (t, 8H, H-3) 7.15-7.28 (m, 10H, H-7, H-8, H-9).

Preparation of Ethylindium-bis(N,N'-diphenylbenzamidinato)

This complex was prepared using a similar procedure to that used for the ethylgallium-bis(N,N'-diphenylacetamidinato) complex above. N,N'-Diphenylbenzamidine (1.39g, 5.10mmol) was added to a solution of Et₃In (0.52g, 2.57mmol) in hexane (30cm³) at room temperature. After heating at 80°C for 4 hours, a white suspension was obtained, which was isolated by filtration and dried *in vacuo*. Yield: 1.10g (62%). Analysis, calculated for C₄₀H₃₅N₄In (M.W. 686.56): C, 69.98; H, 5.13; N, 8.16%. Found: C, 70.09; H, 5.12; N, 8.12%. ¹H N.M.R. (CDCl₃): δ/p.p.m. 1.25 (q, 2H, InCH₂CH₃), 1.46 (t, 3H, InCH₂CH₃), 6.51 (d, 8H, H-2), 6.82 (t, 4H, H-4), 6.95 (t, 8H, H-3) 7.10-7.26 (m, 10H, H-7, H-8, H-9).

Colourless, block-shaped crystals of this complex, suitable for X-ray diffraction work, were grown from the hexane filtrate at -35°C.

Preparation of Ethylindium-bis(N,N'-diphenylacetamidinato)

Again, this complex was prepared using a similar procedure to that used for the ethylgallium-bis(N,N'-diphenylacetamidinato) complex above. N,N'-Diphenylacetamidine (1.39g, 6.61mmol) was reacted with a solution of Et₃In (0.67g, 3.32mmol) in hexane (30cm³). After heating at 80°C for 4 hours, the colourless solution was left to cool to

room temperature, which produced a colourless crystalline solid. Yield: 1.24g (67%). Analysis, calculated for $C_{30}H_{31}N_4In$ (M.W. 562.42): C, 64.98%; H, 6.13%; N, 9.47%. Found: C, 65.04%; H, 5.65%; N, 9.68%. 1H N.M.R. ($CDCl_3$): $\delta/p.p.m.$ 1.18 (q, 2H, $InCH_2CH_3$), 1.47 (t, 3H, $InCH_2CH_3$), 2.10 (s, 6H, CH_3), 6.80 (d, 8H, H-2), 6.99 (t, 4H, H-4), 7.17 (t, 8H, H-3).

Preparation of Aluminium-tris(N,N'-diphenylbenzamidinato)

N,N'-Diphenylbenzamidine (0.85g, 3.12mmol) was partially dissolved in hexane ($40cm^3$) and chilled in a liquid nitrogen bath. A hexane solution of Me_3Al ($0.52cm^3$, 1.04mmol) was added via a syringe and the mixture was allowed to warm to room temperature and stirred for 1 hour. This mixture was heated at $80^\circ C$ for 12 hours which produced a pale yellow powder. This was separated by filtration and recrystallised from chloroform to give a pale yellow microcrystalline product. Yield: 0.63g (72%). Analysis, calculated for $C_{57}H_{45}N_6Al$ (M.W. 841.01): C, 80.86%; H, 5.55%; N, 10.30%. Found: C, 80.50%; H, 5.42%; N, 9.87%. 1H N.M.R. ($CDCl_3$): $\delta/p.p.m.$ 6.64 (d, 12H, H-2), 6.80-6.92 (m, 12H, H-4, H-7), 6.99 (t, 12H, H-3), 7.09 (t, 6H, H-8), 7.19 (t, 3H, H-9).

Preparation of Aluminium-tris(N,N'-diphenylacetamidinato)

This complex was prepared using a similar procedure to that used for aluminium-tris(N,N'-diphenylbenzamidinato). A solution of Me_3Al in hexanes ($0.79cm^3$, 1.58mmol) was added to a suspension of N,N'-diphenylacetamidine (1.0g, 4.76mmol) in hexane. The product is a colourless crystalline solid. Yield: 0.82g (79%). Analysis, calculated for $C_{42}H_{39}N_6Al$ (M.W. 654.79): C, 77.04%; H, 6.00%; N, 12.83%. Found: C, 76.56%; H, 6.09%; N, 12.62%. 1H N.M.R. ($CDCl_3$): $\delta/p.p.m.$ 2.00 (s, 9H, CH_3), 6.73 (d, 12H, H-2), 6.99 (t, 6H, H-4), 7.18 (t, 12H, H-3).

Preparation of Gallium-tris(N,N'-diphenylbenzamidinato)

N,N'-Diphenylbenzamidine (0.95g, 3.49mmol) and methylgallium-bis(N,N'-diphenylbenzamidinato) (2.19g, 3.49mmol) were placed in a sealed tube and heated at

200°C for 30 minutes to produce a melt, over which time 1 mole equivalent of methane was evolved. The pale yellow solid was dissolved in chloroform (15cm³) and the solution cooled to -35°C for 24 hours which produced a microcrystalline yellow solid. The product was isolated by removing the solvent by filtration, washed with hexane (2 x 10cm³) and dried *in vacuo*. Yield: 2.0g (65%). Analysis, calculated for C₅₇H₄₅N₆Ga (M.W. 883.74): C, 77.47; H, 5.13; N, 9.51%. Found: C, 77.10; H, 5.25; N, 9.40%. ¹H N.M.R. (CDCl₃): δ/p.p.m. 6.68 (d, 12H, H-2), 6.87 (t, 6H, H-4), 6.94 (d, 6H, H-7), 7.03 (t, 12H, H-3), 7.13 (t, 6H, H-8), 7.21 (t, 3H, H-9).

Preparation of Gallium-tris(N,N'-diphenylacetamidinato)

This complex was prepared by the same procedure to that used for gallium-tris(N,N'-diphenylbenzamidonato). The product is a colourless solid. Yield: 1.11g (65%). Analysis, calculated for C₄₂H₃₉N₆Ga (M.W. 697.53): C, 72.32; H, 5.64; N, 12.05%. Found: C, 72.02; H, 5.50; N, 11.80%. ¹H N.M.R. (CDCl₃): δ/p.p.m. 1.95 (s, 9H, CH₃), 6.63 (d, 12H, H-2), 6.85 (t, 6H, H-4), 7.00 (t, 12H, H-3).

Preparation of Indium-tris(N,N'-diphenylbenzamidonato)

N,N'-Diphenylbenzamidine (0.55g, 2.02mmol) was reacted with ethylindium-bis(N,N'-diphenylbenzamidine) (1.39g, 2.02mmol) as a melt at 200°C. After 30 minutes, 1 mole equivalent of ethane was evolved. Recrystallisation of the solid from chloroform solution gave a pale yellow solid, which was isolated by filtration and washed with hexane (2 x 10cm³). Yield: 1.24g (66%). Analysis, calculated for C₅₇H₄₅N₆In (M.W. 928.84): C, 73.71; H, 4.88; N, 9.05%. Found: C, 74.44; H, 4.81; N, 8.83%. ¹H N.M.R. (CDCl₃): δ/p.p.m. 6.56 (d, 12H, H-2), 6.80 (t, 6H, H-4), 6.94 (t, 12H, H-3), 7.01-7.05 (d, 6H, H-7), 7.11-7.26 (m, 9H, H-8, H-9).

The crystals used in the X-ray structural analysis were grown from the chloroform filtrate of the recrystallised solid.

Preparation of Indium-tris(N,N'-diphenylacetamidinato)

N,N'-Diphenylacetamide (0.53g, 2.52mmol) was reacted with ethylindium-bis(N,N'-diphenylacetamide) (1.42g, 2.52mmol) in a sealed tube at 200°C and the product washed with hexane (2 x 10cm³). The product is a colourless solid. Yield: 1.57g (84%). Analysis, calculated for C₄₂H₃₉N₆In (M.W. 742.63): C, 67.93; H, 5.29; N, 11.32%. Found: C, 68.29; H, 4.77; N, 11.40%. ¹H N.M.R. (CDCl₃): δ/p.p.m. 1.95 (s, 9H, CH₃), 6.63 (d, 12H, H-2), 6.85 (t, 6H, H-4), 7.02 (t, 12H, H-3).

Table 6.1 Summary of infra-red band frequencies of some dialkyl-metal-amidinato complexes.

Complex	Infra-red bands (cm ⁻¹)
[Me ₂ Al(PhNCPhNPh)]	3040 (w), 1595 (m), 1580 (m), 1497 (s), 1480 (s), 1442 (m-s), 1430 (m-s), 1334 (m), 1278 (w), 1189 (w), 1175 (w), 1126 (w), 1075 (w), 1024 (w), 976 (w), 794 (m-s), 775 (m-s), 769 (m), 708 (s), 696 (s), 675 (m), 552 (w), 508 (w), 503 (w).
[Me ₂ Al(PhNCMeNPh)]	3060 (m), 3020 (m), 1596 (m-s), 1578 (m), 1503 (s), 1417 (s), 1367 (s), 1331 (m), 1305(m), 1277 (w), 1225 (m), 1192 (w), 1170 (w), 1075 (w), 1028 (m), 1012 (m), 996 (w), 910 (w-m), 903 (w), 849 (m), 833 (w), 775 (s), 722 (m-s), 696 (s), 592 (m), 518 (s) 440 (w).
[Me ₂ Ga(PhNCPhNPh)]	3060 (m), 3020 (m), 1596 (m), 1580 (m), 1500 (s), 1441 (s), 1317 (m), 1277 (w), 1216 (w), 1174 (w), 1125 (w), 1074 (w), 1025 (w), 970 (w), 794 (m), 772 (m), 766 (m), 706 (m), 693 (s), 584 (w), 505 (w).
[Me ₂ In(PhNCPhNPh)]	3057 (m), 3020 (m), 1594 (m), 1581 (m), 1543 (m), 1440 (s), 1425 (s), 1310 (m), 1275 (m), 1259 (w-m), 1212 (m), 1124 (w), 1074 (m), 1026 (m), 1000 (w), 959 (m), 921(w), 790 (m-s), 769 (m-s), 695 (s), 615 (w), 593 (w), 541 (w), 516 (m), 465 (w-m).

Table 6.1 (cont.).

Complex	Infra-red bands (cm ⁻¹)
[Et ₂ In(PhNCHNPh)]	3050 (w), 3031 (m), 1621 (m), 1597 (m-s), 1546 (s), 1486 (s), 1418 (m), 1283 (s), 1268(s), 1221 (s), 1174 (m), 1151 (w), 1093 (w), 1078 (w), 1005 (m), 993 (m) 975 (w), 956 (w), 928 (w), 886 (w), 759 (s), 694 (s), 637 (m-s), 599 (w), 521 (m), 498 (w), 485 (w), 467 (w).

Recorded as Nujol mulls, CsI plates

Table 6.2 Summary of infra-red band frequencies of the dialkyl-metal-(N,N'-diphenylbenzamidinato).(4-Bu^t-pyridine) complexes.

Complex	Infra-red bands (cm ⁻¹)
[Me ₂ Ga(PhNCPhNPh).(4-Bu ^t -pyridine)]	3053 (w), 3020 (w), 1616 (m), 1594 (m), 1580 (m), 1534 (m), 1489 (s), 1454 (s), 1441 (m), 1425 (s), 1273 (w), 1215 (m), 1192 (w), 1120 (w), 1069 (w), 1020 (w), 997 (w), 967 (w), 955 (w), 830 (w), 792(m), 760 (m), 708 (w), 695 (m), 571 (w-m), 523 (w), 490 (w).
[Me ₂ In(PhNCPhNPh).(4-Bu ^t -pyridine)]	3060 (w), 1607 (m), 1593 (m), 1579 (m), 1515 (m), 1489 (s), 1470 (s), 1450 (s), 1440 (s), 1419 (s), 1270 (w), 1213 (w-m), 1120 (w), 1071 (w), 1012 (w), 950 (w), 828 (w), 791 (m), 770 (m), 762 (m), 698 (s), 627 (s), 570 (w), 488 (w-m).

Recorded as Nujol mulls, CsI plates

Table 6.3 Summary of infra-red band frequencies of some monoalkyl-metal-bis(amidinato) complexes.

Complex	Infra-red bands (cm ⁻¹)
[MeAl(PhNCPhNPh) ₂]	3040 (w), 1595 (m), 1580 (m), 1495 (s), 1480 (s), 1440 (m-s), 1428 (m-s), 1330 (m), 1278 (w), 1189 (w), 1175 (w), 1120 (w), 1075 (w), 1026 (w), 978 (w), 794 (m-s), 775 (m-s), 768 (m), 708 (s), 696 (s), 675 (m), 550 (w), 502 (w).
[MeGa(PhNCPhNPh) ₂]	3040 (m), 3020 (m), 1594 (m), 1578 (m), 1500 (s), 1441 (s), 1319 (m), 1278 (w), 1215 (w), 1174 (w), 1125 (w), 1075 (w), 1025 (w), 970 (w), 794 (m), 772 (m), 766 (m), 707 (m), 695 (s), 575 (w).
[MeIn(PhNCPhNPh) ₂]	3060 (w), 3018 (w), 1594 (m), 1581 (m), 1497 (s), 1475 (s), 1440 (s), 1312 (m), 1273 (w), 1175 (w), 1123 (w), 1074 (w), 1024 (w), 998 (w), 964 (w-m), 927 (w), 892 (w), 791 (m), 763 (m), 729 (w), 705(m), 692 (s), 530 (w), 503 (w), 495 (w).

Recorded as Nujol mulls, CsI plates

Table 6.4 Summary of infra-red band frequencies of some metal-tris(amidinato) complexes.

Complex	Infra-red bands (cm ⁻¹)
[Al(PhNCPPhNPh) ₃]	3056 (w), 3020 (m), 1595 (m), 1579 (m), 1519 (w), 1491 (s), 1454 (s), 1441 (s), 1427 (s), 1327 (w), 1316 (w), 1281 (m), 1217 (m), 1125 (w), 1076 (m), 1027 (w), 967 (m), 928 (w-m), 895 (w-m), 792 (m), 771 (m), 760 (m), 708 (m), 693 (m-s), 592 (w), 523 (w-m), 508 (w).
[Al(PhNCMeNPh) ₃]	3040, (w), 3020 (w), 1595 (m), 1575 (m), 1493 (s), 1417 (s), 1364 (s), 1313 (m), 1299 (m), 1273 (w), 1226 (m), 1169(w), 1071 (w-m), 1030 (m), 1005 (w), 903 (m), 841 (m), 766 (m), 750 (w), 744 (m), 704 (m-s), 694 (s), 665 (w), 584 (m), 518 (w), 484 (m-s), 419 (m).
[Ga(PhNCPPhNPh) ₃]	3061 (m), 3027 (m), 1593 (m-s), 1578 (m), 1438 (s), 1314 (s), 1277 (m), 1212 (m), 1170 (w), 1125 (m), 1072 (m), 1026 (m), 999 (w-m), 969 (m), 920 (m), 822 (w), 792 (s), 772 (m-s), 762 (m-s), 704 (s), 694 (s), 616 (w), 542 (w), 499 (m), 465 (m).
[In(PhNCPPhNPh) ₃]	3056 (m), 3017 (m), 1595 (m), 1581 (m) 1493 (s), 1474 (s), 1436 (s), 1425 (s), 1310 (m), 1277 (m), 1213 (m), 1171 (w), 1123 (m), 1075 (m), 1027 (w-m), 999 (w), 962 (m), 923 (w), 890 (w), 791 (m-s), 770 (m), 762 (m), 705 (m-s), 692 (m-s), 615 (w), 505 (m), 497 (m), 465 (w), 375 (w).

Recorded as Nujol mulls, CsI plates

EXPERIMENTAL (Chapter 3)

Butyramidinium chloride was purchased from Aldrich. Trifluoroacetamide was supplied by Fluorochem as a colourless liquid (b.p 35–37°C/11mm). This ligand must be kept in cool (–5°C), dark conditions.

Preparation of Dimethylgallium–butyramidinato

The amidine was prepared by the addition of a hexane solution of *n*-butyl–lithium (9.1cm³, 10.92mmol) via a syringe through a Suba–seal to a stirred suspension of butyramidinium chloride (1.49g, 10.92mmol) in hexane (30cm³) cooled at –78°C. This mixture was left to warm to room temperature and stirred for a further hour before the solvent was removed under vacuum leaving a white solid. A water cooled cold finger was quickly inserted. Butyramidine sublimed under vacuum (0.005mm Hg) fairly quickly at 100°C to give a colourless crystalline solid. Yield 0.84g (77%). Analysis, calculated for C₅H₁₂N₂ (M.W. 100.16): C, 59.95; H, 12.08; N, 27.97%. Found: C, 60.20; H, 12.0, N, 27.72%. ¹H N.M.R. (CD₂Cl₂): δ/p.p.m. 1.18 (s, 9H, C{CH₃}₃), 5.54 (s, 3H, NH). ¹³C N.M.R. (CD₂Cl₂): δ/p.p.m. 28.26 (C{CH₃}₃), 37.10 (C{CH₃}₃), 175.31 (NCN).

This amidine is particularly moisture sensitive; exposure of the sublimed product to air for ca. 1 minute gave a sticky material accompanied by a smell of ammonia.

The dimethylgallium derivative was prepared using the same procedure to that used for the preparation of the dimethylgallium–N,N'–diarylamidinato complexes, except that no solvent was used. The reaction mixture gave a white solid. This was sublimed under vacuum (0.005mm Hg) at 80°C to produce a colourless crystalline solid. Yield 0.40g (92%). Analysis, calculated for C₇H₁₇N₂Ga (M.W. 198.95): C, 42.26; H, 8.61; N, 14.08%. Found: C, 41.91; H, 8.52; N, 13.67%. ¹H N.M.R. (C₆D₆): δ/p.p.m. 0.08 (s, 6H, GaMe₂), 0.79 (s, 9H, C{CH₃}₃), 4.73 (s, br, 2H, NH). ¹³C N.M.R. (C₆D₆): δ/p.p.m. –7.74 (GaMe), 27.61 (C{CH₃}₃), 38.38 (C{CH₃}₃), 184.19 (NCN).

Accurate M.S. (C.I.) peak match on MH⁺ and DH⁺ m/z : 199.0726, 397.1373 (theoretical: 199.07258, 397.13733).

I.R. (Nujol): 3409 (m), 3016 (m), 1562 (s), 1536 (m), 1514 (s), 1503 (m), 1372 (m), 1297 (w), 1066 (w), 1033 (m), 799 (s), 722 (s), 699 (s), 608 (s), 574 (s), 531 (s), 409 (w-m).

Preparation of dimethylgallium-N,N'-trifluoroimidoyltrifluoroacetamidinato

Me_2Ga (0.50g, 4.35mmol) was condensed under vacuum onto degassed trifluoroacetamide (0.98g, 8.70mmol) held at -196°C . The mixture was allowed to warm slowly to room temperature and the volume of methane evolved was measured. The viscous colourless liquid was heated to 60°C and then left at room temperature for 24 hours after which time a quantity of a colourless crystalline product appeared. This was obtained by sublimation from the liquid mixture under static vacuum at 70°C . Yield 0.61g. Analysis, calculated for $\text{C}_6\text{H}_8\text{N}_3\text{F}_6\text{Ga}$ (M.W. 305.86): C, 23.56; H, 2.62; N, 13.74%. Found: C, 23.07; H, 2.62; N, 13.36%. Melting point: $91.0 - 91.5^\circ\text{C}$. ^1H N.M.R. (CDCl_3): $\delta/\text{p.p.m.}$ -0.27 (s, 6H, GaCH_3), 7.37 (br s, 2H, NH). ^{13}C N.M.R. (400MHz) (CDCl_3): $\delta/\text{p.p.m.}$ -4.70 (GaCH_3), 117.15 (q, J 1114.6 Hz, CF_3), 162.04 (q, J 141.6 Hz, N-C-N). ^{19}F N.M.R. (400MHz) (CDCl_3): $\delta/\text{p.p.m.}$ -76.17 (CF_3). M.S. (C.I.) m/z (intens.): 309 (7.5), 308 (66.7), 307 (11.3), 306 (100), 208 (4.0), 113 (11.3), 58 (3.7), 52 (1.5).

Accurate M.S. (C.I.) peak match on MH^+ m/z : 305.99560 (theoretical: 305.995647).

I.R. bands (KBr disk) [$\text{Me}_2\text{Ga}\{\text{HNC}(\text{CF}_3)\text{NC}(\text{CF}_3)\text{NH}\}$]: 3331 (m), 3307 (m), 2967 (w-m), 2940 (w, br), 1628 (s), 1561 (s), 1534 (m-s), 1508 (m-s), 1491 (m-s), 1295 (s), 1285 (s), 1219 (s), 1199 (vs), 1163 (vs), 1069 (m), 935 (m), 823 (m), 804 (w), 768 (m-s), 723 (w-m), 675 (m), 614 (w-m), 594 (m), 547 (m), 533 (w-m).

I.R. bands (thin film) [$\text{H}_2\text{NC}(\text{CF}_3)\text{NH}$] : 3600-2400 (s, br), 1680 (vs), 1660 (s), 1511 (m), 1471 (m-s), 1419 (m), 1312 (m), 1201 (vs), 1152 (vs), 1046 (w), 1003 (w), 944 (m), 859 (m), 827 (w-m), 791 (w), 742 (w), 704 (m), 639 (w).

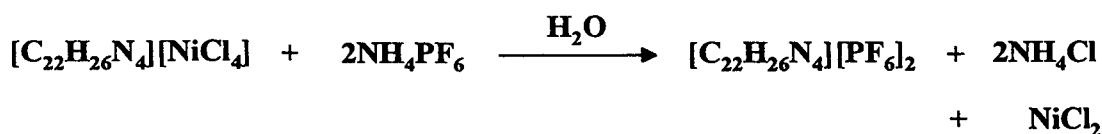
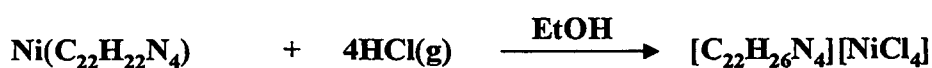
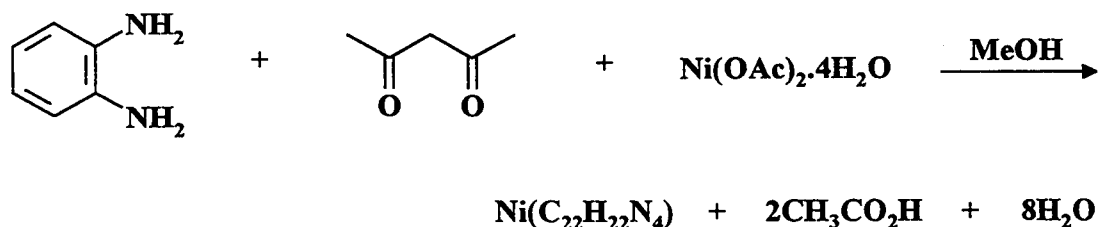
Large, well-formed block-shaped, colourless crystals of [$\text{Me}_2\text{Ga}\{\text{HNC}(\text{CF}_3)\text{NC}(\text{CF}_3)\text{NH}\}$] were obtained by rapid sublimation of the pure compound under vacuum at 60°C .

EXPERIMENTAL (Chapter 4)

1,2-Diamino-benzene, pentane-2,4-dione (Hacac), nickel (II) diacetate tetrahydrate, lithium cyclopentadienyl, lithium bis(trimethylsilyl)amide and lithium trimethylsiloate were obtained from Aldrich and were used without further purification. Lithium methyl was used as a diethyl ether solution and the concentration was assumed to be as quoted by Aldrich (1.4M).

Preparation of 5,7,12,14-tetramethyldibenzo [b,i][1,4,8,11] tetraazacyclotetradecine, H₂tmtaa.

The free ligand H₂tmtaa was synthesised by the standard metal template method²⁶⁰ illustrated below:



The ¹H N.M.R. spectrum showed the product to contain ethanol which could not be removed by pumping under vacuum for several hours. Purification involved dissolving the yellow-brown powder in hot pyridine, followed by the addition of water, which caused the precipitation of a bright yellow solid. This solid was filtered and dried by

pumping under vacuum at 80°C overnight. Typical overall yield: 22%. Analysis, calculated for $C_{22}H_{22}N_4$ (M.W. 344.46): C, 76.61; H, 7.02; N, 16.27 %. Found : C, 76.45; H, 7.08; N, 16.17 %. 1H N.M.R. ($CDCl_3$) δ /p.p.m.: 2.13 (s, 12H, CH_3), 4.87 (s, 2H, methine CH), 6.99 (s, 8H, C_6H_4), 12.58 (s, br, 2H, NH).

The free ligand is soluble in moderately polar solvents such as toluene, benzene and dichloromethane, but only slightly soluble in short chain alkanes, such as hexane.

Preparation of $[Et_2In(Htmtaa)]$

H_2tmtaa (0.63g, 1.83mmol) was partially dissolved in hexane (30cm³) and cooled on a dry ice-acetone bath at -78 °C for 10 minutes. To this stirred suspension was added a solution of Et_3In (0.39g, 1.93 mmol) in hexane (20cm³) via a dropping funnel. The suspension was allowed to warm to room temperature and methane evolution occurred below 0°C, and was stirred for 1 hour. A yellow solid formed with a darker yellow supernatant solution. The suspension was cooled in the freezer at -35°C for 1 hour and the solid was isolated by filtration and dried *in vacuo* for 2 hours to give a lemon yellow powder. Yield: 0.80g (85%). Analysis, calculated for $C_{26}H_{33}N_4In$ (M.W. 516.39): C, 60.47; H, 6.44; N, 10.85%. Found: C, 60.86; H, 6.32; N, 10.67%. 1H N.M.R. (400MHz) ($CDCl_3$) δ /p.p.m.: -0.02, 0.72 (2 × q, 2 × 2H, $InCH_2CH_3$), 0.47, 1.38 (2 × t, 2 × 3H, $InCH_2CH_3$), 1.65, 2.11 (2 × s, 2 × 6H, CH_3), 4.82, 4.84 (2 × s, 2 × 1H, methine CH), 6.97-7.10 (m, 8H, C_6H_4), 12.24 (s, 1H, NH).

Preparation of $[EtIn(tmtaa)]$

The diethylindium complex, $[Et_2In(Htmtaa)]$ (0.40g, 0.78mmol), was dissolved in hexane (40cm³) and heated at reflux under argon for 12 hours. An orange solution was produced. Upon slowly cooling this solution to room temperature, deep orange, block-shaped crystals were deposited. These were suitable for single crystal X-ray diffraction studies. Yield: 0.24g (64%). Analysis, calculated for $C_{24}H_{27}N_4In$ (M.W. 486.33): C, 59.27; H, 5.60; N, 11.52%. Found: C, 59.45; H, 5.38; N, 11.51%. 1H N.M.R. (400MHz)

N.M.R. (400MHz) (CDCl_3) δ /p.p.m.: 0.34 (q, 2H, InCH_2CH_3), 0.76 (t, 3H, InCH_2CH_3), 2.17 (s, 12H, CH_3), 4.66 (s, 2H, methine CH), 6.90-7.10 (AA'BB' multiplet, 8H, C_6H_4).

This complex was also prepared by heating $[\text{Et}_2\text{In}(\text{Htmtaa})]$ in the solid state under dry nitrogen to 180°C . 1 mole equivalent of gas, which was presumed to be ethane, was evolved and an orange solid obtained.

Preparation of $[\text{ClIn}(\text{tmtaa})]$

A typical preparation follows. To a stirred solution of H_2tmtaa (2.50g, 7.26mmol) in toluene (70cm^3) held at -78°C was added via a syringe a solution of LiMe in diethyl ether (10.37cm^3 , 14.52mmol). The reaction mixture was allowed to warm to room temperature, with stirring, and further heated at 60°C for 2 hours. The resulting blood-red solution was transferred via a stainless steel transfer needle to a stirred suspension of InCl_3 (1.61g, 7.26mmol) in toluene (20cm^3) held at -78°C . After allowing the mixture to warm to room temperature, a cloudy orange-red solution was obtained, which was heated at 70°C for 2 hours and cooled to room temperature. Filtration of the resulting orange suspension gave a dark orange solution which was reduced in volume to ca. 20cm^3 by distillation under reduced pressure. Upon the addition of hexane (40cm^3), a dark orange microcrystalline solid was precipitated. This solid was isolated by filtration and dried *in vacuo* for 2 hours. Yield: 2.43g (68%). Analysis, calculated for $\text{C}_{22}\text{H}_{22}\text{N}_4\text{ClIn}$ (M.W. 492.72): C, 53.63; H, 4.50; N, 11.37%. Found: C, 54.02; H, 4.42; N, 11.31%. ^1H N.M.R. (CDCl_3): 2.27 (s, 12H, CH_3), 4.80 (s, 2H, methine CH), 6.98–7.07, 7.09–7.18 (AA'BB' multiplet, 8H, C_6H_4).

Dark orange, block-shaped crystals were grown by slow evaporation of a chloroform/hexane (20/80) solution and these were suitable for single crystal X-ray diffraction.

Preparation of $[\text{MeIn}(\text{tmtaa})]$

The monochloroindium-complex, $[\text{ClIntmtaa}]$ (0.65g, 1.32mmol), was dissolved in toluene (40cm^3) and cooled to -78°C . A solution of LiMe in diethyl ether (0.94cm^3 ,

1.32mmol) was added via syringe. The stirred mixture was warmed to room temperature and further heated at 70°C for 3 hours. The resulting orange suspension was cooled to room temperature, filtered and the deep orange filtrate was reduced in volume to ca. 10cm³ by distillation under reduced pressure. Upon standing at room temperature overnight, an orange crystalline solid was deposited from the solution. This solid was isolated by filtration and dried *in vacuo*. Yield: 0.41g (66%). Analysis, calculated for C₂₃H₂₅N₄In (M.W. 472.30): C, 58.49; H, 5.34; N, 11.86%. Found: C, 58.93, H, 5.44, N, 11.55%. ¹H N.M.R. (CDCl₃): δ/p.p.m. -0.63 (s, 3H, InCH₃), 2.15 (s, 12H, CH₃), 4.65 (s, 2H, methine CH), 6.92–6.99, 7.00–7.07 (AA'BB' multiplet, 8H, C₆H₄).

The following indium(III) tmtaa complexes, of the general formula, [XIn(tmtaa)] (where X = axial substituent) were prepared using a similar procedure to that for the [MeIn(tmtaa)] complex, except that the appropriate lithium reagent was added to a toluene solution of [ClIn(tmtaa)] at room temperature in the glove box.

Preparation of [CpIn(tmtaa)]

Reagents used: [ClIn(tmtaa)] (1.85g, 3.75mmol) and Li(C₅H₅) (0.27g, 3.75mmol). The product is a brick-red solid. Yield: 1.15g (59%). Analysis, calculated for C₂₇H₂₇N₄In (M.W. 522.36): C, 62.08; H, 5.21; N, 10.72%. Found: C, 63.30; H, 5.31; N, 10.21%. ¹H N.M.R. (CD₃C₆D₅): δ/p.p.m. 1.87 (s, 12H, CH₃), 4.42 (s, 2H, methine CH), 6.03 (s, 5H, C₅H₅), 6.89 (s, 8H, C₆H₄). ¹H N.M.R. (CDCl₃): δ/p.p.m. 2.18 (s, 12H, CH₃), 4.62 (2, 2H, methine CH), 5.72 (s, 5H, C₅H₅), 7.01–7.09 (AA'BB' multiplet, 8H, C₆H₄). ¹H N.M.R. (CD₂Cl₂): δ/p.p.m. 2.14 (s, 12H, CH₃), 4.63 (2, 2H, methine CH), 5.60 (s, 5H, C₅H₅), 6.92–7.10 (AA'BB' multiplet, 8H, C₆H₄).

Controlled cooling of a hot toluene solution of the product to room temperature gave a crop of well-defined block-shaped, red crystals, which were suitable for single crystal X-ray diffraction studies.

Preparation of [(Me₃Si)₂NIn(tmtaa)]

Reagents used: [ClIn(tmtaa)] (1.07g, 2.18mmol) and LiN(SiMe₃)₂ (0.55g, 2.18mmol). Recrystallisation of the product from toluene gave a yellow/orange microcrystalline solid. Yield: 0.85g (63%). Analysis, calculated for C₂₈H₄₀N₅InSi₂ (M.W. 617.65): C, 54.45; H, 6.53; N, 11.34%. Found: C, 54.42; H, 6.65; N, 11.00%. ¹H N.M.R. (CDCl₃): δ/p.p.m. -0.24 (s, 18H, Si(CH₃)₃), 2.20 (s, 12H, CH₃), 4.76 (s, 2H, methine CH), 6.95–7.15 (AA'BB'multiplet, 8H, C₆H₄).

Preparation of [(Me₃Si)OIn(tmtaa)]

Reagents used: [ClIn(tmtaa)] (0.86g, 1.74mmol) and LiOSiMe₃ (0.17g, 1.74mmol). The product was recrystallised from toluene as an orange solid. Yield: 0.54g (57%). Analysis, calculated for C₂₅H₃₁N₅InOSi (M.W. 560.46): C, 53.58; H, 5.58; N, 12.50%. Found: C, 54.20; H, 5.54; N, 12.39%. ¹H N.M.R. (CDCl₃): δ/p.p.m. -0.34 (s, 9H, Si(CH₃)₃), 2.25 (s, 12H, CH₃), 4.75 (s, 2H, methine CH), 6.94–7.05, 7.06–7.17 (AA'BB' multiplet, 8H, C₆H₄).

Table 6.5 Summary of infra-red band frequencies of H₂tmtaa and the indium(III) tmtaa complexes.

Complex	Infra-red bands (cm ⁻¹)
H ₂ tmtaa	1615 (s), 1592(s), 1552(m), 1512 (m), 1503 (m), 1366 (s), 1294 (m), 1275 (m), 1187 (m), 744 (s), 735 (s), 610 (w).
[Et ₂ In(Htmtaa)]	3040 (w), 1622 (m-s), 1595 (s), 1549 (s), 1501 (m), 1285 (m), 1266 (m), 1189 (m), 1174 (w), 1107 (w-m), 1008 (m), 926 (w), 833 (m), 796 (w-m), 742 (s), 573 (w), 534 (w), 486 (w), 459 (w).
[EtIn(tmtaa)]	1553 (m), 1530 (w), 1417 (s), 1188 (m-s), 1117 (w), 1049 (w), 1025 (w), 751 (m), 722 (w), 520 (w, br), 480 (w, br).
[CpIn(tmtaa)]	3100–3020 (w, br), 1566 (m), 1548 (s), 1526 (s), 1412 (s), 1277 (w), 1260 (w), 1191 (s), 1121 (w), 1024 (m), 801 (m), 765 (w), 748 (m), 738 (m), 715 (w), 523 (w), 326 (w).
[(Me ₃ Si) ₂ NIn(tmtaa)]	3035 (w), 1621 (w), 1553 (m), 1529 (m), 1417 (s), 1255 (w), 1243 (m), 1190 (m-s), 1117 (w), 1023 (m), 964 (s), 882 (m), 832 (m), 827(m), 766 (w), 749 (s), 675 (w), 355 (w).
[(Me ₃ Si)OIn(tmtaa)]	3040 (w), 1565 (w), 1537 (m), 1413 (s), 1191 (m), 1034 (w-m), 959 (m), 831 (w-m), 741 (m), 468 (w).

Recorded as Nujol mulls, CsI plates

APPENDIX 1

Thermal Decomposition of Some Group 13 Metal–Amidinato Compounds

APPENDIX 1 Thermal Decomposition of Some Group 13 Metal Amidinato Compounds.

Introduction

An important application of group 13 organometallic compounds is their use as precursors for the preparation of semi-conductor materials such as aluminium nitride (AlN), gallium phosphide (GaP) and indium arsenide (InAs), which are known as III-V semi-conductors.²⁶¹

The fabrication of semi-conductor devices, which normally requires the deposition of thin films of the material, is commonly carried out by a technique known as metal organic vapour phase epitaxy (MOVPE). Currently this technique typically involves the thermal decomposition of a mixture of the trialkyl-metal derivatives of aluminium, gallium or indium with group 15 hydrides (EH₃, E = N, P, As, Sb) onto a heated substrate either at atmospheric or reduced pressure. The major drawbacks of this method relate to the pyrophoric nature of the trimethyl-metal derivatives, which poses handling problems, the high temperatures required to effect the vapour deposition (typically 600–1100°C) and, in the case of the heavier group 15 hydrides, the extreme toxic nature of these reagents. These disadvantages have prompted the search for alternative routes to these materials.

For the III-V semi-conductors attention has been focused mainly on the development of new phosphide and arsenide derivatives. There is an increasing need for the nitrides in view of their semiconductor device applications in the blue and ultraviolet wavelengths.²⁶² For example, GaN has a wide band gap of 3.39eV and is used for the production of blue LED devices by Nichia Chemical Industries, Tokyo, Japan (operating at 450nm, 3.6V, 20mA, 1000 mcd). The luminous intensity of these devices is currently 100 times greater than that of alternative LEDs made from SiC. A number of alternative organometallic precursor materials have been developed that contain a group 13 metal-nitrogen bond, and possess suitable volatility for use with this type of deposition method. For example, the aluminium complex [(Me₂AlNPr₂)₂] is used as a precursor for the deposition of AlN using very low pressure MOVPE.²⁶³

Thermal Decomposition Reactions

In order to obtain information about the thermal decomposition products of the group 13 metal amidinato derivatives discussed in Chapter 2, of the type $[R_xM(L)_{3-x}]$ ($M = Al, Ga, In$; $L =$ amidinato ligand; $x = 0, 1, 2$), a number of thermogravimetric analysis (T.G.A.) and differential thermal analysis (D.T.A.) experiments were carried out by our collaborating company (A.O.C.). Thermal decomposition was carried out under a stream of dry nitrogen with the sample (in mg quantities) held in a platinum crucible, which was heated from 25°C to typically 1000°C at a heating rate of 20°C/minute. The residual materials had the appearance of grey powders.

The results are summarised in Table 1 and are discussed briefly here. The main points to note are as follows. Under the experimental conditions employed, stringent exclusion of air / moisture could not be guaranteed and thus it was appreciated that the formation of metal oxy species could be possible. All the compounds decompose rather than sublime at atmospheric pressure and the T.G.A. plots show fairly smooth sigmoid curves. The aluminium and gallium compounds decompose over a temperature range between 250–350°C and the indium compounds between 325–450°C.

The typical residual fragment for the aluminium compounds is 56–67 mass units, although that from $[Me_2Al(PhNCMeNPh)]$ is significantly lower at 39 mass units. Using the assumption that these fragments represent a single compound, the identity of the higher fragments is uncertain. A value of 41 may represent AlN , whereas 51 can be explained by Al_2O_3 . For the dimethylaluminium compounds, values around 56 – 57 are consistent with either $(Me_2Al)_n$ or $(MeAlN)_n$ with the latter being a more likely possibility.

The typical residual fragment mass for the gallium compounds is around 100, however there is considerable variation. The lowest fragment is ca. 83 and a number of results are within the range 83–92. A value of around 84–85 is consistent with $(MeGa)_n$, and this has been claimed to be the product from the thermal decomposition of $GaMe_3$.²⁶⁴ The latter suggestion is clearly excluded in the case of the tris-amidinato compound. A more likely product is GaN . Ga_2O_3 equates to values around 94 mass

Table 1 Summary of T.G.A. Results for the Aluminium, Gallium and Indium Amidinato Derivatives

Compound	M.W.	Final wt. (%)	Final fragment	Approx. decomp. temp. (°C)	Max temp. (°C)
Dimethylaluminium-N,N'-diphenylbenzamidinato	328.39	20.3	66.7	300	1000
Dimethylaluminium-N,N'-diphenylacetamidinato	266.32	14.6	38.9	350	1000
Dimethylaluminium-N,N'-diphenylformamidinato	252.29	25.0	63.1	350	1000
Dimethylgallium-N,N'-diphenylbenzamidinato	371.13	29.6	109.8	300	1000
Dimethylgallium-N,N'-di(3,4-dichlorophenyl)formamidinato	432.81	19.2	83.1	250	1000
Dimethylgallium-N,N'-di(p-chlorophenyl)benzamidinato	440.02	23.0	101	275	950
Diethylindium-N,N'-diphenylbenzamidinato	416.23	29.2 (at 675°C)	121.5	325	1000
Diethylindium-N,N'-di(p-chlorophenyl)benzamidinato	513.18	26	133	350	1000

Compound	M.W.	Final wt. (%)	Final fragment	Approx. decomp. temp. (°C)	Max temp. (°C)
Methylaluminium-bis(N,N'-diphenylacetamidinato)	460.56	12.2	56.2	300	1000
Methylgallium-bis(N,N'-diphenylbenzamidinato)	627.44	13.9	87.2	250	1000
Ethylgallium-bis(N,N'-diphenylacetamidinato)	517.32	19.8	102.4	350	1000
Methylindium-bis(N,N'-diphenylbenzamidinato)	672.54	16.5	111	450	1000
Ethylindium-bis(N,N'-diphenylacetamidinato)	562.42	21 (at 700°C)	118	425	1000
Aluminium-tris(N,N'-diphenylbenzamidinato)	841.01	11.9 (at 450°C)	100.1	275	1000
Gallium-tris(N,N'-diphenylbenzamidinato)	883.74	10.5 (at 350°C)	92.8	250	1000
Indium-tris(N,N'-diphenylbenzamidinato)	928.84	12 (at 700°C)	111	450	1000

units. Additional mass could be attributed to carbon residues resulting from incomplete decomposition of the precursor compound.

The fragments from the indium compounds fall within the range 111–122, except that obtained from diethylindium-*N,N'*-di(*p*-chlorophenyl)benzamidinato with a value of 133. While the former values are consistent with indium metal, it is more likely that these fragments correspond to InN or In₂O₃ with the difference between the expected and experimental determined mass accounted for by experimental errors.

The conclusions drawn from these results regarding the nature of the residues are tentative, but they do show that the compounds decompose over a relatively narrow temperature range to a material of constant weight to 1000°C.

In an effort to gain more information on the nature of the residues obtained from the gallium-amidinato derivatives, the following X-ray powder diffraction (XRD) and energy dispersive X-ray (EDX) experiments were carried out. The bis(amidinato) compound [MeGa(PhNCPhNPh)₂] was chosen for investigation in these preliminary experiments. Two residue samples were prepared by placing the precursor compound (2 x 0.50g) in a silica tube contained in a thermostatically controlled furnace which was heated to a temperature of 600°C under a dry nitrogen atmosphere over a period of approximately 2 hours. After this time, sample 1 was removed from the furnace and allowed to cool under nitrogen to room temperature. Sample 2 was heated for a further 8 hours at 600°C, and the sample left to cool to room temperature slowly in the furnace over a period of about 4 hours. Both samples had the appearance of grey powders and were kept under nitrogen. The final fragment mass of both samples was approximately 125 mass units.

The X-ray powder diffraction spectra of the samples were recorded between 5 – 35° θ . The spectrum of sample 1 showed a number of weak, poorly defined d lines which could not be accurately analysed. This result indicated that this material was primarily structurally amorphous. The spectrum obtained from sample 2 showed slightly more intense d lines, which are characteristic of GaN, at 2.79, 2.58, 2.43, 1.59, 1.46 and 1.38Å.

(4) The surface morphology of sample 2 was examined using transmission electron microscopy (TEM) and an image of this sample is shown in Figure 1. EDX measurements were taken at various points of this sample. It should be noted that although the sensitivity of this spectroscopic technique for the detection of C, N, and O is similar for each element, it is much lower than that for heavier elements ($Z > 11$) such as Ga. Therefore the intensity of the peak corresponding to Ga is expected to be much more intense compared to the intensity of those corresponding to C, N or O.

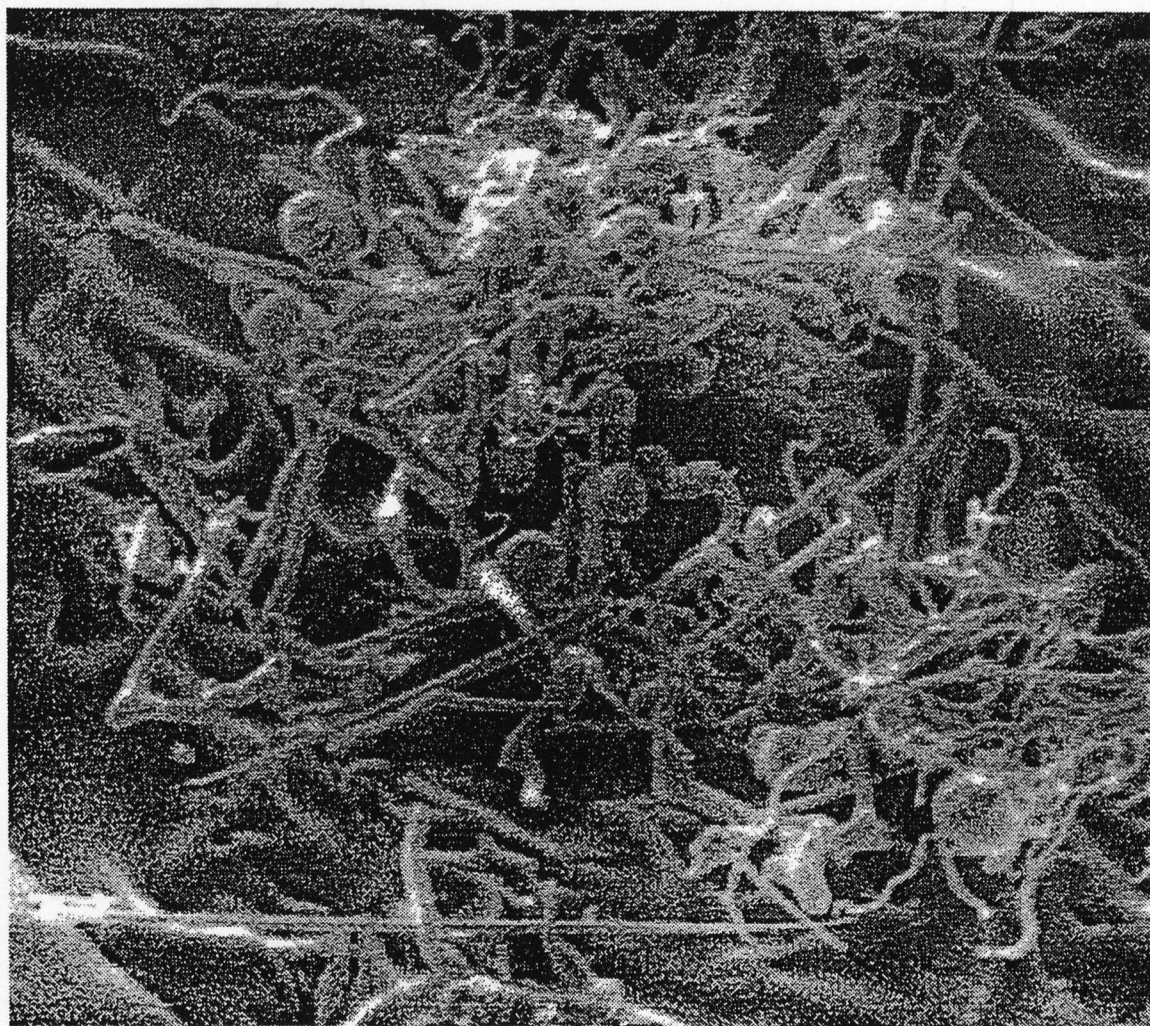
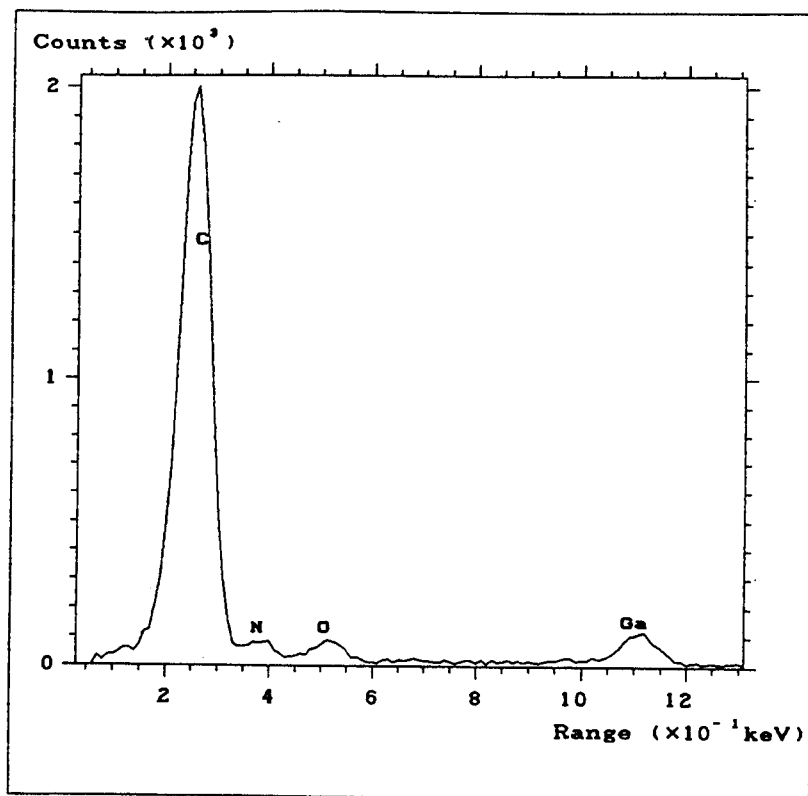


Figure 1 TEM image taken from the thermal decomposition residue of sample 2.

(a)



(b)

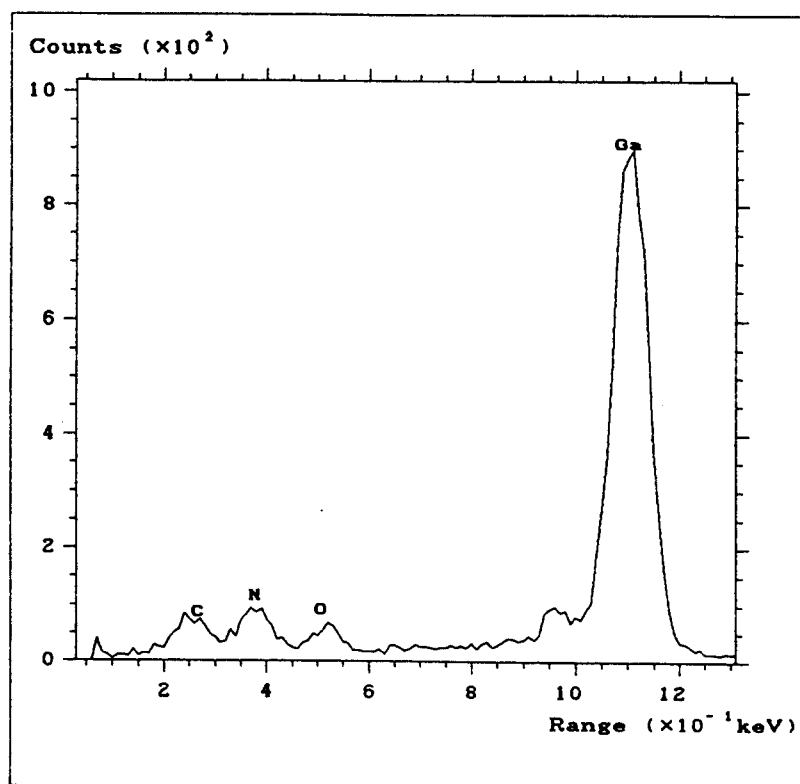


Figure 2 EDX measurements taken from (a) dark areas, (b) light areas.

The measurements obtained from the dark areas as they appeared on the micrograph image showed X-ray emissions that mainly correspond to the K shell of carbon [Figure 2(a)]. The spectrum shown in Figure 2(b) was obtained from the lighter areas, which showed emissions which correspond to the L shell of gallium and the K shell of nitrogen and oxygen, with a smaller proportion of emissions which correspond to carbon. The appearance of the spectrum in relation to the relative proportions of the measurements corresponding to C, N and O varied depending on the location of measurement on the crystal domain. Figure 2(b) shows a representative spectrum. Other spectra showed peaks which mainly correspond to Ga and N only.

Although these preliminary experiments show that the thermal decomposition of $[\text{MeGa}(\text{PhNCPhNPh})_2]$ yields GaN, there is clearly a problem of incorporation of impurities. Attempts at producing high grade metal nitride from this type of precursor compound would therefore need to determine a method of overcoming this problem. The optimum metal complex and the best type of amidinato ligand needs further investigation to achieve minimum decomposition temperatures with a clean decomposition process. The T.G.A. plot obtained from the imidolyamidinato complex, $[\text{Me}_2\text{Ga}\{\text{HNC}(\text{CF}_3)\text{NC}(\text{CF}_3)\text{NH}\}]$, reproduced in Figure 3, shows that this compound has some promising properties in relation to these two requirements. The T.G.A. plot is a smooth sigmoid curve. Decomposition starts at about 80°C and is complete at 120°C, and leaves a grey material which corresponds to 78 mass units. The precursor compound shows significant volatility and can be rapidly sublimed under vacuum (0.005mm Hg, 60°C). Furthermore, it is air stable at room temperature and therefore can be easily handled. Further investigation of the products obtained from thermal decomposition of this compound are planned.

In addition, optimisation of the technical process (varying experimental conditions) is required. For example, the prevention of formation of the oxide could be relatively easily achieved by the use of more rigorously dry conditions.

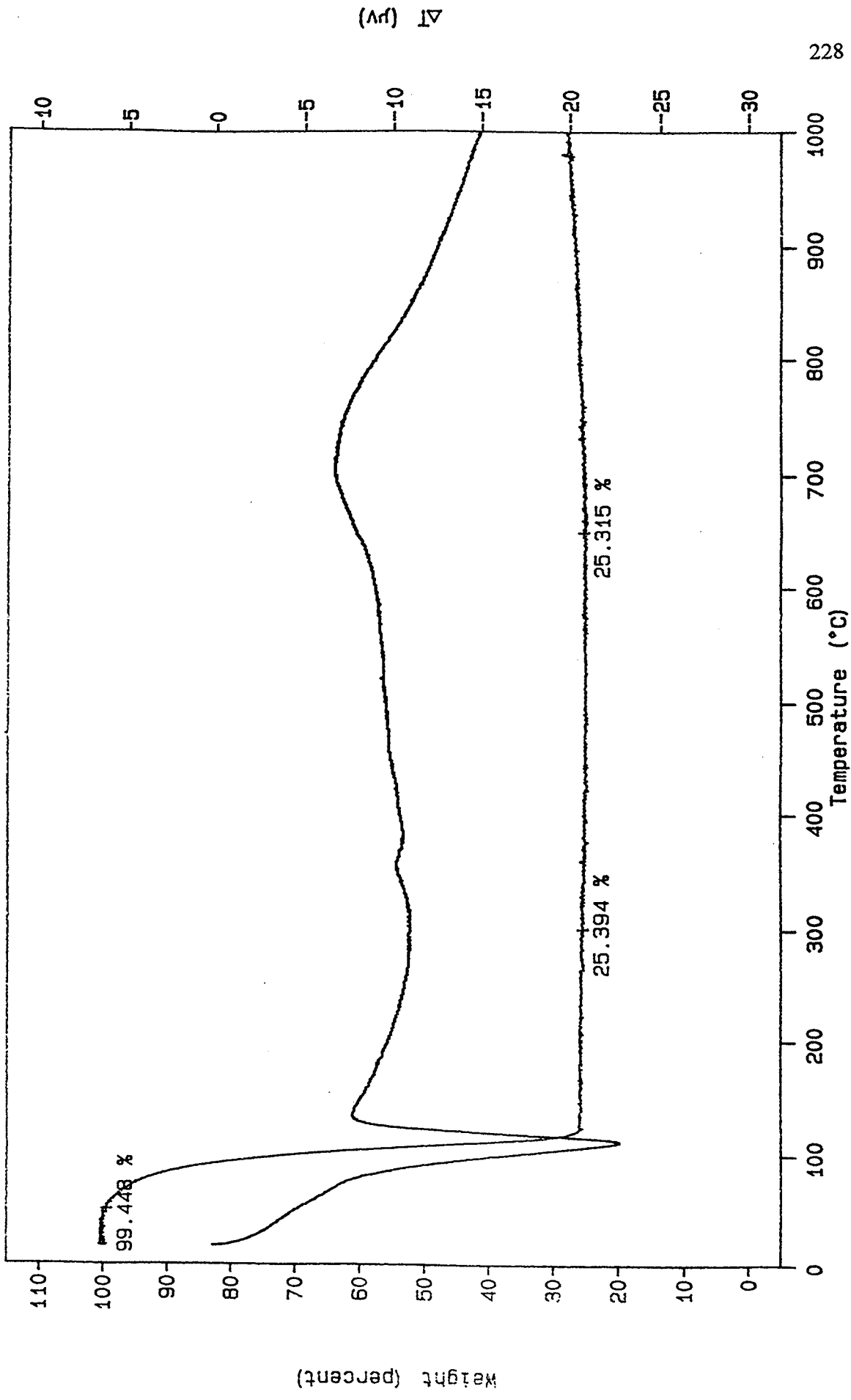


Figure 3 Combined T.G.A. and D.T.A. plot of $[\text{Me}_2\text{Ga}\{\text{HNC}(\text{CF}_3)\text{NC}(\text{CF}_3)\text{NH}\}]$.

APPENDIX 2

X-ray Crystallographic Studies

APPENDIX 2 X-ray Crystallographic Studies

Crystals were grown and mounted by the author. The X-ray crystallographic structure determinations carried out at the University of Warwick described in this work were performed by the author with the help and expert guidance of Drs. W. Errington and N.W. Alcock. The data for the remaining studies described in this work were collected by the EPSRC Crystallographic Service, University of Wales, Cardiff and analysis of the data was carried out by the author.

General Method

All of the crystals used, with the exception of N,N'-diphenylacetamide, were assumed to be air / moisture sensitive and were handled as follows. The crystals were placed under dry paraffin oil to protect them from air and moisture exposure and suitable examples were picked using a glass fibre with the aid of a microscope on the bench. The crystals used were mounted under an argon atmosphere in thin walled quartz Lindemann tubes (0.5 and 1.0 mm diameter) and held in place with a trace of silicon grease. The ends of the Lindemann tubes were heat sealed and further protected with wax. This procedure gave good protection from any deterioration of even the more air sensitive crystals used, provided manipulations were rapid.

The diffraction data for compounds 2, 4, 5, 7, 8 and 10 reported within the tables that follow were collected on a Siemens P3R3 four-circle diffractometer in the ω -2 θ mode, operating with Mo-K α graphite monochromatised radiation, $\lambda = 0.71073\text{\AA}$. Three standard reflections were monitored after every 200 reflections and the data rescaled to correct for any changes in the intensity of these standards that occurred during the data collection. Unit cell dimensions and standard deviations were generally obtained by least squares fit to around 15 high angle reflections. For the data collection, all the reflections were used in the refinement of the structures. They were corrected for Lorentz polarisation and absorption effects using the Analytical method. The structure solution and refinement of each compound is described individually below. Final refinement was

by least squares methods, with anisotropic thermal parameters for all non-H atoms. A weighting scheme of the form $w = 1/[\sigma^2(F_o^2) + (aP)^2 + bP]$ where $P = (F_o^2 + 2F_c^2)/3$ was used and shown to be satisfactory by weight analysis. Computing work for structure solution was carried out using SHELXTL PLUS on a DEC Microvax II.²⁶⁵ Refinement was made using SHELXL 93,²⁶⁶ on a IBM compatible 486 personnel computer. Scattering factors and anomalous dispersion factors were taken from the literature.²⁶⁷

The diffraction data for compounds 1, 3, 6, 9 and 11 were collected by a Delft Instruments FAST TV area detector diffractometer at the EPSRC Crystallographic centre, Cardiff, which is run by Professor M.B. Hursthouse. Structure solution and refinement followed a similar procedure to above.

The unit cell data and the data collection parameters for all of the compounds are given below.

Bond lengths and angles for all non-hydrogen atoms of each compound are listed separately in the tables that follow the description of each structure refinement. For unpublished structures {i.e. all except [MeGa(PhNCPhNPh)₂] and [ClIn(tmtaa)]}, supplementary material comprising atomic co-ordinates of all atoms, thermal parameters and structure factor parameters, can be obtained from Prof. M. G. H Wallbridge (University of Warwick).

Compound	1 [Me ₂ In(PhNCPPhNPh)]	2 [Me ₂ Ga(PhNCPPhNPh) (4-Bu ^t -pyridine)]
Formula	C ₂₁ H ₂₁ InN ₂	C ₃₀ H ₃₄ N ₃ Ga
Molecular weight	416.22	506.34
Crystal system	Orthorhombic	Monoclinic
Space group	P2(1)2(1)2(1)	C2/c
a (Å)	17.262(7)	30.371(13)
b (Å)	34.226(14)	9.982(5)
c (Å)	6.602(5)	20.925(9)
α (°)	90	90
β (°)	90	120.07(3)
γ (°)	90	90
U (Å ³)	3901(4)	5490(4)
Temperature (K)	293(2)	298(2)
Z	8	4
D _c (g cm ⁻³)	1.418	1.225
μ (mm ⁻¹)	1.215	1.02
θ _{min} , θ _{max} (°)	2.14, 24.94	1.99, 24.05
Index ranges	-19/20, -23/40, -7/7	0/34, 0/11, -23/20
Number of data collected	14688	4418
Independent reflections	6034	4333
Absorption correction	–	Analytical
Max., min. transmission	–	0.74, 0.64
R1 (F) [I > 2σ(I)]	0.0479 (R[int] = 0.1619)	0.0471 (R[int] = 0.476)
wR2 (F ²) (all data)	0.0883	0.1313
Goodness of fit on F ²	0.904	1.045
Largest diff. peak & hole (e Å ⁻³)	1.093, -0.395	0.430, -0.347
Data, restraints, parameters	6030/30/433	4330/21/308

	(3)	(4)
Compound	[MeAl(PhNCPPhNPh) ₂]	[MeGa(PhNCPPhNPh) ₂]
Formula	C ₃₉ H ₃₃ N ₄ Al	C ₃₉ H ₃₃ N ₄ Ga
Molecular weight	584.67	627.41
Crystal system	Monoclinic	Triclinic
Space group	C2/c	P $\bar{1}$
a (Å)	24.974(7)	10.206(5)
b (Å)	5.823(2)	10.511(6)
c (Å)	25.173(7)	14.799(9)
α (°)	90	96.89(5)
β (°)	115.86(5)	94.28(4)
γ (°)	90	90.58(4)
U (Å ³)	3294(2)	1571(2)
Temperature (K)	293(2)	293(2)
Z	4	2
D _c (g cm ⁻³)	1.179	1.326
μ (mm ⁻¹)	0.09	0.910
θ_{\min} , θ_{\max} (°)	1.80, 24.96	2.0, 22.1
Index ranges	-26/27, -4/6, -27/25	0/10, -11/11, -15/15
Number of data collected	7175	4152
Independent reflections	2544 R[(int) = 0.0866]	3884 [R(int) = 0.02]
Absorption correction	–	Analytical
Max., min. transmission	–	0.75, 0.66
R1 (F) [I > 2 σ (I)]	0.0553	0.0297
wR2 (F ²) (all data)	0.1689	0.072
Goodness of fit on F ²	0.917	1.085
Largest diff. peak & hole (e Å ⁻³)	0.292/-0.407	±0.2
Data, restraints, parameters	2539/9/200	3883, 46, 399

	(5)	(6)
Compound	[EtGa(PhNCMeNPh) ₂]	[EtIn(PhNCPPhNPh) ₂]
Formula	C ₃₀ H ₃₁ N ₄ Ga	C ₄₀ H ₃₅ N ₄ In
Molecular weight	517.31	686.54
Crystal system	Monoclinic	Monoclinic
Space group	C2/c	Cc
a (Å)	21.715(14)	11.198(2)
b (Å)	15.077(12)	22.456(4)
c (Å)	17.460(11)	13.652(3)
α (°)	90	90
β (°)	115.25(5)	99.96(3)
γ (°)	90	90
U (Å ³)	5170(6)	3381.2(11)
Temperature (K)	230(2)	293(2)
Z	8	4
D _c (g cm ⁻³)	1.329	1.349
μ (mm ⁻¹)	1.09	0.730
θ _{min} , θ _{max} (°)	1.85, 27.56	1.81, 25.06
Index ranges	0/28, -1/19, -22/20	-12/8, -24/24, -12/15
Number of data collected	6572	7498
Independent reflections	5968 [R (int) = 0.0360]	3495 [R (int) = 0.046]
Absorption correction	–	–
Max., min. transmission	–	–
R1 (F) [I > 2σ(I)]	0.0538	0.0341
wR2 (F ²) (all data)	0.1465	0.0813
Goodness of fit on F ²	1.067	0.995
Largest diff. peak & hole (e Å ⁻³)	0.739/-0.653	0.749/-0.287
Data, restraints, parameters	5963/0/316	3495/20/406

Compound	(7) [In(PhNCPPhNPh) ₃]	(8) [Me ₂ Ga(HNC{CF ₃ }NC{CF ₃ }NH)]
Formula	C ₅₇ H ₄₅ N ₆ In	C ₆ H ₈ N ₃ F ₆ Ga
Molecular weight	928.81	305.87
Crystal system	Monoclinic	Orthorhombic
Space group	P2 ₁ /n	P $\bar{4}$ 2 ₁ c
a (Å)	10.868(7)	15.356(5)
b (Å)	22.72(2)	15.356(5)
c (Å)	19.321(12)	9.681(5)
α (°)	90	90
β (°)	105.221(5)	90
γ (°)	90	90
U (Å ³)	4609(5)	2283(2)
Temperature (K)	240(2)	240(2)
Z	4	8
D _c (g cm ⁻³)	1.339	1.780
μ (mm ⁻¹)	0.560	2.468
θ_{\min} , θ_{\max} (°)	1.79, 24.07	1.88, 25.04
Index ranges	0/11, 0/26, -22/21	-12/1, -12/1, -11/0
Number of data collected	6786	1894
Independent reflections	6364 [R (int) = 0.0486]	964 [R (int) = 0.1273]
Absorption correction	Analytical	—
Max., min. transmission	0.88, 0.94	—
R1 (F) [I > 2 σ (I)]	0.0579	0.0553
wR2 (F ²) (all data)	0.1376	0.1164
Goodness of fit on F ²	1.000	1.032
Largest diff. peak & hole (e Å ⁻³)	0.471/-0.670	0.579/-0.404
Data, restraints, parameters	6347/27/577	959/0/145

	(9)	(10)
Compound	[EtIn(tmtaa)]	[ClIn(tmtaa)]
Formula	C ₂₄ H ₂₇ N ₄ In	C ₂₂ H ₂₂ N ₄ ClIn
Molecular weight	486.32	492.71
Crystal system	Monoclinic	Monoclinic
Space group	P2 ₁ /n	P2 ₁ /c
a (Å)	10.014(2)	8.927(4)
b (Å)	16.092(3)	22.457(7)
c (Å)	13.507(3)	10.209(3)
α (°)	90	90.0
β (°)	94.98	101.34(3)
γ (°)	90	90.0
U (Å ³)	2168.4(8)	2006.7(12)
Temperature (K)	140(2)	220(0.2)
Z	4	4
D _c (g cm ⁻³)	1.4909	1.631
μ (mm ⁻¹)	1.107	1.33
θ _{min} , θ _{max} (°)	1.97, 25.08	
Index ranges	-11/10, -17/17, -15/14	0/10, 0/26, -12/11
Number of data collected	9346	3700
Independent reflections	3269 [R (int) = 0.0739]	3472 [R (int) = 0.0417]
Absorption correction	–	Analytical
Max., min. transmission	–	0.81, 0.86
R1 (F) [I > 2σ(I)]	0.0395	0.0472
wR2 (F ²) (all data)	0.0923	0.1460
Goodness of fit on F ²	0.872	1.070
Largest diff. peak & hole (e Å ⁻³)	1.102/-0.438	0.827/-1.524
Data, restraints, parameters	3266/0/262	3463/0/266

	(11)	(12)
Compound	[CpIn(tmtaa)]	PhN(H)CMeNPh
Formula	C ₂₇ H ₂₇ N ₄ In	C ₁₄ H ₁₄ N ₂
Molecular weight	522.35	210.27
Crystal system	Monoclinic	Orthorhombic
Space group	P2 ₁ /n	Pbca
a (Å)	10.283(7)	10.903(2)
b (Å)	15.545(7)	8.603(2)
c (Å)	13.864(2)	26.175(5)
α (°)	90	90
β (°)	92.04(9)	90
γ (°)	90	90
U (Å ³)	2215(2)	2455.2(9)
Temperature (K)	150(2)	293(2)
Z	4	8
D _c (g cm ⁻³)	1.567	1.138
μ (mm ⁻¹)	1.090	0.068
θ _{min} , θ _{max} (°)	1.97, 25.08	2.43, 25.18
Index ranges	-11/8, -17/17, -12/15	-12/11, -9/8, -25/30
Number of data collected	9430	10316
Independent reflections	3372 [R (int) = 0.0690]	2011 [R(int) = 0.0922]
Absorption correction	–	–
Max., min. transmission	–	–
R1 (F) [I > 2σ(I)]	0.0406	0.0458
wR2 (F ²) (all data)	0.0970	0.1149
Goodness of fit on F ²	0.949	0.665
Largest diff. peak & hole (e Å ⁻³)	1.334/-0.454	0.134, -0.103
Data, restraints, parameters	3369/0/289	2007/7/145

Dimethylindium–N,N'–diphenylbenzamidinato

Space group $P2_12_12_1$ was assumed and shown to be correct by satisfactory refinement. Two crystallographically independent indium-containing molecules were found in the unit cell, which differed essentially only in the orientation of the phenyl rings of the amidinato ligand. The structure was solved by the heavy-atom method; the position of the indium atoms were obtained from a Patterson synthesis, and the positions of the remaining non-H atoms determined from a Fourier map using SHELXTL PLUS. Hydrogen atoms were added at calculated positions and refined using a riding model. Anisotropic displacement parameters were used for all non-H atoms. H atoms were given isotropic displacement parameters equal to $U = 0.08 \text{ \AA}^2$. The phenyl groups were restrained to be flat with C_{2v} symmetry. The two indium–nitrogen bond distances within each molecule were restrained to be equal.

Table 2 Bond lengths [Å] for [Me₂In(PhNCPhNPh)].

In(1)-C(12)	2.142(6)	In(1)-C(13)	2.138(7)
In(1)-N(11)	2.239(4)	In(1)-N(12)	2.265(4)
In(2)-C(22)	2.133(6)	In(2)-C(23)	2.143(6)
In(2)-N(22)	2.249(4)	In(2)-N(21)	2.258(5)
N(11)-C(11)	1.328(8)	N(11)-C(111)	1.404(8)
N(12)-C(11)	1.314(8)	N(12)-C(131)	1.416(8)
N(21)-C(21)	1.349(8)	N(21)-C(211)	1.420(8)
N(22)-C(21)	1.302(7)	N(22)-C(231)	1.436(7)
C(11)-C(121)	1.514(8)	C(21)-C(221)	1.487(8)
C(111)-C(112)	1.386(9)	C(111)-C(116)	1.390(8)
C(112)-C(113)	1.361(9)	C(113)-C(114)	1.399(11)
C(114)-C(115)	1.341(11)	C(115)-C(116)	1.370(9)
C(121)-C(126)	1.354(9)	C(121)-C(122)	1.385(10)
C(122)-C(123)	1.390(10)	C(123)-C(124)	1.371(13)
C(124)-C(125)	1.356(14)	C(125)-C(126)	1.391(13)
C(131)-C(136)	1.396(9)	C(131)-C(132)	1.389(9)
C(132)-C(133)	1.359(9)	C(133)-C(134)	1.353(12)
C(134)-C(135)	1.358(12)	C(135)-C(136)	1.406(11)
C(211)-C(212)	1.387(8)	C(211)-C(216)	1.378(9)
C(212)-C(213)	1.403(11)	C(213)-C(214)	1.283(13)
C(214)-C(215)	1.398(12)	C(215)-C(216)	1.376(10)
C(221)-C(226)	1.331(10)	C(221)-C(222)	1.398(10)
C(222)-C(223)	1.390(13)	C(223)-C(224)	1.37(2)
C(224)-C(225)	1.36(2)	C(225)-C(226)	1.331(13)
C(231)-C(236)	1.370(8)	C(231)-C(232)	1.394(9)
C(232)-C(233)	1.353(10)	C(233)-C(234)	1.370(11)
C(234)-C(235)	1.357(11)	C(235)-C(236)	1.387(9)

Table 3 Bond angles [°] for [Me₂In(PhNCPhNPh)].

C(12)-In(1)-C(13)	125.2(3)	C(12)-In(1)-N(11)	116.8(3)
C(13)-In(1)-N(11)	111.6(3)	C(12)-In(1)-N(12)	112.5(2)
C(13)-In(1)-N(12)	113.6(3)	N(11)-In(1)-N(12)	58.8(2)
C(22)-In(2)-C(23)	130.9(3)	C(22)-In(2)-N(22)	107.7(2)
C(23)-In(2)-N(22)	113.3(3)	C(22)-In(2)-N(21)	112.4(2)
C(23)-In(2)-N(21)	111.4(2)	N(22)-In(2)-N(21)	58.9(2)
C(11)-N(11)-C(111)	125.2(5)	C(11)-N(11)-In(1)	94.2(4)
C(111)-N(11)-In(1)	140.3(4)	C(11)-N(12)-C(131)	125.2(5)
C(11)-N(12)-In(1)	93.5(4)	C(131)-N(12)-In(1)	141.1(4)
C(21)-N(21)-C(211)	123.4(5)	C(21)-N(21)-In(2)	93.0(4)
C(211)-N(21)-In(2)	140.6(4)	C(21)-N(22)-C(231)	126.5(5)
C(21)-N(22)-In(2)	94.7(4)	C(231)-N(22)-In(2)	138.5(4)
N(12)-C(11)-N(11)	113.6(5)	N(12)-C(11)-C(121)	124.9(6)
N(11)-C(11)-C(121)	121.5(6)	N(22)-C(21)-N(21)	113.3(5)
N(22)-C(21)-C(221)	125.4(6)	N(21)-C(21)-C(221)	121.3(6)
C(112)-C(111)-C(116)	116.6(6)	C(112)-C(111)-N(11)	124.4(6)
C(113)-C(112)-C(111)	120.9(7)	C(112)-C(113)-C(114)	119.9(7)
C(115)-C(114)-C(113)	120.7(7)	C(114)-C(115)-C(116)	118.4(7)
C(115)-C(116)-C(111)	123.2(7)	C(126)-C(121)-C(122)	120.8(6)
C(126)-C(121)-C(11)	121.0(7)	C(122)-C(121)-C(11)	118.2(6)
C(121)-C(122)-C(123)	117.6(9)	C(124)-C(123)-C(122)	121.6(10)
C(125)-C(124)-C(123)	119.6(8)	C(124)-C(125)-C(126)	119.6(9)
C(121)-C(126)-C(125)	120.7(9)	C(136)-C(131)-C(132)	117.4(6)
C(136)-C(131)-N(12)	123.7(6)	C(132)-C(131)-N(12)	118.9(6)
C(133)-C(132)-C(131)	121.7(7)	C(134)-C(133)-C(132)	120.7(8)
C(133)-C(134)-C(135)	120.3(8)	C(134)-C(135)-C(136)	120.1(8)
C(135)-C(136)-C(131)	119.7(7)	C(212)-C(211)-C(216)	118.9(7)
C(212)-C(211)-N(21)	118.2(7)	C(216)-C(211)-N(21)	122.9(6)
C(211)-C(212)-C(213)	117.5(8)	C(214)-C(213)-C(212)	122.5(9)
C(213)-C(214)-C(215)	122.1(9)	C(214)-C(215)-C(216)	116.7(9)
C(211)-C(216)-C(215)	122.1(7)	C(226)-C(221)-C(222)	118.6(7)
C(226)-C(221)-C(21)	122.7(8)	C(222)-C(221)-C(21)	118.7(7)
C(221)-C(222)-C(223)	118.9(8)	C(224)-C(223)-C(222)	119.3(10)
C(223)-C(224)-C(225)	120.2(11)	C(224)-C(225)-C(226)	119.7(11)
C(221)-C(226)-C(225)	123.3(10)	C(236)-C(231)-C(232)	119.1(6)
C(236)-C(231)-N(22)	116.9(6)	C(232)-C(231)-N(22)	124.0(6)
C(233)-C(232)-C(231)	120.4(7)	C(232)-C(233)-C(234)	120.3(7)
C(235)-C(234)-C(233)	120.2(8)	C(234)-C(235)-C(236)	120.2(8)
C(231)-C(236)-C(235)	119.7(7)		

Dimethylgallium–N,N′–diphenylbenzamidinato.4–*tert*–butyl–pyridine

Space group $C2/c$ was assumed and shown to be correct by satisfactory refinement. The structure was solved by direct methods using SHELXTL PLUS. Hydrogen atoms were added at calculated positions and refined using a riding model. Anisotropic displacement parameters were used for all non-H atoms. H atoms were given isotropic displacement parameters equal to $U = 0.08 \text{ \AA}^2$. The phenyl groups were restrained to be flat with C_{2v} symmetry. The C–Me bonds of the Bu^t group were restrained to be equal in length.

Table 4 Bond lengths [Å] for [Me₂Ga(PhNCPhNPh)(4-Bu^t-pyridine)].

Ga(1)-C(3)	1.950(4)	Ga(1)-C(2)	1.963(5)
Ga(1)-N(1)	2.010(3)	Ga(1)-N(3)	2.210(3)
Ga(1)-N(2)	2.347(3)	N(1)-C(1)	1.344(5)
N(1)-C(11)	1.414(5)	N(2)-C(1)	1.312(5)
N(2)-C(21)	1.394(5)	N(3)-C(45)	1.329(5)
N(3)-C(41)	1.343(5)	C(1)-C(31)	1.491(5)
C(11)-C(12)	1.376(5)	C(11)-C(16)	1.384(5)
C(12)-C(13)	1.373(6)	C(13)-C(14)	1.357(6)
C(14)-C(15)	1.374(6)	C(15)-C(16)	1.380(5)
C(21)-C(22)	1.392(5)	C(21)-C(26)	1.398(6)
C(22)-C(23)	1.376(6)	C(23)-C(24)	1.372(7)
C(24)-C(25)	1.368(7)	C(25)-C(26)	1.383(6)
C(31)-C(36)	1.372(5)	C(31)-C(32)	1.384(5)
C(32)-C(33)	1.380(6)	C(33)-C(34)	1.362(7)
C(34)-C(35)	1.353(7)	C(35)-C(36)	1.386(6)
C(41)-C(42)	1.361(5)	C(42)-C(43)	1.376(6)
C(43)-C(44)	1.386(6)	C(43)-C(46)	1.518(6)
C(44)-C(45)	1.372(6)	C(46)-C(48)	1.493(5)
C(46)-C(49)	1.493(6)	C(46)-C(47)	1.499(6)

Table 5 Bond angles [°] for [Me₂Ga(PhNCPhNPh)(4-Bu^t-pyridine)].

C(3)-Ga(1)-C(2)	124.7(2)	C(3)-Ga(1)-N(1)	115.8(2)
C(2)-Ga(1)-N(1)	117.2(2)	C(3)-Ga(1)-N(3)	99.5(2)
C(2)-Ga(1)-N(3)	95.6(2)	N(1)-Ga(1)-N(3)	89.32(12)
C(3)-Ga(1)-N(2)	99.4(2)	C(2)-Ga(1)-N(2)	93.7(2)
N(1)-Ga(1)-N(2)	60.07(12)	N(3)-Ga(1)-N(2)	148.80(12)
C(1)-N(1)-C(11)	123.6(3)	C(1)-N(1)-Ga(1)	101.1(2)
C(11)-N(1)-Ga(1)	131.4(2)	C(1)-N(2)-C(21)	125.5(3)
C(1)-N(2)-Ga(1)	86.8(2)	C(21)-N(2)-Ga(1)	147.2(3)
C(45)-N(3)-C(41)	115.9(3)	C(45)-N(3)-Ga(1)	125.8(3)
C(41)-N(3)-Ga(1)	117.9(3)	N(2)-C(1)-N(1)	111.9(3)
N(2)-C(1)-C(31)	125.3(3)	N(1)-C(1)-C(31)	122.8(3)
C(12)-C(11)-C(16)	117.3(4)	C(12)-C(11)-N(1)	123.3(4)
C(16)-C(11)-N(1)	119.2(3)	C(13)-C(12)-C(11)	121.7(4)
C(14)-C(13)-C(12)	120.7(4)	C(13)-C(14)-C(15)	118.7(4)
C(14)-C(15)-C(16)	120.8(4)	C(15)-C(16)-C(11)	120.6(4)
C(22)-C(21)-N(2)	124.8(4)	C(22)-C(21)-C(26)	117.8(4)
N(2)-C(21)-C(26)	117.2(4)	C(23)-C(22)-C(21)	121.1(4)
C(24)-C(23)-C(22)	120.0(4)	C(25)-C(24)-C(23)	120.3(4)
C(24)-C(25)-C(26)	120.2(4)	C(25)-C(26)-C(21)	120.5(4)
C(36)-C(31)-C(32)	118.6(4)	C(36)-C(31)-C(1)	121.8(3)
C(32)-C(31)-C(1)	119.6(4)	C(33)-C(32)-C(31)	120.3(4)
C(34)-C(33)-C(32)	120.4(5)	C(35)-C(34)-C(33)	119.7(5)
C(34)-C(35)-C(36)	120.8(5)	C(31)-C(36)-C(35)	120.2(4)
N(3)-C(41)-C(42)	123.5(4)	C(41)-C(42)-C(43)	121.2(4)
C(42)-C(43)-C(44)	115.0(4)	C(42)-C(43)-C(46)	122.0(4)
C(44)-C(43)-C(46)	123.0(4)	C(45)-C(44)-C(43)	121.0(4)
N(3)-C(45)-C(44)	123.3(4)	C(48)-C(46)-C(49)	112.3(6)
C(48)-C(46)-C(47)	105.7(5)	C(49)-C(46)-C(47)	107.5(6)
C(48)-C(46)-C(43)	112.1(4)	C(49)-C(46)-C(43)	107.1(4)
C(47)-C(46)-C(43)	112.1(4)		

Methylaluminium–bis(N,N'–diphenylbenzamidinato)

Space group $C2/c$ was assumed and shown to be correct by satisfactory refinement. The structure was readily solved by direct methods using SHELXTL PLUS. Hydrogen atoms were added at calculated positions and refined using a riding model. Anisotropic displacement parameters were used for all non-H atoms. H atoms were given isotropic displacement parameters equal to $U = 0.08 \text{ \AA}^2$.

Table 6 Bond lengths [\AA] and angles [$^\circ$] for $[\text{MeAl}(\text{PhNCPPhNPh})_2]$.

Al(1)-C(2)	1.941(4)	Al(1)-N(2)#1	1.963(2)
Al(1)-N(2)	1.963(2)	Al(1)-N(1)	1.993(2)
Al(1)-N(1)#1	1.993(2)	Al(1)-C(1)#1	2.414(3)
N(1)-C(1)	1.320(3)	N(1)-C(11)	1.400(3)
N(2)-C(1)	1.318(3)	N(2)-C(31)	1.431(4)
C(1)-C(21)	1.494(4)	C(11)-C(12)	1.383(4)
C(11)-C(16)	1.391(4)	C(12)-C(13)	1.377(4)
C(13)-C(14)	1.375(4)	C(14)-C(15)	1.359(4)
C(15)-C(16)	1.385(4)	C(21)-C(22)	1.374(4)
C(21)-C(26)	1.386(4)	C(22)-C(23)	1.372(4)
C(23)-C(24)	1.373(4)	C(24)-C(25)	1.364(5)
C(25)-C(26)	1.372(5)	C(31)-C(36)	1.371(4)
C(31)-C(32)	1.375(5)	C(32)-C(33)	1.382(6)
C(33)-C(34)	1.351(6)	C(34)-C(35)	1.361(7)
C(35)-C(36)	1.365(5)		
C(2)-Al(1)-N(2)#1	113.81(7)	C(2)-Al(1)-N(2)	113.81(7)
N(2)#1-Al(1)-N(2)	132.37(14)	C(2)-Al(1)-N(1)	105.88(7)
N(2)#1-Al(1)-N(1)	100.59(10)	N(2)-Al(1)-N(1)	66.13(10)
C(2)-Al(1)-N(1)#1	105.88(7)	N(2)#1-Al(1)-N(1)#1	66.13(10)
N(2)-Al(1)-N(1)#1	100.59(10)	N(1)-Al(1)-N(1)#1	148.23(13)
C(2)-Al(1)-C(1)#1	112.25(6)	N(2)#1-Al(1)-C(1)#1	33.06(9)
N(2)-Al(1)-C(1)#1	122.16(10)	N(1)-Al(1)-C(1)#1	129.06(9)
N(1)#1-Al(1)-C(1)#1	33.13(9)	C(1)-N(1)-C(11)	127.7(2)
C(1)-N(1)-Al(1)	91.2(2)	C(11)-N(1)-Al(1)	140.9(2)
C(1)-N(2)-C(31)	124.7(2)	C(1)-N(2)-Al(1)	92.6(2)
C(31)-N(2)-Al(1)	140.8(2)	N(2)-C(1)-N(1)	109.8(2)
N(2)-C(1)-C(21)	125.0(2)	N(1)-C(1)-C(21)	125.2(3)
C(12)-C(11)-C(16)	117.6(3)	C(12)-C(11)-N(1)	118.6(3)
C(16)-C(11)-N(1)	123.6(3)	C(13)-C(12)-C(11)	121.0(3)
C(14)-C(13)-C(12)	120.8(3)	C(15)-C(14)-C(13)	118.9(3)
C(14)-C(15)-C(16)	121.0(3)	C(15)-C(16)-C(11)	120.6(3)
C(22)-C(21)-C(26)	119.1(3)	C(22)-C(21)-C(1)	119.9(3)
C(26)-C(21)-C(1)	121.0(3)	C(23)-C(22)-C(21)	120.7(3)
C(22)-C(23)-C(24)	119.8(3)	C(25)-C(24)-C(23)	120.1(3)
C(24)-C(25)-C(26)	120.4(3)	C(25)-C(26)-C(21)	119.9(3)
C(36)-C(31)-C(32)	118.5(3)	C(36)-C(31)-N(2)	119.2(3)
C(32)-C(31)-N(2)	122.3(3)	C(31)-C(32)-C(33)	120.0(4)
C(34)-C(33)-C(32)	121.1(4)	C(33)-C(34)-C(35)	118.5(4)
C(34)-C(35)-C(36)	121.5(4)	C(35)-C(36)-C(31)	120.3(4)

Symmetry transformations used to generate equivalent atoms: #1 -x,y,-z+1/2

Methylgallium–bis(N,N'–diphenylbenzamidinato)

Space group $P\bar{1}$ was assumed and shown to be correct by satisfactory refinement. The structure was solved by direct methods using SHELXTL PLUS. Hydrogen atoms were added at calculated positions and refined using a riding model. Anisotropic displacement parameters were used for all non-H atoms. H atoms were given isotropic displacement parameters equal to $U = 0.08 \text{ \AA}^2$. The phenyl groups were restrained to be flat with C_{2v} symmetry.

Table 7 Bond lengths [Å] for [MeGa(PhNCPhNPh)₂]

Ga(1)-C(3)	1.940(3)	Ga(1)-N(2)	1.995(2)
Ga(1)-N(3)	2.009(2)	Ga(1)-N(1)	2.112(2)
Ga(1)-N(4)	2.141(2)	N(1)-C(1)	1.326(3)
N(1)-C(11)	1.399(3)	N(2)-C(1)	1.335(3)
N(2)-C(31)	1.409(3)	N(3)-C(2)	1.338(3)
N(3)-C(41)	1.410(3)	N(4)-C(2)	1.319(3)
N(4)-C(61)	1.409(3)	C(1)-C(21)	1.481(4)
C(2)-C(51)	1.479(4)	C(11)-C(16)	1.388(4)
C(11)-C(12)	1.391(4)	C(12)-C(13)	1.380(4)
C(13)-C(14)	1.378(4)	C(14)-C(15)	1.371(5)
C(15)-C(16)	1.379(4)	C(21)-C(26)	1.378(4)
C(21)-C(22)	1.382(4)	C(22)-C(23)	1.373(4)
C(23)-C(24)	1.367(5)	C(24)-C(25)	1.367(5)
C(25)-C(26)	1.389(4)	C(31)-C(32)	1.379(4)
C(31)-C(36)	1.384(4)	C(32)-C(33)	1.390(4)
C(33)-C(34)	1.363(5)	C(34)-C(35)	1.362(5)
C(35)-C(36)	1.374(4)	C(41)-C(46)	1.379(4)
C(41)-C(42)	1.390(4)	C(42)-C(43)	1.381(5)
C(43)-C(44)	1.360(6)	C(44)-C(45)	1.358(6)
C(45)-C(46)	1.380(5)	C(51)-C(52)	1.381(4)
C(51)-C(56)	1.384(4)	C(52)-C(53)	1.374(4)
C(53)-C(54)	1.368(5)	C(54)-C(55)	1.366(5)
C(55)-C(56)	1.379(4)	C(61)-C(66)	1.379(4)
C(61)-C(62)	1.383(4)	C(62)-C(63)	1.376(4)
C(63)-C(64)	1.362(4)	C(64)-C(65)	1.361(5)
C(65)-C(66)	1.370(4)		

Table 8 Bond angles [°] for [MeGa(PhNCPhNPh)₂]

C(3)-Ga(1)-N(2)	129.10(13)	C(3)-Ga(1)-N(3)	132.90(13)
N(2)-Ga(1)-N(3)	97.94(10)	C(3)-Ga(1)-N(1)	106.97(13)
N(2)-Ga(1)-N(1)	63.98(9)	N(3)-Ga(1)-N(1)	94.58(9)
C(3)-Ga(1)-N(4)	102.96(13)	N(2)-Ga(1)-N(4)	97.46(10)
N(3)-Ga(1)-N(4)	63.43(9)	N(1)-Ga(1)-N(4)	150.05(9)
C(1)-N(1)-C(11)	128.3(2)	C(1)-N(1)-Ga(1)	90.2(2)
C(11)-N(1)-Ga(1)	140.3(2)	C(1)-N(2)-C(31)	127.8(2)
C(1)-N(2)-Ga(1)	95.2(2)	C(31)-N(2)-Ga(1)	133.4(2)
C(2)-N(3)-C(41)	125.9(2)	C(2)-N(3)-Ga(1)	95.4(2)
C(41)-N(3)-Ga(1)	131.6(2)	C(2)-N(4)-C(61)	124.8(2)
C(2)-N(4)-Ga(1)	90.1(2)	C(61)-N(4)-Ga(1)	138.4(2)
N(1)-C(1)-N(2)	109.9(2)	N(1)-C(1)-C(21)	124.1(2)
N(2)-C(1)-C(21)	125.9(2)	N(4)-C(2)-N(3)	110.6(2)
N(4)-C(2)-C(51)	125.2(2)	N(3)-C(2)-C(51)	124.1(2)
C(16)-C(11)-C(12)	117.5(3)	C(16)-C(11)-N(1)	125.9(3)
C(12)-C(11)-N(1)	116.4(2)	C(13)-C(12)-C(11)	121.6(3)
C(14)-C(13)-C(12)	120.0(3)	C(15)-C(14)-C(13)	119.0(3)
C(14)-C(15)-C(16)	121.4(3)	C(15)-C(16)-C(11)	120.5(3)
C(26)-C(21)-C(22)	119.7(3)	C(26)-C(21)-C(1)	121.6(3)
C(22)-C(21)-C(1)	118.5(2)	C(23)-C(22)-C(21)	120.1(3)
C(24)-C(23)-C(22)	120.2(3)	C(25)-C(24)-C(23)	120.4(3)
C(24)-C(25)-C(26)	120.0(3)	C(21)-C(26)-C(25)	119.6(3)
C(32)-C(31)-C(36)	118.1(3)	C(32)-C(31)-N(2)	124.1(3)
C(36)-C(31)-N(2)	117.7(3)	C(31)-C(32)-C(33)	119.9(3)
C(34)-C(33)-C(32)	121.2(3)	C(35)-C(34)-C(33)	119.1(3)
C(34)-C(35)-C(36)	120.5(3)	C(35)-C(36)-C(31)	121.2(3)
C(46)-C(41)-C(42)	118.8(3)	C(46)-C(41)-N(3)	117.7(3)
C(42)-C(41)-N(3)	123.4(3)	C(43)-C(42)-C(41)	119.5(3)
C(44)-C(43)-C(42)	120.7(4)	C(45)-C(44)-C(43)	120.5(3)
C(44)-C(45)-C(46)	119.8(4)	C(41)-C(46)-C(45)	120.7(3)
C(52)-C(51)-C(56)	118.9(3)	C(52)-C(51)-C(2)	121.5(3)
C(56)-C(51)-C(2)	119.5(3)	C(53)-C(52)-C(51)	120.6(3)
C(54)-C(53)-C(52)	120.0(3)	C(55)-C(54)-C(53)	120.2(3)
C(54)-C(55)-C(56)	120.2(3)	C(55)-C(56)-C(51)	120.1(3)
C(66)-C(61)-C(62)	118.0(3)	C(66)-C(61)-N(4)	118.7(2)
C(62)-C(61)-N(4)	123.0(3)	C(63)-C(62)-C(61)	120.4(3)
C(64)-C(63)-C(62)	120.9(3)	C(65)-C(64)-C(63)	118.9(3)
C(64)-C(65)-C(66)	121.1(3)	C(65)-C(66)-C(61)	120.6(3)

Ethylgallium–bis(N,N'–diphenylacetamidinato)

Space group $C2/c$ was assumed and shown to be correct by satisfactory refinement. The structure was solved by direct methods using SHELXTL PLUS. Hydrogen atoms were added at calculated positions and refined using a riding model. Anisotropic displacement parameters were used for all non-H atoms. H atoms were given isotropic displacement parameters equal to $U = 0.08 \text{ \AA}^2$.

Table 9 Bond lengths [\AA] for $[\text{EtGa}(\text{PhNCMeNPh})_2]$.

Ga(1)-C(3)	1.983(5)	Ga(1)-N(2)	1.992(3)
Ga(1)-N(3)	1.996(3)	Ga(1)-N(1)	2.137(3)
Ga(1)-N(4)	2.159(3)	N(2)-C(1)	1.338(5)
N(2)-C(31)	1.401(4)	N(1)-C(1)	1.316(4)
N(1)-C(11)	1.412(5)	N(3)-C(2)	1.343(5)
N(3)-C(41)	1.403(4)	N(4)-C(2)	1.315(4)
N(4)-C(61)	1.408(5)	C(1)-C(21)	1.505(5)
C(2)-C(51)	1.494(5)	C(3)-C(4)	1.445(8)
C(11)-C(16)	1.391(5)	C(11)-C(12)	1.392(5)
C(12)-C(13)	1.374(5)	C(13)-C(14)	1.380(6)
C(14)-C(15)	1.395(6)	C(15)-C(16)	1.382(6)
C(31)-C(32)	1.396(5)	C(31)-C(36)	1.403(5)
C(32)-C(33)	1.385(6)	C(33)-C(34)	1.383(6)
C(34)-C(35)	1.390(7)	C(35)-C(36)	1.384(5)
C(41)-C(46)	1.393(5)	C(41)-C(42)	1.400(5)
C(42)-C(43)	1.376(5)	C(43)-C(44)	1.388(6)
C(44)-C(45)	1.372(6)	C(45)-C(46)	1.394(5)
C(61)-C(66)	1.392(5)	C(61)-C(62)	1.399(5)
C(62)-C(63)	1.384(6)	C(63)-C(64)	1.382(6)
C(64)-C(65)	1.375(6)	C(65)-C(66)	1.378(5)

Table 10 Bond angles [°] for [EtGa(PhNCMeNPh)₂].

C(3)-Ga(1)-N(2)	120.2(2)	C(3)-Ga(1)-N(3)	123.2(2)
N(2)-Ga(1)-N(3)	116.40(13)	C(3)-Ga(1)-N(1)	114.6(2)
N(2)-Ga(1)-N(1)	63.39(12)	N(3)-Ga(1)-N(1)	94.51(12)
C(3)-Ga(1)-N(4)	104.5(2)	N(2)-Ga(1)-N(4)	96.82(12)
N(3)-Ga(1)-N(4)	63.00(12)	N(1)-Ga(1)-N(4)	140.91(12)
C(1)-N(2)-C(31)	129.8(3)	C(1)-N(2)-Ga(1)	96.3(2)
C(31)-N(2)-Ga(1)	133.9(2)	C(1)-N(1)-C(11)	125.6(3)
C(1)-N(1)-Ga(1)	90.4(2)	C(11)-N(1)-Ga(1)	143.7(2)
C(2)-N(3)-C(41)	129.1(3)	C(2)-N(3)-Ga(1)	96.8(2)
C(41)-N(3)-Ga(1)	134.0(2)	C(2)-N(4)-C(61)	126.4(3)
C(2)-N(4)-Ga(1)	90.3(2)	C(61)-N(4)-Ga(1)	143.1(2)
N(1)-C(1)-N(2)	109.9(3)	N(1)-C(1)-C(21)	125.0(3)
N(2)-C(1)-C(21)	124.9(3)	N(4)-C(2)-N(3)	109.9(3)
N(4)-C(2)-C(51)	125.5(3)	N(3)-C(2)-C(51)	124.4(3)
C(4)-C(3)-Ga(1)	116.8(4)	C(16)-C(11)-C(12)	118.3(3)
C(16)-C(11)-N(1)	123.0(3)	C(12)-C(11)-N(1)	118.6(3)
C(13)-C(12)-C(11)	121.3(4)	C(12)-C(13)-C(14)	120.6(4)
C(13)-C(14)-C(15)	118.5(4)	C(16)-C(15)-C(14)	121.0(4)
C(15)-C(16)-C(11)	120.2(4)	C(32)-C(31)-N(2)	117.3(3)
C(32)-C(31)-C(36)	117.8(3)	N(2)-C(31)-C(36)	124.7(3)
C(33)-C(32)-C(31)	121.3(4)	C(34)-C(33)-C(32)	120.4(4)
C(33)-C(34)-C(35)	119.1(4)	C(36)-C(35)-C(34)	120.7(4)
C(35)-C(36)-C(31)	120.7(4)	C(46)-C(41)-C(42)	118.6(3)
C(46)-C(41)-N(3)	123.7(3)	C(42)-C(41)-N(3)	117.5(3)
C(43)-C(42)-C(41)	120.9(4)	C(42)-C(43)-C(44)	120.2(4)
C(45)-C(44)-C(43)	119.4(4)	C(44)-C(45)-C(46)	121.2(4)
C(41)-C(46)-C(45)	119.7(4)	C(66)-C(61)-C(62)	118.2(3)
C(66)-C(61)-N(4)	118.5(3)	C(62)-C(61)-N(4)	123.1(3)
C(63)-C(62)-C(61)	120.4(4)	C(64)-C(63)-C(62)	120.5(4)
C(65)-C(64)-C(63)	119.4(4)	C(64)-C(65)-C(66)	120.7(4)
C(65)-C(66)-C(61)	120.8(4)		

Ethylindium–bis(N,N'–diphenylbenzamidinato)

Space group Cc was assumed and shown to be correct by satisfactory refinement. The structure was solved by the heavy-atom method; the position of the indium atom was obtained from a Patterson synthesis, and the positions of the remaining non-H atoms determined from a Fourier map using SHELXTL PLUS. Hydrogen atoms were added at calculated positions and refined using a riding model. Anisotropic displacement parameters were used for all non-H atoms. H atoms were given isotropic displacement parameters equal to $U = 0.08 \text{ \AA}^2$. The phenyl groups were restrained to be flat with C_{2v} symmetry.

Table 11 Bond lengths [Å] for [EtIn(PhNCPhNPh)₂].

In(1)-C(3)	2.147(6)	In(1)-N(3)	2.169(5)
In(1)-N(2)	2.190(4)	In(1)-N(4)	2.314(4)
In(1)-N(1)	2.338(5)	N(1)-C(1)	1.330(7)
N(1)-C(11)	1.415(7)	N(2)-C(1)	1.334(7)
N(2)-C(31)	1.421(7)	N(3)-C(2)	1.350(7)
N(3)-C(41)	1.417(8)	N(4)-C(2)	1.311(7)
N(4)-C(61)	1.428(9)	C(1)-C(21)	1.495(9)
C(2)-C(51)	1.491(8)	C(3)-C(4)	1.526(11)
C(11)-C(16)	1.380(9)	C(11)-C(12)	1.381(8)
C(12)-C(13)	1.387(10)	C(13)-C(14)	1.395(14)
C(14)-C(15)	1.344(14)	C(15)-C(16)	1.369(11)
C(21)-C(22)	1.379(11)	C(21)-C(26)	1.387(11)
C(22)-C(23)	1.387(12)	C(23)-C(24)	1.393(13)
C(24)-C(25)	1.35(2)	C(25)-C(26)	1.363(13)
C(31)-C(32)	1.349(10)	C(31)-C(36)	1.386(9)
C(32)-C(33)	1.393(11)	C(33)-C(34)	1.383(13)
C(34)-C(35)	1.367(13)	C(35)-C(36)	1.382(11)
C(41)-C(42)	1.362(9)	C(41)-C(46)	1.391(9)
C(42)-C(43)	1.408(12)	C(43)-C(44)	1.341(14)
C(44)-C(45)	1.383(14)	C(45)-C(46)	1.360(10)
C(51)-C(52)	1.369(10)	C(51)-C(56)	1.399(9)
C(52)-C(53)	1.398(13)	C(53)-C(54)	1.39(2)
C(54)-C(55)	1.34(2)	C(55)-C(56)	1.366(13)
C(61)-C(66)	1.368(12)	C(61)-C(62)	1.413(12)
C(62)-C(63)	1.400(11)	C(63)-C(64)	1.363(14)
C(64)-C(65)	1.378(14)	C(65)-C(66)	1.371(11)

Table 12 Bond angles [°] for [EtIn(PhNCPPhNPh)₂].

C(3)-In(1)-N(3)	131.9(2)	C(3)-In(1)-N(2)	114.1(2)
N(3)-In(1)-N(2)	114.0(2)	C(3)-In(1)-N(4)	114.4(2)
N(3)-In(1)-N(4)	59.0(2)	N(2)-In(1)-N(4)	96.9(2)
C(3)-In(1)-N(1)	103.4(2)	N(3)-In(1)-N(1)	101.4(2)
N(2)-In(1)-N(1)	58.5(2)	N(4)-In(1)-N(1)	141.3(2)
C(1)-N(1)-C(11)	125.5(5)	C(1)-N(1)-In(1)	90.8(3)
C(11)-N(1)-In(1)	136.8(4)	C(1)-N(2)-C(31)	127.1(5)
C(1)-N(2)-In(1)	97.3(3)	C(31)-N(2)-In(1)	135.1(4)
C(2)-N(3)-C(41)	120.8(4)	C(2)-N(3)-In(1)	97.1(3)
C(41)-N(3)-In(1)	137.6(4)	C(2)-N(4)-C(61)	123.4(5)
C(2)-N(4)-In(1)	91.7(3)	C(61)-N(4)-In(1)	144.1(4)
N(1)-C(1)-N(2)	112.6(5)	N(1)-C(1)-C(21)	122.6(5)
N(2)-C(1)-C(21)	124.8(5)	N(4)-C(2)-N(3)	112.3(5)
N(4)-C(2)-C(51)	125.0(5)	N(3)-C(2)-C(51)	122.7(5)
C(4)-C(3)-In(1)	112.0(5)	C(16)-C(11)-C(12)	117.3(6)
C(16)-C(11)-N(1)	125.1(5)	C(12)-C(11)-N(1)	117.5(5)
C(11)-C(12)-C(13)	121.9(8)	C(12)-C(13)-C(14)	118.6(9)
C(15)-C(14)-C(13)	119.7(7)	C(14)-C(15)-C(16)	121.4(9)
C(15)-C(16)-C(11)	121.2(7)	C(22)-C(21)-C(26)	119.2(6)
C(22)-C(21)-C(1)	120.7(7)	C(26)-C(21)-C(1)	120.1(6)
C(21)-C(22)-C(23)	120.8(8)	C(22)-C(23)-C(24)	118.9(8)
C(25)-C(24)-C(23)	119.2(8)	C(24)-C(25)-C(26)	122.7(12)
C(25)-C(26)-C(21)	119.1(9)	C(32)-C(31)-C(36)	118.1(6)
C(32)-C(31)-N(2)	117.1(6)	C(36)-C(31)-N(2)	124.5(6)
C(31)-C(32)-C(33)	123.8(9)	C(34)-C(33)-C(32)	116.9(9)
C(35)-C(34)-C(33)	120.4(7)	C(34)-C(35)-C(36)	121.0(8)
C(35)-C(36)-C(31)	119.7(8)	C(42)-C(41)-C(46)	118.7(6)
C(42)-C(41)-N(3)	120.9(6)	C(46)-C(41)-N(3)	120.4(6)
C(41)-C(42)-C(43)	120.2(7)	C(44)-C(43)-C(42)	119.9(8)
C(43)-C(44)-C(45)	120.4(8)	C(46)-C(45)-C(44)	119.9(8)
C(45)-C(46)-C(41)	120.9(7)	C(52)-C(51)-C(56)	121.0(6)
C(52)-C(51)-C(2)	119.4(6)	C(56)-C(51)-C(2)	119.5(6)
C(51)-C(52)-C(53)	119.3(9)	C(54)-C(53)-C(52)	118.7(10)
C(55)-C(54)-C(53)	120.8(9)	C(54)-C(55)-C(56)	121.6(11)
C(55)-C(56)-C(51)	118.5(9)	C(66)-C(61)-C(62)	117.8(7)
C(66)-C(61)-N(4)	125.0(8)	C(62)-C(61)-N(4)	117.1(8)
C(63)-C(62)-C(61)	119.3(9)	C(64)-C(63)-C(62)	120.4(9)
C(63)-C(64)-C(65)	120.6(8)	C(66)-C(65)-C(64)	119.0(9)
C(61)-C(66)-C(65)	122.9(9)		

Indium–tris(N,N'–diphenylbenzamidinato)

Space group $P2_1/n$ was assumed and shown to be correct by satisfactory refinement. The structure was solved by the heavy-atom method; the position of the indium atom was obtained from a Patterson synthesis, and the positions of the remaining non-H atoms determined from a Fourier map using SHELXTL PLUS. Hydrogen atoms were added at calculated positions and refined using a riding model. Anisotropic displacement parameters were used for all non-H atoms. H atoms were given isotropic displacement parameters equal to $U = 0.08 \text{ \AA}^2$. The phenyl groups were restrained to be flat with C_{2v} symmetry.

Table 13 Bond lengths [Å] for [In(PhNCPPhNPh)₃].

In(1)-N(2)	2.217(5)	In(1)-N(4)	2.221(6)
In(1)-N(6)	2.242(7)	In(1)-N(5)	2.252(8)
In(1)-N(1)	2.260(6)	In(1)-N(3)	2.278(7)
N(1)-C(1)	1.313(9)	N(1)-C(11)	1.418(10)
N(2)-C(1)	1.336(10)	N(2)-C(31)	1.408(10)
N(3)-C(2)	1.335(10)	N(3)-C(41)	1.409(11)
N(4)-C(2)	1.315(10)	N(4)-C(61)	1.419(10)
N(5)-C(3)	1.333(10)	N(5)-C(71)	1.420(10)
N(6)-C(3)	1.338(11)	N(6)-C(91)	1.393(11)
C(1)-C(21)	1.486(10)	C(2)-C(51)	1.516(11)
C(3)-C(81)	1.479(9)	C(11)-C(16)	1.385(12)
C(11)-C(12)	1.387(11)	C(12)-C(13)	1.382(12)
C(13)-C(14)	1.367(13)	C(14)-C(15)	1.348(13)
C(15)-C(16)	1.381(12)	C(21)-C(22)	1.373(11)
C(21)-C(26)	1.395(11)	C(22)-C(23)	1.381(11)
C(23)-C(24)	1.372(11)	C(24)-C(25)	1.369(11)
C(25)-C(26)	1.380(10)	C(31)-C(36)	1.374(11)
C(31)-C(32)	1.406(12)	C(32)-C(33)	1.370(11)
C(33)-C(34)	1.366(12)	C(34)-C(35)	1.373(12)
C(35)-C(36)	1.378(11)	C(41)-C(42)	1.380(12)
C(41)-C(46)	1.394(13)	C(42)-C(43)	1.363(13)
C(43)-C(44)	1.39(2)	C(44)-C(45)	1.344(14)
C(45)-C(46)	1.378(13)	C(51)-C(52)	1.375(11)
C(51)-C(56)	1.395(12)	C(52)-C(53)	1.416(12)
C(53)-C(54)	1.384(14)	C(54)-C(55)	1.35(2)
C(55)-C(56)	1.365(12)	C(61)-C(66)	1.370(11)
C(61)-C(62)	1.380(10)	C(62)-C(63)	1.385(11)
C(63)-C(64)	1.386(12)	C(64)-C(65)	1.343(11)
C(65)-C(66)	1.386(11)	C(71)-C(72)	1.381(11)
C(71)-C(76)	1.393(11)	C(72)-C(73)	1.387(11)
C(73)-C(74)	1.375(12)	C(74)-C(75)	1.402(13)
C(75)-C(76)	1.367(11)	C(81)-C(86)	1.367(10)
C(81)-C(82)	1.405(11)	C(82)-C(83)	1.399(11)
C(83)-C(84)	1.368(12)	C(84)-C(85)	1.347(12)
C(85)-C(86)	1.386(11)	C(91)-C(92)	1.377(12)
C(91)-C(96)	1.401(13)	C(92)-C(93)	1.389(12)
C(93)-C(94)	1.369(13)	C(94)-C(95)	1.358(14)
C(95)-C(96)	1.382(13)		

Table 14 Bond angles [°] for [In(PhNCPhNPh)₃].

N(2)-In(1)-N(4)	149.3(2)	N(2)-In(1)-N(6)	114.9(3)
N(4)-In(1)-N(6)	93.0(3)	N(2)-In(1)-N(5)	107.5(2)
N(4)-In(1)-N(5)	97.5(2)	N(6)-In(1)-N(5)	59.1(2)
N(2)-In(1)-N(1)	59.1(3)	N(4)-In(1)-N(1)	104.2(3)
N(6)-In(1)-N(1)	102.5(3)	N(5)-In(1)-N(1)	152.4(3)
N(2)-In(1)-N(3)	103.0(3)	N(4)-In(1)-N(3)	58.9(3)
N(6)-In(1)-N(3)	136.0(2)	N(5)-In(1)-N(3)	89.5(3)
N(1)-In(1)-N(3)	116.2(2)	C(1)-N(1)-C(11)	123.4(7)
C(1)-N(1)-In(1)	93.3(5)	C(11)-N(1)-In(1)	141.5(5)
C(1)-N(2)-C(31)	125.9(6)	C(1)-N(2)-In(1)	94.7(5)
C(31)-N(2)-In(1)	135.5(6)	C(2)-N(3)-C(41)	126.5(8)
C(2)-N(3)-In(1)	91.8(5)	C(41)-N(3)-In(1)	141.1(6)
C(2)-N(4)-C(61)	126.2(7)	C(2)-N(4)-In(1)	94.9(5)
C(61)-N(4)-In(1)	133.9(5)	C(3)-N(5)-C(71)	124.0(8)
C(3)-N(5)-In(1)	93.4(5)	C(71)-N(5)-In(1)	136.5(6)
C(3)-N(6)-C(91)	124.9(8)	C(3)-N(6)-In(1)	93.7(5)
C(91)-N(6)-In(1)	141.3(7)	N(1)-C(1)-N(2)	112.9(7)
N(1)-C(1)-C(21)	123.7(8)	N(2)-C(1)-C(21)	123.3(7)
N(4)-C(2)-N(3)	113.3(7)	N(4)-C(2)-C(51)	123.7(7)
N(3)-C(2)-C(51)	123.0(8)	N(5)-C(3)-N(6)	112.1(6)
N(5)-C(3)-C(81)	122.9(9)	N(6)-C(3)-C(81)	124.8(9)
C(16)-C(11)-C(12)	117.3(9)	C(16)-C(11)-N(1)	120.5(9)
C(12)-C(11)-N(1)	122.1(9)	C(13)-C(12)-C(11)	121.0(9)
C(14)-C(13)-C(12)	120.9(9)	C(15)-C(14)-C(13)	118.2(10)
C(14)-C(15)-C(16)	122.5(10)	C(15)-C(16)-C(11)	120.1(10)
C(22)-C(21)-C(26)	119.5(8)	C(22)-C(21)-C(1)	121.6(9)
C(21)-C(22)-C(23)	120.7(9)	C(24)-C(23)-C(22)	119.4(9)
C(25)-C(24)-C(23)	120.7(8)	C(24)-C(25)-C(26)	120.3(9)
C(25)-C(26)-C(21)	119.3(8)	C(36)-C(31)-C(32)	118.4(8)
C(36)-C(31)-N(2)	119.7(8)	C(32)-C(31)-N(2)	121.6(8)
C(33)-C(32)-C(31)	119.4(9)	C(34)-C(33)-C(32)	122.3(10)
C(33)-C(34)-C(35)	117.8(9)	C(34)-C(35)-C(36)	121.7(9)
C(31)-C(36)-C(35)	120.3(9)	C(42)-C(41)-C(46)	117.4(10)
C(42)-C(41)-N(3)	117.0(10)	C(46)-C(41)-N(3)	125.1(10)
C(43)-C(42)-C(41)	121.2(11)	C(42)-C(43)-C(44)	120.8(11)
C(45)-C(44)-C(43)	118.6(10)	C(44)-C(45)-C(46)	121.5(12)
C(45)-C(46)-C(41)	120.4(11)	C(52)-C(51)-C(56)	120.4(9)
C(52)-C(51)-C(2)	118.7(8)	C(56)-C(51)-C(2)	120.5(8)
C(51)-C(52)-C(53)	119.3(10)	C(54)-C(53)-C(52)	117.6(10)
C(55)-C(54)-C(53)	123.0(11)	C(54)-C(55)-C(56)	119.6(11)
C(55)-C(56)-C(51)	120.1(10)	C(66)-C(61)-C(62)	118.7(9)
C(66)-C(61)-N(4)	117.9(8)	C(62)-C(61)-N(4)	123.4(8)
C(61)-C(62)-C(63)	119.7(10)	C(62)-C(63)-C(64)	120.7(9)
C(65)-C(64)-C(63)	119.2(9)	C(64)-C(65)-C(66)	120.4(9)
C(61)-C(66)-C(65)	121.1(9)	C(72)-C(71)-C(76)	118.5(8)

C(72)-C(71)-N(5)	122.8(8)	C(76)-C(71)-N(5)	118.6(8)
C(71)-C(72)-C(73)	120.4(8)	C(74)-C(73)-C(72)	121.7(9)
C(73)-C(74)-C(75)	117.3(9)	C(76)-C(75)-C(74)	121.4(9)
C(75)-C(76)-C(71)	120.6(9)	C(86)-C(81)-C(82)	119.2(7)
C(86)-C(81)-C(3)	120.4(8)	C(82)-C(81)-C(3)	120.3(7)
C(83)-C(82)-C(81)	118.7(8)	C(84)-C(83)-C(82)	119.6(9)
C(85)-C(84)-C(83)	122.2(9)	C(84)-C(85)-C(86)	118.8(9)
C(81)-C(86)-C(85)	121.5(8)	C(92)-C(91)-N(6)	126.2(10)
C(92)-C(91)-C(96)	116.3(9)	N(6)-C(91)-C(96)	117.3(9)
C(91)-C(92)-C(93)	122.3(10)	C(94)-C(93)-C(92)	119.6(10)
C(95)-C(94)-C(93)	119.7(11)	C(94)-C(95)-C(96)	120.7(11)
C(95)-C(96)-C(91)	121.2(11)		

Dimethylgallium–N,N′–trifluoroacetimidoyltrifluoroacetamidinato

Systematic reflection conditions $hhl, l = 2n; h00, h = 2n$ indicate space group $P\bar{4}2_1c$. The structure was solved by direct methods using SHELXTL (TREF). H atoms were added at calculated positions and refined using a riding model. Anisotropic displacement parameters were used for all non-H atoms. H atoms were given isotropic displacement parameters equal to $U = 0.08 \text{ \AA}^2$. The NH hydrogen atoms were not clearly visible on difference Fourier maps, but the orientation of the CF_3 groups and the bond length parameters within the imidoamidinato ring indicated NH positions associated with N(1) and N(3).

Table 15 Bond lengths [Å] and angles [°] for [Me₂Ga{HNC(CF₃)NC(CF₃)NH}].

Ga(1)-C(5)	1.900(12)	Ga(1)-C(6)	1.93(2)
Ga(1)-N(1)	1.992(9)	Ga(1)-N(3)	2.012(9)
N(1)-C(2)	1.315(14)	N(2)-C(2)	1.294(14)
N(2)-C(3)	1.354(14)	N(3)-C(3)	1.274(13)
C(1)-F(12)	1.27(2)	C(1)-F(13)	1.309(14)
C(1)-F(11)	1.32(2)	C(1)-C(2)	1.58(2)
C(3)-C(4)	1.49(2)	C(4)-F(42)	1.262(14)
C(4)-F(41)	1.319(14)	C(4)-F(43)	1.331(14)
C(5)-Ga(1)-C(6)	125.5(7)	C(5)-Ga(1)-N(1)	111.0(5)
C(6)-Ga(1)-N(1)	108.1(5)	C(5)-Ga(1)-N(3)	108.8(5)
C(6)-Ga(1)-N(3)	109.9(5)	N(1)-Ga(1)-N(3)	86.7(4)
C(2)-N(1)-Ga(1)	125.2(7)	C(2)-N(2)-C(3)	118.7(10)
C(3)-N(3)-Ga(1)	127.2(8)	F(12)-C(1)-F(13)	108.5(13)
F(12)-C(1)-F(11)	109.4(13)	F(13)-C(1)-F(11)	108.1(12)
F(12)-C(1)-C(2)	110.5(11)	F(13)-C(1)-C(2)	108.6(11)
F(11)-C(1)-C(2)	111.7(11)	N(2)-C(2)-N(1)	132.4(10)
N(2)-C(2)-C(1)	111.8(11)	N(1)-C(2)-C(1)	115.8(10)
N(3)-C(3)-N(2)	129.8(10)	N(3)-C(3)-C(4)	118.9(12)
N(2)-C(3)-C(4)	111.2(10)	F(42)-C(4)-F(41)	107.9(11)
F(42)-C(4)-F(43)	103.9(13)	F(41)-C(4)-F(43)	105.3(11)
F(42)-C(4)-C(3)	113.4(11)	F(41)-C(4)-C(3)	113.3(12)
F(43)-C(4)-C(3)	112.3(10)		

[EtIn(tmtaa)]

Space group $P2_1/n$ was assumed and shown to be correct by satisfactory refinement. The structure was solved by direct methods using SHELXTL PLUS. Hydrogen atoms were added at calculated positions and refined using a riding model. Anisotropic displacement parameters were used for all non-H atoms. H atoms were given isotropic displacement parameters equal to $U = 0.08 \text{ \AA}^2$.

Figure 4 shows a space filling representation of [EtIn(tmtaa)], showing the positions of the benzenoid protons and the methyl groups of the molecule.

Table 16 Bond lengths [Å] and angles [°] for [EtIn(tmtaa)].

In(1)-C(23)	2.158(6)	In(1)-N(2)	2.193(4)
In(1)-N(4)	2.207(4)	In(1)-N(1)	2.213(4)
In(1)-N(3)	2.216(4)	N(1)-C(2)	1.320(6)
N(1)-C(22)	1.431(7)	N(2)-C(4)	1.335(6)
N(2)-C(6)	1.424(7)	N(3)-C(12)	1.338(6)
N(3)-C(11)	1.403(6)	N(4)-C(15)	1.331(6)
N(4)-C(17)	1.406(7)	C(1)-C(2)	1.523(7)
C(2)-C(3)	1.409(7)	C(3)-C(4)	1.400(7)
C(4)-C(5)	1.513(7)	C(6)-C(7)	1.387(7)
C(6)-C(11)	1.438(7)	C(7)-C(8)	1.379(8)
C(8)-C(9)	1.385(8)	C(9)-C(10)	1.378(8)
C(10)-C(11)	1.392(7)	C(12)-C(14)	1.383(8)
C(12)-C(13)	1.520(7)	C(14)-C(15)	1.425(7)
C(15)-C(16)	1.518(7)	C(17)-C(18)	1.378(8)
C(17)-C(22)	1.430(7)	C(18)-C(19)	1.380(8)
C(19)-C(20)	1.387(8)	C(20)-C(21)	1.381(8)
C(21)-C(22)	1.394(8)	C(23)-C(24)	1.451(9)
C(23)-In(1)-N(2)	112.7(2)	C(23)-In(1)-N(4)	116.0(2)
N(2)-In(1)-N(4)	131.2(2)	C(23)-In(1)-N(1)	118.5(2)
N(2)-In(1)-N(1)	85.9(2)	N(4)-In(1)-N(1)	73.9(2)
C(23)-In(1)-N(3)	110.0(2)	N(2)-In(1)-N(3)	74.5(2)
N(4)-In(1)-N(3)	86.4(2)	N(1)-In(1)-N(3)	131.5(2)
C(2)-N(1)-C(22)	125.2(4)	C(2)-N(1)-In(1)	127.5(4)
C(22)-N(1)-In(1)	106.7(3)	C(4)-N(2)-C(6)	124.5(4)
C(4)-N(2)-In(1)	127.6(4)	C(6)-N(2)-In(1)	107.4(3)
C(12)-N(3)-C(11)	126.5(4)	C(12)-N(3)-In(1)	126.5(4)
C(11)-N(3)-In(1)	106.7(3)	C(15)-N(4)-C(17)	125.1(4)
C(15)-N(4)-In(1)	126.9(3)	C(17)-N(4)-In(1)	107.3(3)
N(1)-C(2)-C(3)	123.2(5)	N(1)-C(2)-C(1)	121.2(5)
C(3)-C(2)-C(1)	115.4(5)	C(4)-C(3)-C(2)	131.8(5)
N(2)-C(4)-C(3)	123.3(5)	N(2)-C(4)-C(5)	121.4(5)
C(3)-C(4)-C(5)	115.1(5)	C(7)-C(6)-N(2)	125.5(5)
C(7)-C(6)-C(11)	118.8(5)	N(2)-C(6)-C(11)	115.4(4)
C(8)-C(7)-C(6)	121.7(5)	C(7)-C(8)-C(9)	119.8(5)
C(10)-C(9)-C(8)	119.9(5)	C(9)-C(10)-C(11)	121.9(5)
C(10)-C(11)-N(3)	125.4(4)	C(10)-C(11)-C(6)	117.9(5)
N(3)-C(11)-C(6)	116.3(4)	N(3)-C(12)-C(14)	124.2(5)
N(3)-C(12)-C(13)	120.3(5)	C(14)-C(12)-C(13)	115.4(5)
C(12)-C(14)-C(15)	131.9(5)	N(4)-C(15)-C(14)	123.4(5)
N(4)-C(15)-C(16)	120.8(5)	C(14)-C(15)-C(16)	115.8(5)
C(18)-C(17)-N(4)	125.5(5)	C(18)-C(17)-C(22)	118.6(5)
N(4)-C(17)-C(22)	115.6(5)	C(17)-C(18)-C(19)	122.0(5)
C(18)-C(19)-C(20)	119.6(6)	C(21)-C(20)-C(19)	120.0(6)

C(20)-C(21)-C(22)	121.1(5)	C(21)-C(22)-C(17)	118.7(5)
C(21)-C(22)-N(1)	125.3(5)	C(17)-C(22)-N(1)	115.6(5)
C(24)-C(23)-In(1)	116.1(5)		

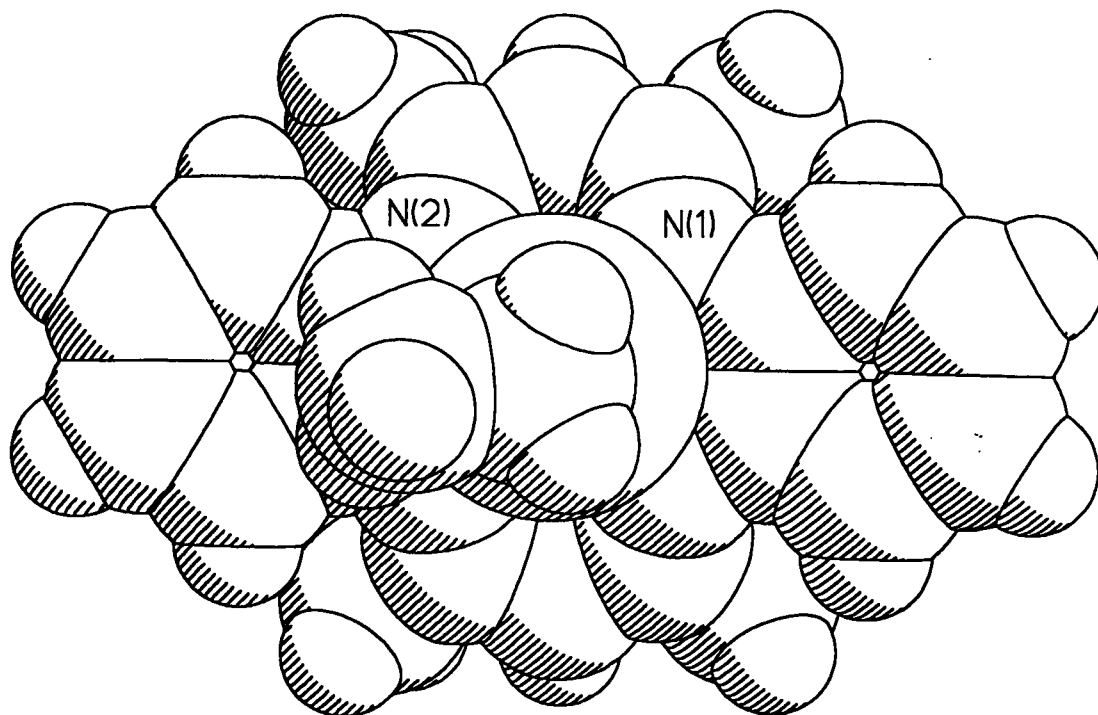


Figure 4 Space filling representation of [EtIn(tmtaa)] to indicate the interaction of the benzenoid rings and the methyl protons.

[ClIn(tmtaa)]

Space group $P2_1/c$ was assumed and shown to be correct by satisfactory refinement. The structure was solved by direct methods using SHELXTL PLUS. Hydrogen atoms were added at calculated positions and refined using a riding model. Anisotropic displacement parameters were used for all non-H atoms. H atoms were given isotropic displacement parameters equal to $U = 0.08 \text{ \AA}^2$.

Table 17 Bond lengths [Å] and angles [°] for [ClIn(tmtaa)].

In(1)-N(4)	2.159(6)	In(1)-N(2)	2.161(5)
In(1)-N(3)	2.168(5)	In(1)-N(1)	2.173(5)
In(1)-Cl(1)	2.380(2)	N(1)-C(2)	1.350(9)
N(1)-C(22)	1.420(9)	N(2)-C(4)	1.328(9)
N(2)-C(6)	1.407(9)	N(3)-C(12)	1.334(9)
N(3)-C(11)	1.416(8)	N(4)-C(15)	1.344(9)
N(4)-C(17)	1.423(9)	C(1)-C(2)	1.509(10)
C(2)-C(3)	1.397(9)	C(3)-C(4)	1.403(9)
C(4)-C(5)	1.514(9)	C(6)-C(7)	1.405(10)
C(6)-C(11)	1.426(10)	C(7)-C(8)	1.386(10)
C(8)-C(9)	1.393(12)	C(9)-C(10)	1.397(11)
C(10)-C(11)	1.417(10)	C(12)-C(14)	1.414(10)
C(12)-C(13)	1.499(9)	C(14)-C(15)	1.406(10)
C(15)-C(16)	1.519(9)	C(17)-C(18)	1.395(10)
C(17)-C(22)	1.446(10)	C(18)-C(19)	1.398(10)
C(19)-C(20)	1.374(11)	C(20)-C(21)	1.385(10)
C(21)-C(22)	1.373(10)	N(4)-In(1)-N(2)	140.3(2)
N(4)-In(1)-N(3)	90.6(2)	N(2)-In(1)-N(3)	76.7(2)
N(4)-In(1)-N(1)	76.5(2)	N(2)-In(1)-N(1)	89.5(2)
N(3)-In(1)-N(1)	140.1(2)	N(4)-In(1)-Cl(1)	107.5(2)
N(2)-In(1)-Cl(1)	112.2(2)	N(3)-In(1)-Cl(1)	109.7(2)
N(1)-In(1)-Cl(1)	110.2(2)	C(2)-N(1)-C(22)	126.6(6)
C(2)-N(1)-In(1)	124.1(4)	C(22)-N(1)-In(1)	108.4(4)
C(4)-N(2)-C(6)	125.3(6)	C(4)-N(2)-In(1)	124.7(5)
C(6)-N(2)-In(1)	108.1(4)	C(12)-N(3)-C(11)	127.6(6)
C(12)-N(3)-In(1)	124.3(5)	C(11)-N(3)-In(1)	107.7(4)
C(15)-N(4)-C(17)	127.4(6)	C(15)-N(4)-In(1)	124.1(5)
C(17)-N(4)-In(1)	108.1(4)	N(1)-C(2)-C(3)	124.1(6)
N(1)-C(2)-C(1)	119.8(6)	C(3)-C(2)-C(1)	116.1(6)
C(2)-C(3)-C(4)	132.1(6)	N(2)-C(4)-C(3)	124.2(6)
N(2)-C(4)-C(5)	120.7(6)	C(3)-C(4)-C(5)	115.0(6)
C(7)-C(6)-N(2)	123.7(6)	C(7)-C(6)-C(11)	119.2(6)
N(2)-C(6)-C(11)	116.7(6)	C(8)-C(7)-C(6)	120.7(7)
C(7)-C(8)-C(9)	120.5(7)	C(8)-C(9)-C(10)	120.2(7)
C(9)-C(10)-C(11)	120.2(7)	N(3)-C(11)-C(10)	124.0(6)
N(3)-C(11)-C(6)	116.4(6)	C(10)-C(11)-C(6)	119.1(6)
N(3)-C(12)-C(14)	123.7(6)	N(3)-C(12)-C(13)	121.5(6)
C(14)-C(12)-C(13)	114.6(6)	C(15)-C(14)-C(12)	133.1(7)
N(4)-C(15)-C(14)	123.9(6)	N(4)-C(15)-C(16)	120.8(6)
C(14)-C(15)-C(16)	115.2(6)	C(18)-C(17)-N(4)	124.4(7)
C(18)-C(17)-C(22)	118.8(6)	N(4)-C(17)-C(22)	116.4(6)
C(17)-C(18)-C(19)	119.2(7)	C(20)-C(19)-C(18)	122.0(7)
C(19)-C(20)-C(21)	119.0(7)	C(22)-C(21)-C(20)	121.8(7)
C(21)-C(22)-N(1)	125.4(7)	C(21)-C(22)-C(17)	119.1(6)
N(1)-C(22)-C(17)	115.1(6)		

[CpIn(tmtaa)]

Space group $P2_1/n$ was assumed and shown to be correct by satisfactory refinement. The structure was solved by direct methods using SHELXTL PLUS. Hydrogen atoms were added at calculated positions and refined using a riding model. Anisotropic displacement parameters were used for all non-H atoms. H atoms were given isotropic displacement parameters equal to $U = 0.08 \text{ \AA}^2$. Refinement of the parameters within the cyclopentadienyl ring was less satisfactory (see Chapter 4). It is suggested that this may be because of some form of crystallographic disorder within this group. Furthermore, unfortunately no absorption correction was performed on the crystal sample (the X-ray diffraction data collection was carried out at the University of Cardiff). Had this correction been obtained, it could have improved the model of the structure, particularly in relation to the cyclopentadienyl unit.

Table 18 Bond lengths [Å] for [CpIn(tmtaa)].

In(1)-N(4)	2.171(4)	In(1)-N(1)	2.191(5)
In(1)-N(2)	2.191(4)	In(1)-N(3)	2.191(5)
In(1)-C(23)	2.229(6)	N(1)-C(2)	1.344(7)
N(1)-C(22)	1.412(7)	N(2)-C(4)	1.336(7)
N(2)-C(6)	1.418(7)	N(3)-C(12)	1.333(6)
N(3)-C(11)	1.426(7)	N(4)-C(15)	1.343(7)
N(4)-C(17)	1.413(7)	C(1)-C(2)	1.527(8)
C(2)-C(3)	1.393(8)	C(3)-C(4)	1.408(8)
C(4)-C(5)	1.527(8)	C(6)-C(7)	1.387(8)
C(6)-C(11)	1.434(7)	C(7)-C(8)	1.367(8)
C(8)-C(9)	1.398(8)	C(9)-C(10)	1.388(8)
C(10)-C(11)	1.382(8)	C(12)-C(14)	1.421(8)
C(12)-C(13)	1.522(8)	C(14)-C(15)	1.385(8)
C(15)-C(16)	1.520(7)	C(17)-C(18)	1.392(8)
C(17)-C(22)	1.445(7)	C(18)-C(19)	1.381(8)
C(19)-C(20)	1.389(8)	C(20)-C(21)	1.364(8)
C(21)-C(22)	1.402(8)	C(23)-C(24)	1.369(10)
C(23)-C(27)	1.439(10)	C(24)-C(25)	1.280(10)
C(25)-C(26)	1.386(10)	C(26)-C(27)	1.449(10)

Table 19 Bond angles [°] for [CpIn(tmtaa)].

N(4)-In(1)-N(1)	75.7(2)	N(4)-In(1)-N(2)	136.6(2)
N(1)-In(1)-N(2)	88.5(2)	N(4)-In(1)-N(3)	88.0(2)
N(1)-In(1)-N(3)	134.4(2)	N(2)-In(1)-N(3)	74.6(2)
N(4)-In(1)-C(23)	115.4(2)	N(1)-In(1)-C(23)	111.3(2)
N(2)-In(1)-C(23)	108.0(2)	N(3)-In(1)-C(23)	114.1(2)
C(2)-N(1)-C(22)	127.0(5)	C(2)-N(1)-In(1)	124.9(4)
C(22)-N(1)-In(1)	108.0(3)	C(4)-N(2)-C(6)	125.9(5)
C(4)-N(2)-In(1)	125.6(4)	C(6)-N(2)-In(1)	108.4(3)
C(12)-N(3)-C(11)	125.6(5)	C(12)-N(3)-In(1)	126.5(4)
C(11)-N(3)-In(1)	107.6(3)	C(15)-N(4)-C(17)	125.4(5)
C(15)-N(4)-In(1)	125.9(4)	C(17)-N(4)-In(1)	108.3(3)
N(1)-C(2)-C(3)	124.0(5)	N(1)-C(2)-C(1)	120.7(5)
C(3)-C(2)-C(1)	115.2(5)	C(2)-C(3)-C(4)	133.2(5)
N(2)-C(4)-C(3)	123.2(5)	N(2)-C(4)-C(5)	121.0(5)
C(3)-C(4)-C(5)	115.6(5)	C(7)-C(6)-N(2)	126.7(5)
C(7)-C(6)-C(11)	118.0(5)	N(2)-C(6)-C(11)	115.1(5)
C(8)-C(7)-C(6)	122.3(5)	C(7)-C(8)-C(9)	119.9(6)
C(10)-C(9)-C(8)	119.2(6)	C(11)-C(10)-C(9)	121.5(6)
C(10)-C(11)-N(3)	124.8(5)	C(10)-C(11)-C(6)	119.1(5)
N(3)-C(11)-C(6)	115.8(5)	N(3)-C(12)-C(14)	121.9(5)
N(3)-C(12)-C(13)	121.5(5)	C(14)-C(12)-C(13)	116.5(4)
C(15)-C(14)-C(12)	133.5(5)	N(4)-C(15)-C(14)	123.7(5)
N(4)-C(15)-C(16)	120.7(5)	C(14)-C(15)-C(16)	115.5(5)
C(18)-C(17)-N(4)	125.9(5)	C(18)-C(17)-C(22)	118.1(5)
N(4)-C(17)-C(22)	115.7(5)	C(19)-C(18)-C(17)	122.3(5)
C(18)-C(19)-C(20)	118.9(6)	C(21)-C(20)-C(19)	121.1(6)
C(20)-C(21)-C(22)	121.5(5)	C(21)-C(22)-N(1)	125.8(5)
C(21)-C(22)-C(17)	118.0(5)	N(1)-C(22)-C(17)	115.9(5)
C(24)-C(23)-C(27)	109.7(6)	C(24)-C(23)-In(1)	99.8(5)
C(27)-C(23)-In(1)	107.8(5)	C(25)-C(24)-C(23)	108.2(8)
C(24)-C(25)-C(26)	112.5(8)	C(25)-C(26)-C(27)	106.5(7)
C(23)-C(27)-C(26)	102.1(6)		

N,N'-Diphenylacetamide

Sublimation of the ligand under vacuum (0.003mm Hg) at 100°C onto a cold finger (water cooled) produced colourless needle-shaped crystals. A regular shaped example was picked and used for the X-ray diffraction study.

Space group *Pbca* was assumed and shown to be correct by satisfactory refinement. The structure was solved by direct methods using SHELXTL PLUS. The hydrogen atoms associated with the phenyl and methyl groups were added at calculated positions and refined using a riding model. The co-ordinates of the hydrogen atom associated with the nitrogen atom were refined, with a restrained bond distance (0.92Å). Anisotropic displacement parameters were used for all non-H atoms. H atoms were given isotropic displacement parameters equal to $U = 0.08 \text{ \AA}^2$. The molecular structure is shown in Figure 5.

Table 20 Bond lengths [\AA] and angles [$^\circ$] for [PhN(H)CMeNPh].

N(1)-C(17)	1.279(3)	N(1)-C(11)	1.409(3)
N(2)-C(17)	1.363(3)	N(2)-C(21)	1.415(3)
C(11)-C(12)	1.348(4)	C(11)-C(16)	1.374(4)
C(12)-C(13)	1.389(4)	C(13)-C(14)	1.343(5)
C(14)-C(15)	1.333(5)	C(15)-C(16)	1.373(4)
C(17)-C(18)	1.501(3)	C(21)-C(26)	1.378(3)
C(21)-C(22)	1.378(3)	C(22)-C(23)	1.367(4)
C(23)-C(24)	1.373(4)	C(24)-C(25)	1.359(4)
C(25)-C(26)	1.390(4)		
C(17)-N(1)-C(11)	119.6(2)	C(17)-N(2)-C(21)	127.9(2)
C(12)-C(11)-C(16)	117.3(3)	C(12)-C(11)-N(1)	122.1(3)
C(16)-C(11)-N(1)	120.3(3)	C(11)-C(12)-C(13)	121.5(4)
C(14)-C(13)-C(12)	119.8(4)	C(15)-C(14)-C(13)	119.6(5)
C(14)-C(15)-C(16)	121.1(4)	C(15)-C(16)-C(11)	120.7(4)
N(1)-C(17)-N(2)	121.6(3)	N(1)-C(17)-C(18)	124.7(3)
N(2)-C(17)-C(18)	113.7(2)	C(26)-C(21)-C(22)	118.9(3)
C(26)-C(21)-N(2)	118.4(3)	C(22)-C(21)-N(2)	122.8(3)
C(23)-C(22)-C(21)	120.2(3)	C(22)-C(23)-C(24)	120.9(3)
C(25)-C(24)-C(23)	119.6(3)	C(24)-C(25)-C(26)	119.9(3)
C(21)-C(26)-C(25)	120.4(3)		

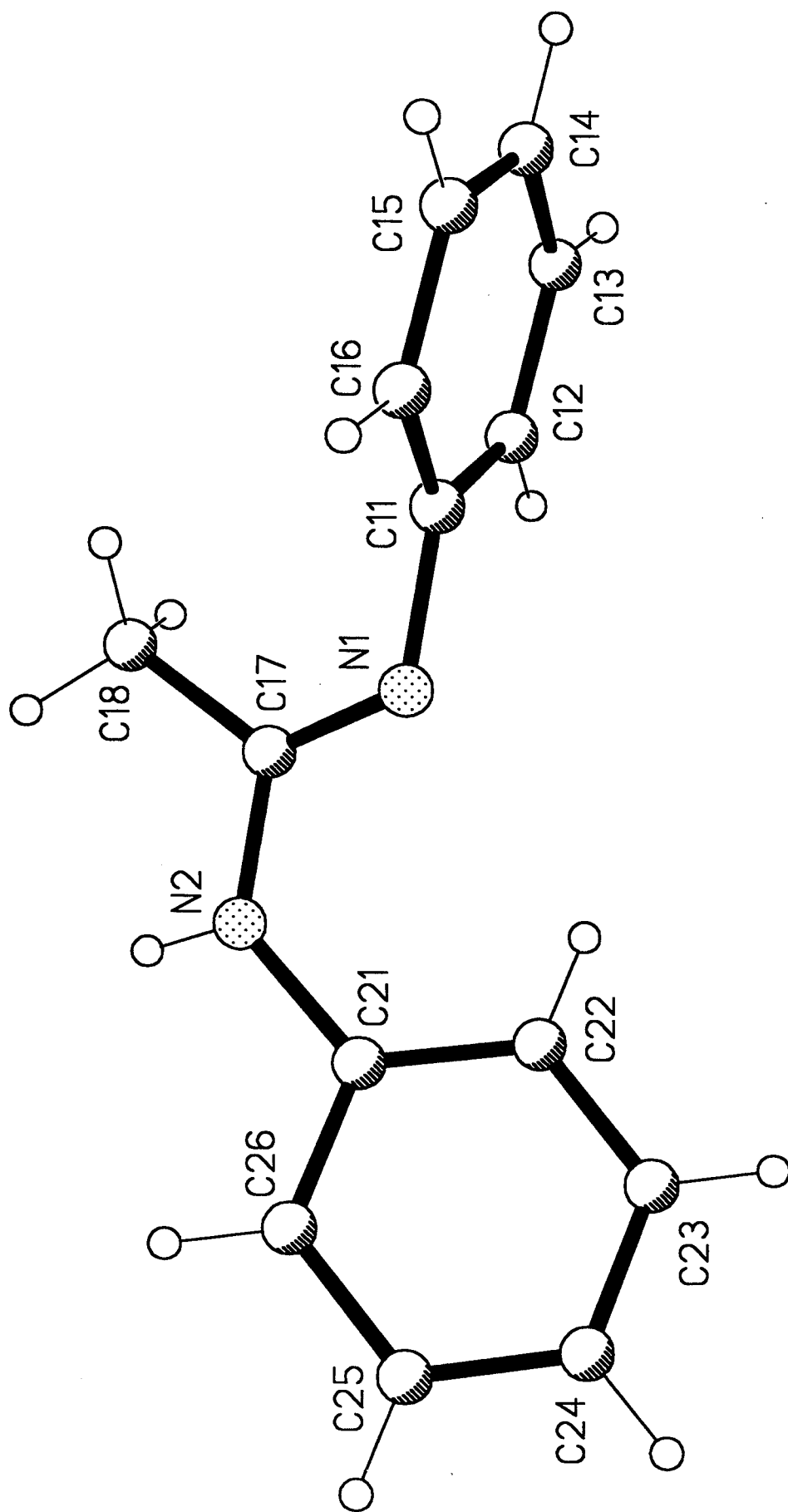


Figure 5 The molecular structure of N,N'-diphenylacetamide.

APPENDIX 3

Mass Spectra

PAGES MISSING IN
ORIGINAL

Table 21 Summary of E.I. mass spectroscopic data of dimethylaluminium-amidinato complexes.

Complex	m/z (% intensity)
[Me ₂ Al(PhNCPhNPh)]	329 (3.1), 328 (11.3), 327 (2.1), 314 (18.1), 313 (77.7), 299 (3.6), 298 (20.2), 297 (69.5), 296 (5.3), 295 (2.5), 272 (14.4), 271 (26.3), 181 (21.4), 180 (100), 168 (4.1), 167 (10.1), 77 (75.5), 65 (6.7), 51 (33.3).
[Me ₂ Al{(4-Cl-C ₆ H ₄)N CPhN(4-Cl-C ₆ H ₄)}]	399 (0.9), 398 (4.3), 397 (0.9), 396 (6.6), 385 (5.6), 384 (5.1), 383 (28.8), 382 (7.9), 381 (44.4), 370 (2.1), 369 (4.3), 368 (11.5), 367 (14.7), 366 (17.0), 365 (16.4), 343 (1.9), 342 (2.1), 341 (2.1), 339 (3.0), 216 (10.5), 214 (32.6), 140 (9.3), 138 (13.1), 113 (29.2), 111 (100), 77 (8.4), 51 (3.5).
[Me ₂ Al(PhNCMeNPh)]	266 (2.2), 251 (100), 210 (5.5), 209 (3.4), 191 (2.6), 158 (4.1), 118 (39.0), 93 (4.0), 77 (36.8), 51 (5.8).
[Me ₂ Al{(4-Cl-C ₆ H ₄)N CMeN(4-Cl-C ₆ H ₄)}]	337 (0.5), 336 (2.4), 335 (0.5), 334 (3.7), 323 (4.3), 322 (3.0), 321 (2.4), 320 (5.6), 319 (34.8), 308 (2.8), 307 (8.5), 306 (10.0), 305 (44.0), 304 (15.7), 303 (68.6), 282 (0.5), 281 (1.3), 280 (2.3), 279 (5.1), 278 (3.5), 277 (8.0), 276 (1.5), 155 (3.7), 154 (33.4), 153 (9.9), 152 (100), 113 (12.7), 111 (36.8), 76 (2.9), 75 (13.8).
[Me ₂ Al(PhNCHNPh)]	252 (4.6), 237 (69.7), 221 (39.5), 196 (23.3), 195 (17.3), 104 (8.7), 93 (100), 92 (5.2), 77 (64.4).

Table 22 Summary of E.I (and C.I. where specified) mass spectroscopic data of dialkylgallium-amidinato complexes.

Complex	m/z (% intensity)
[Me ₂ Ga(PhNCPhNPh)]	372 (13.4), 370 (20.0), 357 (76.3), 355 (100), 341 (4.0), 339 (6.1), 272 (8.0), 271 (11.5), 180 (96.5), 163 (35.5), 161 (37.2), 101 (7.5), 99 (11.1), 77 (85.5), 71 (12.2), 69 (18.1), 51 (21.1).
[Et ₂ Ga(PhNCPhNPh)]	400 (6.0), 398 (10.2), 371 (50.0), 369 (73.5), 341 (14.5), 340 (12.5), 272 (9.1), 271 (8.3), 270 (4.0), 180 (100), 177 (5.4), 175 (8.0), 104 (3.0), 103 (6.0), 77 (21.5), 71 (6.3), 69 (9.5), 51 (9.5).
[Me ₂ Ga{(4-NO ₂ -C ₆ H ₄)N CPhN(4-NO ₂ -C ₆ H ₄)}]	462 (4.5), 460 (6.7), 447 (59.9), 445 (90.3), 431 (2.1), 429 (2.2), 362 (11.5), 361 (3.3), 330 (8.0), 226 (15.8), 225 (100), 180 (10.4), 179 (60.0), 163 (16.1), 161 (21.3), 101 (23.3), 99 (30.4), 86 (4.3), 84 (6.9), 77 (12.5), 76 (44.8), 71 (13.0), 69 (23.4), 57 (13.0), 55 (10.0), 50 (14.4).
[Me ₂ Ga{(4-Cl-C ₆ H ₄)N CPhN(4-Cl-C ₆ H ₄)}]	444 (0.2), 443 (0.2), 442 (0.8), 441 (0.5), 440 (2.1), 439 (0.4), 438 (1.6), 429 (0.5), 428 (0.6), 427 (3.6), 426 (2.1), 425 (7.9), 424 (1.5), 423 (6.4), 344 (1.2), 343 (1.5), 342 (7.5), 341 (4.4), 340 (10.2), 339 (3.5), 217 (4.9), 216 (40.1), 215 (18.5), 214 (100), 163 (2.9), 161 (4.6), 114 (1.0), 113 (8.8), 112 (3.0), 111 (28.0), 101 (5.2), 99 (8.8), 77 (14.3), 75 (19.4), 71 (8.5), 69 (12.6).
[Me ₂ Ga(PhNCPhNPh). (4-Bu ^t -pyridine)]	372 (13.9), 370 (25.5), 357 (38.5), 355 (45.1), 343 (1.7), 341 (1.9), 339 (1.4), 272 (29.9), 271 (14.4), 181 (59.7), 180 (100), 163 (9.8), 161 (15.0), 135 (39.1), 121 (11.5), 120 (70.3), 118 (8.9), 104 (12.8), 103 (10.9), 101 (5.6), 99 (7.0), 93 (9.9), 92 (37.5), 91 (16.2), 77 (86.4), 71 (12.7), 69 (17.8), 65 (18.6). C.I. (NH ₃): 508 (3.0), 506 (3.9).

Table 23 Summary of E.I. (and C.I. where specified) mass spectroscopic data of dialkylindium-amidinato complexes.

Complex	m/z (% intensity)
[Me ₂ In(PhNCPPhNPh)]	417 (4.6), 416 (17.0), 415 (2.8), 402 (20.3), 401 (87.6), 399 (5.7), 387 (4.5), 386 (25.9), 385 (88.7), 384 (7.3), 383 (4.5), 272 (12.8), 271 (18.3), 270 (3.8), 207 (3.0), 181 (18.7), 180 (100), 168 (5.0), 167 (11.2), 145 (21.5), 130 (5.1), 115 (94.1), 113 (5.5), 77 (85.6), 65 (5.7), 51 (30.7).
[Et ₂ In(PhNCPPhNPh)]	445 (1.7), 444 (5.7), 416 (21.4), 415 (64.2), 401 (8.8), 387 (6.0), 386 (30.0), 385 (63.7), 384 (7.1), 360 (5.5), 272 (18.7), 271 (12.6), 270 (5.6), 221 (1.9), 181 (21.7), 180 (73.7), 115 (81.8), 113 (8.8), 103 (6.9), 78 (13.5), 77 (80.2), 69 (6.1), 65 (8.4), 51 (51.3), 50 (8.1).
[Et ₂ In{(4-Cl-C ₆ H ₄)N CPhN(4-Cl-C ₆ H ₄)}]	515 (0.4), 514 (1.9), 513 (0.4), 512 (2.9), 487 (3.7), 486 (3.4), 485 (19.1), 484 (5.4), 483 (29.7), 458 (2.0), 457 (4.0), 456 (11.1), 455 (14.0), 454 (16.2), 453 (17.1), 387 (1.1), 385 (2.6), 343 (0.9), 342 (1.0), 341 (1.0), 339 (1.4), 218 (2.2), 216 (5.7), 214 (17.7), 201 (2.4), 180 (2.4), 173 (6.0), 115 (100), 113 (14.3), 111 (19.4), 77 (7.4), 51 (5.5).
[Et ₂ In(PhNCHNPh)]	369 (2.1), 368 (10.7), 340 (8.2), 339 (39.6), 311 (9.6), 310 (48.7), 309 (25.6), 308 (6.6), 196 (8.6), 195 (6.7), 173 (3.3), 144 (2.1), 115 (71.0), 113 (7.3), 104 (7.2), 94 (3.0), 93 (37.6), 92 (4.9), 78 (3.6), 77 (31.3), 66 (4.7), 65 (7.6), 51 (17.6).
[Et ₂ In(PhNCPPhNPh). (4-Bu ^t -pyridine)]	444 (0.5), 416 (2.1), 415 (6.5), 386 (3.2), 385 (6.1), 272 (1.5), 271 (1.7), 180 (21.8), 173 (9.8), 136 (40.0), 135 (98.0), 120 (98.5), 115 (35.8), 113 (2.0), 104 (27.7), 92 (100), 77 (15.0), 50 (31.3). C.I. (NH ₃): 580 (10.1), 579 (2.1).

Table 24 Summary of E.I. mass spectroscopic data of monoalkyl-metal-bis(amidinato) complexes.

Complex	m/z (% intensity)
[MeAl(PhNCPhNPh) ₂]	585 (0.5), 584 (1.1), 570 (6.5), 569 (16.7), 375 (10.6), 313 (25.1), 299 (4.2), 298 (14.9), 272 (13.3), 271 (14.5), 181 (24.9), 180 (100), 173 (21.2), 77 (98.0), 57 (11.5), 51 (60.6).
[MeAl(PhNCMeNPh) ₂]	461 (0.3), 460 (2.1), 446 (2.1), 445 (86.4), 251 (19.5), 236 (23.4), 235 (35.4), 210 (8.3), 209 (29.7), 167 (10.8), 118 (100), 117 (25.5), 93 (17.6), 77 (76.1), 65 (6.1), 51 (13.8).
[MeGa(PhNCPhNPh) ₂]	629 (1.5), 628 (4.3), 627 (8.1), 626 (7.8), 625 (6.6), 615 (1.8), 614 (8.8), 613 (32.4), 612 (8.9), 611 (43.4), 420 (1.2), 419 (6.0), 418 (1.5), 417 (9.4), 358 (1.1), 357 (7.4), 356 (1.7), 355 (13.5), 354 (0.9), 353 (4.4), 272 (5.3), 271 (5.6), 226 (5.3), 223 (8.8), 181 (10.0), 180 (100), 163 (16.5), 161 (23.5), 115 (2.1), 77 (81.7), 71 (6.5), 69 (10.0), 65 (4.7), 51 (24.1).
[EtGa(PhNCMeNPh) ₂]	519 (1.0), 518 (1.1), 517 (1.9), 516 (1.0), 491 (8.4), 490 (52.7), 489 (87.4), 488 (65.7), 487 (91.5), 309 (9.4), 307 (14.3), 295 (4.9), 293 (7.4), 279 (19.5), 277 (25.0), 211 (10.8), 210 (46.9), 209 (44.8), 208 (10.5), 167 (12.5), 119 (36.9), 118 (100), 117 (11.3), 93 (19.2), 78 (22.5), 77 (98.1), 71 (52.0), 69 (68.4), 65 (15.4), 51 (58.6), 50 (10.6).
[MeIn(PhNCPhNPh) ₂]	658 (1.7), 657 (3.9), 386 (0.6), 385 (3.9), 273 (1.8), 272 (10.3), 271 (9.1), 270 (1.8), 269 (5.5), 268 (1.4), 243 (1.6), 195 (2.1), 181 (11.0), 180 (100), 167 (4.7), 115 (7.7), 93 (14.2), 77 (71.6), 65 (12.9), 51 (33.5).

[EtIn(PhNCPPhNPh)₂] 687 (0.2), 686 (0.4), 658 (11.5), 657 (26.9),
655 (2.2), 558 (0.5), 463 (1.5), 445 (0.9), 444 (1.3),
415 (19.2), 387 (15.4), 386 (6.3), 385 (16.0),
272 (26.0), 271 (13.5), 269 (3.0), 181 (26.9),
180 (100), 173 (21.2), 115 (40.4), 77 (98.0), 57 (11.5),
51 (60.6).

[MeIn(PhNCMeNPh)₂] 563 (0.2), 562 (0.6), 534(1.4), 533 (57.9), 353 (7.3),
324 (7.3), 323 (22.0), 283 (0.9), 210 (6.7), 209 (17.1),
167 (6.7), 118 (51.2), 117 (43.9), 115 (100), 113 (3.5),
77 (66.5), 65 (9.7), 5.1 (30.5).

Table 25 Summary of E.I. mass spectroscopic data of metal-tris(amidinato) complexes.

Complex	m/z (% intensity)
[Al(PhNCPhNPh) ₃]	841 (12.2), 840 (17.0), 839 (9.3), 571 (2.8), 570 (15.2), 569 (54.8), 420 (4.0), 376 (4.9), 375 (26.5), 324 (3.3), 285 (3.4), 272 (3.8), 271 (14.5), 270 (4.3), 194 (3.2), 181 (39.4), 180 (100), 168 (9.3), 167 (21.0), 152 (3.5), 91 (2.8), 77 (97.4), 65 (4.3).
[Al(PhNCMeNPh) ₃]	656 (0.5), 655 (2.0), 654 (11.9), 445 (6.8), 444 (9.1), 236 (3.9), 235 (4.0), 210 (7.8), 209 (4.0), 167 (5.5), 119 (8.1), 118 (85.9), 92 (5.2), 76 (100).
[Ga(PhNCPhNPh) ₃]	887 (0.7), 886 (2.5), 885 (5.7), 884 (7.2), 883 (7.7), 882 (7.0), 842 (0.9), 841 (1.9), 840 (1.0), 614 (4.8), 613 (16.0), 612 (6.4), 611 (26.4), 572 (1.9), 570 (2.8), 420 (1.1), 419 (3.3), 418 (1.4), 417 (5.5), 342 (1.0), 340 (1.4), 271 (6.9), 225 (13.5), 223 (20.1), 180 (68.1), 167 (8.3), 76 (100), 71 (6.5), 69 (9.7), 50 (7.3).
[Ga(PhNCMeNPh) ₃]	700 (1.3), 699 (2.7), 698 (3.8), 697 (3.9), 696 (4.5), 489 (7.9), 488 (10.1), 487 (11.9), 486 (14.2), 280 (4.9), 279 (4.0), 278 (7.4), 277 (6.8), 210 (14.1), 209 (5.9), 167 (1.3), 119 (8.0), 118 (95.5), 92 (10.4), 76 (100), 71 (45.0), 69 (68.3).
[In(PhNCPhNPh) ₃]	929 (19.7), 928 (33.8), 926 (13.6), 748 (0.6), 659 (16.2), 657 (43.9), 655 (5.2), 465 (1.2), 463 (4.7), 386 (3.8), 385 (17.3), 272 (7.5), 271 (10.1), 269 (9.7), 181 (12.7), 180 (100), 167 (10.0), 115 (48.6), 113 (2.6), 77 (94.8), 65 (5.2), 51 (16.8).
[In(PhNCMeNPh) ₃]	744 (1.0), 743 (3.4), 742 (7.9), 535 (6.1), 534 (23.9), 324 (2.2), 323 (9.0), 210 (6.7), 209 (14.8), 194 (3.0), 167 (4.7), 119 (6.0), 118 (78.1), 117 (47.7), 115 (48.6), 113 (2.0), 92 (3.2), 90 (3.0), 76 (100), 64 (8.3), 50 (18.7).

Table 26 E.I. (and C.I. where specified) mass spectroscopic data of H_2tmtaa and indium (III) $tmtaa$ complexes.

Complex	m/z (% intensity)
H_2tmtaa	344 (100), 343 (5.8), 329 (86.3), 212 (13.3), 211 (31.2), 200 (14.4), 199 (48.7), 198 (26.7), 197 (98.9), 186 (6.4), 185 (22.6), 184 (12.3), 183 (12.7), 182 (19.6), 181 (10.0), 173 (38.8), 172 (36.4), 171 (29.4), 170 (11.9), 169 (10.0), 158 (20.3), 157 (28.4), 156 (20.3), 146 (12.6), 145 (22.1), 144 (12.7), 143 (11.9), 133 (68.9), 132 (25.1), 131 (23.2), 130 (24.5), 92 (40.2), 91 (26.3), 77 (28.8), 76 (11.0).
$[Et_2In(Htmtaa)]$	516 (1.2), 487 (13.1), 486 (35.2), 458 (27.1), 457 (100), 345 (6.6), 344 (25.8), 329 (24.4), 243 (7.2), 211 (17.8), 199 (13.7), 198 (13.6), 197 (33.0), 196 (11.9), 182 (7.4), 173 (13.0), 172 (13.7), 171 (11.0), 157 (9.6), 156 (8.7), 145 (6.6), 144 (5.2), 133 (19.3), 132 (10.3), 131 (10.2), 130 (8.7), 115 (87.3), 113 (3.7), 77 (10.0), 65 (9.0). C.I. (NH_3): 517 (14.0), 487 (100), 345 (78.5), 344 (21.5), 329 (22.4), 197 (25.0), 115 (37.5).
$[EtIn(tmtaa)]$	486 (20.5), 458 (15.8), 457 (60.8), 344 (5.6), 329 (7.4), 211 (7.7), 197 (16.6), 173 (4.5), 172 (7.5), 169 (8.1), 157 (9.6), 156 (8.7), 145 (4.8), 144 (2.8), 133 (9.2), 132 (14.4), 131 (23.2), 119 (14.5), 115 (49.8), 113 (6.2), 77 (10.5), 69 (53.4), 57 (21.6).
$[MeIn(tmtaa)]$	473 (20.8), 472 (80.3), 458 (24.9), 457 (100), 327 (5.9), 236 (17.7), 211 (9.9), 198 (8.6), 196 (7.3), 149 (9.7), 115 (78.6), 113 (5.2), 77 (6.0), 57 (6.1).
$[CpIn(tmtaa)]$	522 (5.9), 494 (5.7), 492 (16.0), 472 (6.2), 458 (15.7), 457 (55.5), 344 (6.5), 329 (6.2), 211 (5.8), 199 (5.8), 198 (6.0), 197 (11.0), 196 (6.5), 149 (9.3), 133 (12.9), 132 (21.8), 131 (17.3), 115 (58.1), 113 (5.5), 92 (18.4), 91 (26.5), 77 (12.4), 71 (13.7), 69 (18.9), 67 (13.0), 66 (100), 65 (55.3), 63 (13.5), 57 (18.3), 55 (15.1).

$[(\text{SiMe}_3)_2\text{NIn}(\text{tmtaa})]$	617 (1.4), 546 (1.0), 492 (1.4), 457 (39.3), 344 (2.3), 329 (8.9), 311 (2.8), 211 (10.3), 199 (6.3), 198 (8.7), 197 (14.1), 195 (5.4), 173 (5.8), 172 (5.7), 171 (5.7), 133 (9.7), 132 (7.9), 131 (7.6), 130 (4.8), 115 (75.7), 113 (3.9).
$[(\text{SiMe}_3)\text{OIn}(\text{tmtaa})]$	546 (5.0), 457 (6.5), 344 (2.3), 329 (2.0), 221 (1.0), 211 (1.0), 199 (1.4), 197 (2.5), 173 (1.4), 172 (2.1), 147 (19.8), 146 (20.0), 133 (3.7), 132 (2.0), 131 (2.7), 130 (4.1), 115 (3.6), 113 (0.4).
$[\text{ClIn}(\text{tmtaa})]$	495 (8.0), 494 (33.1), 493 (25.9), 492 (89.5), 327 (8.1), 215 (20.2), 198 (4.5), 197 (17.1), 196 (10.0), 195 (9.0), 183 (11.5), 182 (8.3), 173 (9.8), 172 (11.3), 171 (13.3), 157 (10.9), 149 (15.9), 143 (11.9), 137 (14.9), 133 (31.6), 132 (100), 131 (68.4), 130 (15.4), 115 (27.5), 113 (7.4), 92 (37.9), 91 (47.3), 81 (43.5), 77 (29.4), 71 (32.2), 69 (85.4), 65 (28.7), 57 (53.9), 55 (55.6).

REFERENCES

REFERENCES

1. C.R.C. Handbook of Chemistry and Physics, 69th Edition (1988-1989) Eds. R.C. Weast, M.J. Astle and W.H. Beyer. C.R.C. Press, Inc., Boca Raton, Florida.
2. H. Sinn, W. Kaminsky, H.J. Vollmer and R. Woldt, *Angew. Chem., Int. Ed. Engl.*, 1980, **19**, 390.
3. J.J. Eisch, in "Comprehensive Organic Synthesis", Eds. B.M. Trost, I. Fleming, Pergamon Press, Oxford, 1992, Vol. 8, p. 773.
4. A.H. Cowley and R.A. Jones, *Angew. Chem.*, 1989, **101**, 1235; *Angew. Chem., Int. Ed. Engl.*, 1989, **28**, 1208.
5. R.L. Wells, *Coord. Chem. Rev.*, 1992, **112**, 273.
6. G. Wilkinson, F.G.A. Stone, E.W. Abel (Eds.), "Comprehensive Organometallic Chemistry", Pergamon Press, Oxford, 1982.
 - (a) "Non-cyclic Three and Four Co-ordinated Boron Compounds" by J.D. Odom (Vol. 1).
 - (b) "Aluminium" by J.J. Eisch, (Vol. 1).
 - (c) "Gallium and Indium" by D.G. Tuck, (Vol. 1).
 - (d) "Thallium" by H. Kurosawa, (Vol. 1).
7. E.W. Abel, F.G.A. Stone, G. Wilkinson, (Eds.), "Comprehensive Organometallic Chemistry II", Pergamon Press, Oxford, 1995.
 - (a) "Aluminum" by J.J. Eisch, (Vol. 1).
 - (b) "Gallium, Indium and Thallium, Excluding Transition Metal Derivatives" by M.A. Paver, C.A. Russell and D.S. Wright, (Vol. 1).
8. C. Dohmeier, C. Robl, M. Tacke and H. Schnöckel, *Angew. Chem.*, 1991, **103**, 594, *Angew. Chem., Int. Ed. Engl.*, 1991, **30**, 564.
9. D. Loos, H. Schnöckel, J. Gauss and U. Schneider, *Angew. Chem.*, 1992, **104**, 1376; *Angew. Chem., Int. Ed. Engl.*, 1992, **31**, 1362.
10. O.T. Beachley, Jr., M.R. Churchill, J.C. Fenttinger, J.C. Pazik and L. Victoriano, *J. Am. Chem. Soc.*, 1986, **108**, 4666.

11. A.J. Carty, M.J.S. Gynane, M.F. Lappert, S.J. Miles, A. Singh and N.J. Taylor, *Inorg. Chem.*, 1980, **19**, 3637.
12. H. Schmidbaur, *Angew. Chem.*, 1985, **97**, 893; *Angew. Chem., Int. Ed. Engl.*, 1985, **24**, 893.
13. E.G. Hoffmann, *Liebigs Ann. Chem.*, 1960, **629**, 104.
14. C.H. Henrickson and D.P. Eyman, *Inorg. Chem.*, 1967, **6**, 1461.
15. A.W. Laubengayer and W.F. Gilliam, *J. Am. Chem. Soc.*, 1941, **63**, 477.
16. K.S. Pitzer and H.S. Gutowsky, *J. Am. Chem. Soc.*, 1946, **68**, 2204.
17. M.J. Albright, W.M. Butler, T.J. Anderson, M.D. Glick and J.P. Oliver, *J. Am. Chem. Soc.*, 1976, **98**, 3995.
18. J.F. Malone and W.S. McDonald, *J. Chem. Soc., Chem. Commun.*, 1967, 444.
19. N. Muller, A.L. Otermat, *Inorg. Chem.*, 1965, **4**, 296.
20. E.L. Amma and R.E. Rundle, *J. Am. Chem. Soc.*, 1958, **80**, 4141.
21. G. Allegra, G. Perego and A. Immirzi, *Makromol. Chem.*, 1963, **61**, 69.
22. H.D. Hausen, K. Mertz, E. Veigel and J. Weidlein, *Z. Naturforsch., Teil B*, 1975, **30**, 159.
23. M.J.S. Gynane and I.J. Worrall, *Inorg. Nucl. Chem. Lett.*, 1972, **8**, 547.
24. J.S. Poland and D.G. Tuck, *J. Organomet. Chem.*, 1972, **452**, 315.
25. A.W. Laubengayer and G.F. Lengnick, *Inorg. Chem.*, 1966, **5**, 503.
26. H. Schmidbaur, J. Weidlein, H.F. Klein and K. Eiglmeier, *Chem. Ber.*, 1968, **101**, 2268.
27. J.P. Maher and D.F. Evans, *J. Chem. Soc.*, 1963, 5534.
28. R. Köster, *Angew. Chem.*, 1961, **73**, 66.
29. B.M. Mikhailov, L.S. Vasil'ev and E.N. Safonova, *Dokl. Akad. Nauk. SSSR*, 1962, **147**, 630.
30. R. Köster and G. Benedikt, *Angew. Chem.*, 1963, **75**, 23.
31. P.A. McCusker, J.V. Marra and G.F. Hennion, *J. Am. Chem. Soc.*, 1961, **83**, 1924.
32. E.A. Jeffrey, T. Mole and J.K. Saunders, *Aust. J. Chem.*, 1968, **21**, 137.

33. E.A. Jeffrey, T. Mole and J.K. Saunders, *Aust. J. Chem.*, 1968, **21**, 649.
34. T. Mole and J.R. Surtees, *Aust. J. Chem.*, 1964, **17**, 310.
35. E.A. Jeffrey, T. Mole and J.K. Saunders, *J. Chem. Soc., Chem. Commun.*, 1967, 696.
36. J.R. Surtess, *Chem. Ind. (London)*, 1964, 1260.
37. K.S. Pitzer and H.S. Gutowsky, *J. Am. Chem. Soc.*, 1946, **68**, 2204.
38. G.E. Coates and R.A. Whitcombe, *J. Chem. Soc.*, 1956, 3351.
39. N.N. Greenwood, P.G. Perkins and M.E. Twentyman, *J. Chem. Soc., (A)*, 1969, 249.
40. G.E. Coates, M.L.H. Green, K. Wade, "Organometallic Compounds", 3rd edition, Vol 1. "The Main Group Elements" by G.E. Coates and K. Wade. Methuen and Co. Ltd., London (1967).
41. L.E. Manzer and G.W. Parshall, *Inorg. Chem.*, 1976, **15**, 3114.
42. T. Onak, "Organoborane Chemistry", Academic Press, New York, 1975.
43. H. Lehmkuhl, *Angew. Chem.*, 1963, **75**, 1090.
44. C.A. Smith and M.G.H. Wallbridge, *J. Chem. Soc., (A)*, 1967, 7.
45. F.A. Cotton and J.R. Leto, *J. Chem. Phys.*, 1959, **30**, 993.
46. N.N. Greenwood and T.S. Srivastava, *J. Chem. Soc. A.*, 1966, 270.
47. N.N. Greenwood and T.S. Srivastava, *J. Chem. Soc. A.*, 1966, 267.
48. M.F. Lappert and J.K. Smith, *J. Chem. Soc.*, 1965, 5826.
49. H.C. Brown and N. Davidson, *J. Am. Chem. Soc.*, 1942, **64**, 316.
50. G. Bahr and G.E. Müller, *Chem. Ber.*, 1955, **88**, 251.
51. F. Schindler, H. Schmidbaur and G. Jonas, *Angew. Chem. Int. Ed. Engl.*, 1965, **4**, 153.
52. G.E. Coates and N.D. Huck, *J. Chem. Soc.*, 1952, 4501.
53. G.E. Coates, *J. Chem. Soc.*, 1951, 2003.
54. V.G. Tsvetkov, B.I. Kozyrkin, K.K. Furkin and R.F. Galiullina, *Zh. Obshch. Khim.*, 1977, **47**, 2155.
55. A. Lieb, M.T. Emerson and J.P. Oliver, *Inorg. Chem.*, 1965, **4**, 1825.

56. G.E. Coates and J. Graham, *J. Chem. Soc.*, 1963, 233.
57. D. Ulmschneider and J. Goubeau, *Chem. Ber.*, 1957, **90**, 2733.
58. R.B. Booth and C.A. Kraus, *J. Am. Chem. Soc.*, 1952, **74**, 1415.
59. H. Meerwein, G. Hinz, H. Majert and H. Sönke, *J. Prakt. Chem.*, 1936, **47**, 251.
60. J. Goubeau, R. Epple, D. Ulmschneider and H. Lehmann, *Angew. Chem.*, 1955, **67**, 710.
61. H.C. Brown and K. Murray, *J. Am. Chem. Soc.*, 1959, **81**, 4108.
62. M.E. Kenney and A.W. Laubengayer, *J. Am. Chem. Soc.*, 1954, **76**, 4839.
63. G.S. Smith and J.L. Hoard, *J. Am. Chem. Soc.*, 1959, **81**, 3907.
64. J.J. Eisch, *J. Am. Chem. Soc.*, 1962, **84**, 3830.
65. F. Runge, W. Zimmermann, H. Pfeiffer and I. Pfeiffer, *Z. Anorg. Allg. Chem.*, 1951, **267**, 39.
66. H. Gilman and R.G. Jones, *J. Am. Chem. Soc.*, 1946, **68**, 517.
67. H.P.A. Groll, *J. Am. Chem. Soc.*, 1930, **52**, 2998.
68. S.F. Birch, *J. Chem. Soc.*, 1934, 1132.
69. A.N. Nesmeyanov and N.N. Novikova, *Bull. Acad. Sci. USSR, Div. Chem. Sci.*, 1942, 372 (*Chem. Abstr.*, 1945, **39**, 1637).
70. E. Wiberg, T. Johannsen and O. Stecher, *Z. Anorg. Allg. Chem.*, 1943, **251**, 114.
71. J.P. Oliver and L.G. Stevens, *J. Inorg. Nucl. Chem.*, 1962, **24**, 953.
72. H. Gilman and R.G. Jones, *J. Am. Chem. Soc.*, 1940, **62**, 980.
73. L.M. Dennis, R.W. Work, E.G. Rochow and E.M. Chamot, *J. Am. Chem. Soc.*, 1934, **56**, 1047.
74. W.C. Schumb and H.I. Crane, *J. Am. Chem. Soc.*, 1938, **60**, 306.
75. L.C. Chao and R.D. Riecke, *Synth. React. Inorg. Metal–Org. Chem.*, 1974, **4**, 373.
76. J.J. Jerius, J.M. Hahn, A.F.M. Maqsudur Rahman, O. Mols, W.H. Ilsley and J.P. Oliver, *Organometallics*, 1986, **5**, 1812.
77. T. Mole, *Aust. J. Chem.*, 1963, **16**, 794.
78. H. Hartmann and H. Lutsche, *Naturwiss*, 1961, **48**, 601.

79. H. Hartmann and H. Lutsche, *Naturwiss*, 1962, **49**, 182.
80. O.T. Beachley, Jr., M.R. Churchill, J.C. Pazik and J.W. Ziller, *Organometallics*, 1986, **5**, 1814.
81. J.T. Leman and A.R. Barron, *Organometallics*, 1989, **8**, 2214.
82. E. Todt and R. Dötzer, *Z. Anorg. Allg. Chem.*, 1963, **321**, 120.
83. V.A. Fedorov and V.G. Makarenko, *Tr. Khim. Tekhnol.*, 1975, **19**, (*Chem. Abstr.*, 1976, **85**, 143 170).
84. L.I. Zakharkin, O.Y. Okhlobystin and B.N. Strunin, *Bull. Acad. Sci. USSR, Engl. Transl.*, 1962, 1913, and references therein.
85. H.C. Clark and A.L. Pickard, *J. Organomet. Chem.*, 1967, **8**, 427.
86. A.A. Korotkov and V.M. Nepyshnevskii, *Plasticheskie Massy*, 1964, **46**, *Chem. Abstr.*, 1965, **62**, 14710g.
87. H. Lehmkuhl, *Ann. Chem.*, 1968, **719**, 40.
88. J.J.Eisch, *J. Am. Chem. Soc.*, 1962, **84**, 3605.
89. K. Zeigler, H. Martin and F. Krupp, *Liebigs Ann. Chem.*, 1960, **629**, 14.
90. K. Ziegler, F. Krupp and K. Zosel, *Angew. Chem.*, 1955, **67**, 425.
91. A. Boardman, R.W.H. Small and I.J. Worrall, *Inorg. Chim. Acta*, 1986, **119**, L13.
92. D.C. Bradley, H. Chudzynska, M.M. Faktor, D.M. Frigo, M.B. Hursthouse, B. Hussain and L.M. Smith, *Polyhedron*, 1988, **7**, 1289.
93. H.D. Hodes and A.D. Berry, *J. Organomet. Chem.*, 1987, **336**, 299.
94. R.B. Hallock, W.E. Hunter, J.L. Atwood and O.T. Beachley, Jr., *Organometallics*, 1985, **4**, 547.
95. G.H. Robinson, W.T. Pennington, B. Lee, M.F. Self and D. Hrcir, *Inorg. Chem.*, 1991, **30**, 809.
96. G.H. Robinson, W.E. Hunter, S.G. Bott and J.L. Atwood, *J. Organomet. Chem.*, 1987, **326**, 9.
97. J.J. Beyers, W.T. Pennington and G.H. Robinson, *Acta Crystallogr., Sect. C*, 1992, **48**, 2023.

98. G.H. Robinson, M.F. Self, S.A. Sangokoya and W.T. Pennington, *J. Cryst. Spectrosc.*, 1988, **18**, 285.
99. H. Schumann, U. Hratmann, A. Dietrich and J. Pickardt, *Angew. Chem. Int. Ed. Engl.*, 1988, **27**, 1077.
100. H. Schumann, U. Hartmann, W. Wassermann, O. Just, A. Dietrich, L. Pohl, M. Hostalek and M. Lokai, *Chem. Ber.*, 1991, **124**, 1113.
101. H. Schumann, U. Hartmann, W. Wassermann, A. Dietrich, F.H. Gorlitz, L. Pohl and M. Hostalek, *Chem. Ber.*, 1990, **123**, 2093.
102. D.K. Coggin, P.E. Fanwick and M.A. Green, *J. Chem. Soc., Chem. Commun.*, 1993, 1127.
103. R.S. Steevensz, D.G. Tuck, H.A. Meinema and J.G. Noltes, *Can. J. Chem.*, 1985, **63**, 755.
104. H. Schumann, T.D. Seuss and H. Hemling, unpublished results, 1994.
105. D.C. Bradley, D.M. Frigo, I.S. Harding and M.B. Hursthouse, *J. Chem. Soc., Chem. Commun.*, 1992, 577.
106. J.F. Malone and W.S. McDonald, *J. Chem. Soc., Chem. Commun.*, 1967, 444.
107. H.D. McBride, *Dissertation Abstr.*, 1967, **B27**, 3891; *Chem. Abstr.*, 1967, **67**, 94825f.
108. D.C. Bradley, H. Dawes, D.M. Frigo, M.B. Hursthouse and B. Hussain, *J. Organomet. Chem.*, 1987, **325**, 55.
109. F. Gerstner and J. Weidlein, *Z. Naturforsch B*, 1978, **33**, 24; H.D. Hausen, F. Gerstner and W. Schwarz, *J. Organomet. Chem.*, 1978, **145**, 277.
110. F. Gerstner, W. Schwarz, H.D. Hausen and J. Weidlein, *J. Organomet. Chem.*, 1979, **175**, 33.
111. R. Lechler, H.D. Hausen and J. Weidlein, *J. Organomet. Chem.*, 1989, **359**, 1.
112. K. Wade and J.E. Lloyd, *J. Chem. Soc.*, 1965, 2662.
113. K. Wade and J.E. Lloyd, *J. Chem. Soc.*, 1965, 5083.
114. H. Reineckel and D. Jahnke, *Chem. Ber.*, 1964, **97**, 2661.

115. T. Hirabayashi, K. Itoh, S. Sakai and Y. Ishii, *J. Organomet. Chem.*, 1970, **21**, 273.
116. J.T. Leman, A.R. Barron, J.W. Ziller and R.M. Kren, *Polyhedron*, 1989, **8**, 1909.
117. J.T. Leman, J. Braddock-Wilking, A.J. Coolong and A.R. Barron, *Inorg. Chem.*, 1993, **32**, 4324.
118. J.T. Leman, H.A. Roman and A.R. Barron, *Organometallics*, 1993, **12**, 2986.
119. G.E. Coates and R.N. Mukherjee, *J. Chem. Soc.*, 1964, 1295.
120. P.B. Hitchcock, H.A. Jasim, M.F. Lappert and H.D. Williams, *J. Chem. Soc., Chem. Commun.*, 1986,
121. H. Schmidbaur, K. Schwirten and H.H. Pickel, *Chem. Ber.*, 1969, **102**, 564.
122. P. Cocolios, R. Guilard and P. Fournari, *J. Organomet. Chem.*, 1979, **179**, 311.
123. A. Coutsolelos and R. Guilard, *J. Organomet. Chem.*, 1983, **253**, 273.
124. A. Tabard, R. Guilard and K.M. Kadish, *Inorg. Chem.*, 1986, **25**, 4277.
125. C. Lecomte, J. Protas, P. Cocolios and R. Guilard, *Acta Crystallogr., Sect. B*, 1980, **36**, 2769.
126. O.T. Beachley, Jr. and G.E. Coates, *J. Chem. Soc.*, 1965, 3241.
127. O.T. Beachley, G.E. Coates and G. Kohnstan, *J. Chem. Soc.*, 1965, 3248.
128. F. Zettler and H. Hess, *Chem. Ber.*, 1977, **110**, 3943.
129. K. Mertz, W. Schwartz, B. Eberwein, J. Weidlein, H. Hess and H.D. Hausen, *Z. Anorg. Allg. Chem.*, 1977, **429**, 99.
130. D.A. Atwood, A.H. Cowley, P.R. Harris, R.A. Jones, S.U. Koschmieder and C.M. Nunn, *J. Organomet. Chem.*, 1993, **449**, 61.
131. M.J. Almond, M.G.B. Drew, C.E. Jenkins and D.A. Rice, *J. Chem. Soc., Dalton Trans.*, 1992, 5.
132. D.A. Atwood, A.H. Cowley, P.R. Harris, R.A. Jones, S.U. Koschmieder, C.M. Nunn, J.L. Atwood and S.G. Bott, *Organometallics*, 1993, **12**, 24.
133. A.H. Cowley, P.R. Harris, R.A. Jones and C.M. Nunn, *Organometallics*, 1991, **10**, 652.

134. L.V. Interrante, G.A. Sigel, M. Garbaskas, C. Hejna and G.A. Slack, *Inorg. Chem.*, 1989, **28**, 252.
135. K.M. Waggoner, K. Ruhlandt-Senge, R.J. Wehmschulte, X. He, M.M. Olmstead and P.P. Power, *Inorg. Chem.*, 1993, **32**, 2557.
136. M.A. Petrie, K. Ruhlandt-Senge and P.P. Power, *Inorg. Chem.*, 1993, **31**, 4038.
137. H. Bürger, J. Cictron, U. Goetze, U. Wannagat and W.J. Wismar, *J. Organomet. Chem.*, 1971, **33**, 1.
138. G.M. Sheldrick and W.S. Sheldrick, *J. Chem. Soc.*, 1969, 2279.
139. N.W. Alcock, I.A. Degnan, M.G.H. Wallbridge, H.R. Powell, M. McPartlin and G.M. Sheldrick, *J. Organomet. Chem.*, 1989, **361**, C33.
140. A.H. Cowley, R.A. Jones, M.A. Mardones, J. Ruiz, J.L. Atwood and S.G. Bott, *Angew. Chem. Int. Ed. Engl.*, 1990, **29**, 1150.
141. A.H. Cowley, F.P. Gabbai, D.A. Atwood, C.J. Carrano, L.M. Mokry and M.R. Bond, *J. Am. Chem. Soc.*, 1994, **116**, 1559.
142. M.R. Mason, J.M. Smith, S.G. Bott and A.R. Barron, *J. Am. Chem. Soc.*, 1993, **115**, 4971.
143. R.S. Tobias, M.J. Sprague and G.E. Glass, *Inorg. Chem.*, 1968, **7**, 1714.
144. G.E. Coates and R.G. Hayter, unpublished results.
145. H.C. Clark and A.L. Pickard, *J. Organometal. Chem.*, 1968, **13**, 61.
146. M.B. Power and A.R. Barron, *J. Chem. Soc., Chem. Commun.*, 1991, 1315.
147. A.H. Cowley, R.A. Jones, P.R. Harris, D.A. Atwood, L. Contreras and C. Burek, *Angew. Chem.*, 1991, **103**, 1164.; *Angew. Chem., Int. Ed. Engl.*, 1991, **30**, 1143.
148. M.B. Power, J.W. Ziller, A.N. Tyler and A.R. Barron, *Organometallics*, 1992, **11**, 1055.
149. E.G. Hoffmann, *Ann. Chim.*, 1960, **629**, 104.
150. D.A. Drew, *Z. Anorg. Allg. Chem.*, 1973, **398**, 241.
151. D.J. Brauer and G.D. Stucky, *J. Am. Chem. Soc.*, 1969, **91**, 5462.

152. G.E. Coates and R.G. Hayter, *J. Chem. Soc.*, 1953, 2519.
153. T. Hirabayashi, T. Sakakibara and Y. Ishii, *J. Organomet. Chem.*, 1972, **35**, 19.
154. H. Schmidbaur, *J. Organomet. Chem.*, 1963, **1**, 28.
155. H. Schmidbaur and F. Schindler, *Chem. Ber.*, 1966, **99**, 2178.
156. B. Armer and H. Schmidbaur, *Chem. Ber.*, 1967, **100**, 1521.
157. A.W. Apblett and A.R. Barron, *Organometallics*, 1990, **9**, 2137.
158. O.T. Beachley, Jr., T.E. Getman, R.U. Kirss, R.B. Hallock, W.E. Hunter and J.L. Atwood, *Organometallics*, 1985, **4**, 751.
159. A.H. Cowley, S.K. Mehrotra, J.L. Atwood and W.E. Hunter, *Organometallics*, 1985, **4**, 1115.
160. T. Mole, *Aust. J. Chem.*, 1966, **19**, 373.
161. K.W. Egger, *J. Chem. Soc. (A)*, 1971, 3603.
162. K.B. Starowieyski, S. Pasynekiewicz and M. Skowronska-Ptasinska, *J. Organomet. Chem.*, 1975, **90**, C43.
163. A.P. Shreve, R. Mulhaupt, W. Fultz, J. Calabrese, W. Robbins and S.D. Ittel, *Organometallics*, 1988, **7**, 409.
164. M.A. Banks, O.T. Beachley, Jr., H.J. Gysling and H.R. Luss, *Organometallics*, 1990, **9**, 1979.
165. O.T. Beachley, Jr., J.C. Lee, H.J. Gysling, S.H.L. Chao, M.R. Churchill and C.H. Lake, *Organometallics*, 1992, **11**, 3144.
166. J. Weidlein, *Angew. Chem. Int. Ed. Engl.*, 1969, **8**, 927.
167. H.D. Hausen and H.U. Schwering, *Z. Anorg. Allg. Chem.*, 1973, **398**, 119.
168. H.D. Hausen, K. Sille, J. Weidlein and W. Schwartz, *J. Organomet. Chem.*, 1978, **160**, 411.
169. W. Lindel and F. Huber, *Z. Anorg. Allg. Chem.*, 1974, **408**, 167.
170. F.W.B. Einstein, M.M. Gilbert and D.G. Tuck, *J. Chem. Soc., Dalton Trans.*, 1973, 248.
171. J.J. Habeeb and D.G. Tuck, *Can. J. Chem.*, 1974, **52**, 3950.
172. J. Weidlein, *Z. Anorg. Allg. Chem.*, 1971, **386**, 129.

173. H.D. Hausen, *J. Organomet. Chem.*, 1972, **39**, C37.
174. H.D. Hausen, K. Mertz and J. Weidlein, *J. Organomet. Chem.*, 1974, **67**, 7.
175. W.R. Kroll and W. Naegele, *J. Organomet. Chem.*, 1969, **19**, 439.
176. B. Ballarin, G.A. Battiston, F. Benetollo, R. Gerbasi, M. Porchia, D. Favretto and P. Traldi, *Inorg. Chim. Acta*, 1994, **217**, 71.
177. H. Olapinski, B. Schaible and J. Weidlein, *J. Organomet. Chem.*, 1972, **43**, 107.
178. H.U. Schwering and J. Weidlein, *Chimica*, 1973, **27**, 535.
179. H. Yasuda, T. Araki and H. Tani, *J. Organomet. Chem.*, 1973, **49**, 103.
180. Y. Kai, N. Yasuoka, N. Kasai, M. Kakudo, H. Yasuda and H. Tani, *J. Chem. Soc., Chem. Commun.*, 1968, 1332.
181. H.U. Schwering, J. Weidlein and P. Fischer, *J. Organomet. Chem.*, 1975, **84**, 17.
182. P. Fischer, R. Gräf, J.J. Stezowski and J. Weidlein, *J. Am. Chem. Soc.*, 1977, **99**, 6131.
183. M.D. Healy and A.R. Barron, *J. Am. Chem. Soc.*, 1989, **111**, 398.
184. J.C. Cannadine, PhD Thesis, University of Warwick, 1994.
185. S. Patei (Ed.), "The Chemistry of Amidines and Imidates", Wiley, New York, 1975; Vol. 2, 1991.
186. V.G. Granik, *Russ. Chem. Rev.*, 1983, **52**, 377.
187. J. Barker, R.O. Gould and M Kilner, *J. Chem. Soc., Dalton Trans.*, 1987, 2687.
188. J. Barker and M. Kilner, *Coord. Chem. Rev.*, 1994, **133**, 219.
189. R. Lechler, H.D. Hausen and J. Weidlein, *J. Organomet. Chem.*, 1989, **359**, 1.
190. D. Kottmair-Maieron, R. Lechler and J. Weidlein, *Z. Anorg. Allg. Chem.*, 1991, **593**, 111.
191. C. Ergezinger, F. Weller and K. Dehnicke, *Z. Naturforsch B*, 1988, **43**, 1621.
192. H. Borgholte, K. Dehnicke, H. Goesmann and D. Fenske, *Z. Anorg. Allg. Chem.*, 1991, **600**, 7.
193. K. Dehnicke, *Chemiker-Zeitung*, 1990, **114**, 295.
194. F.T. Edelman, *Coord. Chem. Rev.*, 1994, **137**, 403.

195. J.T. Leman, H.A. Roman and A.R. Barron, *J. Chem. Soc., Dalton Trans.*, 1992, 2183.
196. D.C. Prevorsek, *J. Phys. Chem.*, 1962, **66**, 769.
197. C. Ergezinger, F. Weller and K. Dehnicke, *Z. Naturforsch., Teil B*, 1988, **43**, 1621.
198. J. Weidlein, *Z. Anorg. Allg. Chem.*, 1970, **378**, 245.
199. A.F.M.J. van der Ploeg, G. van Koten and K. Vrieze, *Inorg. Chem.*, 1982, **21**, 2026.
200. N.C. Blacker, PhD Thesis, University of Warwick, 1992.
201. F. Glockling and R.G. Strafford, *J. Chem. Soc. (A)*, 1971, 1761.
202. J. Barker, M. Jones and M. Kilner, *Org. Mass Spectrom.*, 1985, **20**, 619.
203. H. Borgholte, K. Dehnicke, H. Golsmann and D. Fenske, *Z. Anorg. Allg. Chem.*, 1991, **600**, 7.
204. F. Weller and U. Müller, *Chem. Ber.*, 1977, **112**, 2039.
205. M. Veith and O. Recktenwald, *J. Organomet. Chem.*, 1984, **264**, 19.
206. D.A. Atwood, R.A. Jones, A.H. Cowley, S.G. Bott and J.L. Atwood, *J. Organomet. Chem.*, 1992, **434**, 143.
207. W.W. Porterfield, *"Inorganic Chemistry"*, Addison-Wesley Ltd. (1983).
208. N.W. Alcock, J. Barker and M.G.H. Wallbridge, *Acta Crystallogr., Sect. C*, 1988, **44**, 712.
209. F.J. Lahoz, A. Tiripicchio, M.T. Camellini, L.A. Oro and M.T. Pinillos, *J. Chem. Soc., Dalton Trans.*, 1985, 1487.
210. C.L. Yao, L.P. He, J.D. Korp and J.L. Bear, *Inorg. Chem.*, 1988, **27**, 4389.
211. B. Lee, W.T. Pennington and G.H. Robinson, *Organometallics*, 1990, **9**, 1709.
212. S.J. Rettig, A. Storr and J. Trotter, *Can. J. Chem.*, 1975, **53**, 58; *ibid*, **53**, 753.
213. A.H. Cowley, R.A. Jones, M.A. Mardones, J. Ruiz, J.L. Atwood and S.G. Bott, *Angew. Chem. Int. Ed. Engl.*, 1990, **29**, 1150.

214. A.M. Arif, D.C. Bradley, D.M. Frigo, M.B. Hursthouse and B. Hussain, *J. Chem. Soc., Chem Commun.*, 1985, 783.
215. M.A. Khan, R.S. Steevensz, D.G. Tuck, J.G. Noltes and P.W.R. Corfield, *Inorg. Chem.*, 1980, **19**, 3407.
216. C.A. Olazábal, F.P. Gabbaï, A.H. Cowley, C.J. Carrano, L.M. Mokry and M.R. Bond, *Organometallics*, 1994, **13**, 421.
217. R.G. Ball, K.M. Lee, A.G. Marshall and J. Trotter, *Inorg. Chem.*, 1980, **19**, 1463.
218. R.B. King, *J. Am. Chem. Soc.*, 1969, **91**, 7211.
219. V.L. Goedkin, H. Ito and T. Ito, *J. Chem. Soc., Chem. Commun.*, 1984, 1453.
220. I. Crossland and F.S. Grevil, *Acta Chem. Scand.*, 1981, **Ser. B. 35**, 605.
221. L. Tschugsev and W. Lebedinski, *C.R. Acad. Sci. (Paris)*, 1915, **161**, 563.
222. N.C. Stephenson, *J. Inorg. Nucl. Chem.*, 1962, **24**, 801.
223. H. Hoberg and J.B. Muir, *J. Organomet. Chem.*, 1969, **17**, 30.
224. T. Hirabayashi, K. Itoh, S. Sakai and Y. Ishii, *J. Organomet. Chem.*, 1970, **21**, 273.
225. R.S. Garigipati, *Tetra. Lett.*, 1990, **31**, 1969.
226. M. Bottrill, R. Goddard, M. Green, R.P. Hughes, M.K. Lloyd, S.H. Taylor and P. Woodward, *J. Chem. Soc., Dalton Trans.*, 1975, 1150.
227. V. Robinson, G.E. Taylor, P. Woodward, M. I. Bruce and R. C. Wallis, *J. Chem. Soc., Dalton Trans.*, 1981, 1169.
228. W.J. Bland, R.D.W. Kemmitt, I.W. Nowell and D.R. Russell, *J. Chem. Soc., Chem. Commun.*, 1968, 1065.
229. J. Barker and M. Kilner, *J. Chem. Soc., Dalton Trans.*, 1989, 837.
230. B.M. Mikhailov, V.A. Dorokhov and V.I. Seredenko, *Dokl., Akad. Nauk SSSR*, 1971, **199**, 1328.
231. M.B. Hursthouse, M. A. Mazid, S.D. Robinson and A. Sahajpal, *J. Chem. Soc., Dalton Trans.*, 1994, 3615.
232. K. Dymock and G.J. Palenik, *Acta Crystallogr., Sect. B*, 1974, **30**, 1364.

233. R. Guilard and K.M. Kadish, *Chem. Rev.*, 1988, **88**, 1121.
234. Y. Hosokawa, M. Kuroko, T. Aida and S. Inoue, *Macromolecules*, 1991, **24**, 824.
235. M.J. Taylor, D.G. Tuck and L. Victoriano, *J. Chem. Soc., Dalton Trans.*, 1981, 928.
236. G.H. Robinson, A.D. Rae, C.F. Camapana and S.K. Byram, *Organometallics*, 1987, **6**, 1227.
237. G.H. Robinson and S.A. Sangokoya, *J. Am. Chem. Soc.*, 1987, **109**, 6852.
238. G.H. Robinson, E.S. Appel, S.A. Sangokoya, H. Zhang and J.L. Atwood, *J. Coord. Chem.*, 1988, **17**, 373.
239. G.H. Robinson, M.F. Self, S.A. Sangokoya and W.T. Pennington, *J. Am. Chem. Soc.*, 1989, **111**, 1521.
240. G.H. Robinson, W.T. Pennington, B. Lee, M.F. Self and D. Hencir, *Inorg. Chem.*, 1991, **30**, 809.
241. B. Lee, W.T. Pennington and G.H. Robinson, *Organometallics*, 1990, **9**, 1709.
242. B. Lee, W.T. Pennington, G.H. Robinson and R.D. Rogers, *J. Organomet. Chem.*, 1990, **396**, 269.
243. V.L. Goedken, J.J. Pluth, S.M. Peng and B. Bursten, *J. Am. Chem. Soc.*, 1976, **98**, 8014.
244. M.C. Weiss, B. Bursten, S.M. Peng and V.L. Goedken, *J. Am. Chem. Soc.*, 1976, **98**, 8021.
245. F.A. Cotton and J. Czuchajowska, *Polyhedron*, 1990, **9**, 2553.
246. J.L. Hoard, *Science*, 1971, **174**, 1295.
247. D.A. Atwood, V.O. Atwood and A.H. Cowley, *Inorg. Chem.*, 1992, **31**, 3871.
248. F.W.B. Einstein, M.M. Gilbert and D.G. Tuck, *Inorg. Chem.*, 1972, **11**, 2832.
249. S. Shibata, L.S. Bartell, R.M. Gavin, Jr., *J. Chem. Phys.*, 1964, **41**, 717.
250. O.T. Beachley, Jr., J.C. Pazik, T.E. Glassman, M.R. Churchill, J.C. Fettinger and R. Blom, *Organometallics*, 1988, **7**, 1051.
251. J.S. Poland and D.G. Tuck, *J. Organomet. Chem.*, 1972, **42**, 307.

252. M. Kuroki, T. Aida and S. Inoue, *J. Am. Chem. Soc.*, 1987, **109**, 4739.
253. M. Kuroki, T. Watanabe, T. Aida and S. Inoue, *Macromol.*, 1988, **21**, 3114.
254. S. Tero-Kubota, N. Hoshino, M. Kato, V.L. Goedken and T. Ito, *J. Chem. Soc., Chem. Commun.*, 1985, 959.
255. H. Oshio, S. Tero-Kubota and T. Ito, *Bull. Chem. Soc. Jpn.*, 1987, **60**, 3047.
256. V.E. Zubarev and V.N. Belevskii, L.T. Bugaenko, *Russian Chem. Rev.*, 1979, **48**, 729.
257. K.M. Kadish, G.B. Maiya and Q.Y. Xu, *Inorg. Chem.*, 1989, **28**, 2518.
258. M. Hoshino, K. Yasufku, H. Seki and H. Yamazaki, *J. Phys. Chem.*, 1985, **89**, 3080.
259. M. Hoshino and T. Hirai, *J. Phys. Chem.*, 1987, **91**, 4510.
260. V.L. Goedken and M.C. Weiss, *Inorg. Synth.*, 1980, **20**, 115.
261. S. Jena and K.C. Dash, *Indian J. Chem.*, 1994, **33A**, 699.
262. S. Strite and H. Morjoc, *J. Vac. Sci. Technol. B*, 1992, **10**, 1237.
263. D.C. Bradley, D.M. Frigo and E.A.D. White, "Forming aluminium nitride films", UK Pat. Appl. 8804707 & 8805524.
264. M.G. Jacko and S.J.W. Price, *Can. J. Chem.*, 1963, **41**, 1560.
265. G.M. Sheldrick, SHELXTL-PLUS user's manual, Nicolet Instr. Co., Madison, Wisconsin, 1990.
266. G. M. Sheldrick, (1993). SHELXL93. *Program for the Refinement of Crystal Structures*. University of Göttingen, Germany.
267. International Tables for X-ray Crystallography, 1974, Vol IV, Kynoch Press, Birmingham.